NAVIGATION STUDY FOR

JACKSONVILLE HARBOR, FLORIDA

DRAFT INTEGRATED GENERAL REEVALUATION REPORT II

AND

SUPPLEMENTAL ENVIRONMENTAL IMPACT STATEMENT

APPENDIX A

ATTACHMENT L

# ENGINEERING – Hydrodynamic and Water Quality Modeling for Environmental Impacts

**Ecological Modeling for Jacksonville Harbor Deepening GRR-2**

**Draft Report**

Prepared for

U.S. Army Corps of Engineers, Jacksonville District
Jacksonville, Florida

W912EP-10-D-0011 0004

by

Taylor Engineering, Inc.
10151 Deerwood Park Blvd.
Bldg. 300, Ste. 300
Jacksonville, Florida 32256
(904) 731-7040

C2012-010

March 2013

DRAFT

## TABLE OF CONTENTS


TABLE OF CONTENTS ..... I
LIST OF FIGURES ..... III
LIST OF TABLES ..... VI
1.0 INTRODUCTION ..... 1
1.1 Purpose ..... 1
1.2 Proposed Deepening Alternatives ..... 1
1.3 Potential Ecological Changes Due to Deepening ..... 1
1.4 Evaluation Methods ..... 2
1.5 Geographic Scope of the Study ..... 3
2.0 ECOLOGICAL EVALUATION FRAMEWORK ..... 7
2.1 Introduction ..... 7
2.2 Jacksonville Harbor Deepening Alternatives ..... 7
2.3 WSIS Model Systems ..... 8
2.4 Jacksonville Harbor Deepening Ecological Evaluation Approach ..... 9
3.0 SUBMERGED AQUATIC VEGETATION ..... 15
3.1 WSIS SAV Model ..... 15
3.3 Application of the SAV Model for Jacksonville Harbor Deepening GRR-2 Ecological Effects Evaluation ..... 16
3.4 SAV Model Results ..... 17
4.0 WETLANDS ..... 46
4.1 WSIS Wetlands Model ..... 46
4.2 Application of the WSIS Wetlands Model for Jacksonville Harbor Deepening GRR-2 Ecological Effects Evaluation ..... 48
4.3 Recommendations ..... 51
5.0 FISH ..... 55
5.1 Introduction ..... 55
5.2 Methods ..... 56
5.3 Results ..... 57
5.4 Potential Impacts of Channel Deepening on LSJR Fish Communities ..... 59
5.5 Recommendations ..... 59
6.0 BENTHIC MACROINVERTEBRATES ..... 67
6.1 Introduction and Existing Conditions ..... 67
6.2 Potential River Deepening Effects on Macroinvertebrates ..... 71


DRAFT

**6.3 BMI Analysis Methods** ..... **72**
*6.3.1 BMI Taxa Population and Community Abundance and Salinity* ..... *72*
*6.3.2 Partial Duration Frequency Analysis of Salinity* ..... *75*
**6.4 Results** ..... **77**
*6.4.1 Salinity Zones and BMI Community Abundance* ..... *77*
*6.4.2 Changes in Salinity Zone Areas* ..... *87*
*6.4.3 Changes in BMI Densities* ..... *88*
*6.4.4 Partial Duration Frequency Analysis of Salinity Behaviors* ..... *88*
*6.4.5 Effects of Salinity Changes on Commercially Important Species* ..... *105*
*6.4.6 Potential Effects of Channel on Estuarine Benthic Communities* ..... *111*
*6.4.7 Uncertainties* ..... *112*
**6.5 Recommendations** ..... **113**
**7.0 PHYTOPLANKTON** ..... **114**
**7.1 WSIS Plankton Empirical Models** ..... **114**
**7.2 Application of the Phytoplankton Model for Jacksonville Harbor Deepening GRR-2 Ecological Effects Evaluation** ..... **116**
**7.3 Results** ..... **116**
**7.4 Recommendations** ..... **118**
**8.0 WATER QUALITY** ..... **122**
**8.1 WSIS Water Quality Model** ..... **122**
**8.2 Jacksonville Harbor Deepening GRR-2 Water Quality Model** ..... **122**
**9.0 REFERENCES** ..... **124**

**APPENDIX A** **Calculation of Moving Average Salinities for Fish Analyses**

**APPENDIX B** **Benthic Macroinvertebrates (BMI) Moving Average Salinity Calculations**

**APPENDIX C** **EFDC Hydrodynamic Modeling for Water Quality Model Input for the Jacksonville Harbor Deepening GRR-2**

**APPENDIX D** **Application of CE-QUAL-ICM to the Jacksonville Harbor Deepening GRR-2 in the Lower St. Johns River**

DRAFT

## LIST OF FIGURES


**Figure 1.1** Jacksonville Harbor Segments (Source: USACE) ..... 2
**Figure 1.2** GRR-2 Ecological Evaluation Study Area (Source: SJRWMD, 2012) ..... 4
**Figure 2.1** EFDC Model Mesh ..... 12
**Figure 3.1** WSIS *V. americana* Stress Levels (Source: Dobberfuhl 2012) ..... 21
**Figure 3.2** SAV Evaluation Cells ..... 22
**Figure 3.3** Frequency of Moderate or Extreme SAV Stress — 40-ft Baseline ..... 23
**Figure 3.4** Frequency of Moderate or Extreme SAV Stress — 44-ft Project ..... 24
**Figure 3.5** Extreme Frequency of Moderate or Extreme SAV Stress — 46-ft Project ..... 25
**Figure 3.6** Frequency of Moderate or Extreme SAV Stress — 50-ft Project ..... 26
**Figure 3.7** Increase in Moderate/Extreme SAV Stress — Baseline to 44-ft Project ..... 27
**Figure 3.8** I ncrease in Moderate/Extreme SAV Stress — Baseline to 46-ft Project ..... 28
**Figure 3.9** Increase in Moderate/Extreme SAV Stress — Baseline to 50-ft Project ..... 29
**Figure 3.10** Frequency of Moderate/Extreme SAV Stress — 50-yr, 40-ft Baseline ..... 30
**Figure 3.11** Frequency of Moderate/Extreme SAV Stress — 50-yr 44-ft Project ..... 31
**Figure 3.12** Frequency of Moderate/Extreme SAV Stress — 50-yr, 46-ft Project ..... 32
**Figure 3.13** Frequency of Moderate/Extreme SAV Stress — 50-yr, 50-ft Project ..... 33
**Figure 3.14** Increase in Moderate/Extreme SAV Stress — Baseline to 50-yr Baseline ..... 34
**Figure 3.15** Increase in Moderate/Extreme SAV Stress — 50-yr Baseline to 50-yr, 44-ft Project ..... 35
**Figure 3.16** Increase in Moderate/Extreme SAV Stress — 50-yr Baseline to 50-yr, 46-ft Project ..... 36
**Figure 3.17** Increase in Moderate/Extreme SAV Stress — 50-yr Baseline to 50-yr, 50-ft Project ..... 37
**Figure 3.18** Littoral Area Subject To No Stress Effect ..... 38
**Figure 3.19** Littoral Area Subject To Low Stress Condition ..... 38
**Figure 3.21** Littoral area subject to extreme stress condition ..... 39
**Figure 3.20** Littoral Area Subject To Moderate Stress Condition ..... 39
**Figure 3.22** Littoral Area Subject To No Stress Effect At 50-yr Condition ..... 40
**Figure 3.23** Littoral Area Subject To Low Stress At 50-yr Condition ..... 40
**Figure 3.25** Littoral Area Subject To Extreme Stress At 50-yr Condition ..... 41
**Figure 3.24** Littoral Area Subject To Moderate Stress At 50-yr Condition ..... 41
**Figure 3.27** Temporal Distribution of Low Stress ..... 42
**Figure 3.26** Temporal Distribution of No Stress Effect ..... 42
**Figure 3.29** Temporal Distribution of Extreme Stress ..... 43
**Figure 3.28** Temporal Distribution of Moderate Stress ..... 43
**Figure 3.31** Temporal Distribution of Low Stress For 50-yr Condition ..... 44


DRAFT

**Figure 3.30** Temporal Distribution of No Stress Effect For 50-yr Condition ..... 44
**Figure 3.33** Temporal Distribution of Extreme Stress For 50-yr Condition ..... 45
**Figure 3.32** Temporal Distribution of Moderate Stress For 50-yr Condition ..... 45
**Figure 4.1** WSIS Wetland Breaklines ..... 52
**Figure 4.2** 95% Salinity for 40-ft Baseline Condition..... 53
**Figure 4.3** Location of Wetland Breaklines ..... 54
**Figure 5.1** Inter-annual Variability of Salinity Zone Areas for Baseline Conditions..... 60
**Figure 5.2** Comparison of Salinity Zone Areas for All Alternatives ..... 61
**Figure 5.3** Average Percent Changes in Water Column Salinity Zone Areas from the Current to 50-yr Horizon Conditions for Each Alternative ..... 62
**Figure 5.4** Baseline Maximum Water Column Salinity, LSJR North, 30-Day Moving Average, Baseline, 44-ft, 46-ft, and 50-ft Channels..... 63
**Figure 5.5** Baseline Maximum Water Column Salinity, LSJR South, 30-Day Moving Average, Baseline, 44-ft, 46-ft, and 50-ft Channels..... 64
**Figure 5.6** 50-yr Horizon Maximum Water Column Salinity, LSJR North, 30-Day Moving Average: Baseline, 44-ft, 46-ft, and 50-ft Channels..... 65
**Figure 5.7** 50-yr Horizon Maximum Water Column Salinity, LSJR South, 30-Day Moving Average: Baseline, 44-ft, 46-ft, and 50-ft Channels..... 66
**Figure 6.1** Maximum Bottom Salinity, LSJR, 30-Day Moving Average, Baseline Simulation ..... 79
**Figure 6.2** Inter-annual Variability in Salinity Zones for the Baseline Conditions of the Simulation80
**Figure 6.3** Maximum Bottom Salinity, LSJR North, 30-Day Moving Average, Baseline, 46-ft and 50-ft Channels..... 81
**Figure 6.4** Maximum Bottom Salinity, LSJR South, 30-Day Moving Average, Baseline, 46-ft and 50-ft Channels..... 82
**Figure 6.5** Maximum Bottom Salinity, LSJR North, 30-Day Moving Average, Comparison: Baseline and 50-yr Horizon Baseline ..... 83
**Figure 6.6** Maximum Bottom Salinity, LSJR South, 30-Day Moving Average, Comparison: Baseline and 50-yr Horizon Baseline ..... 84
**Figure 6.7** Maximum Bottom Salinity, LSJR North, 30-Day Moving Average, 50-yr Horizon: Baseline, 46-ft and 50-ft Channels..... 85
**Figure 6.8** Maximum Bottom Salinity, LSJR South, 30-Day Moving Average, 50-yr Horizon: Baseline, 46-ft and 50-ft Channels..... 86
**Figure 6.9** Average Salinity Zone Percent Changes Comparing the Current Baseline to Each Alternative Considered at the 50-yr Horizon..... 87

DRAFT

**Figure 6.10** Total BMI Densities for Baseline and Alternative Current Condition Simulations and 50-Yr Horizon Condition Simulations ..... 89
**Figure 6.11** Partial Duration Frequencies for Current and 50-yr Horizon Project Alternatives: 30ppt Salinity Duration Probabilities at Site SJR17 ..... 91
**Figure 6.12** Partial Duration Frequencies for Current and 50-yr Horizon Project Alternatives: 24 ppt Salinity Duration Probabilities at Site SJR17 ..... 92
**Figure 6.13** Partial Duration Frequencies for Alternatives under Current Conditions: 18 ppt Salinity Duration Probabilities at Site SJR17 ..... 93
**Figure 6.14** Partial Duration Frequencies for the 50-yr Horizon: 18 ppt Salinity Duration Probabilities at Site SJR17 ..... 94
**Figure 6.15** Partial Duration Frequencies for Current and 50-yr Horizon Conditions: 12 ppt Salinity Duration Probabilities at Site SJR17 ..... 95
**Figure 6.16** Partial Duration Frequencies for Current and 50-yr Horizon Conditions: 12 ppt Salinity Duration Probabilities at Site SJR17 ..... 96
**Figure 6.17** Partial Duration Frequencies for 1 ppt Salinity at SJR 40. ..... 97
**Figure 6.18** Partial Duration Frequencies for 0.5 ppt Salinity at SJR 40. ..... 98
**Figure 6.19** Duration Frequencies for 5.0 ppt Salinity at SR16. ..... 99
**Figure 6.20** Partial Duration Frequencies for 4.0 ppt Salinity at SR16. ..... 100
**Figure 6.21** Partial Duration Frequencies for 3.0 ppt Salinity at SR16. ..... 101
**Figure 6.22** Partial Duration Frequencies for 2.0 ppt Salinity at SR16 ..... 102
**Figure 6.23** Partial Duration Frequencies for 1.0 ppt Salinity at SR16 ..... 103
**Figure 6.24** Partial Duration Frequencies for 0.50 ppt Salinity at SR16 ..... 104
**Figure 6.25** Annual Blue Crab Landings from Five Northeast Florida Counties 1986 – 2011 ..... 106
**Figure 6.26** Soft-shell Crab Landings 1998 – 2011, for Five-County Northeast Florida Region. ..... 107
**Figure 6.27** White Shrimp Landings Recorded by Florida Fish and Wildlife Conservation Commission. Monthly, 1986 – 2011 ..... 110
**Figure 6.28** Brown and Pink Shrimp Landings Recorded by Florida Fish and Wildlife Conservation Commission. Monthly, 1986 – 2011 ..... 110
**Figure 7.1** Phytoplankton Sampling Stations ..... 119
**Figure 7.3** Regression Results — Nitrogen Fixation, Segment 3, Racy Point. ..... 120
**Figure 7.2** Regression Results — Marine Algal Bloom, Segment 2, Doctors Lake. ..... 120
**Figure 7.4** Regression Results — Freshwater Maximum Chl-A, Segment 3, Racy Point. ..... 121
**Figure 7.5** Regression Results — Freshwater Bloom Duration, Segment 2, Doctors Lake. ..... 121

DRAFT

## LIST OF TABLES

**Table 2.1** EFDC Model Simulations ..... 13
**Table 3.1** Salinity Stress Acres/Day ..... 20
**Table 4.1** WSIS Wetland Community Transition Salinity Break Points ..... 47
**Table 4.2** Salinity Breakpoint[1] Locations ..... 49
**Table 4.3** Movement of Salinity Breakpoints[1] ..... 50
**Table 5.1** Salinity Categories (from Miller et al., 2012) ..... 57
**Table 6.1** Salinity Breakpoints and Related Salinity Ranges for Salinity Area Estimates ..... 74
**Table 6.2** Locations of Salinity Data Used for PDFA Analysis From Mattson Et al.(2012). ..... 76
**Table 7.1** Input Variables For The Phytoplankton Empirical Regression Models ..... 116

DRAFT

# 1.0 INTRODUCTION

## 1.1 Purpose

The U.S. Army Corps of Engineers (USACE), Jacksonville District is preparing a General Revaluation Report (GRR) to evaluate proposed deepening of the Jacksonville Harbor navigation project. The Jacksonville Harbor Deepening GRR-2 will evaluate engineering, economic, and environmental factors related to the proposed St. Johns River navigation channel deepening. The USACE contracted with Taylor Engineering to prepare an evaluation of ecological effects in the lower St. Johns River (LSJR) from the proposed deepening. The USACE directed Taylor Engineering to base the evaluation on methods developed for assessment of estuarine portions of the St. Johns River described in St. Johns River Water Management District's (SJRWMD) recently completed evaluation of impacts of proposed water withdrawals from the middle and upper St. Johns River.

Potential environmental changes due to channel deepening include alteration of salinity and water circulation in the LSJR. These alterations could affect ecologically important communities in the river. This report evaluates potential effects on five of those communities — fishes, benthic macroinvertebrates, submerged aquatic vegetation, wetlands, and phytoplankton. It also examines potential effects on two key water quality parameters — dissolved oxygen and chlorophyll a. The results reported herein provide supporting documentation for the Jacksonville Harbor Deepening GRR-2 evaluation and associated Supplemental Environmental Impact Statement (SEIS).

## 1.2 Proposed Deepening Alternatives

The Jacksonville Harbor Deepening GRR-2 will describe in detail the proposed St. Johns River Federal navigation channel deepening alternatives. Generally, the deepening alternatives would increase the depth of the navigation channel from its currently authorized depth of 40 ft up to a maximum depth of 50 ft from the river entrance up to navigation channel mile 14 (located approximately at the northwest end of Bartram Island). Depth alternatives evaluated in this report include the current 40 ft depth and 44 ft, 46 ft and 50 ft deep channels (Figure 1.1).

## 1.3 Potential Ecological Changes Due to Deepening

The LSJR is an estuarine system in which salt water from the ocean mixes with fresh water flowing into the system from the upper reaches of the river and from tributaries discharging into the river.

**Figure 1.1** Jacksonville Harbor Segments (Source: USACE)

Salinity in the LSJR varies from oceanic levels at the river entrance to freshwater levels in the upper river. Many of the ecological communities and individual plant and animal species inhabiting the river respond to specific salinity conditions, which set their habitat range or affect their life cycles. As water mixes and flows into and out of the river, the length of time that any particular parcel of water resides in the river also varies. The water residence time (or "water age") may also affect some ecological communities. By changing the configuration of the river channel, the proposed deepening will affect water circulation, which, in turn, affects salinity and water age. Although some estuarine communities could be affected by changes in water elevation, the proposed channel deepening scenarios would have negligible effects on water elevation. This ecological evaluation therefore, does not examine any deepening-induced water level changes.

Numerical hydrodynamic models using EFDC (Environmental Fluid Dynamics Code) provide a tool for simulating salinity concentrations and water age for the current ("baseline") condition and the proposed project alternatives. Comparison of differences from baseline that occur under simulated conditions provides a means of assessing effects of the proposed deepening on some of the salinity-dependent LSJR ecological communities.

### 1.4 Evaluation Methods

A recently completed St. Johns River Water Management District study of the LSJR provides a framework for assessing ecological impacts of salinity changes. The *St. Johns River Water Supply Impact Study* (SJRWMD 2012) evaluated effects of proposed water withdrawals on St. Johns River ecological communities. The water supply impact study (WSIS) evaluated ecological impacts due to water level, salinity, and water age changes that could occur under various proposed surface water withdrawal

DRAFT

scenarios. Developed over a four-year period by a team comprised of dozens of scientists and engineers and with review by the National Research Council, the WSIS provides the most comprehensive and up to date set of information upon which to base an ecological impact assessment in the lower St. Johns River.

Pertinent to the Jacksonville Harbor Deepening GRR-2 evaluation of channel deepening effects on salinity and water age, the water supply impact study (WSIS) developed ecological models to evaluate the effects of salinity and water age changes on phytoplankton, submerged aquatic vegetation, wetland, benthic macroinvertebrate, and fish communities in the LSJR. Although the WSIS focused on evaluation of the effects of changes in flow entering the upper reaches of the river, the numerical and ecological models developed for the WSIS address salinity and water age effects in the LSJR. For the channel deepening evaluation, this report reviews the WSIS ecological models and adapts them, where possible, for use in the deepening evaluation. Differences in channel configuration, geographic scope, simulation time frames, and evaluation focus meant that not all of the WSIS ecological models could be directly applied for the Jacksonville Harbor Deepening GRR-2 evaluation. Subsequent chapters in this report provide details of each of the five ecological models and their adaption for the Jacksonville Harbor Deepening GRR-2 study.

In addition to the ecological models, the WSIS used the CE-QUAL-ICM water quality model to evaluate selected water quality parameters. Likewise, the Jacksonville Harbor Deepening GRR-2 evaluation included application of a CE-QUAL-ICM model to evaluate the same water quality parameters in the LSJR. The Jacksonville Harbor Deepening GRR-2 CE-QUAL-ICM modeling efforts are described in Appendices A and B.

This report does not address all potential environmental effects of the harbor deepening project. The SEIS prepared for the harbor deepening will include discussion of pertinent environmental effects not addressed in this report.

### 1.5 Geographic Scope of the Study

Though the proposed channel deepening extends about 14 miles upstream from the river mouth, salinity changes caused by the deepening could extend much further upstream. The Jacksonville Harbor Deepening GRR-2 ecological evaluation study area therefore begins at the confluence of St. Johns River and the Atlantic Ocean, and extends some 101 river miles upriver to a point slightly downstream of Lake George. The Jacksonville Harbor Deepening GRR-2 ecological study area, shown in Figure 1.2, comprises River Segments 1, 2, and 3 as defined in the WSIS (SJRWMD 2012):

Segment 1 – Mayport to Fuller Warren Bridge, river mile 0 to 24.6[1]

Segment 2 – Fuller Warren Bridge to Fleming Island, river mile 24.6 to 40.4

Segment 3 – Fleming Island to Little Lake George, river mile 40.4 to 101.3

Salinity changes due to channel deepening do not propagate upriver beyond the Shands Bridge (river mile 50) in the northern part of Segment 3 (Taylor 2012).

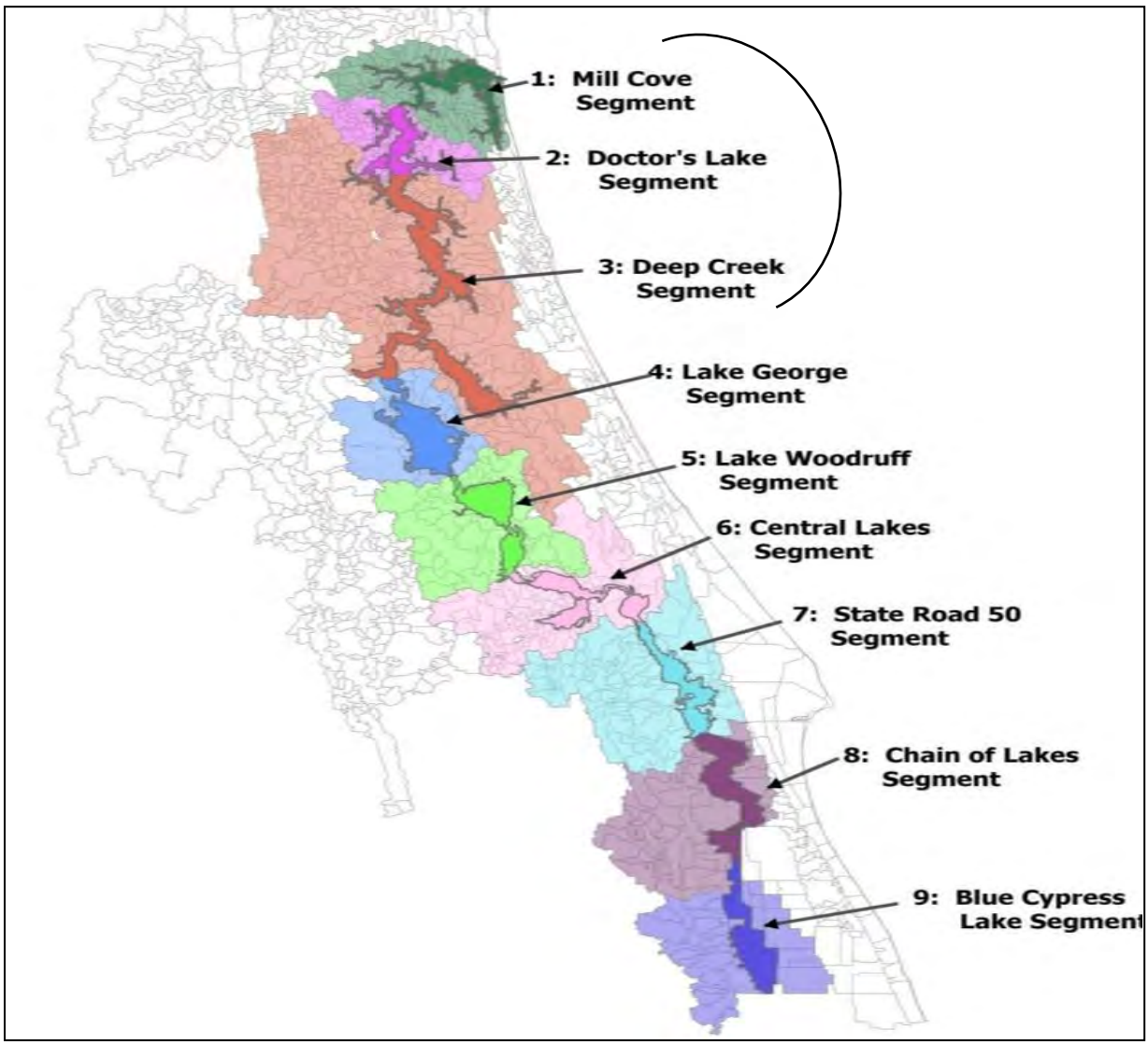


**Figure 1.2** GRR-2 Ecological Evaluation Study Area (Source: SJRWMD, 2012)

[1] River miles cited in this report refer to the SJRWMD river miles used for ecological evaluation. This river mile system is slightly different than the USACE river miles.

Nassau, Duval, Clay, St. Johns, and Putnam counties have riverfront along the river's main channel in the study area. The paragraphs below provide a summary of river conditions in the study area.

The area near the mouth of the St. Johns River (river miles 0 - 7) includes the U.S. Naval Station at Mayport, the confluence of the Florida Intracoastal Waterway and the river immediately west of the Naval Station, extensive salt marshes north and south of the main river channel and along the intracoastal waterway north and south. The shoreline along river miles 7 to 25 (slightly upstream of the Fuller Warren Bridge) is largely urbanized, comprising the City of Jacksonville, port facilities, electric generation facilities, and other waterfront features such as dredged material management facilities.

Though largely urbanized, this area includes several tributaries and associated wetland systems, including the Trout, Broward, and Arlington Rivers, Dunn Creek and a large embayment, Mill Cove. Urbanization continues upstream from river miles 25 to 43, where much of the shoreline comprises urban or suburban communities. Within this region, tributaries include the Cedar, and Ortega Rivers, Doctors Lake, and Julington Creek with their associated wetland systems. Between river miles 43 and 68 (Federal Point) fringing swamps and marshes, farmland, and minor residential areas occur near the river shoreline. Upstream of Federal Point, the west bank of the river is dominated by farmland with expanding river edge residential development and the towns of East Palatka (about river mile 80). On the west side of the river upstream of Federal Point, areas of swampland, the confluence of Rice Creek with the river and the town of Palatka waterfront (river mile 80) are dominant shoreline features. Upstream of river mile 80 to the study area terminus, swamps and interspersed residential development are the primary shoreline land forms and uses.

From river miles 0 to 25, the main stem of the river is subject to large tidal fluctuation and strong currents. Outside of the Federal navigation channel, river depth varies with maximum depths 50 ft occurring in the downtown Jacksonville area. Upstream of downtown Jacksonville, beginning roughly at river mile 25, the river channel becomes shallow, generally less than 6.6 ft (Miller et al. 2012). Tidal range is diminished but still a notable factor affecting shoreline wetland communities. Submerged aquatic vegetation (SAV), typically dominated by eelgrass (*Vallisneria americana*), is a key ecological community that occurs commonly along the shoreline from about river mile 25 upstream. Moving upstream from river mile 25, as the water becomes fresher, a diverse submerged and emergent wetland community occurs along the shoreline where not supplanted with armoring (revetments, seawalls, etc.).

The remainder of this report is organized as follows: Chapter 2 describes the ecological evaluation framework, including the identification of the deepening alternatives, application of the

hydrodynamic model that provides input data for the ecological evaluation, general applicability of the WSIS ecological models. Chapters 3 – 7 describe evaluation of each of the five ecological communities. Chapter 8 briefly discusses the water quality modeling while Appendices C and D contain separate reports of water quality modeling details. Appendix C describes the EFDC model developed to provide input data to the ICM-CEQUAL water quality model. Appendix B describes calibration of the CE-QUAL model.

DRAFT

# 2.0 ECOLOGICAL EVALUATION FRAMEWORK

## 2.1 Introduction

The ecological evaluation reported herein focuses on key LSJR ecological components — submerged aquatic vegetation, wetlands, fish, benthic macroinvertebrates, and phytoplankton — for which the SJRWMD WSIS provides ecological models (SJRWMD, 2012). The various ecological models were developed by the SJRWMD to evaluate the effects of water withdrawals in the upper St. Johns River from the river mouth up to Blue Cypress Lake (river mile 275). Representing the most recent and comprehensive assessment of the St. Johns River, the models addressed ecological effects of water level changes upstream of Deltona and salinity and water age changes downstream of Palatka.

Hydrodynamic modeling of the proposed Jacksonville Harbor deepening alternatives provided information about the potential effects of channel deepening on water levels and salinity (Taylor 2012). The modeling results indicated that a deeper channel would have negligible effects on riverine water levels. The WSIS models dealing with water level were thus not applicable to the harbor deepening evaluation. The hydrodynamic modeling showed that the deeper channel would alter salinity distribution in the LSJR. This ecological evaluation therefore used the WSIS report as the basis for assessing effects based on alteration of salinity patterns.

This chapter provides a brief review of the Jacksonville Harbor deepening alternatives, an overview of the WSIS model systems and review of the potential applicability of the WSIS models to the harbor deepening ecological evaluation. Subsequent chapters provide in-depth discussion about the application of the WSIS models to the harbor deepening study.

## 2.2 Jacksonville Harbor Deepening Alternatives

Segment 1 of the Jacksonville Harbor project, extending from the mouth of the river up to USACE river mile 14 near the northwest end of Blount Island, is authorized for 40-ft depth. The proposed Jacksonville Harbor deepening would increase the authorized depth of Segment 1. As described in the Jacksonville Harbor Deepening GRR-2 the USACE is considering and evaluating several project depth alternatives, up to a maximum depth of 50 ft. This ecological evaluation considered alternative project depths of 44 ft, 46 ft and 50 ft, comparing the effects of each of those alternatives to the project baseline condition.

The project baseline against which the deepening alternatives were compared represents the project area condition at time of construction, projected to occur in 2018. The baseline condition therefore includes river bathymetry as will exist following completion of the Mayport deepening and Mile Point project construction.

This study also included consideration of project area conditions 50 years after project completion. The 50-yr condition includes a 0.39-ft sea level rise and 155 million gallons per day (MGD) water withdrawals from the upper St. Johns River. This sea level rise represents a continuation of the recent historical rate of sea level rise. Taylor (2012) provides more detail about the deepening alternatives summarized in this section.

### 2.3 WSIS Model Systems

The WSIS methodology and report (SJRWMD, 2012), reviewed by the National Research Council, describes a comprehensive data set and analytical system for evaluation of the LSJR. The WSIS ecological models for the LSJR describe, in various formats, predictive relationships between salinity or water age and characteristics of the five LSJR river ecological components. Each model represented the consensus of a group of experts assembled to study a specific ecological component.

To apply the ecological models, the WSIS study group first used the Environmental Fluid Dynamics Code (EFDC) hydrodynamic model to simulate baseline and various water withdrawal scenarios. The WSIS baseline scenario represented LSJR basin conditions as existed in 1995. Forecast scenarios included several combinations of future water withdrawal, land use scenarios, and sea level rise (0.46 ft) as estimated for the year 2030. Notably, the 2030 condition included estimated land use patterns that resulted in greater water runoff and discharge into the river than occurred with the 1995 land use.

The WSIS EFDC model simulated each scenario for an 11-year period using rainfall and evapotranspiration records from 1995 through 2005. Allowing for a one-year “spin-up” period, the WSIS study group based its evaluations on the simulation results for the 10-year period from 1996 – 2005.

Output from the EFDC model simulations provided salinity and water age data for application of the ecological “models”. The ecological models developed by the WSIS study team employed differing evaluative approaches which depended on the particular derivatives of salinity or water age that best

described observed ecological effects. Briefly, the five ecological models evaluated effects based on the following approaches:

- Submerged aquatic vegetation – frequency and spatial extent of salinity stress on eelgrass (*Vallisneria americana*)
- Wetlands – location of salinity values defining transitions between wetland community types
- Fish – distribution of species or "pseudospecies" in relation to freshwater inflows
- Benthic macroinvertebrates – distribution of species in relation to salinity zones
- Plankton – regression equations using water age statistics as independent variables to calculate phytoplankton bloom metrics

Comparison of the modeled differences in ecological community indicators among baseline and water withdrawal scenarios allowed the WSIS study team to make quantitative or qualitative estimates of the magnitude of effects due to the withdrawals. Subsequent chapters of this report review of each of the five WSIS ecological models and discuss their applicability for the Jacksonville Harbor Deepening GRR-2 study.

### 2.4 Jacksonville Harbor Deepening Ecological Evaluation Approach

The Jacksonville Harbor Deepening ecological evaluation began with review of the WSIS models to determine how they could be applied to predict the effects of salinity and water age changes in the river due to the deepening. Initial EFDC modeling of the harbor deepening project showed that the project would not alter salinity patterns upstream of the Shands Bridge in WSIS River Segment 3. Each of the five WSIS models provided methods for assessing impacts of salinity or water age changes in one or more of River Segments 1 – 3. The deepened channel would not alter water levels, land use, runoff, nutrient loading, or other factors considered in the WSIS study. Application of the WSIS models for salinity and water age changes therefore formed the starting point for the Jacksonville Harbor Deepening GRR-2 ecological evaluation.

The ecological evaluation approach adopted for the Jacksonville Harbor Deepening GRR-2 ecological modeling is based on the WSIS model approaches, with some differences intended to give a more conservative (i.e., overestimate) assessment of potential impacts. Similar to the WSIS, the Jacksonville Harbor Deepening GRR-2 ecological modeling begins with EFDC model simulations of

project baseline and several project alternative scenarios. The following paragraphs summarize the Jacksonville Harbor Deepening GRR-2 EFDC model simulations. Taylor (2011, 2012) provides additional technical details and model results.

The EFDC model is a three-dimensional numerical model with the ability to simulate flow and transport in surface water systems. As applied for the Jacksonville Harbor Deepening GRR-2 ecological evaluation, the model contains 4,824 horizontal cells with six vertical layers in each cell. The model domain extends from the Atlantic Ocean near the river mouth upstream to the south end of Lake George (Figure 2.1).

The SJRWMD provided the EFDC model from the WSIS study, including all boundary conditions data. Taylor Engineering modified the model for application with the Jacksonville Harbor Deepening GRR-2 study. Notable modifications include repositioning the southern model boundary at Lake George, adding model cells along the project area navigation channel, and adding depths based on USACE bathymetric surveys conducted in 2009/10 and the design depths of the Mayport Deepening and the Mile Point Projects. These changes were made to focus the model on the LSJR portion of the river where deepening effects will occur, to better define the river bathymetry in the project area, and to provide a "baseline" condition that represents the river bathymetry at the anticipated time of the Jacksonville Harbor deepening.

Each of the Jacksonville Harbor Deepening GRR-2 EFDC model simulations included the following conditions:

- 1995 land use condition and inflows associated with that condition
- 7-year simulation period (1995 – 2001)
- Boundary condition input data as provided by the SJRWMD

The selected seven-year simulation period includes the three driest consecutive years (1999 – 2001) recorded for the LSJR basin. Selection of this time period thus provides a conservative estimate of salinity impacts in that the dry conditions should allow increases in salinity farther up the river than under a more typical rainfall period. Taylor (2012) provides additional discussion of these model details.

Table 2.1 identifies the eight conditions simulated for the Jacksonville Harbor Deepening GRR-2 ecological modeling study and identifies the combination of project, water withdrawal, and sea level condition represented by each simulation. We ran all simulations for a 7-year period from 1995 – 2001.

Allowing 1995 to be a spin-up year, the model results from 1996 to 2001 were saved in output data files for use in the ecological models. Each simulation output file contained hourly results for each of the vertical layers in each of the model cells. As discussed in succeeding chapters, we applied post-processing routines to the output data to generate the specific salinity or water age data required by the ecological models.

DRAFT

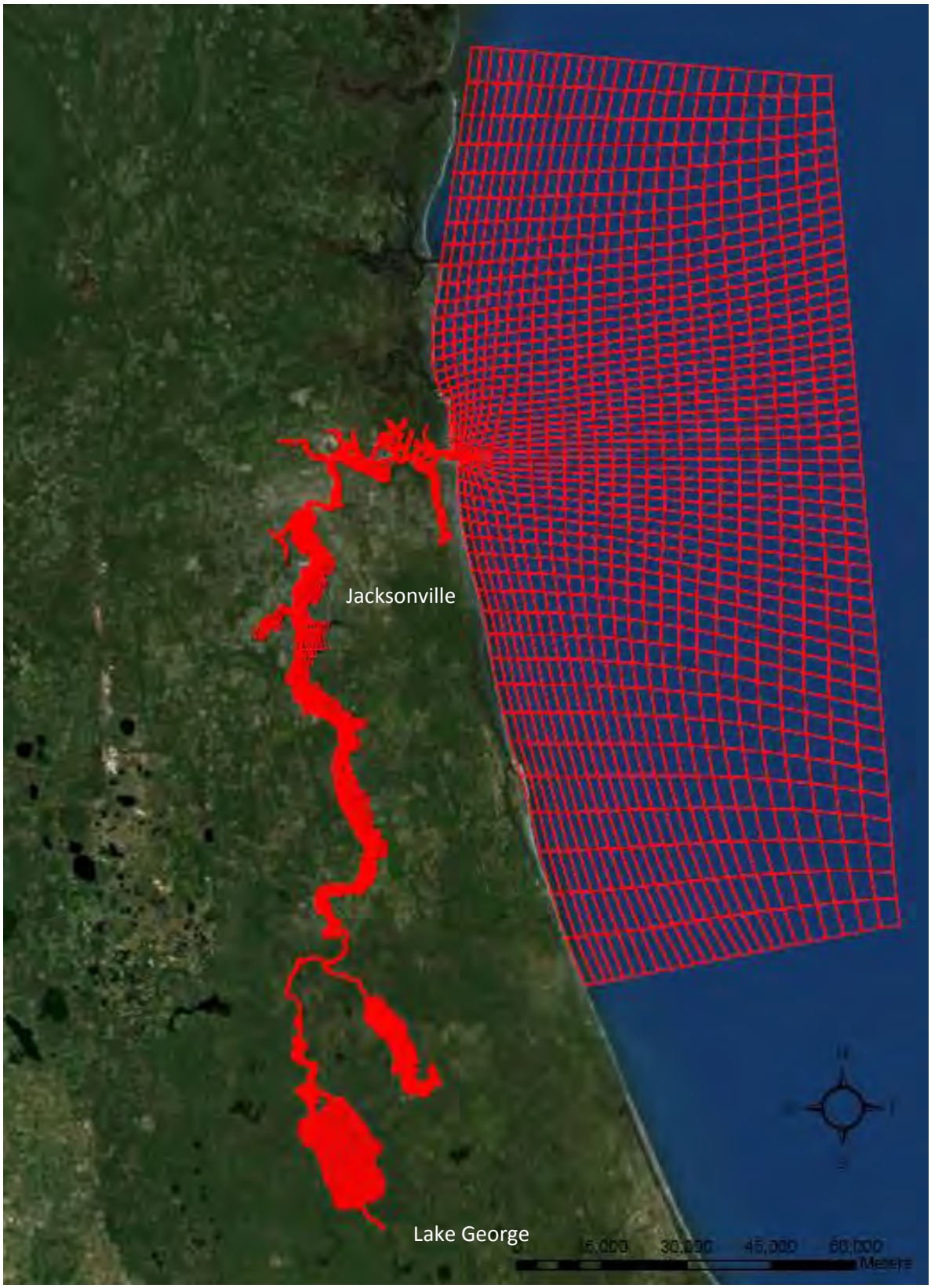


**Figure 2.1** EFDC Model Mesh

**Table 2.1** EFDC Model Simulations

| Scenario | Depth (ft) | | | | Water Withdrawal | | Sea Level | |
|---|---|---|---|---|---|---|---|---|
| | 40 | 44 | 46 | 50 | None | 155 MGD | No Change | Const. +50 yr, Curve 1 (0.39 ft) |
| 40ft_B95_SL0[1] | x | | | | x | | x | |
| 40ft_FSJ_SF1 | x | | | | | x | | x |
| 44ft_B95_SL0 | | x | | | x | | x | |
| 44ft_FSJ_SF1 | | x | | | | x | | x |
| 46ft_B95_SL0 | | | x | | x | | x | |
| 46ft_FSJ_SF1 | | | x | | | x | | x |
| 50ft_B95_SL0 | | | | x | x | | x | |
| 50ft_FSJ_SF1 | | | | x | | x | | x |

[1]Baseline condition

The Jacksonville Harbor Deepening GRR-2 ecological evaluation based on the WSIS analytical models was not intended to address all potential environmental effects of the deepening project. Other ongoing USACE efforts, including preparation of a Supplemental Environmental Impact Statement (SEIS) for the Jacksonville Harbor Deepening, will address other project effects.

The WSIS models were designed to address ecological effects in the main stem (including along the shoreline) of the LSJR. Identification of effects in the main stem may allow inference of potential effects upstream of the model domain; the model systems do not, however, directly address impacts of salinity changes that may occur upstream in marshes and tributaries.

The EFDC model configuration used for the Jacksonville Harbor Deepening GRR-2 study was well-calibrated to simulate salinity conditions in the LSJR. However, because the EFDC model domain and simulation period were not identical to those used for the WSIS, some of the ecological models—wetlands and phytoplankton in particular — did not perform well under the simulation conditions set for the Jacksonville Harbor Deepening GRR-2 study. The results from these two model systems suggested

that the models are highly specific for the particular EFDC configuration used in the WSIS study. Consequently, we adapted and modified as practicable the model concepts for the Jacksonville Harbor Deepening GRR-2 evaluation. Subsequent chapters of this report describe all of the ecological model approaches, application, and results in detail.

DRAFT

## 3.0 SUBMERGED AQUATIC VEGETATION

The WSIS submerged aquatic vegetation (SAV) working group evaluated potential effects of water withdrawal on SAV communities of the St. Johns River. Dobberfuhl et al. (2012) describe the working group's SAV evaluation and development of the SAV evaluation "models." This chapter reviews aspects of Dobberfuhl et al. (2012) report, identifies the model's applicability for evaluation of effects of the Jacksonville Harbor deepening project, and describes application of the model for the Jacksonville Harbor Deepening GRR-2 evaluation.

The submerged aquatic vegetation community (SAV) in the LSJR is dominated by *Vallisneria americana*, with other oligohaline/freshwater species — including *Najas guadalupensis*, *Ruppia maritima*, and others — observed on a less-frequent basis. The downstream extent of the LSJR SAV community occurs in the vicinity of river mile 25 near the Fuller Warren Bridge. SAV is sparsely distributed in that lower end of its range and its distribution varies from year to year. SAV become more abundant and dense upstream, with persistent beds occurring at a SJRWMD monitoring station near the Bolles School at about river mile 31. The Bolles School monitoring station likely represents the most downstream extent of persistent SAV beds in the LSJR. SJRWMD monitoring shows that SAV from the Bolles School site upstream to a monitoring station at Moccasin Slough near river mile 37 is subject to periodic salinity stress, which affects both distribution and abundance. SAV in this area is also subject to low-light stress due to higher water coloration during high runoff conditions.

### 3.1 WSIS SAV Model

For the WSIS, Dobberfuhl et al. (2012) determined that the two most important potential effects of water withdrawal on SAV communities relate to (1) alterations to stage (water levels) and (2) elevated salinity. Given its cosmopolitan nature, dominance in the estuarine portions of the river, biological importance, and well-studied physiology and ecology, the working group used *Vallisneria americana* as the representative species for all SAV analyses. Because the proposed Jacksonville Harbor deepening does not alter water levels affecting SAV, the water level effects model is not applicable to the Jacksonville Harbor Deepening GRR-2 study. This report therefore focusses on application of the WSIS SAV salinity stress model.

The WSIS SAV working group used existing literature to develop the salinity exposure model and performed additional field and experimental analyses (i.e., microcosm experiments, intensive SAV

sampling, and in situ reciprocal transplant experiments) to further refine the stress thresholds within the model. The group found that salinity stress on *V. Americana* depends on both salinity level and duration of exposure, as illustrated in Figure 3.1[2]. The working group found that 7-day and 30-day average salinity best predicted salinity stress on *V. Americana* and used these indicators to evaluate the modeled salinity changes due to water withdrawal.

The WSIS salinity stress model compared EFDC salinity output (daily average salinity for surface cells within the model domain) to the stress levels shown in Figure 3.1. The model considered salinity only in River Segments 2 and 3, from river miles 24.5 to 48 (Fuller Warren Bridge to Green Cove Springs) and only in littoral zone cells (i.e., those contiguous to the shoreline). This area, described by 140 model cells, represents the downstream limit of *V. Americana* habitat in the LSJR. Frequent salinity stress prevents occurrence of the species farther downstream in River Segment 1. The model littoral cells represent the shallow shoreline habitat where *V. americana* may grow in this area.

Each model cell was assigned a daily stress condition four stress categories defined in the SAV salinity exposure model. From the resulting data, the Dobberfuhl (2012) calculated both frequency and total acreage of salinity stress on potential SAV habitat.

### 3.3 Application of the SAV Model for Jacksonville Harbor Deepening GRR-2 Ecological Effects Evaluation

Initial review of EFDC simulation results indicated that the salinity changes due to the harbor deepening would not reach Green Cove Springs. We therefore elected to evaluate SAV stress in the same 140 modeled cells as the WSIS study. Figure 3.2 shows the SAV model cells, which cover 13,947 acres. These cells represent potential littoral zone SAV habitat. SAV has historically occurred along the shoreline within the area covered by these cells. However, SAV is absent from some of the cells when stressed by salinity or other factors. In addition, as noted by the WSIS SAV study group, the model cell widths are four to six times greater than the observed widths of SAV beds so the total area of potential seagrass habitat equals less than 13,947 acres. In considering the number of acres affected by salinity stress, the WSIS study group multiplied the modeled acreage by a factor of 0.25 to obtain a more likely estimate of affected acreage.

[2] Figures referenced in this chapter appear at the end of the chapter.

From the EFDC simulation output files, we calculated the daily, vertically averaged salinity for each of the 140 littoral zone model cells. From those values, we calculated the 7-day, 30-day, and 90-day average salinity[3] in each cell for each day of the simulation period. Comparing the salinity values to the WSIS salinity-duration exposure model we classified the daily stress level in each of the cells as no effect, low stress, moderate stress, or extreme stress. The results indicated that SAV would experience the greatest number of days under a stressed condition when stress was determined by the 90-day average salinity. The results presented below are based on SAV stress assessment from 90-day average salinity values. With the first 90-day average value occurring on day 90 of the simulation period, this salinity data set contained 2,103 daily values for each cell for the six-year simulation period. From this data set we examined several measures of spatial and temporal distribution of SAV stress conditions. For each model cell, we calculated the stress frequency as percentage of simulation time the cell was in one of the four stress conditions and magnitude of stress frequency increase as the difference between stress frequency values for different simulation conditions. We summed the total acres in each stress category for each day of the simulation and then determined cumulative probability of the number of acres falling within each category. Lastly, we calculated the number of acre-days in a stress condition by summing the total number of acres under each stress condition and dividing by the total number of days that condition occurred in one or more cells[4].

### 3.4 SAV Model Results

Figure 3.3 illustrates the percentage of time each of the littoral cells is under moderate/extreme/stress for the modeled baseline 40-ft condition. As expected, the most downstream cells, near the Fuller Warren Bridge, exhibit the greatest time under stress. Ten cells in this area are under salinity stress for greater than 30% of the simulation period (1996 – 2001). About three miles upstream, near river mile 28, stress frequency decreases to 20% or less of the simulation period. Near the Bolles School SJRWMD SAV monitoring site, the model predicts salinity stress during about 10% of the simulation period. Moving upstream, stress frequency continues to decrease. Stress frequencies of 1 – 5% occur south of river mile 32 (near Naval Air Station (NAS) Jacksonville). The model-predicted stress frequency drops to 0% on the west side of the river at the Buckman Bridge (river mile 34). The 0% stress frequency zone begins at about river mile 35 on the east side of the river.

[3] e.g., The first 7-day average salinity value occurred on day 7 of the simulation and was the average of the daily salinities from days 1 – 7.

[4] Acres/day in a stress condition = $\sum_{d=1}^{n}$ acres /n, where d = simulation day, n = total number of days, and acres = total number acres under stress condition on the nth day.

Figures 3.4, 3.5 and 3.6 show the percentage of time each of the littoral cells is under moderate/ extreme stress for the modeled 44-ft, 46-ft, and 50-ft project conditions. The model predicts little change in the area of the LSJR subject to no salinity stress for any of the simulated project conditions. The only change in the no stress area occurs, with all project alternatives, on the west side of the river immediately south of the Buckman Bridge (river mile 34 – 35) where two cells change from no stress to the 1 – 5% stress category. Downstream of the Buckman Bridge, stress frequencies progressively increase with increased simulated channel depths.

Figures 3.7, 3.8, and 3.9 illustrate the magnitude of salinity stress frequency increase in each cell for the 44-ft, 46-ft, and 50-ft project conditions relative to the baseline condition. Stress frequency increase is shown as the number of percentage points difference from the baseline condition (e.g. if the stress frequency increases from 12% for baseline to 16% for a project condition, the stress magnitude increase is 4). Given the 2,103 daily salinity data points for each six-year simulation, an increase of one percentage point equates to 3.5 days of stress per year.

For the 44-ft project simulation, salinity stress frequency increases 1 to 2 percentage points from the no stress zone downstream to about river mile 28. Downstream of river mile 28, stress frequency increases 1 to 3 points to about river mile 25. Five cells near river mile 25 and the Fuller Warren Bridge experience 4 to 6 point increases in stress frequency. The 46-ft project simulation showed several more cells from river mile 26 to 29 having up to a 3-point increase in stress frequency, along with the cells near the Fuller Warren Bridge having greater magnitude stress frequency increase. With the 50-ft project depth salinity stress frequency increased up to eight percentage points at one cell near the Fuller Warren Bridge. Increases in stress percentage of up to four points occur in several cells between the Fuller Warren Bridge and NAS Jacksonville.

Figure 3.10 shows the percentage of time each of the littoral cells is under moderate/extreme stress for the 50-yr baseline condition (i.e., 40 ft depth, 0.39 ft sea level rise, 155 MGD water withdrawal). The model shows that the no stress zone moves about one mile upriver relative to its location for the baseline 40-ft simulation. The most apparent increase in salinity stress frequency occurs between the Fuller Warren Bridge and river mile 29.

Figures 3.11, 3.12 and 3.13 show the percentage of time each of the littoral cells is under moderate or extreme stress for the 50-yr 44-ft, 46-ft, and 50-ft project conditions. For each of these projects, SAV would not experience salinity stress upstream of Doctors Lake (river mile 37).The northern

DRAFT

extent of the no stress zone occurs about a mile upstream of its location for the 50-yr baseline condition. With all three project depths, all cells downstream of river mile 29 experience salinity stress frequencies greater than 20%.

Figures 3.14 illustrates the magnitude of salinity stress frequency increase in each cell for the 50-yr 40-ft baseline relative to the current baseline condition. Stress frequency generally increases 1 – 3 percentage points from the Fuller Warren Bridge upriver to river mile 35, with scattered cells showing up to a 4 point increase.

Figures 3.15, 3.16, and 3.17 illustrate the magnitude of salinity stress frequency increase in each cell for the 50-yr 44-ft, 46-ft, and 50-ft projects relative to the 50-yr 40-ft baseline. The magnitude of stress frequency increase is generally greater with the projects at the 50-yr time horizon than it is under the current project conditions.

Figures 3.18 – 3.21 illustrate the probability of total littoral acres in each of the stress categories for the baseline and 44-ft, 46-ft, and 50-ft project depths. These figures indicate that the greatest difference in acres subject to salinity stress between baseline and the three project conditions occurs when salinity stress begins to noticeably increase at about the 50%, 35% and 5% probability levels.

Figures 3.22 – 3.25 illustrate the probability of total littoral acres in each of the stress categories for the current baseline, 50-yr baseline and 50-yr 44-ft, 46-ft, and 50-ft project depths. The overall patterns are similar to the current conditions but differences among project alternatives are greater at the 50-yr condition.

Figures 3.26 – 3.29 show the temporal distribution of salinity stress effects in terms of total acres in each stress condition for the baseline and 44-ft, 46-ft, and 50-ft projects. Figures 3.30 – 3.33 show the same plots for the 50-yr condition. Both sets of figures illustrate that the total number of acres of potential littoral habitat affected by salinity stress varies from year to year. During relatively dry years (e.g., 1999, 2000, 2001), moderate to extreme salinity stress may occur continuously for several months under all of the simulated conditions, including the baseline and 50-yr baseline.

Table 3.1 summarizes the SAV results in terms of acres/day under salinity stress. As noted by the WSIS study group, a more likely estimate of affected acreage may be obtained by multiplying these by a factor of 0.25. The acres/day measure provides a simple means to compare total SAV stress effects of the

different simulated conditions. However, these numbers do not consider the spatial and temporal distributions of salinity stress, which are important factors in determining actual effects of salinity on SAV beds. As the duration or frequency of salinity stress increases, the ability of SAV to recover from the stress would diminish.

The results of the baseline simulation indicate temporally and spatially variable salinity stress on SAV populations from the Fuller Warren Bridge to approximately NAS Jacksonville. Long (up to several months), widespread periods of salinity stress occur during the driest modeled years. These results appear consistent with field observations of declines in SAV beds during recent dry years. Increasing the channel depth causes progressively greater salinity stress superimposed on the already variable patterns of the baseline condition. Generally, the differences due to the project alternatives are much less than the annual differences due to variable hydrologic conditions. Nonetheless, the additional stress imposed by any of the proposed project alternatives will likely contribute to upstream migration of the northern extent of SAV in the LSJR.

**Table 3.1** Salinity Stress Acres/Day

| Stress Condition | Acres/day | | | | | | | |
|---|---|---|---|---|---|---|---|---|
| | Current Condition | | | | 50-yr Condition | | | |
| | Base 40 ft | 44 ft | 46 ft | 50 ft | Base 40 ft | 44 ft | 46 ft | 50 ft |
| No Effect | 10,983 | 10,845 | 10,826 | 10,764 | 10,627 | 10,303 | 10,282 | 10,212 |
| Low | 2,721 | 2,739 | 2,738 | 2,754 | 3,014 | 3,077 | 3,074 | 3,088 |
| Moderate | 1,378 | 1,407 | 1,410 | 1,402 | 1,553 | 1,591 | 1,597 | 1,606 |
| Extreme | 298 | 389 | 401 | 446 | 380 | 582 | 604 | 664 |

Due to the annual salinity stress variability inherent in the system, it is difficult to predict specific project induced alterations in potential SAV habitat. Nonetheless, the potential SAV habitat acreages subject to salinity stress conditions can provide a measure of impact. As noted by the Dobberfuhl (2012), the acreages obtained from the SAV model system overestimate the amount of potentially affected SAV habitat.

DRAFT

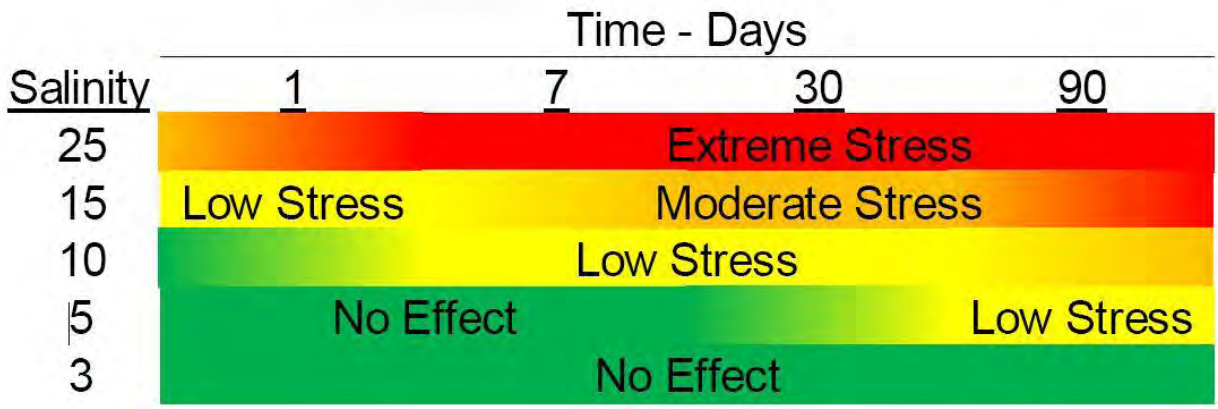


**Figure 3.1** WSIS *V. americana* Stress Levels (Source: Dobberfuhl 2012)

DRAFT

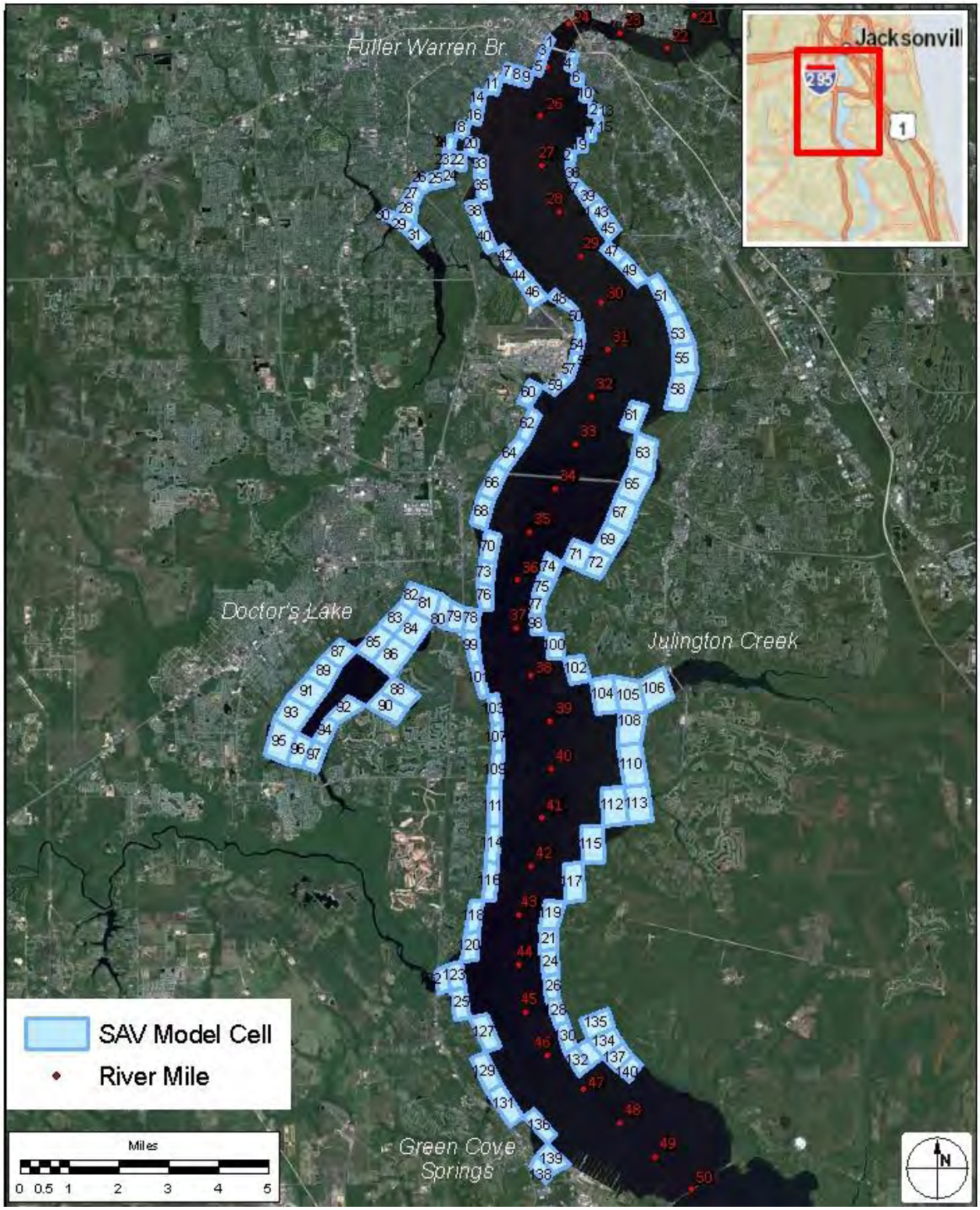


**Figure 3.2** SAV Evaluation Cells

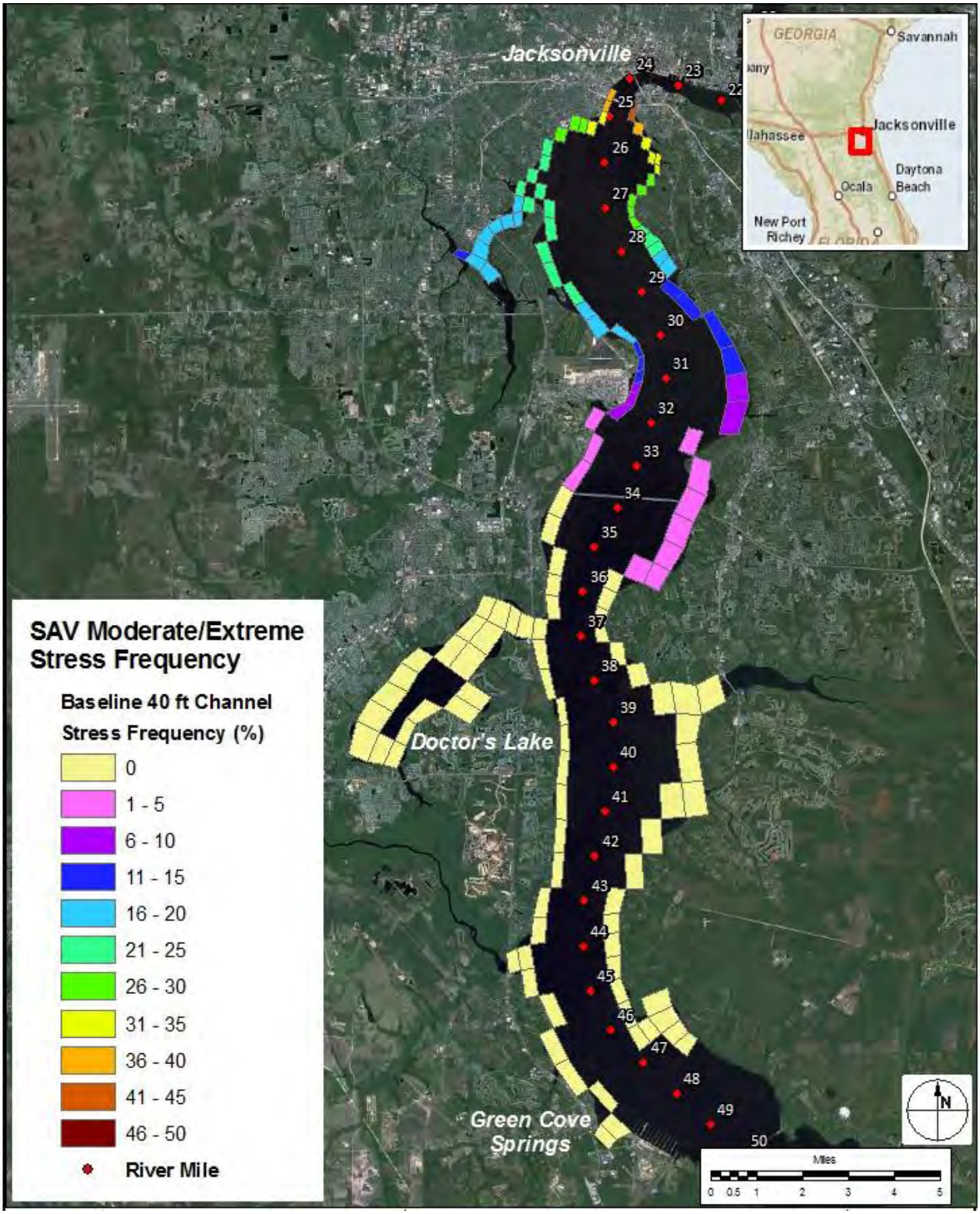


**Figure 3.3** Frequency of Moderate or Extreme SAV Stress — 40-ft Baseline

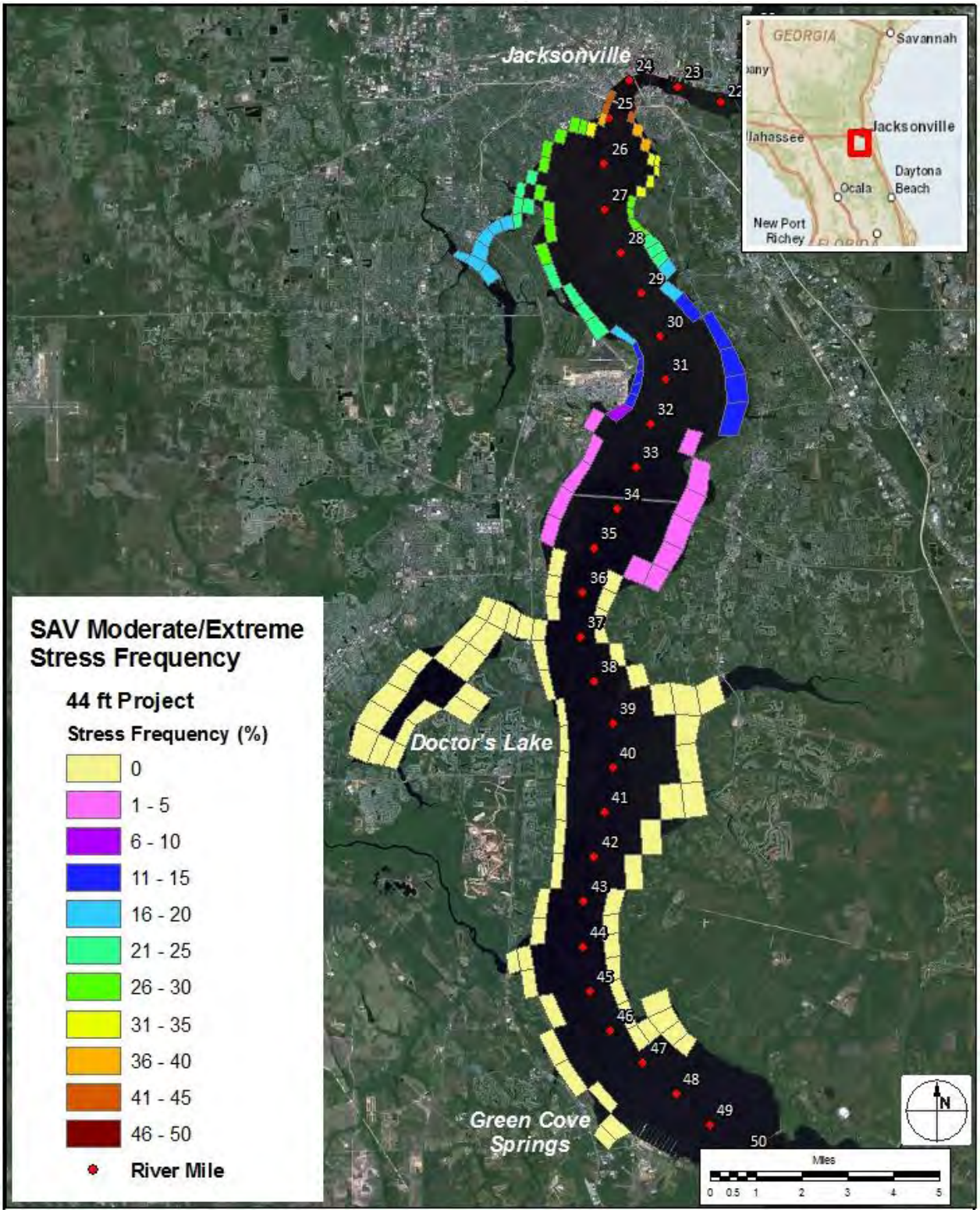


**Figure 3.4** Frequency of Moderate or Extreme SAV Stress — 44-ft Project

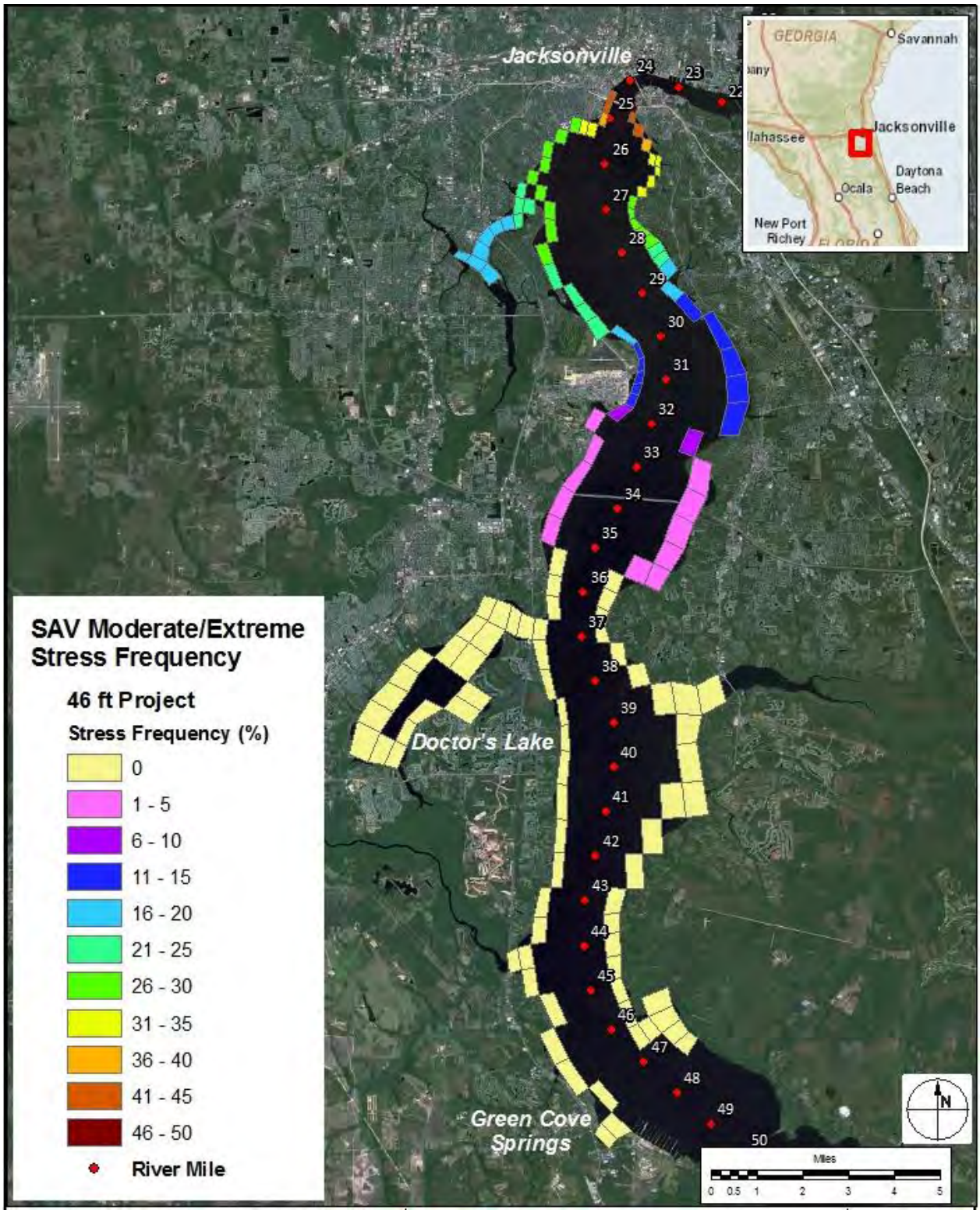


**Figure 3.5** Extreme Frequency of Moderate or Extreme SAV Stress — 46-ft Project

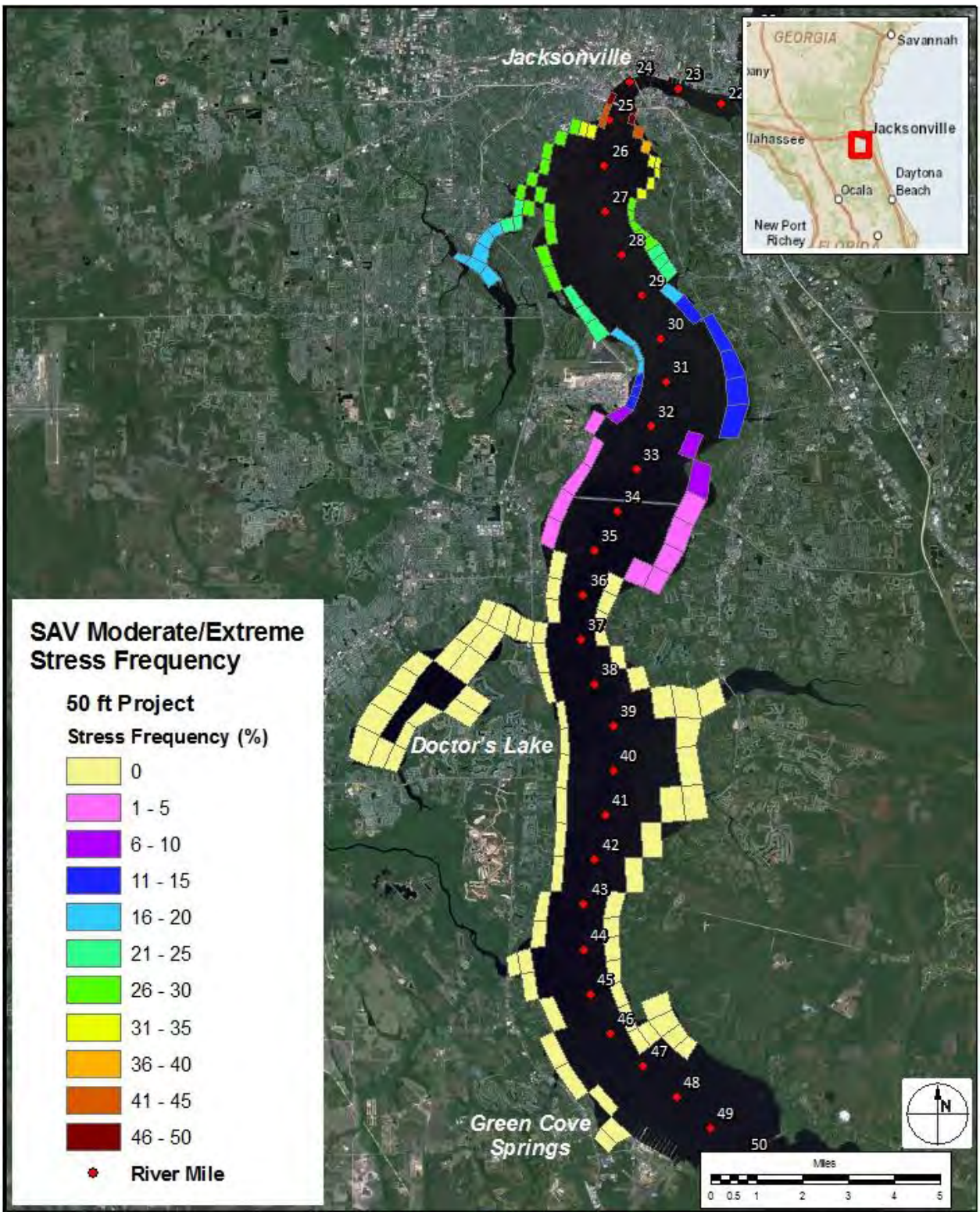


**Figure 3.6** Frequency of Moderate or Extreme SAV Stress — 50-ft Project

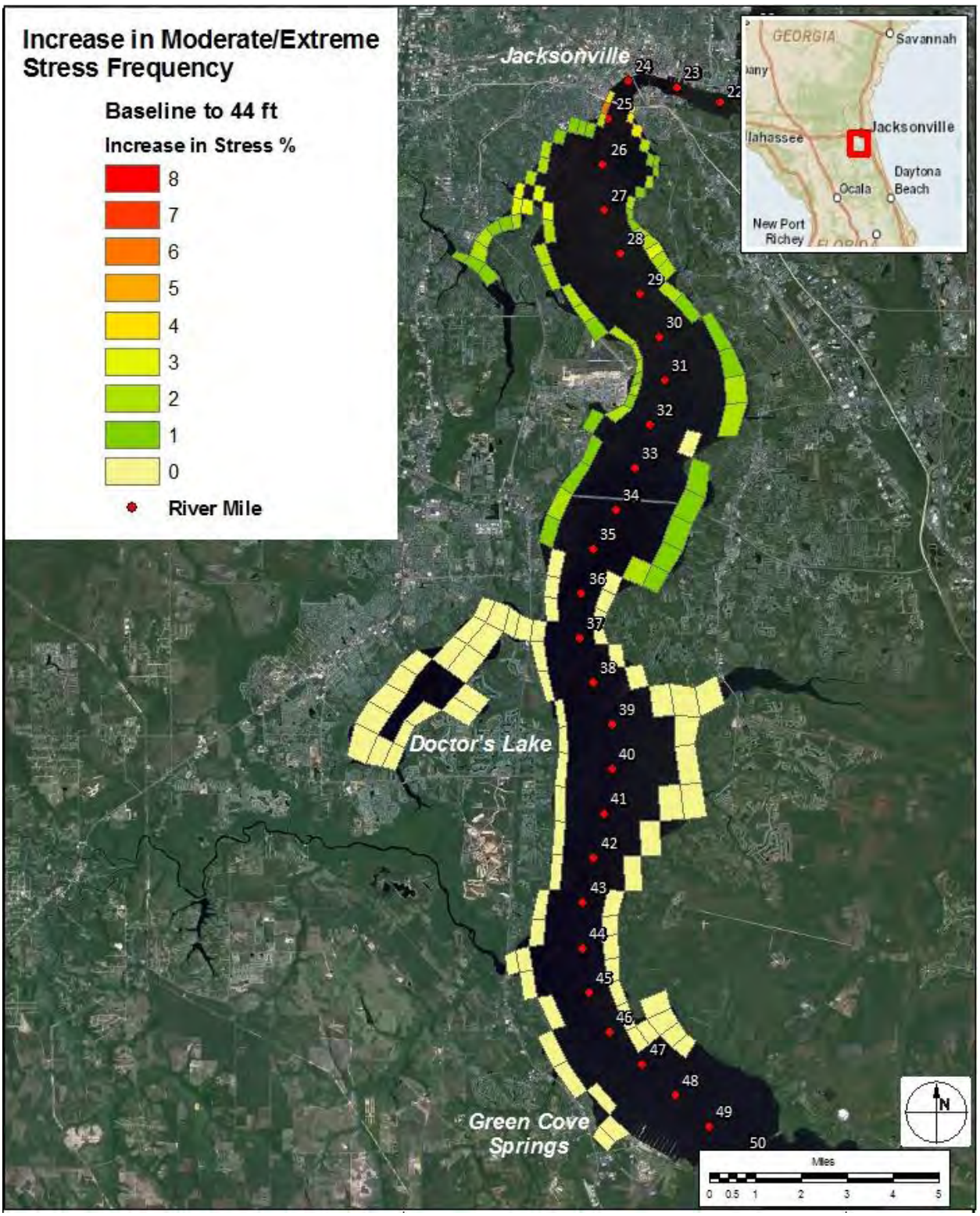


**Figure 3.7** Increase in Moderate/Extreme SAV Stress — Baseline to 44-ft Project

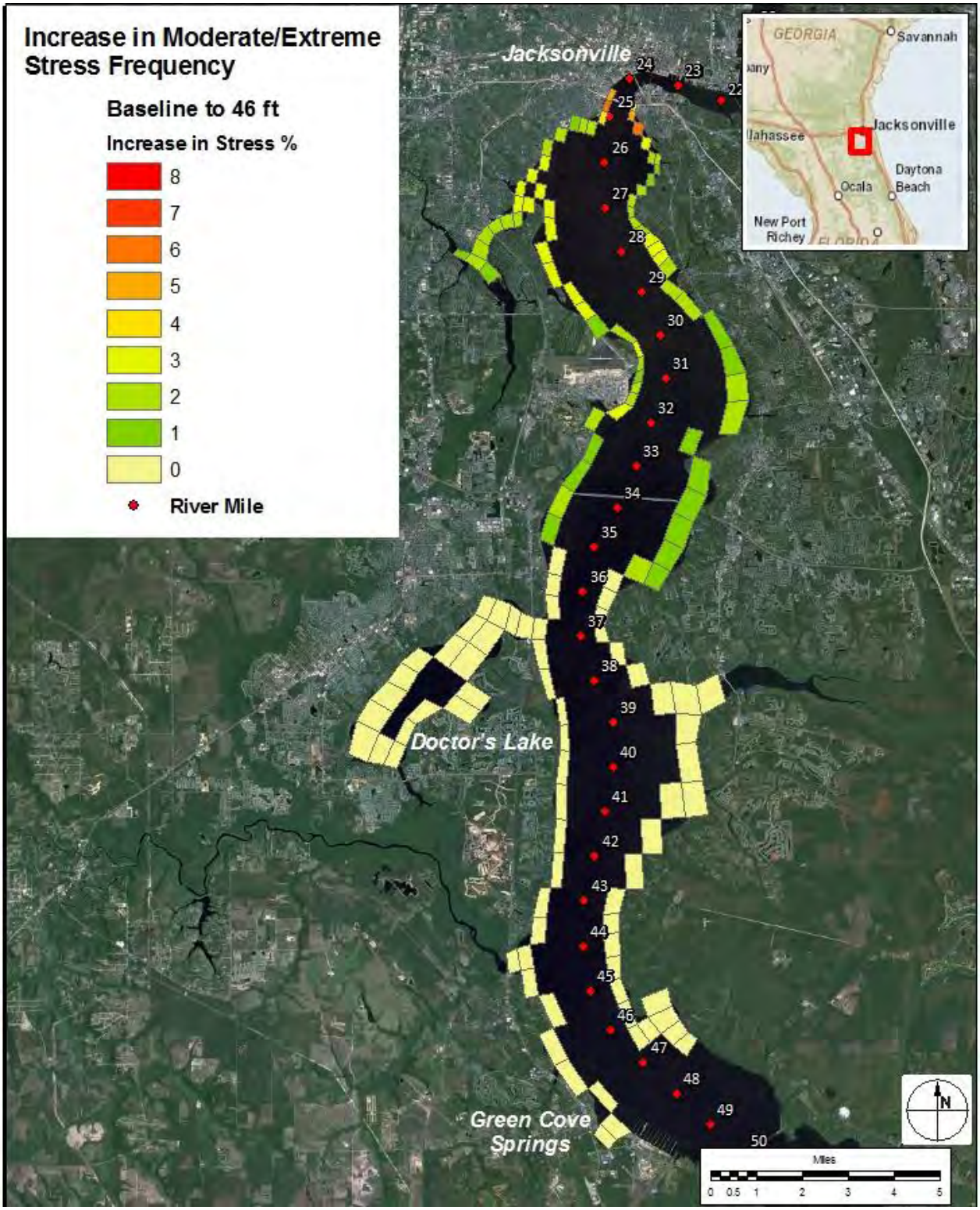


**Figure 3.8** Increase in Moderate/Extreme SAV Stress — Baseline to 46-ft Project

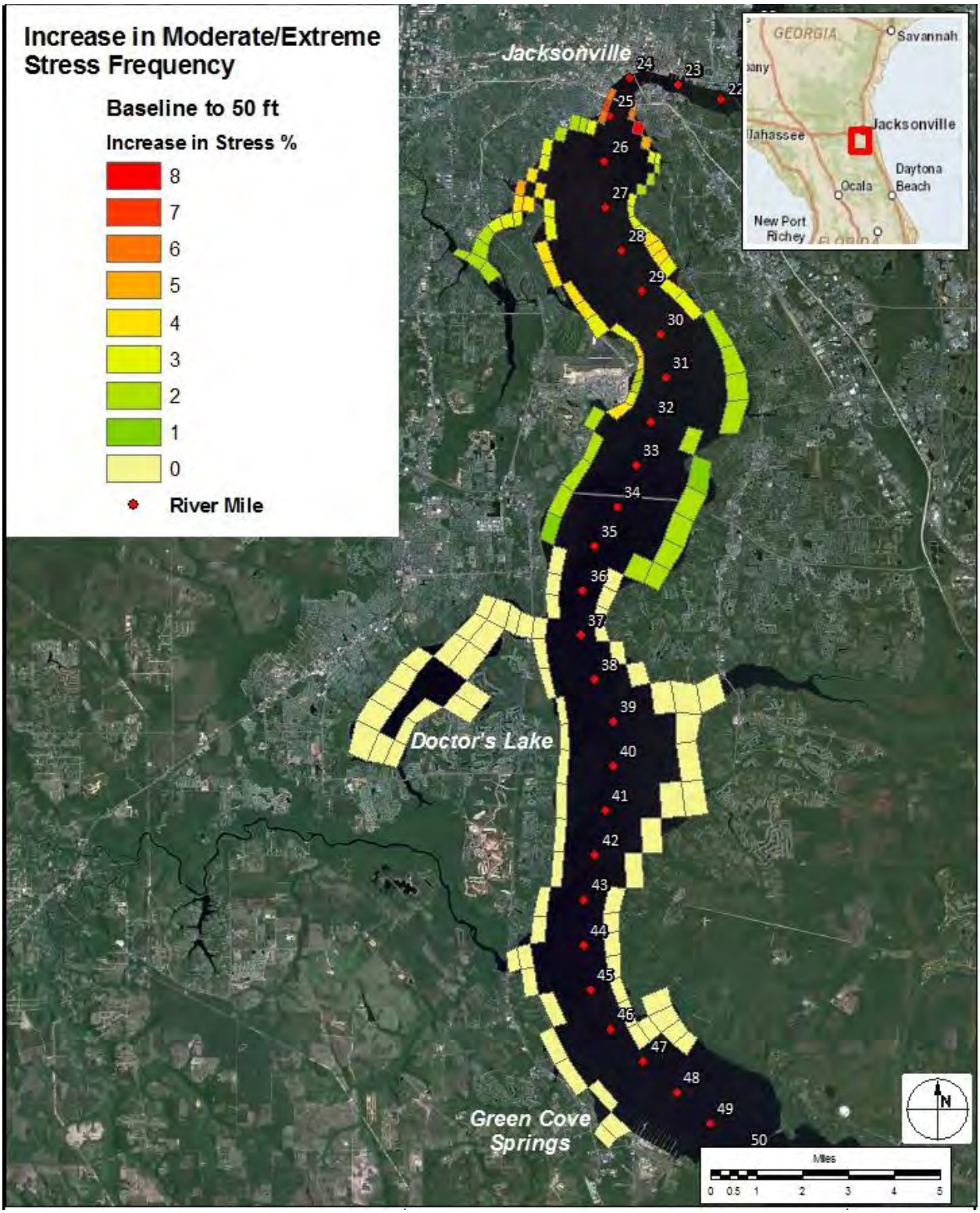


**Figure 3.9** Increase in Moderate/Extreme SAV Stress — Baseline to 50-ft Project

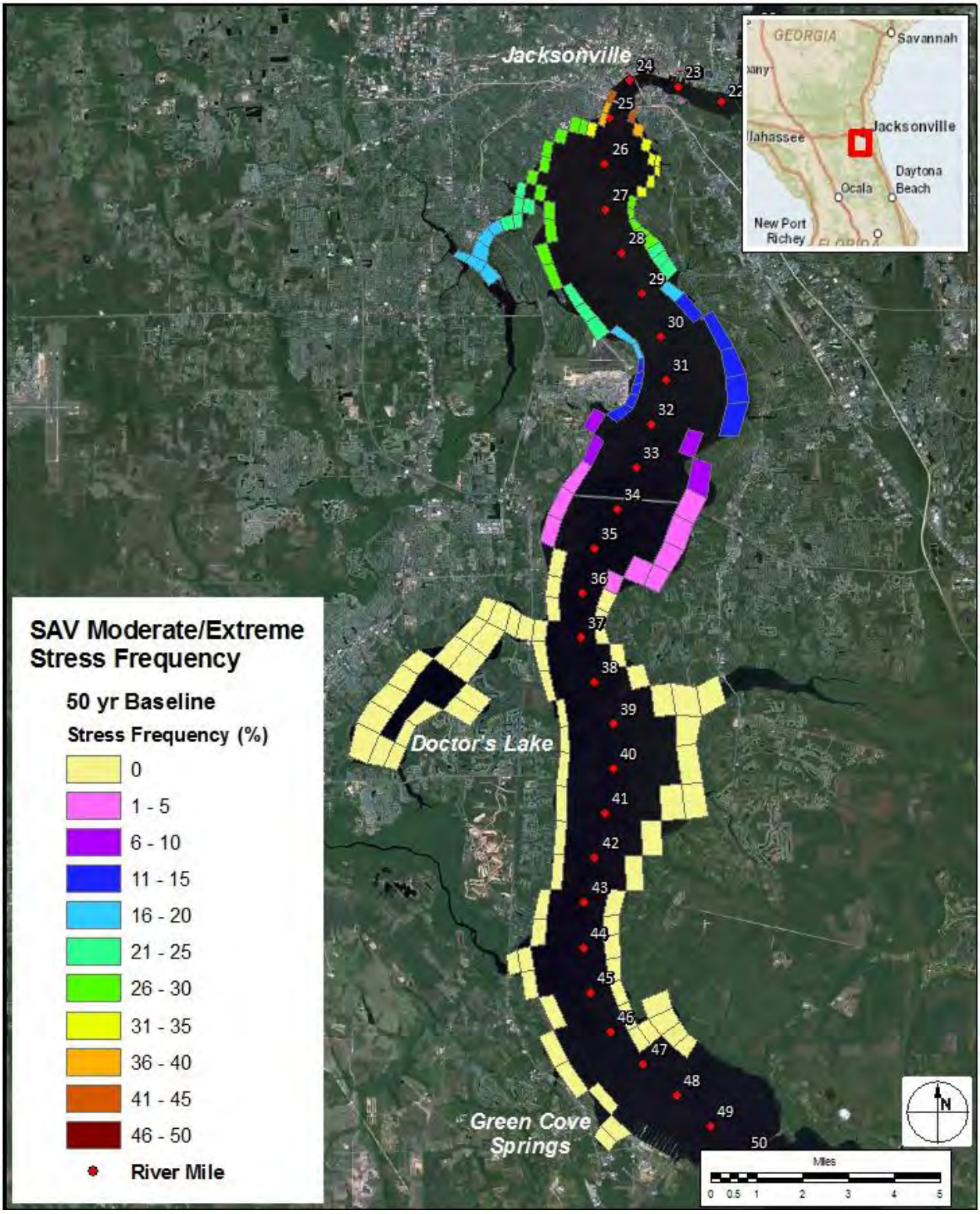


**Figure 3.10** Frequency of Moderate/Extreme SAV Stress — 50-yr, 40-ft Baseline

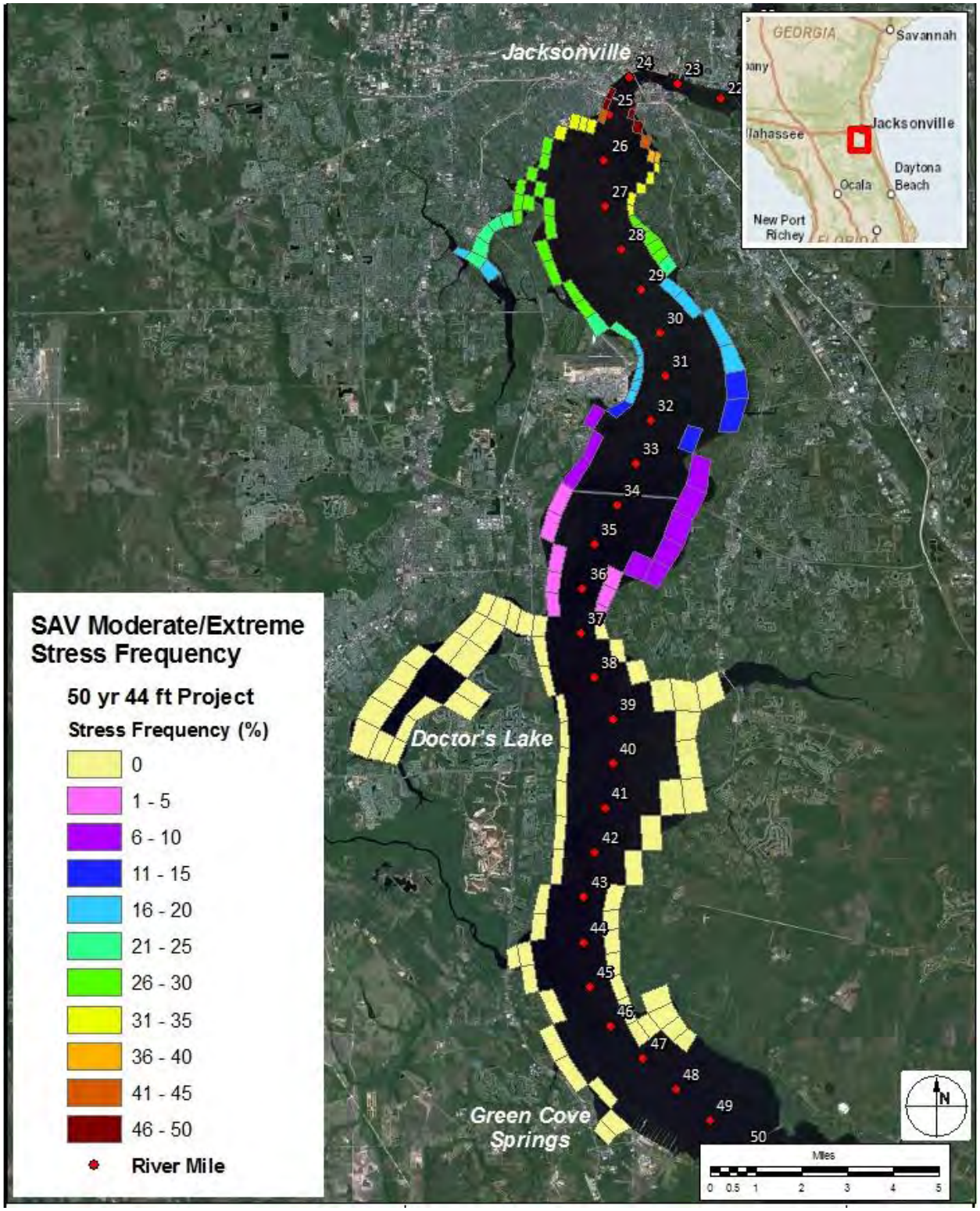


**Figure 3.11** Frequency of Moderate/Extreme SAV Stress — 50-yr 44-ft Project

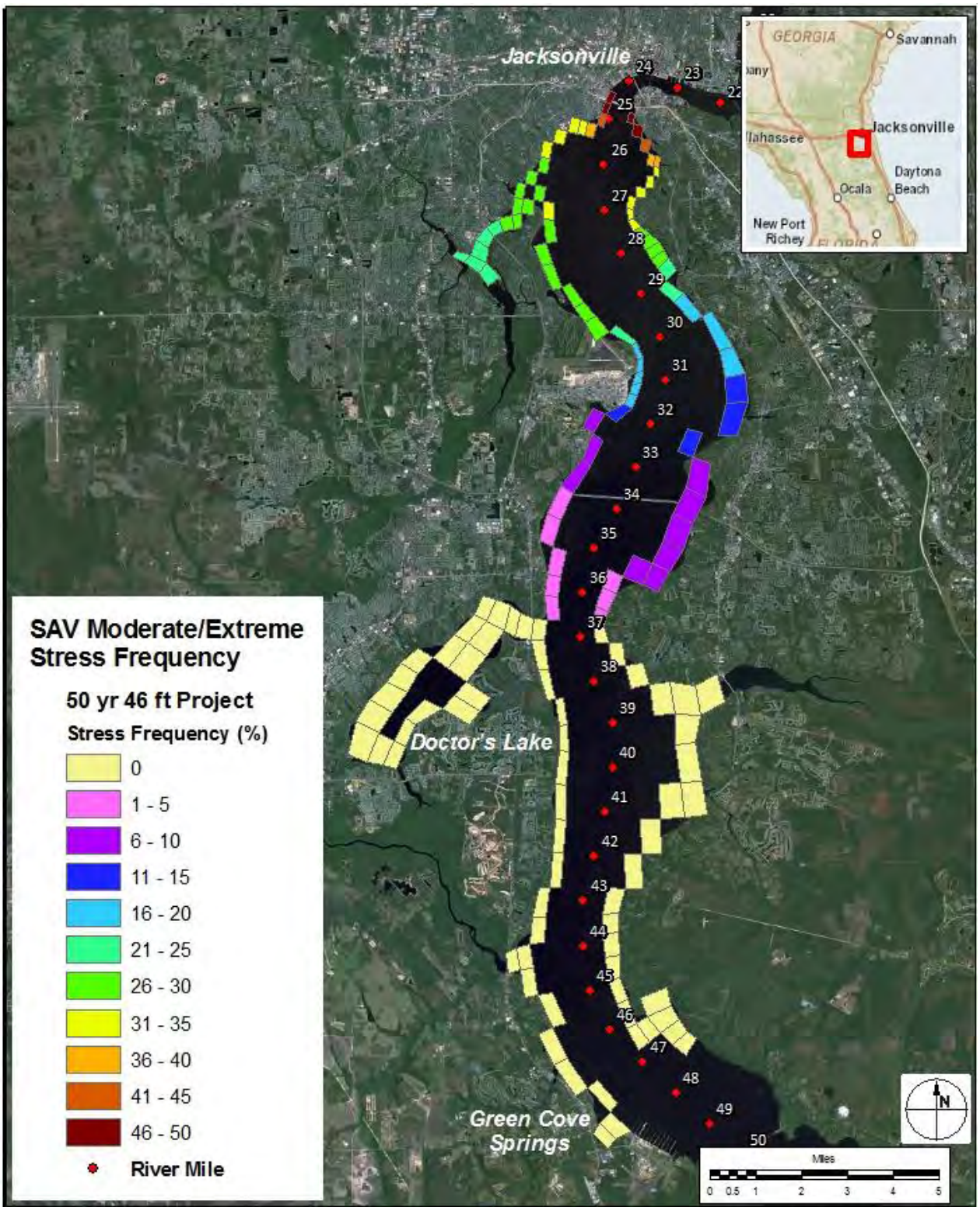


**Figure 3.12** Frequency of Moderate/Extreme SAV Stress — 50-yr, 46-ft Project

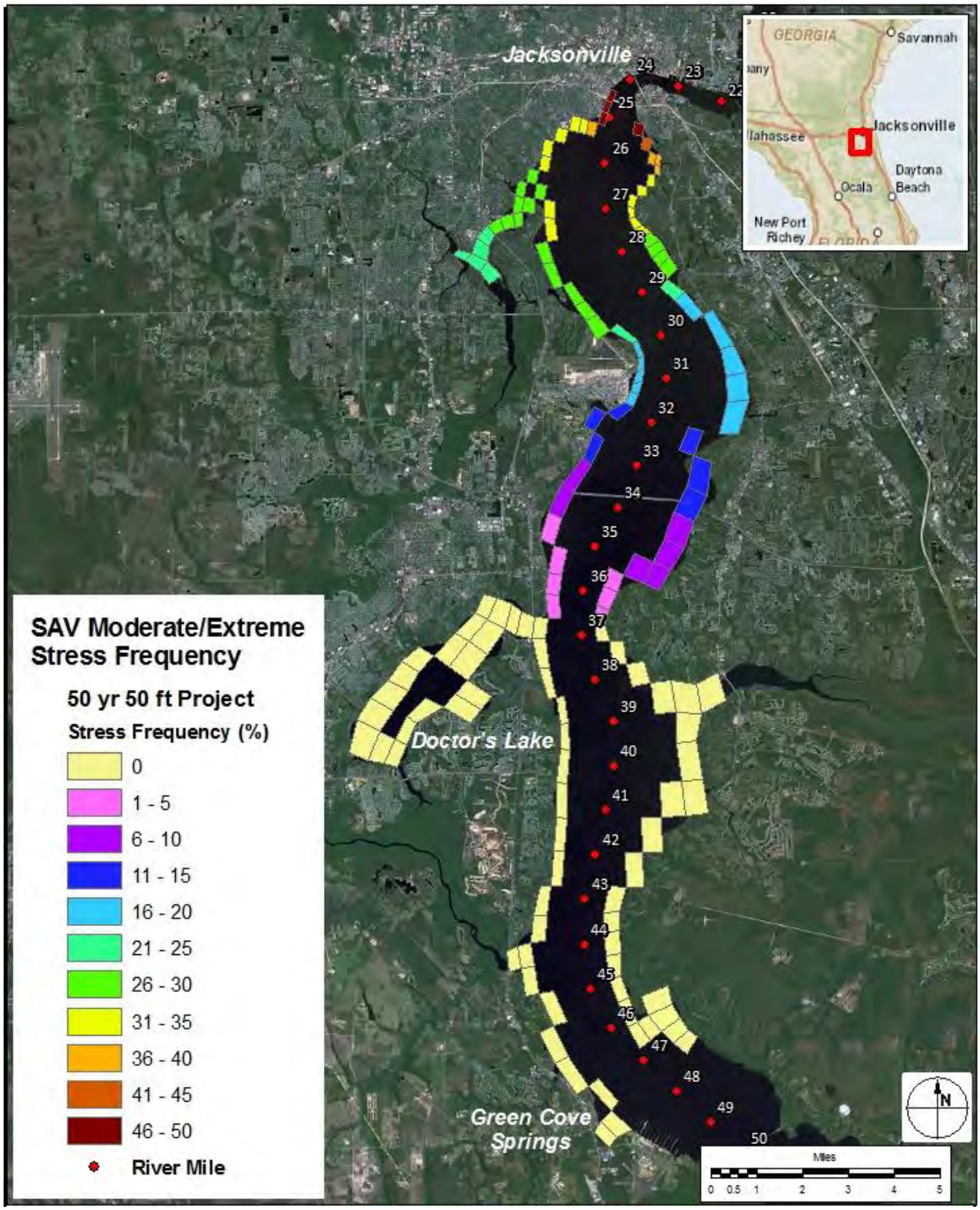


**Figure 3.13** Frequency of Moderate/Extreme SAV Stress — 50-yr, 50-ft Project

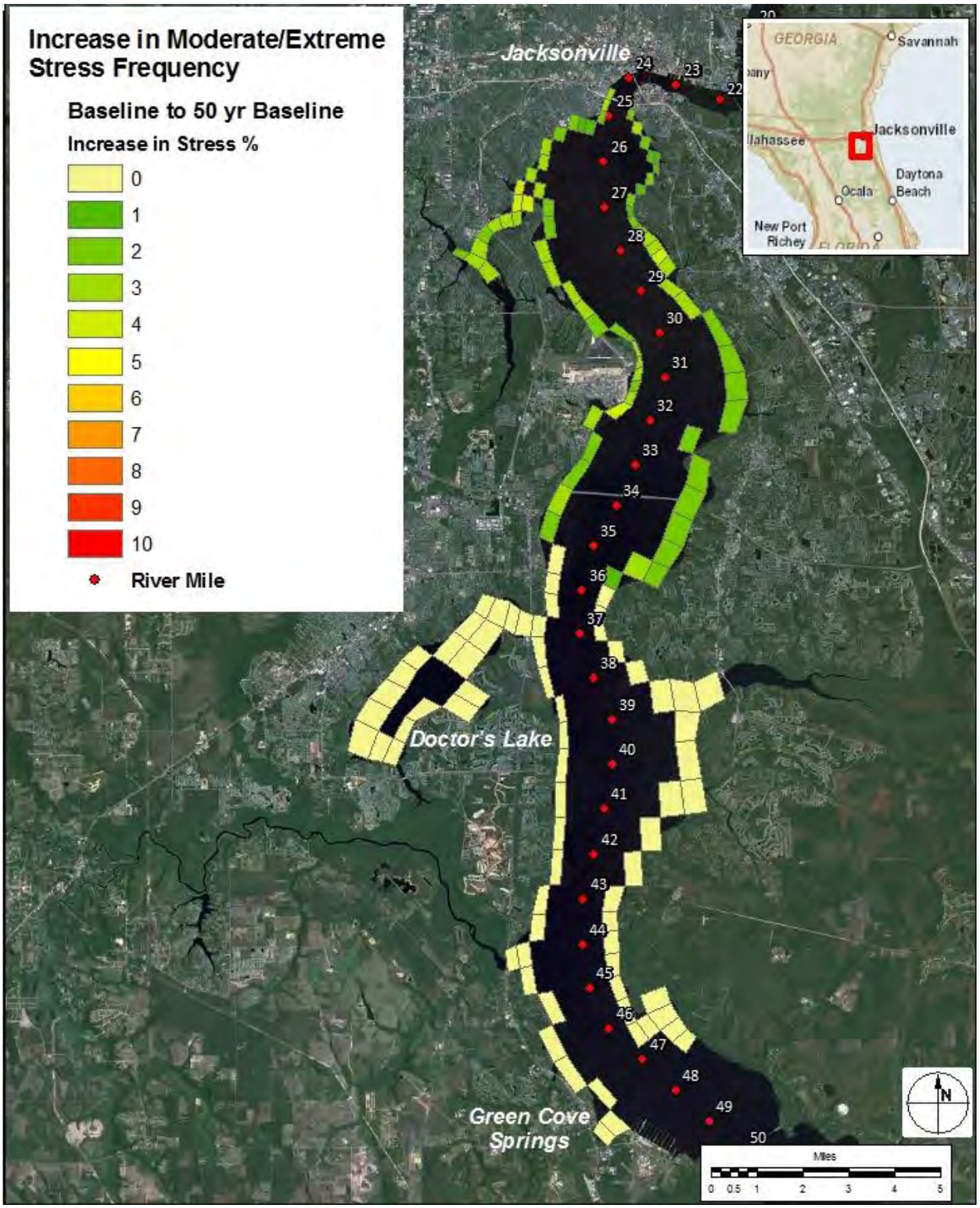


**Figure 3.14** Increase in Moderate/Extreme SAV Stress — Baseline to 50-yr Baseline

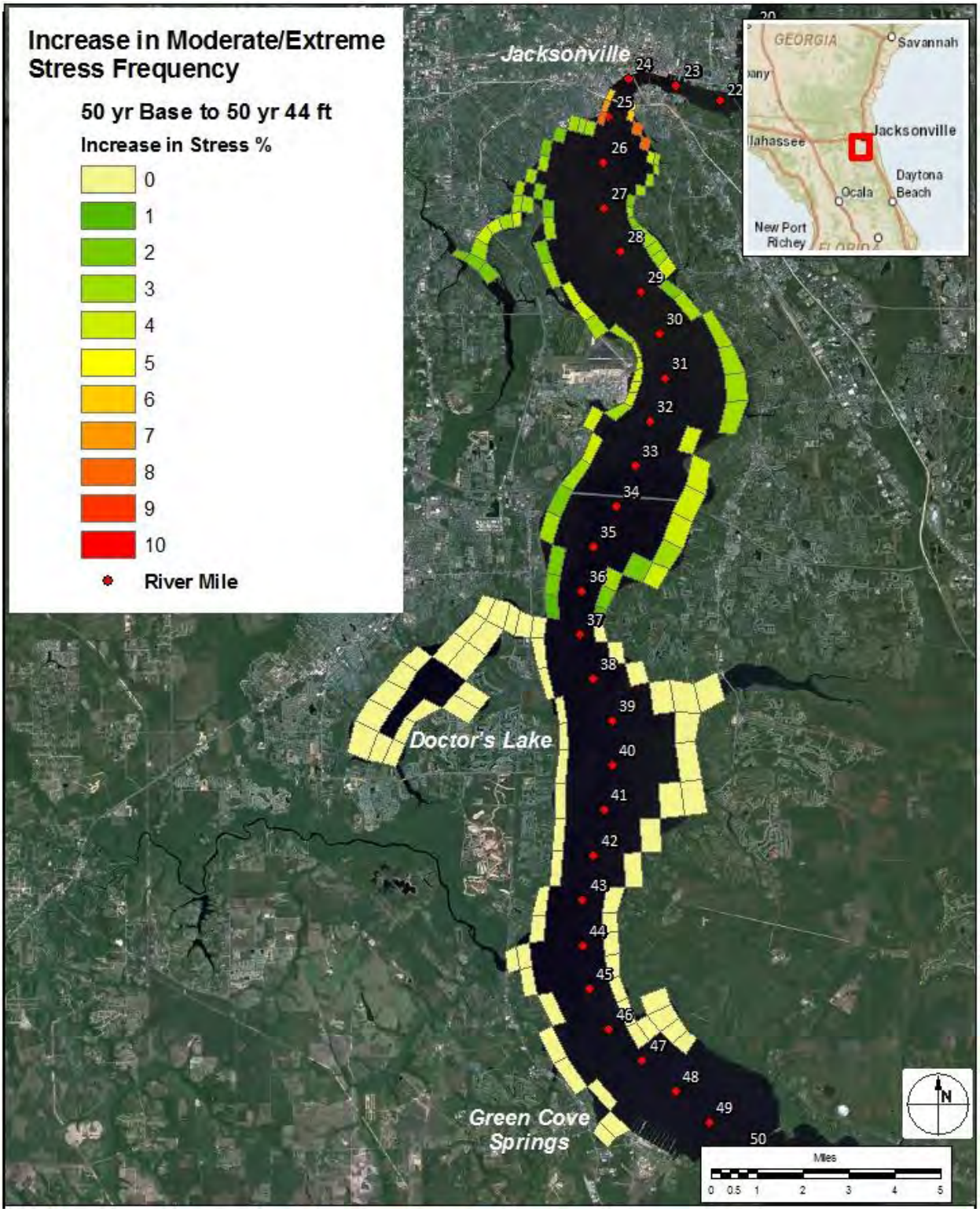


**Figure 3.15** Increase in Moderate/Extreme SAV Stress — 50-yr Baseline to 50-yr, 44-ft Project

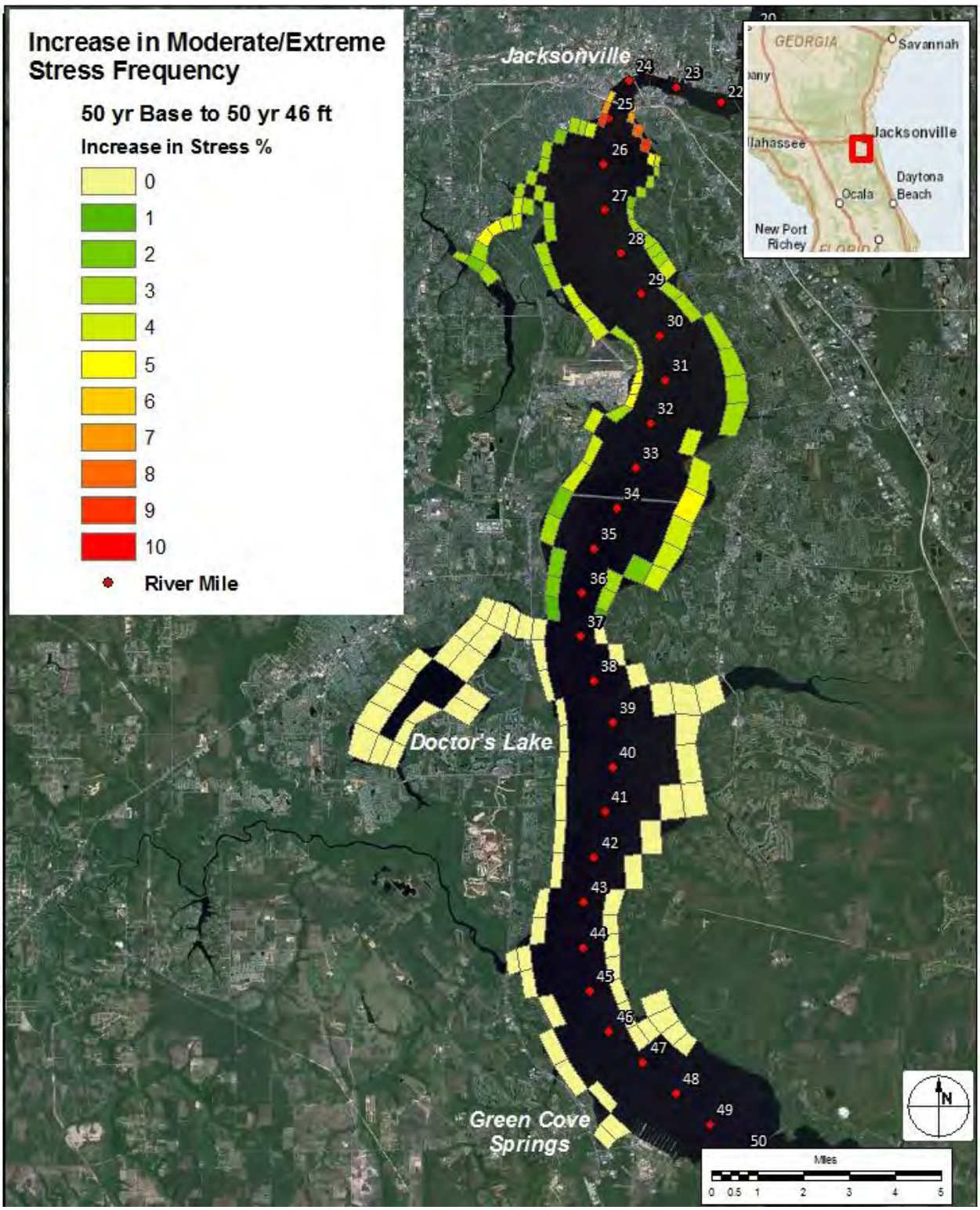


**Figure 3.16** Increase in Moderate/Extreme SAV Stress — 50-yr Baseline to 50-yr, 46-ft Project

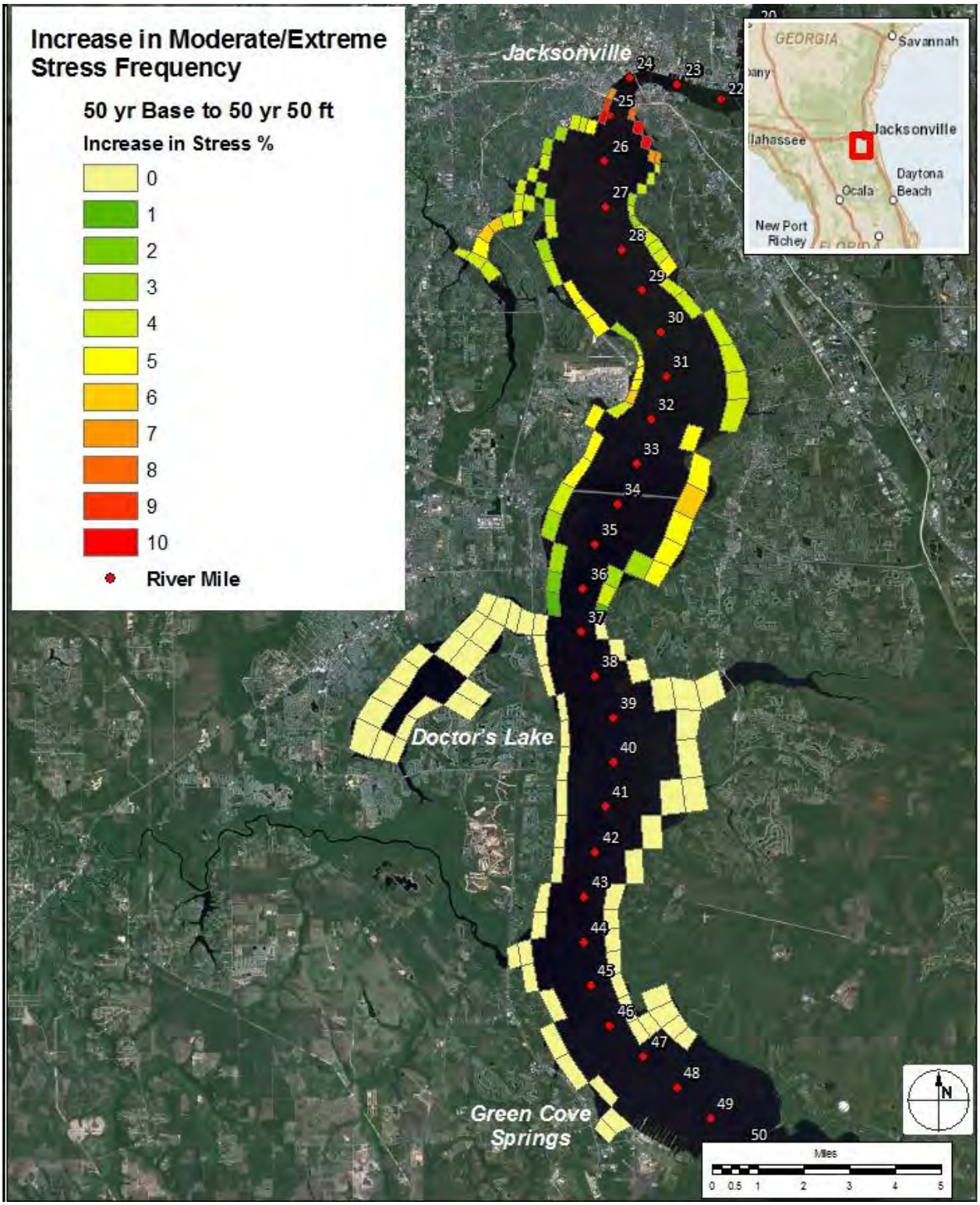


**Figure 3.17** Increase in Moderate/Extreme SAV Stress — 50-yr Baseline to 50-yr, 50-ft Project

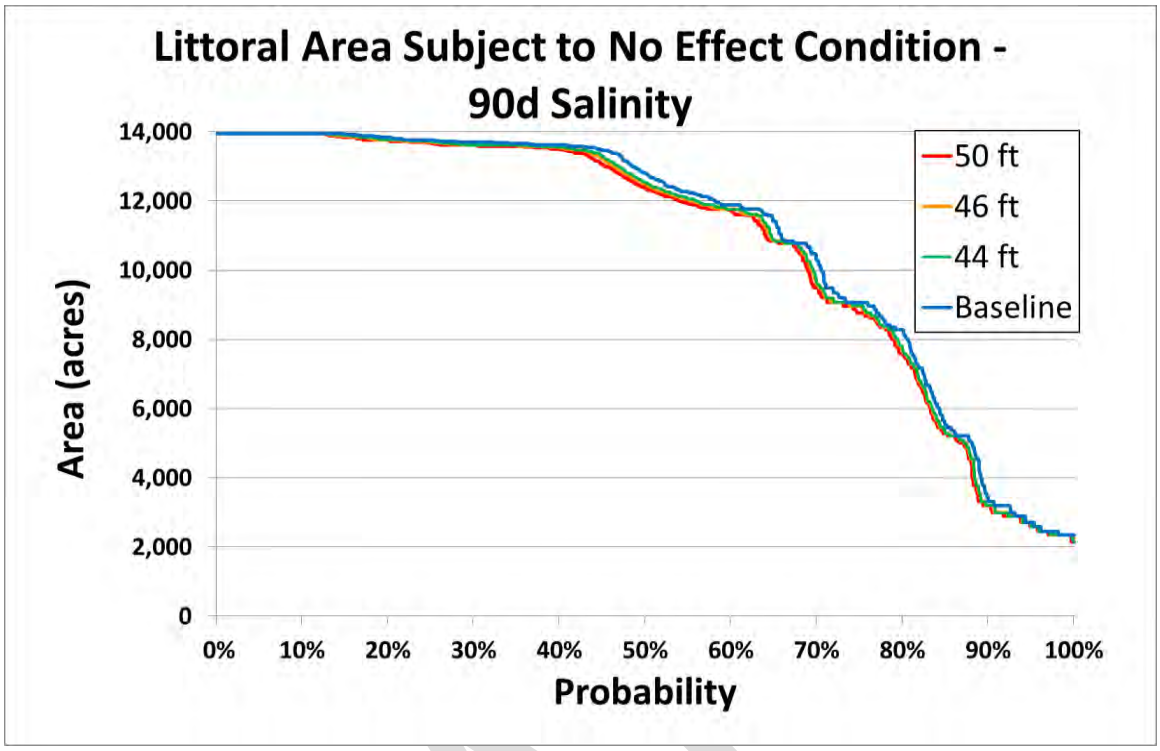


**Figure 3.18** Littoral Area Subject To No Stress Effect

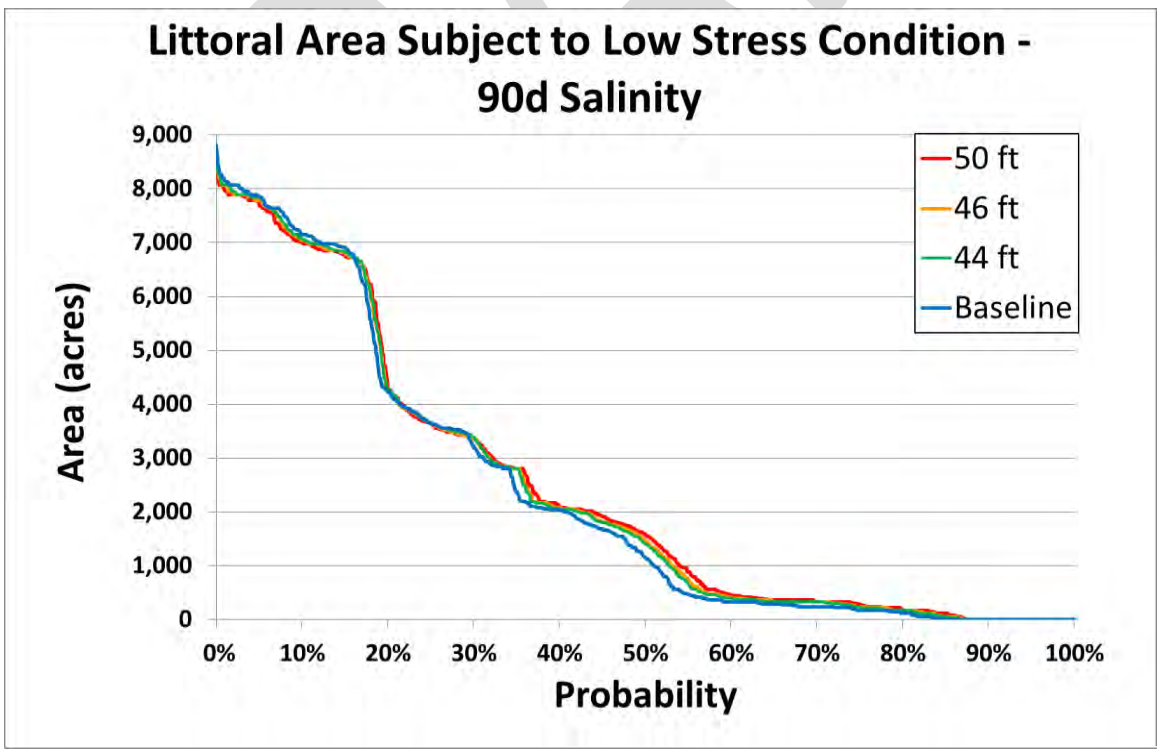


**Figure 3.19** Littoral Area Subject To Low Stress Condition

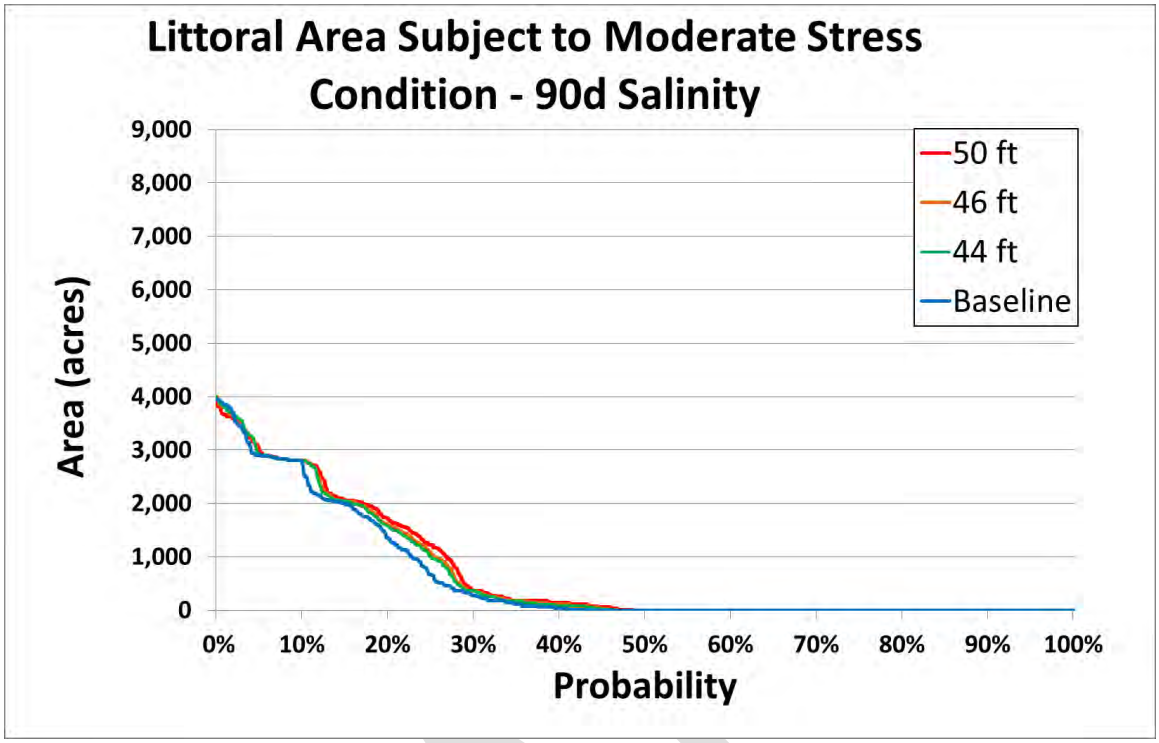


**Figure 3.20** Littoral Area Subject To Moderate Stress Condition

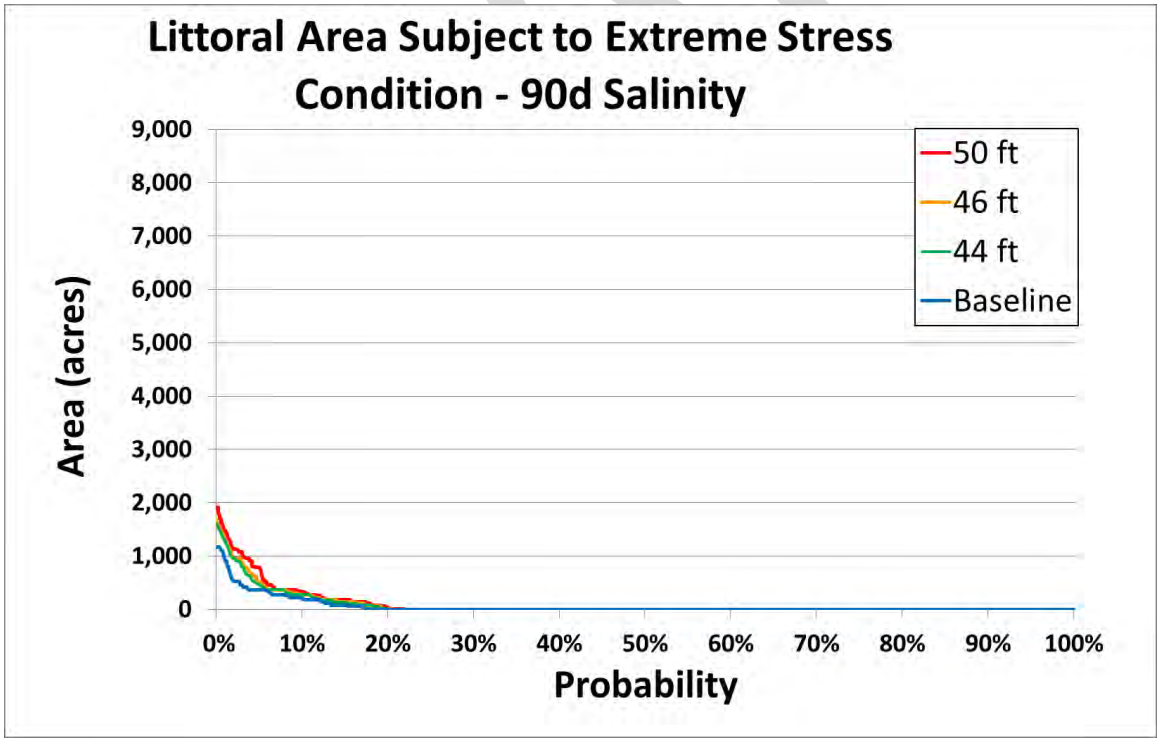


**Figure 3.21** Littoral area subject to extreme stress condition

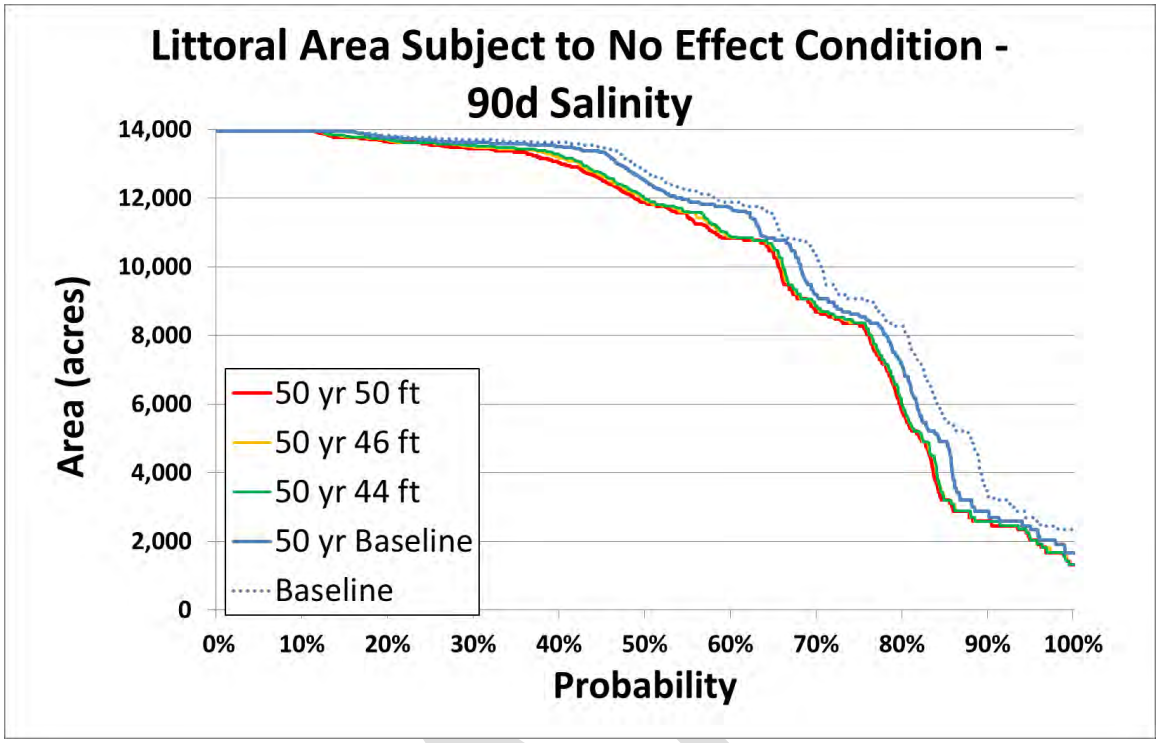


**Figure 3.22** Littoral Area Subject To No Stress Effect At 50-yr Condition

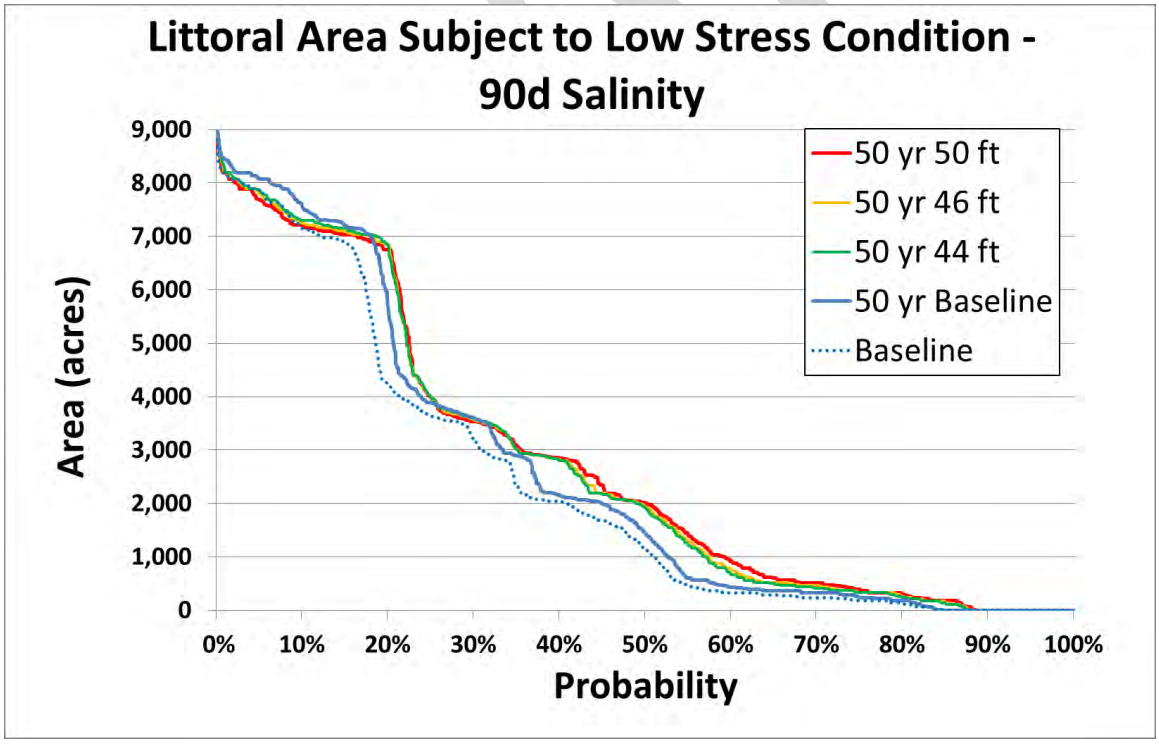


**Figure 3.23** Littoral Area Subject To Low Stress At 50-yr Condition

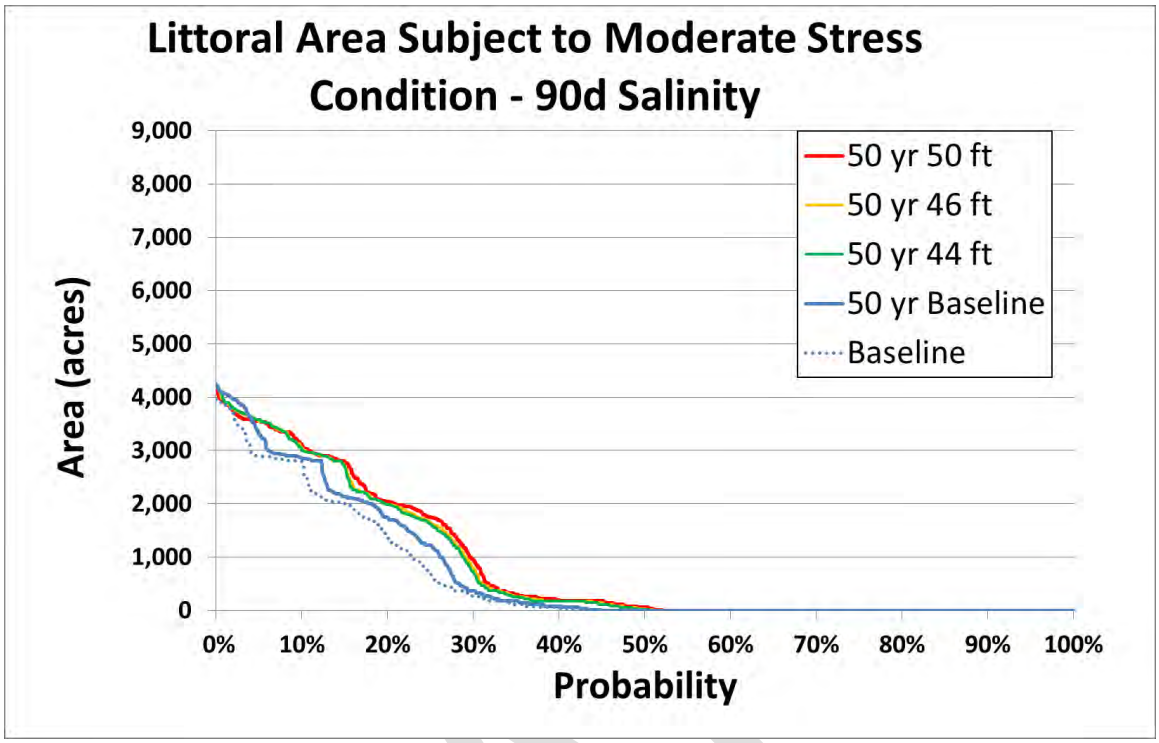


**Figure 3.24** Littoral Area Subject To Moderate Stress At 50-yr Condition

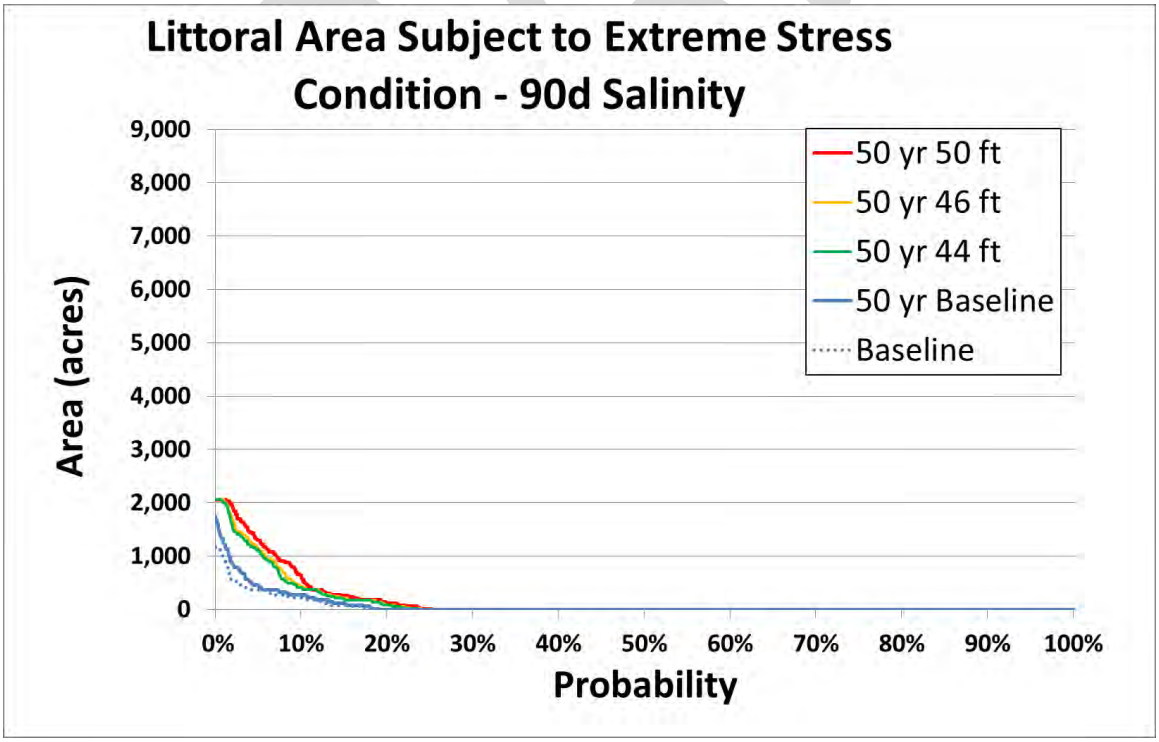


**Figure 3.25** Littoral Area Subject To Extreme Stress At 50-yr Condition

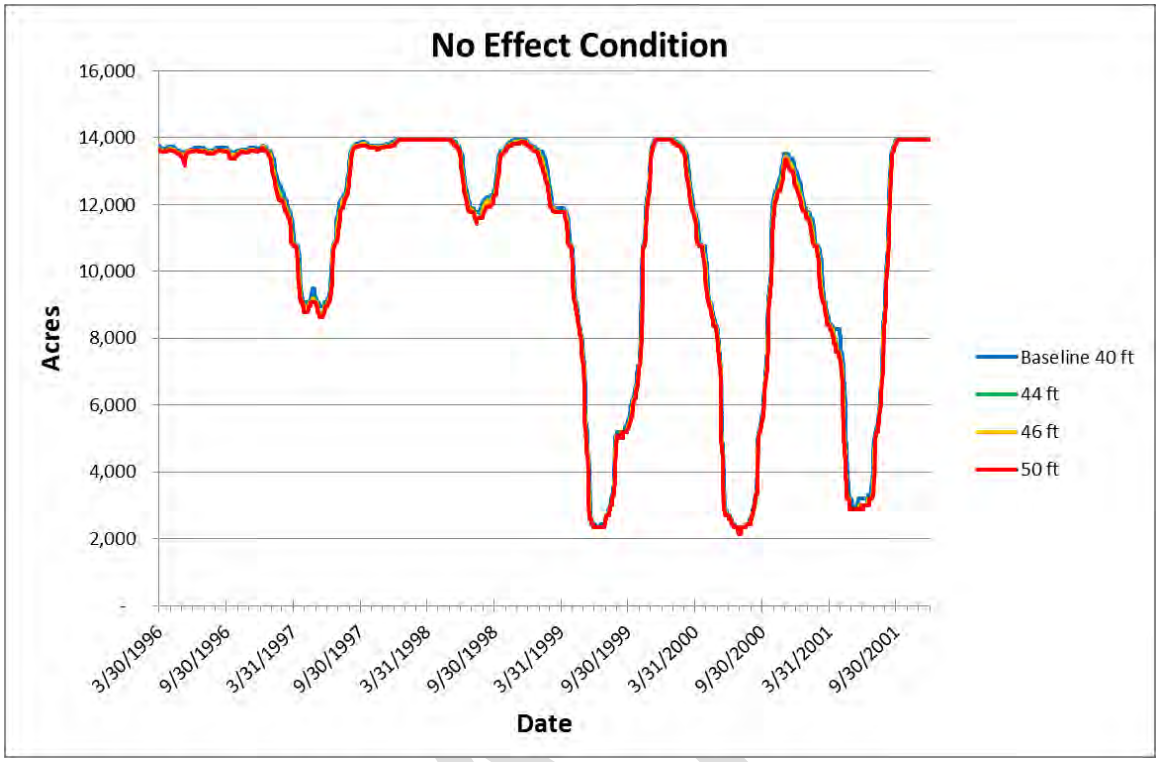


**Figure 3.26** Temporal Distribution of No Stress Effect

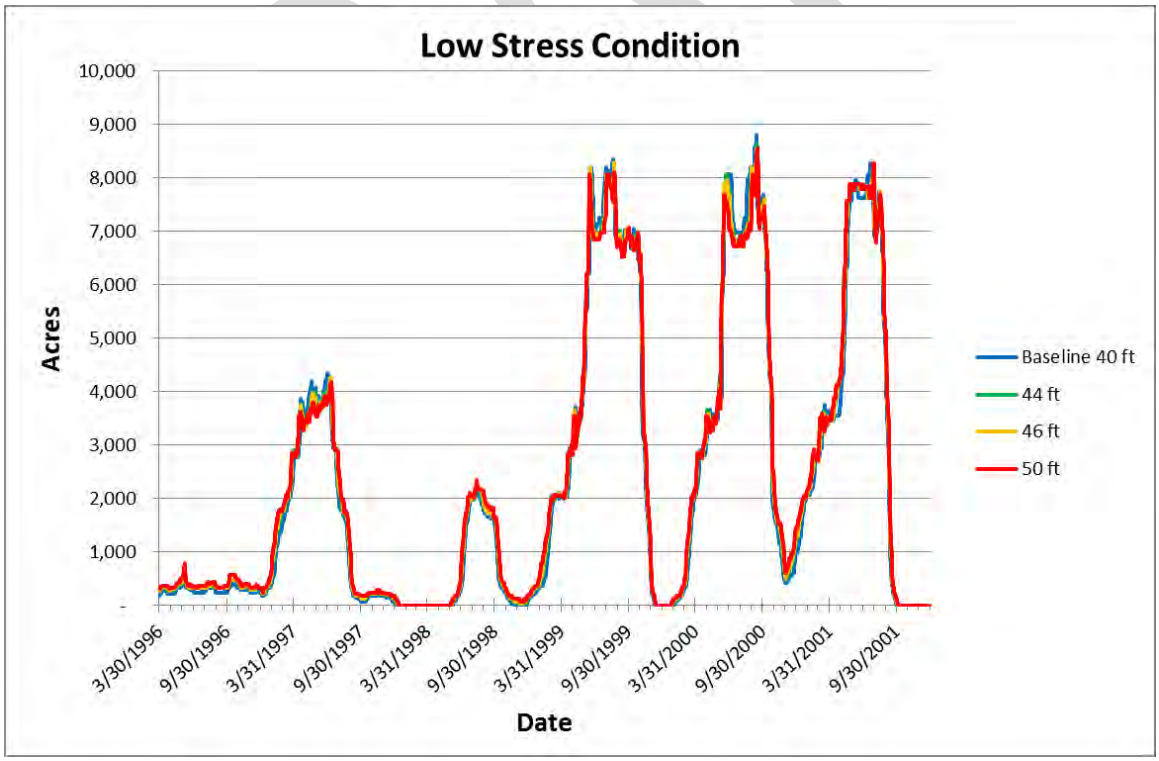


**Figure 3.27** Temporal Distribution of Low Stress

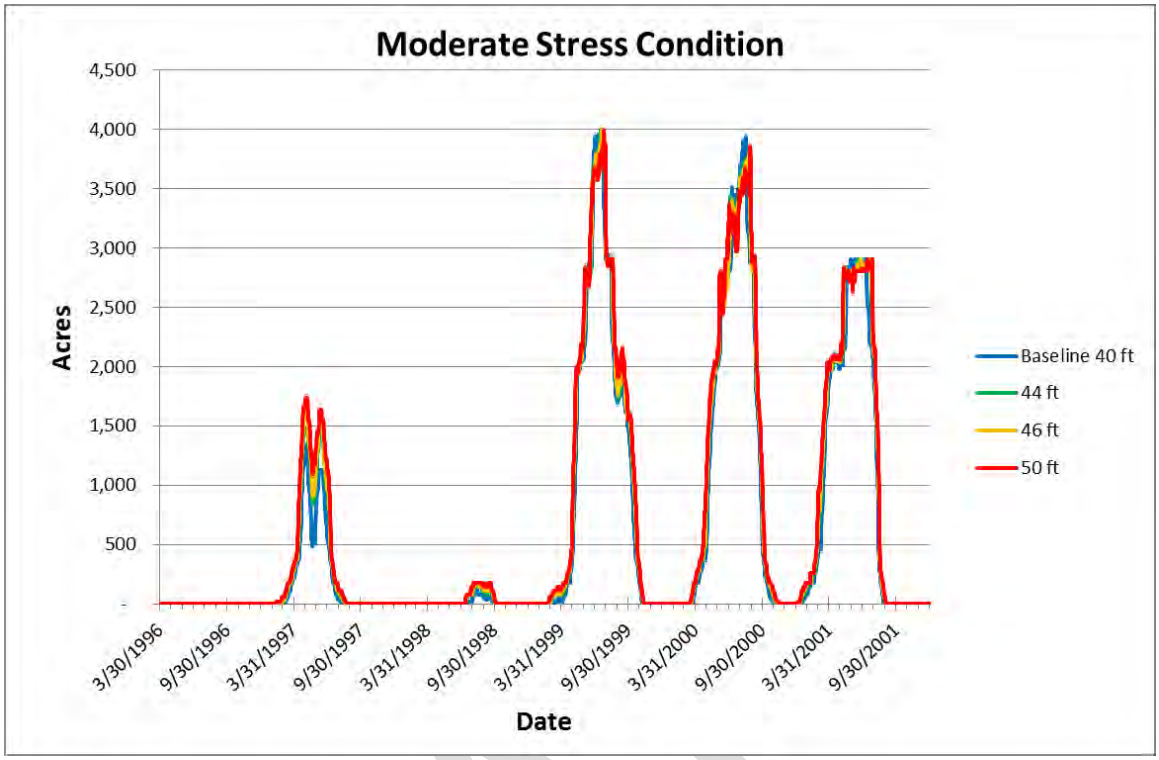


**Figure 3.28** Temporal Distribution of Moderate Stress

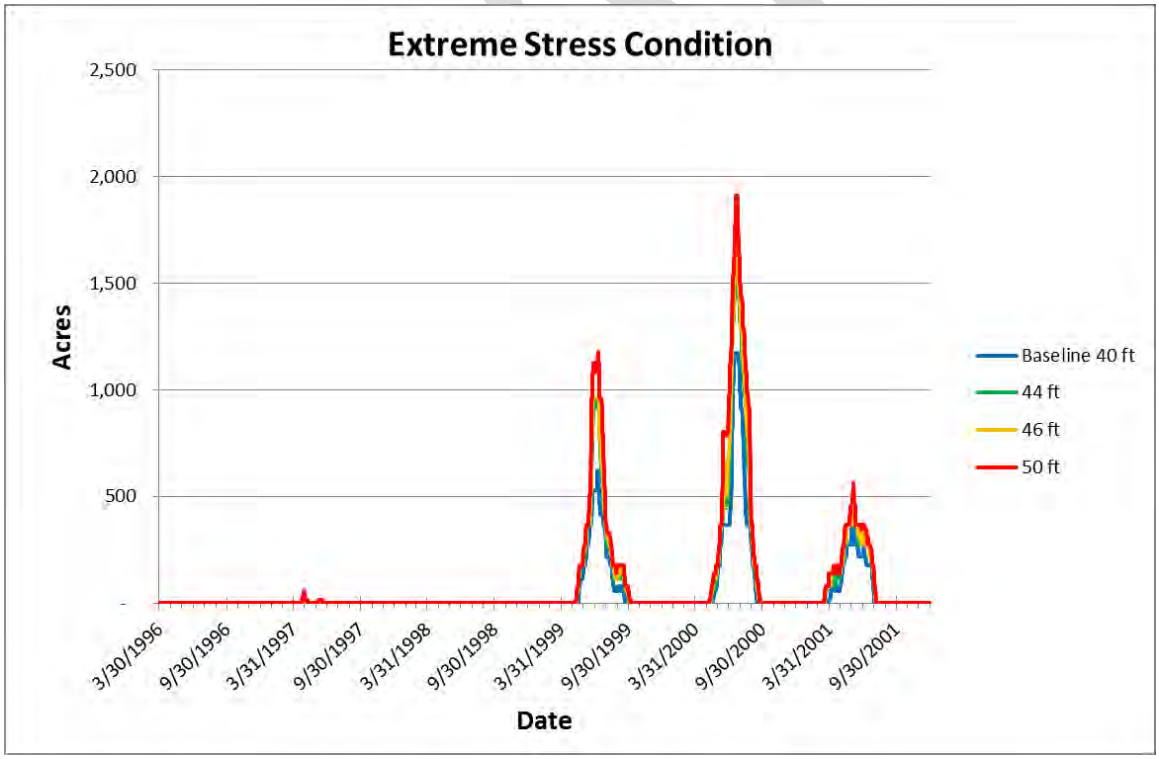


**Figure 3.29** Temporal Distribution of Extreme Stress

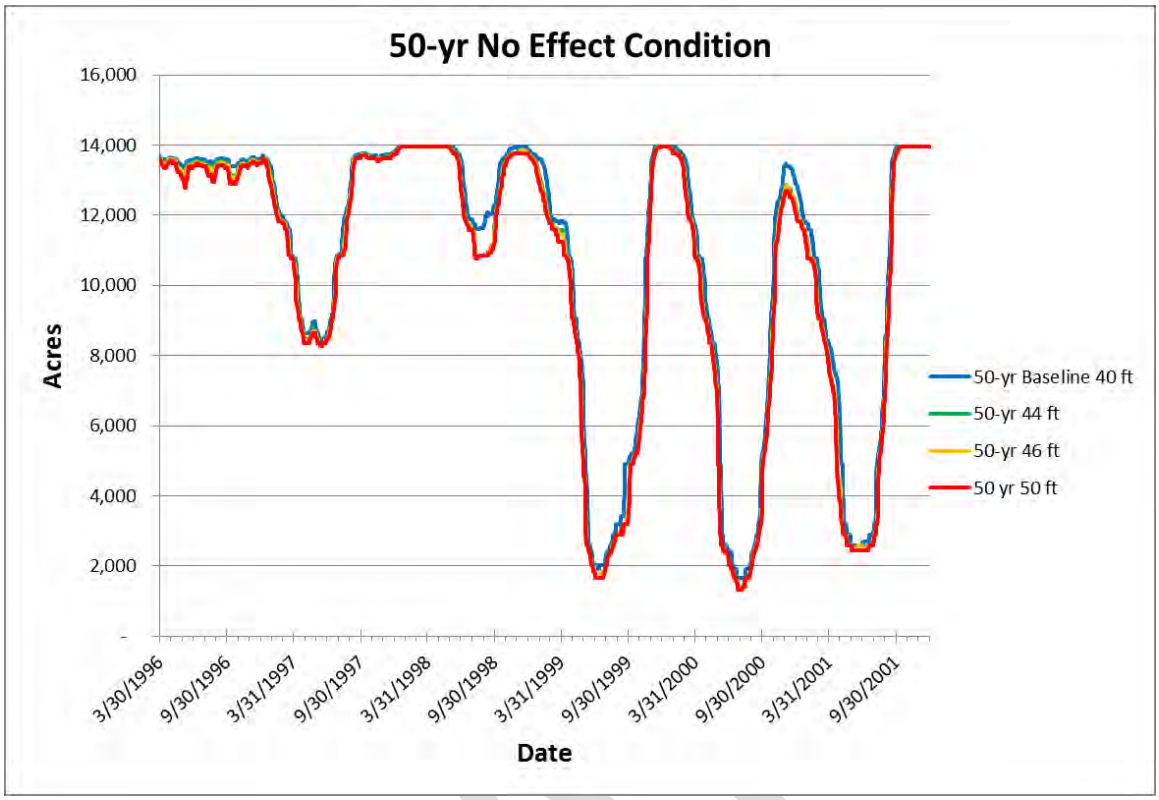


**Figure 3.30** Temporal Distribution of No Stress Effect For 50-yr Condition

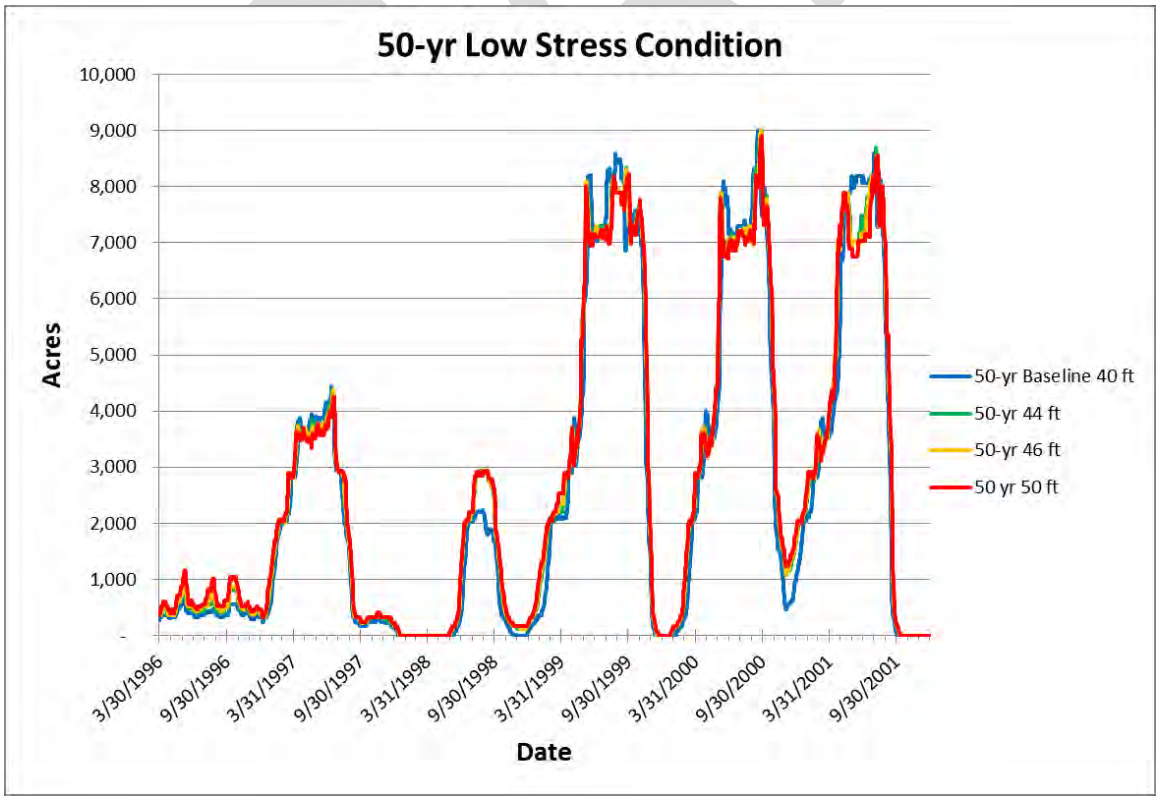


**Figure 3.31** Temporal Distribution of Low Stress For 50-yr Condition

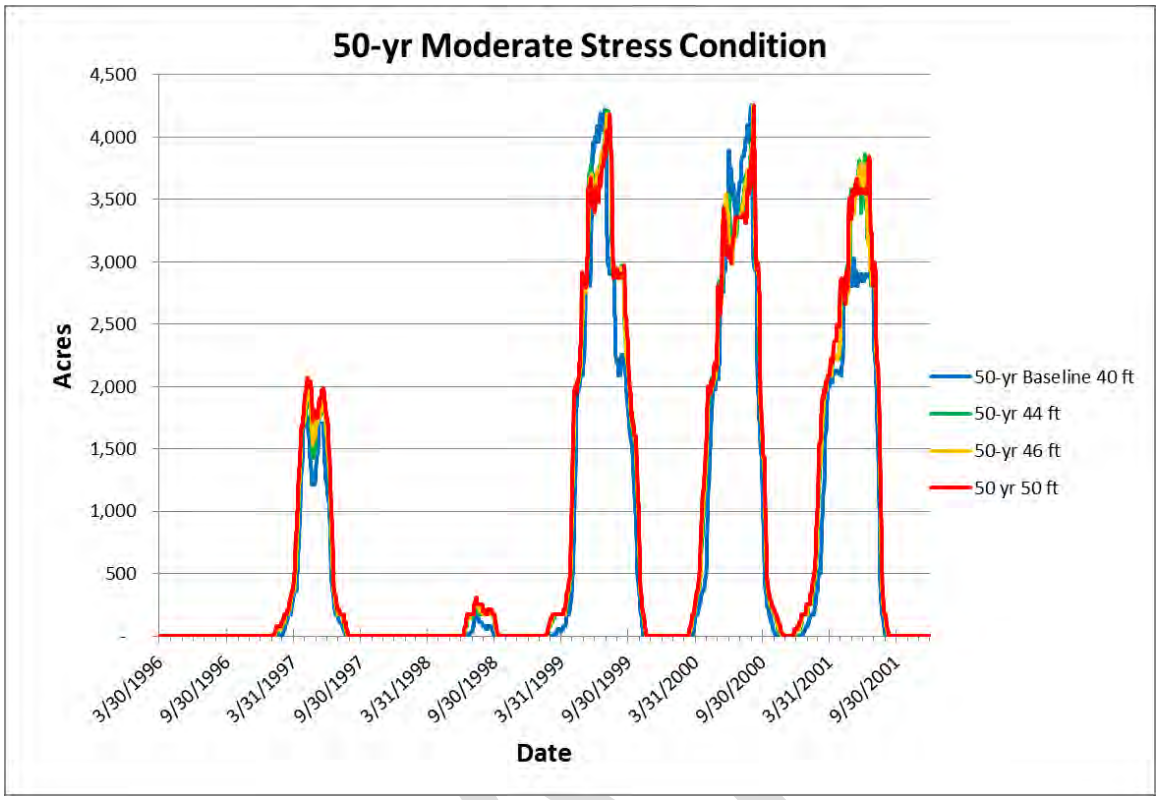


**Figure 3.32** Temporal Distribution of Moderate Stress For 50-yr Condition

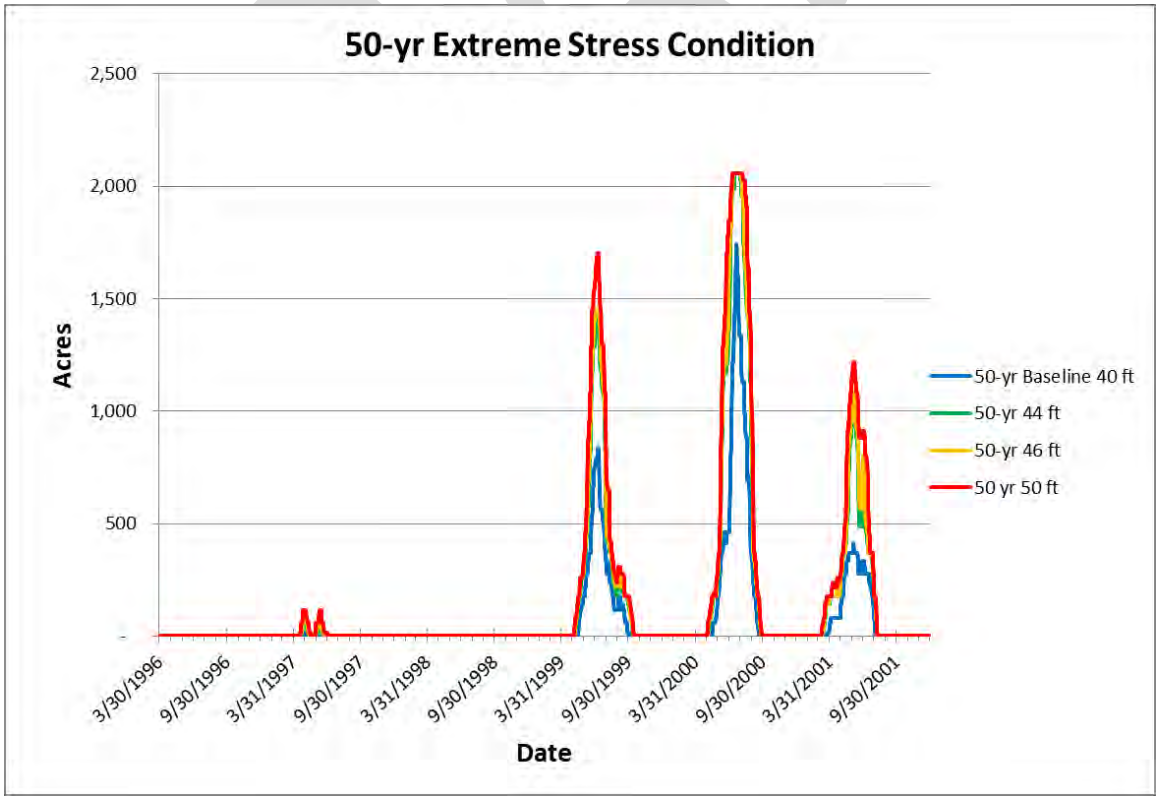


**Figure 3.33** Temporal Distribution of Extreme Stress For 50-yr Condition

## 4.0 WETLANDS

The District's wetland vegetation working group for the WSIS evaluated potential effects of water withdrawal on floodplain wetland vegetation communities of the St. Johns River. Kinser et al. (2012) describe the working group's wetland vegetation evaluation and development of the wetland evaluation models. This review summarizes pertinent content of the Kinser et al. (2012) WSIS wetlands report and identifies the models' applicability for evaluation of effects of the Jacksonville Harbor deepening project.

Wetlands in the LSJR range from tidal salt marsh with salinities near ocean concentrations to freshwater marsh and hardwood swamps. In the Jacksonville Harbor Deepening GRR-2 study area (River Segments 1 – 3) salinity appears a major factor in determining wetland character. Some wetland areas near the river appear in a state of transition from freshwater to brackish or saline conditions as evidenced by the appearance of salt tolerant vegetation in areas that were once freshwater swamp. In contrast, some areas in tributaries appear to have become fresher with increasing stormwater runoff (Kinser et al., 2012).

### 4.1 WSIS Wetlands Model

The WSIS wetland vegetation working group determined that the most important potential effects of water withdrawal on wetland vegetation communities are related to changes in temporal and spatial patterns of inundation and water depth in the middle and upper parts of the river and to movement of salinity concentrations in the lower part of the river.

The working group focused its attention on evaluation of the hydrologic effects in River Segments 5 – 8 where water withdrawal could have the greatest influence on water surface elevation. Because water withdrawal scenarios did not substantially affect water elevation in the lower segments, the group did not assess hydrologic effects on wetlands in River Segments 1 – 4. The Jacksonville Harbor deepening project is unlikely to affect any of the areas encompassed by these analyses for River Segments 5 – 8. The WSIS assessments in these segments are not, therefore, pertinent to the deepening project Jacksonville Harbor Deepening GRR-2 ecological evaluation.

The WSIS wetlands group focused its evaluation of salinity effects on river kilometer 40 to kilometer 80 which corresponds to River Segment 2 and the downstream end of Segment 3 (north of the Shands Bridge). The group determined that the normally high salinity in River Segment 1 limits wetlands to estuarine salt marsh communities unlikely affected by any salinity changes that would occur under water withdrawal scenarios. Consequently, the group did not evaluate marshes in Segment 1.

The SJRWMD wetlands group selected the Ortega River as the model system from which to derive a tool for evaluation of salinity effects in River Segments 2 and 3. The group conducted a field sampling campaign to obtain wetland vegetation and soil salinity data within a series of plots along the Ortega River. From these data, the group identified five wetland community types — freshwater swamp, tidal swamp, lower tidal swamp, intermediate marsh, and sand cordgrass marsh. Transition from one community to another occurred in predictable fashion along a salinity gradient which allowed identification of soil salinity "break points" between community types. Comparing soil salinities obtained during the field campaign to 95$^{th}$ percentile salinities generated by EFDC model simulations, the group found good correlation between the salinity pairs and therefore translated soil salinity break points to river salinity break points. Table 4.1 lists the wetland community soil salinity and river salinity break points.

**Table 4.1** WSIS Wetland Community Transition Salinity Break Points

| | **Salinity Break Points (PSU)** | |
|---|---|---|
| **Wetland Community Transition** | **Soil** | **River** |
| Hardwood swamp/Tidal swamp | 0.47 | 3.32 |
| Tidal swamp/Lower tidal swamp | 1.53 | 4.13 |
| Lower tidal swamp/Intermediate marsh | 2.44 | 4.93 |
| Intermediate marsh/Sand cordgrass marsh | 3.41 | 5.77 |

From the results of EFDC model simulations of baseline and water withdrawal scenarios, the group plotted the river salinity concentration lines in the main stem of the river and considered changes in break line position under different scenarios indicative of potential shifts in the wetland community boundaries. Figure 4.1[5] shows the locations of the salinity breakpoints (salinities that distinguish different wetland communities) for the WSIS study baseline simulation (1996 – 2005). The figure also shows the locations of saltmarsh and freshwater wetlands as mapped by Florida Land Use, Cover, and Forms Classification System (FLUCCS) codes in the SJRWMD 2009 land use GIS data set.

The methods applied by SJRWMD for assessment of wetlands are applicable in Segment 2 and Segment 3. We expect that the salinities in Segment 1 within the model domain are above the highest salinity threshold in the SJRWMD model. If the model indicates salinity changes in Segment 1, those

[5] Figures referenced in this chapter appear at the end of the chapter.

changes could potentially affect the distribution of wetland communities at the upstream end of the marshes, but those areas are outside of the model domain and outside of the river segment for which the WSIS tool was developed.

### 4.2 Application of the WSIS Wetlands Model for Jacksonville Harbor Deepening GRR-2 Ecological Effects Evaluation

Initial review of Jacksonville Harbor Deepening GRR-2 EFDC simulation results indicated that the salinity changes due to the harbor deepening would not reach Green Cove Springs. We therefore used salinity values in the same 140-cell shoreline set (Fuller Warren Bridge to Green Cove Springs) used for the SAV evaluation (see Figure 3.2 in Chapter 3). From the EFDC model results, we obtained vertically averaged, daily salinity values for each cell. Following the WSIS approach, we calculated the 95$^{th}$ percentile salinity value for each cell for the baseline six-year simulation period. Figure 4.2 shows the results, classifying each cell according to WSIS wetland type salinity ranges as defined by the breakpoints.

Examination of Figure 4.2 suggested that we should not apply the WSIS wetland salinity breakpoints to the Jacksonville Harbor Deepening GRR-2 EFDC model results. Relative to the WSIS baseline breakpoint locations, the Jacksonville Harbor Deepening GRR-2 baseline salinities placed the breakpoints several miles upstream. For example, whereas the WSIS 5.77 PSU breakpoint occurs near river mile 34 (Buckman Bridge), the Jacksonville Harbor Deepening GRR-2 baseline 5.77 PSU breakpoint occurs nine miles upstream near river mile 43. The WSIS 4.93 PSU breakpoint occurs at river mile 36 whereas the Jacksonville Harbor Deepening GRR-2 4.93 breakpoint occurs at seven miles upstream at river mile 43. The upstream shift of the salinity breakpoints for the Jacksonville Harbor Deepening GRR-2 baseline simulation is likely due to the shorter simulation period (6 years for Jacksonville Harbor Deepening GRR-2 study; 10 years for WSIS study), the influence of 3 very dry years in the Jacksonville Harbor Deepening GRR-2 simulation period, and the Mayport and Mile Point channel cross section modifications. Additionally, examination of the WSIS 95$^{th}$ percentile wetland breakpoint line locations in relation to the 2009 mapped wetlands shows that the lines lie several miles upstream of the most upstream mapped saltmarsh wetlands along the main stem of the river. Because the WSIS study used a different wetland classification system than the 2009 land use data set, we could not assess the suitability of the WSIS salinity breakpoints for estimating wetland transitions along the main stem. Based on the above results, we concluded that we should not use the 95$^{th}$ percentile salinity breakpoints to predict Jacksonville Harbor deepening salinity impacts on wetlands.

To explore the applicability of using the WSIS wetland community transition breakpoints with another measure of salinity, we used GIS software to calculate and plot the position of four breakpoint lines based on average salinity for the six-year baseline simulation and for the 44-ft, 46-ft, and 50-ft project simulations. Figure 4.3 shows position of the breakpoint lines for the baseline and 50-ft project. The breakpoints based on average salinity moved downstream relative to the 95$^{th}$ percentile breakpoints. The most saline breakpoint, 5.77 PSU, located at river mile 29 near the north end of NAS Jacksonville and about five miles upstream of the WSIS 5.77 PSU breakpoint. In the Ortega River, the 5.77 PSU location roughly coincided with the most upstream salt marsh mapped in the 2009 SJRWMD land use data set. Each of the remaining breakpoints also shifted downstream relative to the 95$^{th}$ percentile breakpoints. Table 4.2 lists the locations of the salinity breakpoints based on average salinity for each of the simulated project alternatives.

**Table 4.2** Salinity Breakpoint[1] Locations

| Wetland Community | Salinity Break Point | River Mile | | | | | | | |
|---|---|---|---|---|---|---|---|---|---|
| | | Baseline 40 ft | 44 ft | 46 ft | 50 ft | 50-yr 40 ft Baseline | 50-yr 44 ft | 50-yr 46 ft | 50 yr 50 ft |
| Freshwater swamp/ Freshwater tidal swamp | 3.21 | 34.8 | 35.4 | 35.4 | 35.4 | 35.6 | 36.4 | 36.5 | 36.6 |
| Freshwater tidal swamp/ Lower tidal swamp | 4.13 | 31.8 | 31.9 | 32.0 | 32.0 | 32.1 | 33.1 | 33.2 | 33.7 |
| Lower tidal swamp/ Intermediate marsh | 4.93 | 29.7 | 29.9 | 30.0 | 30.2 | 30.2 | 31.8 | 31.8 | 31.9 |
| Intermediate Marsh/ Sand cordgrass marsh | 5.77 | 28.9 | 29.2 | 29.2 | 29.3 | 29.3 | 29.7 | 29.8 | 29.9 |

[1]Breakpoint based on average salinity of the six-year simulations

The simulated projects would move average salinity breakpoints varying distances upstream relative to the baseline condition (Table 4.3). The maximum breakpoint shifts occur with the 50-year, 50-ft project which moves breakpoints up to 1.7 miles upstream relative to the 50-year baseline.

While the information in Tables 4.2 and 4.3 may give an indication of the magnitude of spatial shift of salinity values affecting wetland vegetation, the specific locations of the breakpoints should not be used to predict the location of wetland impacts. Few fringing wetlands occur along the main stem of the

river from the Fuller Warren Bridge upstream to Doctors Lake. And, as noted by Kinser et al. (2012), wetlands that occur in this area (River Segment 2) presently exhibit signs of increasing salinity due perhaps to past river modifications and rising sea level. It is difficult, therefore to assess the validity of the salinity breakpoints, whether based on the 95th percentile or the average salinity, for prediction of channel deepening effects on wetland communities. Assessment of the breakpoints as a prediction tool is further complicated by the difference in WSIS wetland classification and the mapped wetlands based on FLUCCS codes. However, based on the FLUCCS mapping of large freshwater wetlands beginning in the vicinity of Doctors Lake and Julington Creek, the breakpoints generated from 95th percentile salinity appear to lie too far upstream while those based on average salinity may lie too far downstream.

**Table 4.3** Movement of Salinity Breakpoints[1]

| Wetland Community | Salinity Break Point | Distance (Miles) Moved Upstream from Baseline | | | | Distance (Miles) Moved Upstream from 50 yr Baseline | | |
|---|---|---|---|---|---|---|---|---|
| | | 44 ft | 46 ft | 50 ft | 50-yr 40 ft Baseline | 50-yr 44 ft | 50-yr 46 ft | 50 yr 50 ft |
| Freshwater swamp/ Freshwater tidal swamp | 3.21 | 0.6 | 0.6 | 0.6 | 0.8 | 0.8 | 0.9 | 1.0 |
| Freshwater tidal swamp/ Lower tidal swamp | 4.13 | 0.1 | 0.2 | 0.2 | 0.3 | 1.0 | 1.1 | 1.5 |
| Lower tidal swamp/ Intermediate marsh | 4.93 | 0.2 | 0.3 | 0.5 | 0.5 | 1.6 | 1.6 | 1.7 |
| Intermediate Marsh/ Sand cordgrass marsh | 5.77 | 0.3 | 0.3 | 0.4 | 0.3 | 0.4 | 0.5 | 0.6 |

[1]Breakpoint based on average salinity of the six-year simulations

To better understand the transition from salt marsh to freshwater wetlands in River Segment 2, we performed a limited field observation on December 19, 2012 to note presence or absence of salt-tolerant vegetation in wetlands fringing the river. During the field observation, we observed wetlands on both sides of the river from readily accessible shorelines from about a mile south of the Fuller Warren Bridge (river mile 26) to the Shands Bridge (river mile 50). We noted the presence of salt-tolerant vegetation as far south as Black Creek near river mile 44, several miles upstream of the FLUCCS-mapped salt marsh communities. The distribution of salt tolerant vegetation suggests that wetland communities along the

main stem of the river exhibit vegetation characteristics and transition from salt tolerant to freshwater vegetation that is determined by periodic influence of saline water excursions upstream and penetration of salt into the wetlands with high tides.

### 4.3 Recommendations

Given the observations detailed above, we recommend development of wetland salinity breakpoints based on the frequency of occurrence of specific salinities at high tide. Such relationship between high tide salinity and wetland community characteristics has been observed in other east coast river/marsh systems (Courtney Hackney, personal communication, 2012). We intend to use salinity/high tide relationships from the baseline EFDC simulations to test such relationships for the St. Johns River.

In addition, supplemental hydrodynamic modeling simulations of salinity in several tributaries outside of the current EFDC model domain could provide insight about potential impacts to marshes that do not lie along the main stem of the river.

DRAFT

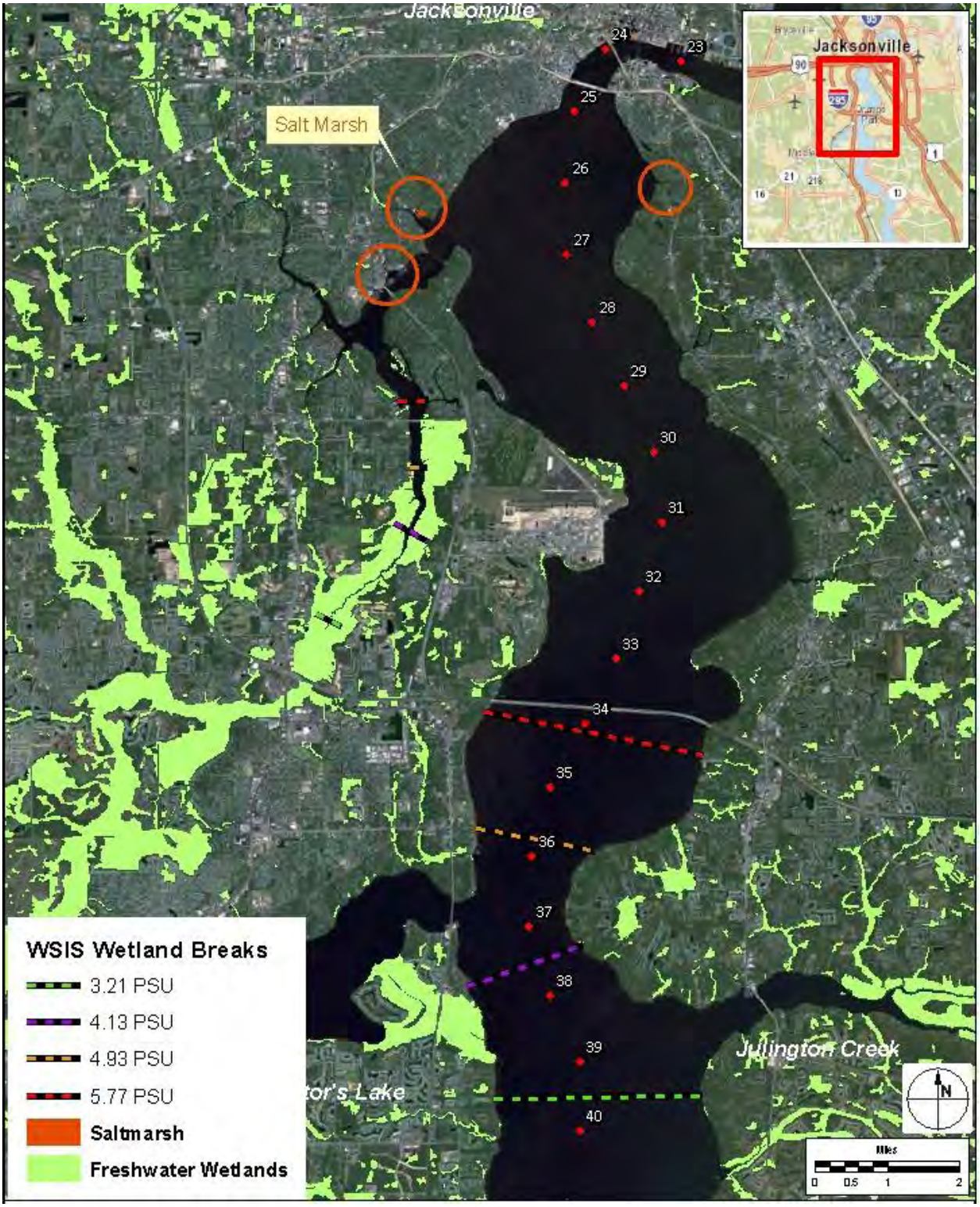


**Figure 4.1** WSIS Wetland Breaklines

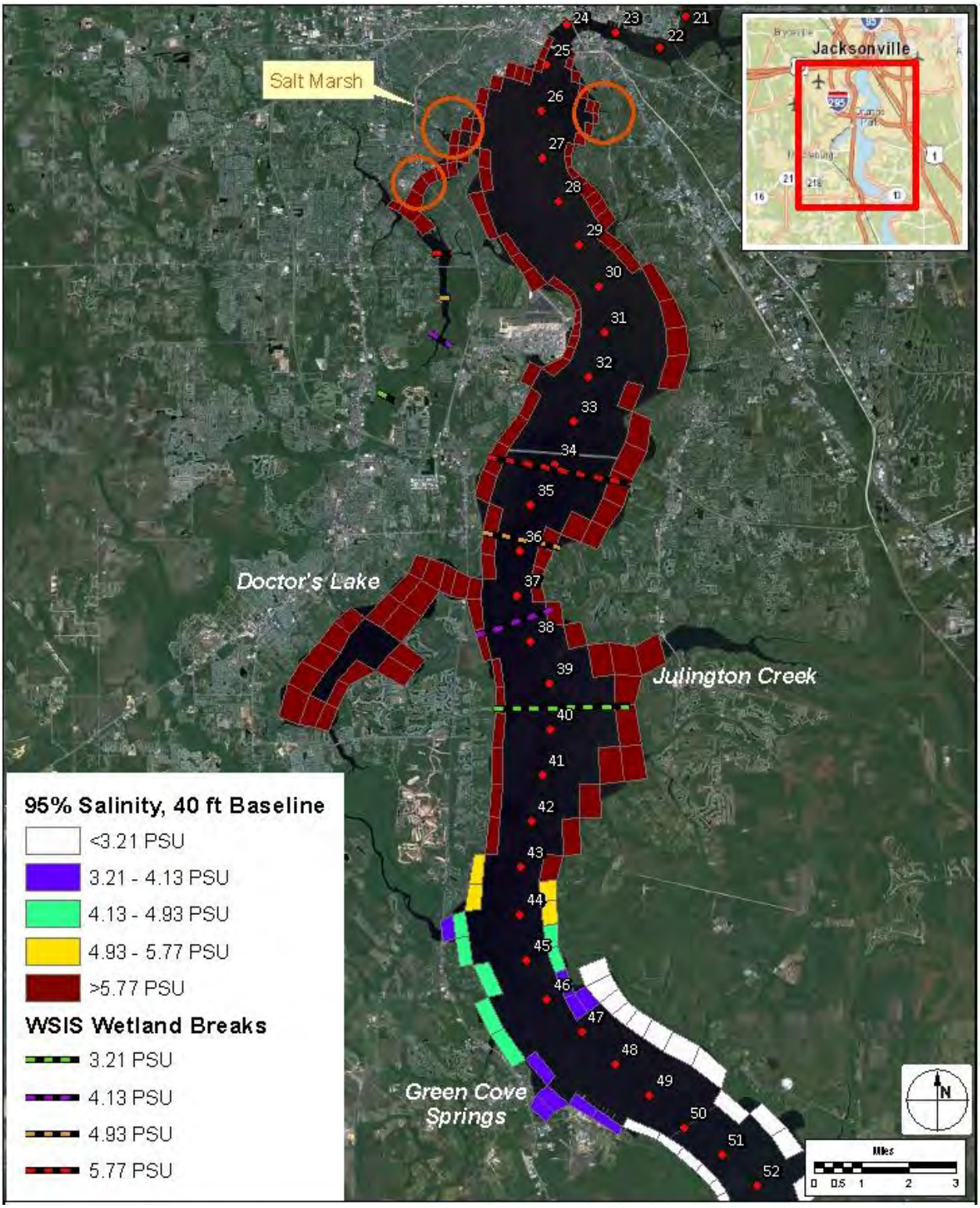


**Figure 4.2** 95% Salinity for 40-ft Baseline Condition

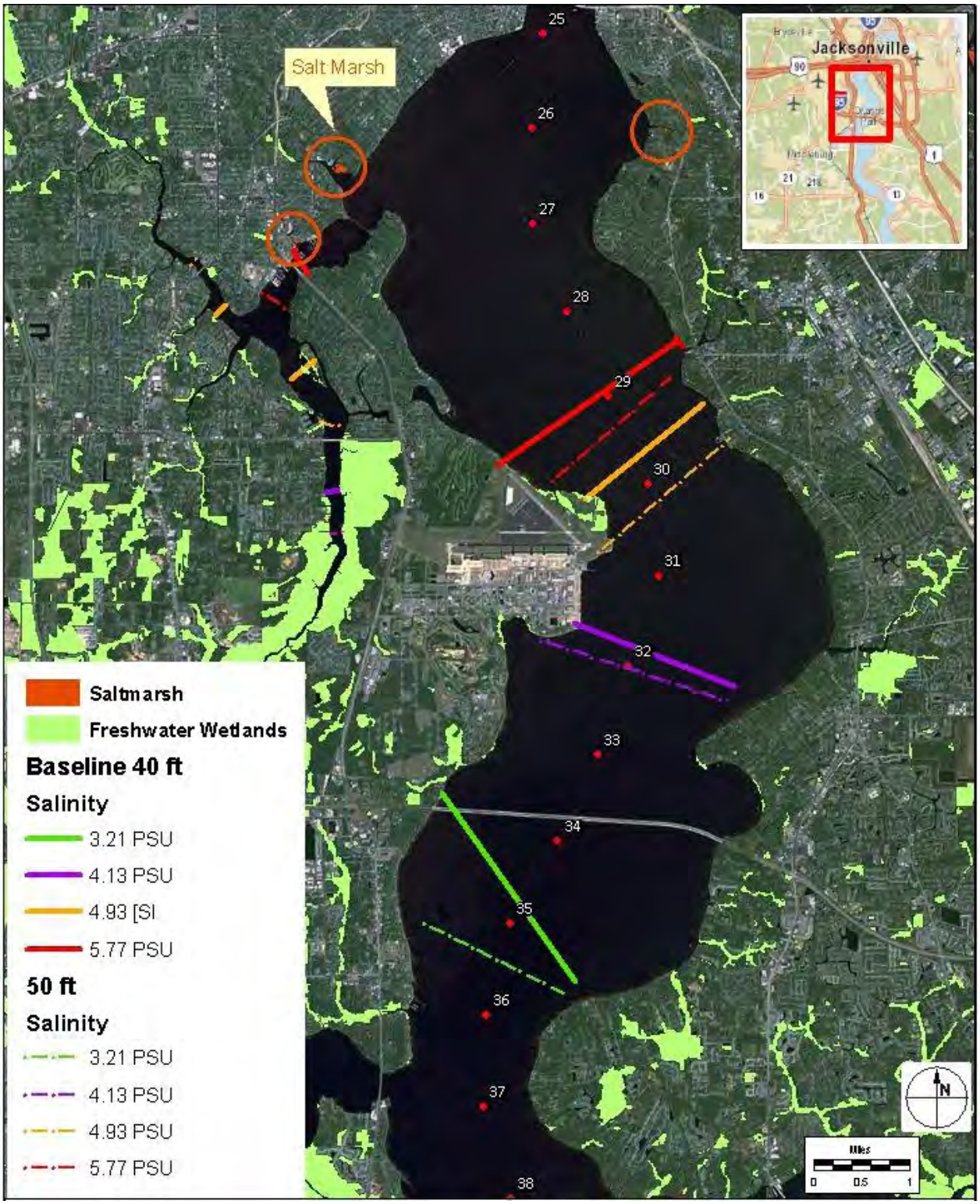


**Figure 4.3** Location of Wetland Breaklines

# 5.0 FISH

## 5.1 Introduction

The lower St. Johns River (LSJR) has a large, diverse fish community associated with the wide range of salinity conditions encountered in the estuary and tidally influenced areas of the river. Freshwater, estuarine marine, anadromous, and catadromous species are included in the species list. SJRWMD 2012: Chapter 12, pp. 12-3 and 12-44) summarizes the importance of this community:

> The fish community of the St. Johns River is a productive, diverse composite of freshwater, estuarine, and marine species populations. The LSJR fish community is a biologically unique community in North America because several estuarine species have established nonmigratory breeding populations in upstream freshwater reaches. The St. Johns River also supports some of the most valuable commercial and recreational fisheries in the state (Bass and Cox 1985; DeMort 1990; Holder et al. 2006; McLane 1955)..Two hundred and twenty-five fish species have been collected from the St. Johns River (Cox et al. 1980; MacDonald et al. 2009; McLane 1955; Tagatz 1968) — 63 freshwater species, 138 euryhaline species, and 24 marine species. Euryhaline species use the estuary for some or all of their life stages. Several species considered strictly estuarine inhabitants, including stingray (*Dasyatis* spp.), goby (*Microgobius* spp.), and pipefish (*Syngnathus* spp.), have established subpopulations that spend their entire life cycles within the freshwater portions of the river (Burgess and Franz 1978; Johnson and Snelson 1996).

Commercial fishing since the 1850s has been an important component of the local community (Miller et al.2012). Since the 1950s, commercial fishing has declined, but recreational sport fishing remains an important activity in the lower and upper river. Brody (1994) identified largemouth bass, black crappie, and other sunfishes (centrarchidae) as the main interests of sport fishermen in the LSJR. Striped bass and sunshine-striped bass, stocked from state-run hatcheries, maintain that fishery. Emergent and submerged vegetation provide key areas for game fishes. As noted in Brody (1994, p. 58), “When submerged and emergent aquatic vegetation are reduced, game fish populations are diminished.” Popular saltwater or estuarine species for recreational fishing include red drum (Sciaenops ocellatus), spotted sea trout (*Cynoscion nebulosus*), black drum (*Pogonias cromis*), and Atlantic croaker (*Micropogonias undulatus*) (DeMort, 1990 as cited in Miller et al., 2012). Both Brody (1994) and Miller (2012) consider the LSJR fish community diminished over the past 50 years.

DRAFT

Miller et al. (2012) considered that water withdrawals from the middle and upper portions of the river could potentially affect fishes in estuarine reaches by reducing freshwater inflow and changing the spatial coverage and distribution of salinity zones. Such changes could directly influence estuarine fish distribution, abundance, and community structure. Inputs to the estuarine fisheries analysis from other working groups include potential changes in benthic macroinvertebrate communities, potential loss of SAV, and potential for increased phytoplankton blooms and a resultant decline in dissolved oxygen (SJRWMD, 2012: Chapter 12). Salinity changes in the LSJR due to channel deepening could also change the spatial coverage and distribution of salinity zones and affect estuarine fish communities as described above.

### 5.2 Methods

The USACE's intent for this study was to apply the methods developed by SJRWMD and described in Miller et al. (2012) to assess potential changes in the fish community resulting from water withdrawals in the middle and upper St. Johns River. The USACE wishes to better understand the potential effects of salinity changes resulting from proposed deepening of the Federal channel in the first 13 miles of the St. Johns River. This study was unable to apply the methods that comprise the central focus of the WSIS assessment. The WSIS study applied data developed during almost 10 years of fish community field sampling conducted by the Florida Fish and Wildlife Conservation Commission (FWC) Fisheries-Independent Monitoring (FIM) program (MacDonald et al., 2009). As part of the WSIS efforts, analysts with the FWC used regression analysis to relate fisheries data from the FIM program to river flows (freshwater inflows) and developed quantitative relationships between fish species and "pseudospecies" (defined in Miller et al., 2012) abundances and river discharges. Miller et al. (2012) did not use salinity in the regression and correlation analyses because the wide salinity tolerances of many fish, their general mobility, and the rapid variability of salinity reduced its potential value to identify fish distribution patterns. In addition, Miller noted, "Freshwater inflow is also an easily quantifiable variable that will directly respond to water withdrawals." The statistical relationships developed from freshwater flows are not useful in developing salinity-abundance relationships.

Miller et al. (2012) identified six salinity categories (Table 1) to investigate effects of upstream water withdrawal on the LSJR. USACE added one additional salinity zone (low polyhaline) to provide the opportunity to identify linkages with BMI salinity zone changes, because the BMI assessment (Chapter 6) included that salinity category. The SJRWMD investigation looked at the LSJR estuary as extending from the mouth of the river to Buffalo Bluff upstream of Palatka (Table 1). Within the LSJR, the SJRWMD calculated the average river surface area associated with each salinity category in each year

of the salinity simulation. It compared the annual average areas of each habitat in various water withdrawal scenarios to assess whether different alternatives caused significant changes in the area of the several salinity habitat categories. The ecological modeling for channel deepening applies the same salinity zone analysis for the various deepening scenarios.

This study applied GIS analysis of the estimated highest salinity condition of each year to estimate changes in the areas of salinity ranges in the river. The baseline simulation provided the highest 30-day, 60-day, and 90-day moving average (MA) salinity days of each year (see Appendix A for calculation details) input to ArcGIS for calculation of salinity breakpoints and salinity zone areas (Table 5.1). For the salinity breakpoint values shown in Table 5.1, ArcGIS provided salinity isolines (isohalines) for each year's data. The same software provided the area (salinity zones) between isohalines. Because the 30-day MA data provided the greatest differences between the baseline and project alternative conditions, those results are provided here. The analysis of salinity zones of the 50-year horizon alternatives used the same method.

**Table 5.1** Salinity Categories (from Miller et al., 2012)

| Salinity Zone (ppt) | Salinity Category | Salinity Breakpoint (ppt) |
|---|---|---|
| x<0.5 | limnetic | |
| 0.5 ≤x <5.0 | oligohaline | 0.5 |
| 5.0≤x<12.0 | low mesohaline | 5.0 |
| 12 ≤x <18.0 | high mesohaline | 12.0 |
| 18 ≤x <24.0 | low polyhaline | 18.0 |
| 24 ≤x <30.0 | high polyhaline | 24.0 |
| X ≥30.0 | euhaline | 30.0 |

## 5.3 Results

### Salinity Zone Changes

Salinity zones varied both in average area and by year (Figure 5.1). Salinities less than 5 ppt accounted for between 60 and 76% of the total project area (94,822 acres) in relatively wet years (1996 – 1998) and for 41% – 48% in relatively dry years (1999 – 2001), a 35% decrease in area from wet to dry years. In particular, the <0.5 ppt zone, which when present occupied the river main channel between the upstream end of the project area (just downstream of Lake George) to a location near Green Cove Springs

varied dramatically. For the baseline, the average area of the <0.5 ppt salinity zone equaled 24,528 acres. In 1999, that zone included only 349 acres, and in the 2001 simulation, that zone did not exist.

The areas associated with salinity zones higher than 5 ppt varied somewhat less dramatically, but showed clear differences between years. Of the salinity zones between 5 ppt and 30 ppt, the 12 ppt –18 ppt zone increased by the greatest fraction between relatively wet years and dry years. The 12 ppt – 18 ppt zone included 3% to 8% of the total area in dry years and 12% – 13% of the total areas in wet years. The other, higher salinity zones also increased in area during the dry years. The three salinity zones between 12 and 30 ppt, with an average of about 5% each of total project area in the wet years, increased to between 6% and 13% of the total in wet years. The largest increase occurred in the 12 ppt – 18 ppt range. Salinities > 30 ppt showed the greatest fractional increase, accounting for 2.5% of the total in wet years and more than twice that area in dry years.

A comparison of each alternative (baseline, 44-ft Channel, 46-ft Channel, and 50-ft Channel) to its 50-yr horizon counterpart showed the amount each zone changed at the project 50-yr horizon (Figure 5.2). The <0.5 ppt and the 0.5 ppt – 5.0 ppt salinity zones lost acreage that was transferred to the other salinity zones. The zone of salinities 24 ppt – 30 ppt showed almost no changes between alternatives. This probably resulted from that salinity zone's location in the river — in the narrowest part of the river near Talleyrand Terminal. This area also includes an abrupt bottom elevation change from deep (> 35 ft) to relatively shallow (20 ft or less). The other channel deepening alternatives included similar patterns. Note also the similarity between the 44-ft and 46-ft channel depth alternatives (Figures 5.4, 5.5, 5.6, and 5.7).

When compared in terms of percent area changes (Figure 5.3), the two largest salinity zones (<0.5 ppt and 0.5 – 5 ppt) lost between about 4% and about 12% of their areas. The 24 – 30 ppt zone lost a small percent of area in each alternative, for the reasons discussed above.

Maximum average water column salinity zones changed with alternatives and time (the 50-yr horizon alternative results) in ways similar to those seen in the analysis of maximum bottom salinity zone changes in Chapter 6 (Benthic Macroinvertebrates). Generally, the alternative channel depths produced only small changes in the location of each salinity zone, typically by small shifts upstream (Figures 5.4 and 5.5: Maximum 30-day MA salinities for 1999 simulation; Figures 5.6 and 5.7: 50-yr Horizon Maximum 30-day MA salinities for 1999 simulation). In figures 5.5 and 5.7, the <0.5 ppt zone is constrained to an area of a hundred acres or so at the mouth of a small tributary. The rest of the river in that area has salinities between 0.5 and 5 ppt.

Note that the figures show the approximate northern and southern halves of the project area separately. The salinity zone boundary changes are small; a map showing the entire project area would obscure the changes. In addition, the figures do not show the 44-ft alternative. The 44-ft alternative changes were very similar to the 46-ft effects and therefore did not display effectively.

### 5.4 Potential Impacts of Channel Deepening on LSJR Fish Communities

The available analyses for the fish environment are consistent with similar analyses for benthic macroinvertebrates (Chapter 6) and SAV (Chapter 3). However, the analyses are insufficient to provide a clear understanding of potential effects of the deepening alternative on fish populations.

### 5.5 Recommendations

Additional analysis of the FIM dataset (MacDonald et al. 2009) to examine relationships between salinity and fish species and pseudospecies defined for the analysis of the lower river fish community (MacDonald et al. 2009; Miller et al. 2012) would provide direct relationships (if they exist). Salinity modeling in the marshes may shed additional light on potential changes in that marsh that could change the availability of fixed habitat (the appropriate salinity in the marshes at the appropriate season). Examination of salinity patterns in the main channel river adjacent to the access points to the extensive river mouth marshes could help assess the potential effect of salinity regime changes on salinity related behaviors in fish species / pseudospecies.

A number of species show very discrete cohort growth patterns, at least for recruitment and initial growth stages. This pattern allows direct examination of salinity and life history events in samples collected as part of the FIM dataset. Other species show clear periods of presence and absence, which may also serve as effective example species to consider salinity effects. Such analyses combined with salinity modeling of the marshes would do a great deal to clarify the potential effects of the proposed channel deepening alternatives.

DRAFT

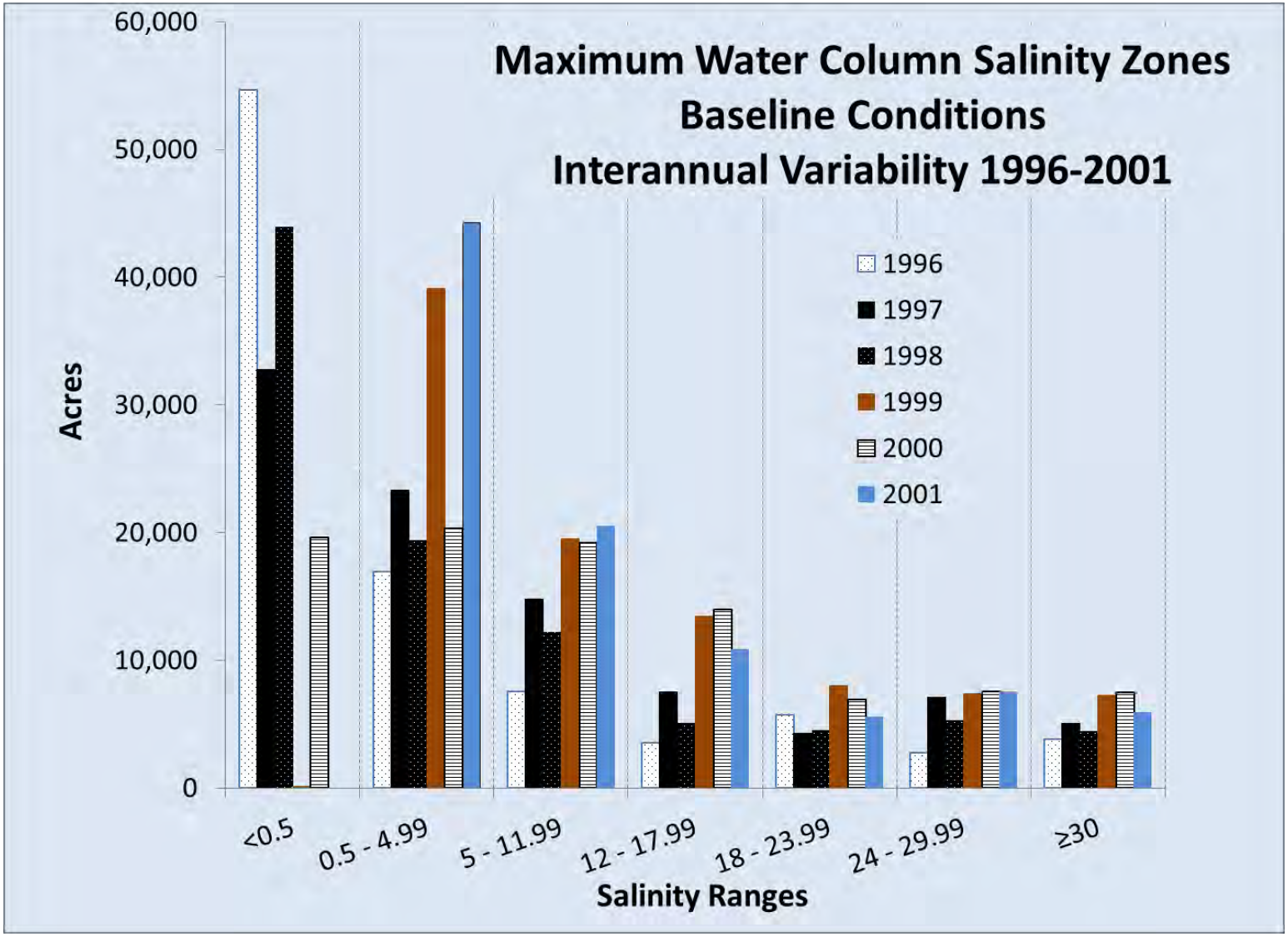


**Figure 5.1** Inter-annual Variability of Salinity Zone Areas for Baseline Conditions.

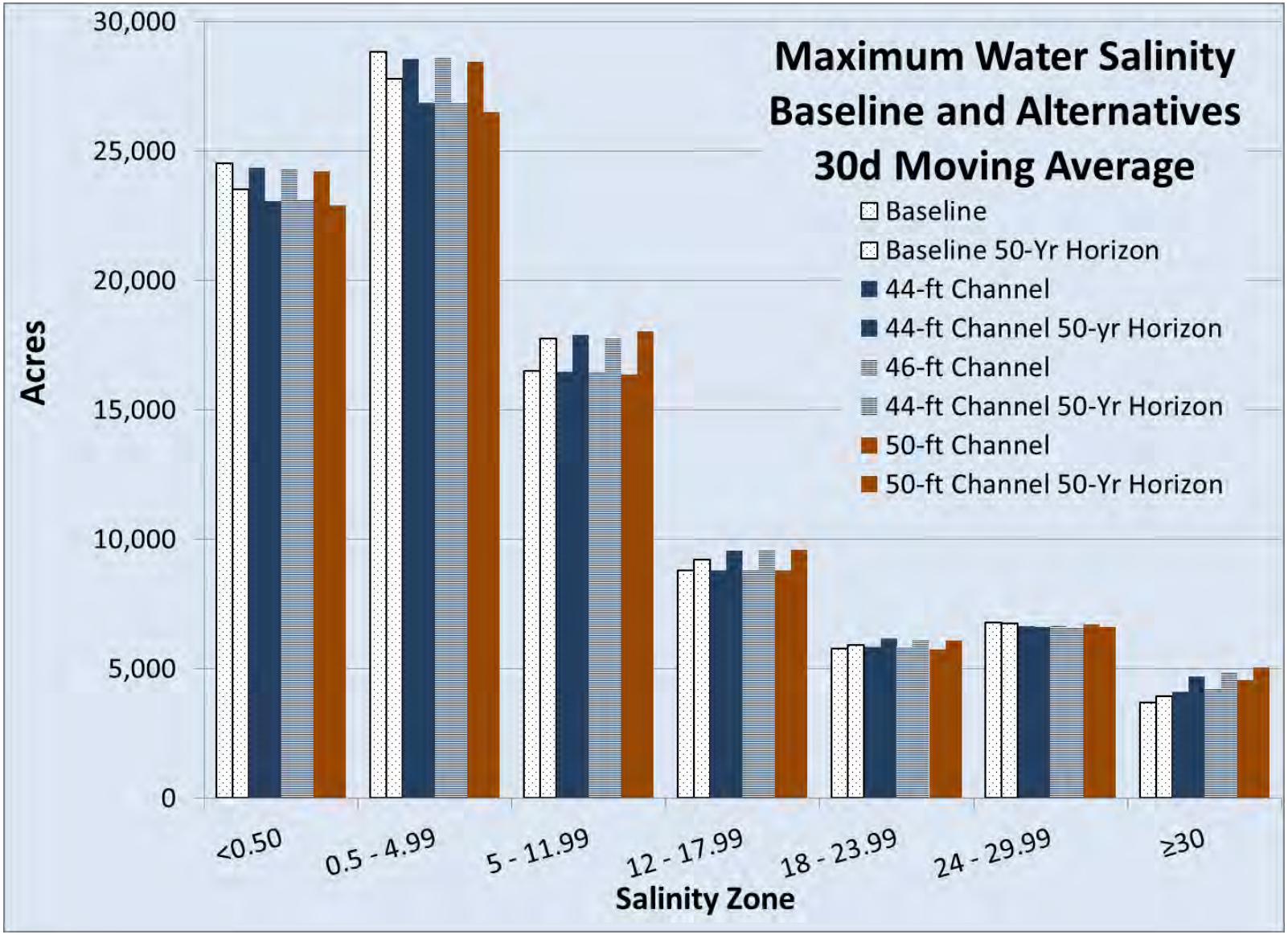


**Figure 5.2** Comparison of Salinity Zone Areas for All Alternatives

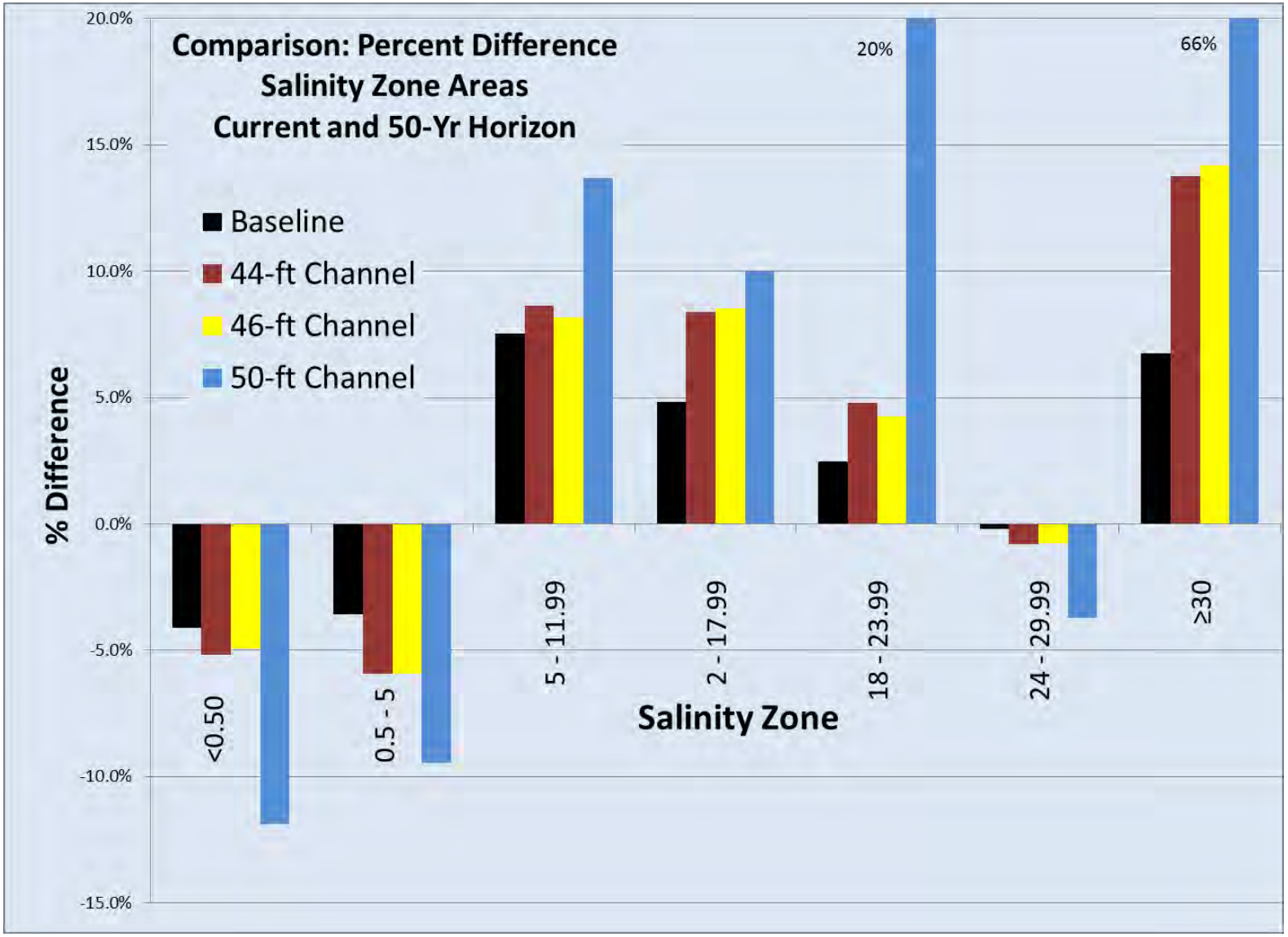


**Figure 5.3** Average Percent Changes in Water Column Salinity Zone Areas from the Current to 50-yr Horizon Conditions for Each Alternative

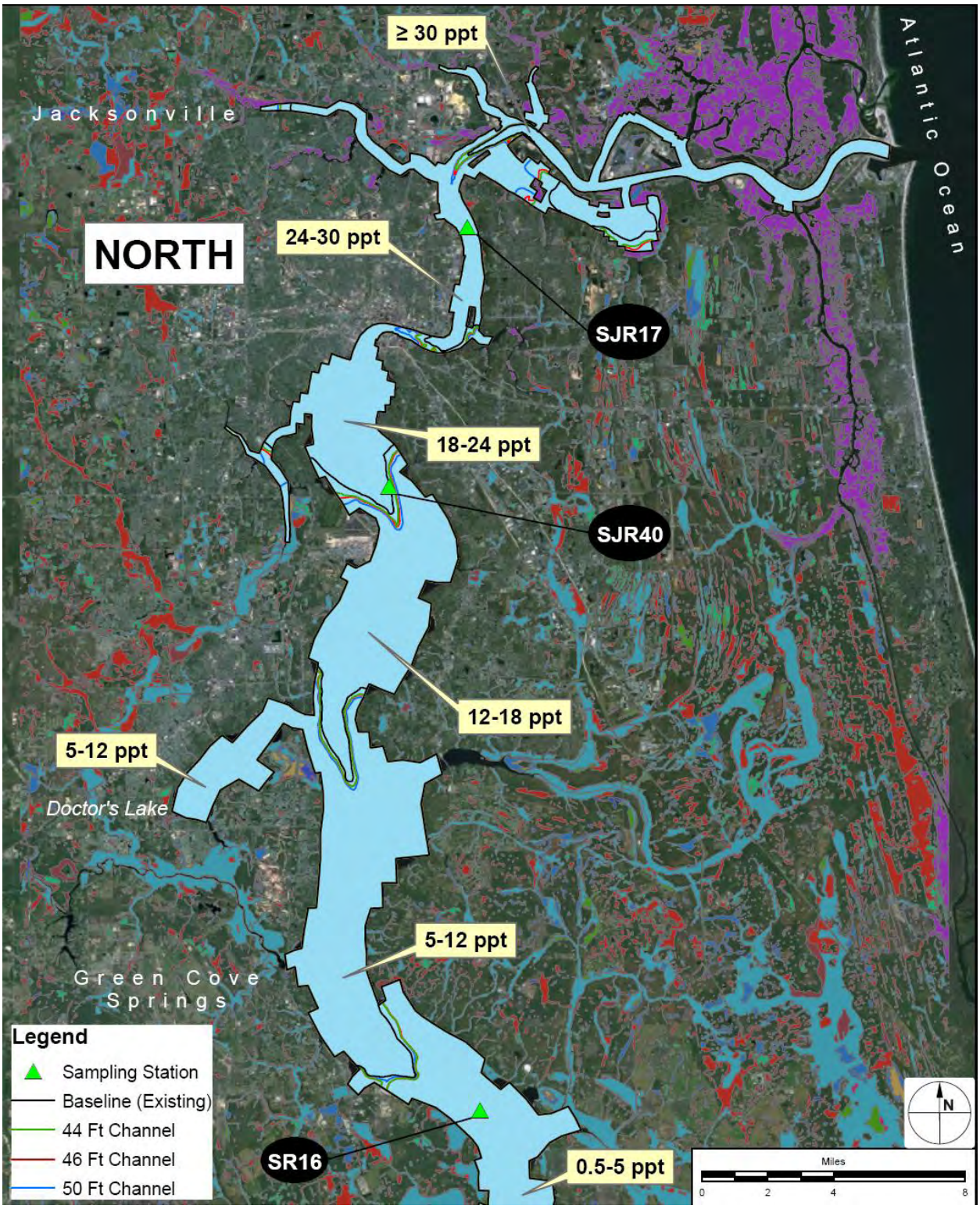


**Figure 5.4** Baseline Maximum Water Column Salinity, LSJR North, 30-Day Moving Average, Baseline, 44-ft, 46-ft, and 50-ft Channels

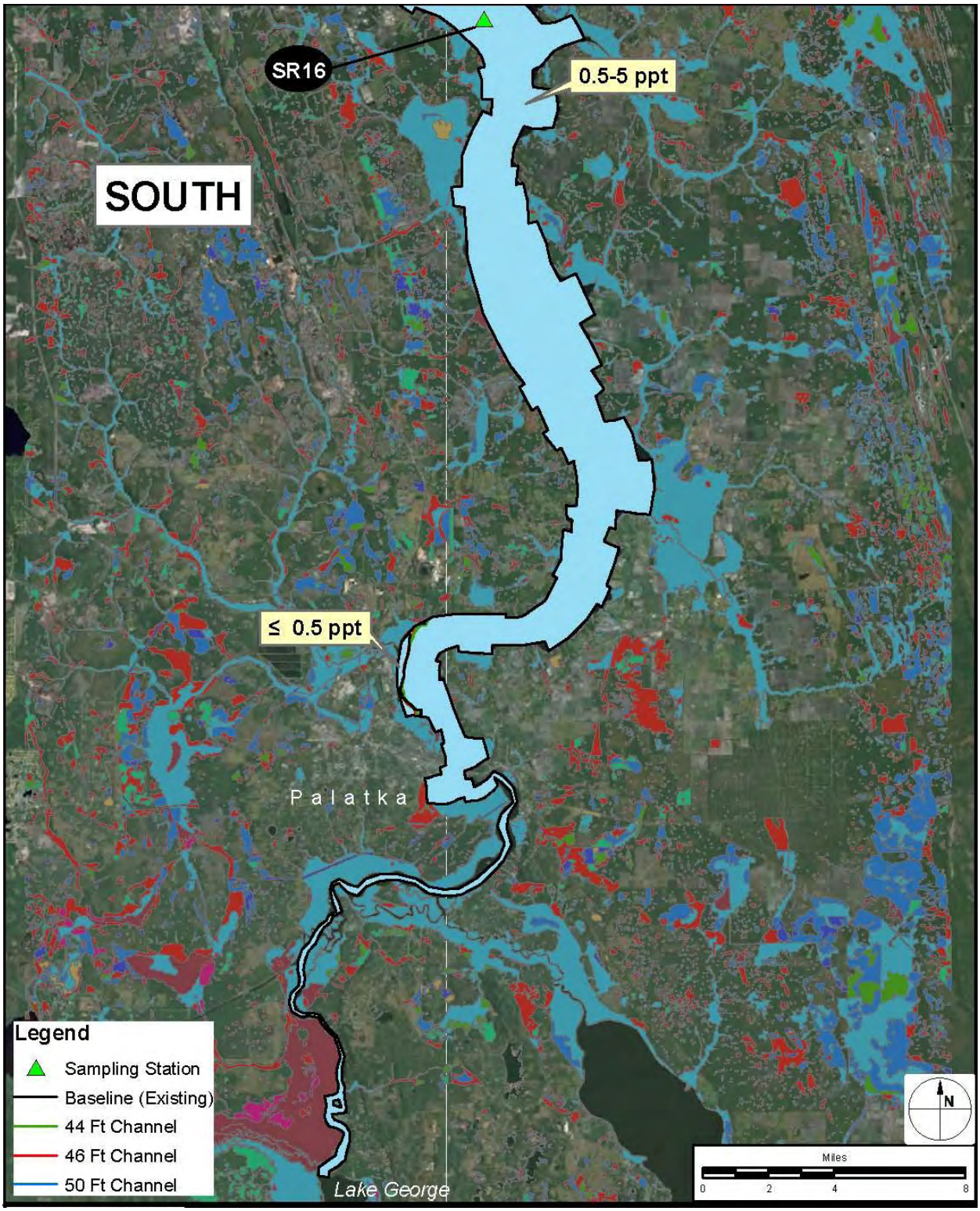


**Figure 5.5** Baseline Maximum Water Column Salinity, LSJR South, 30-Day Moving Average, Baseline, 44-ft, 46-ft, and 50-ft Channels

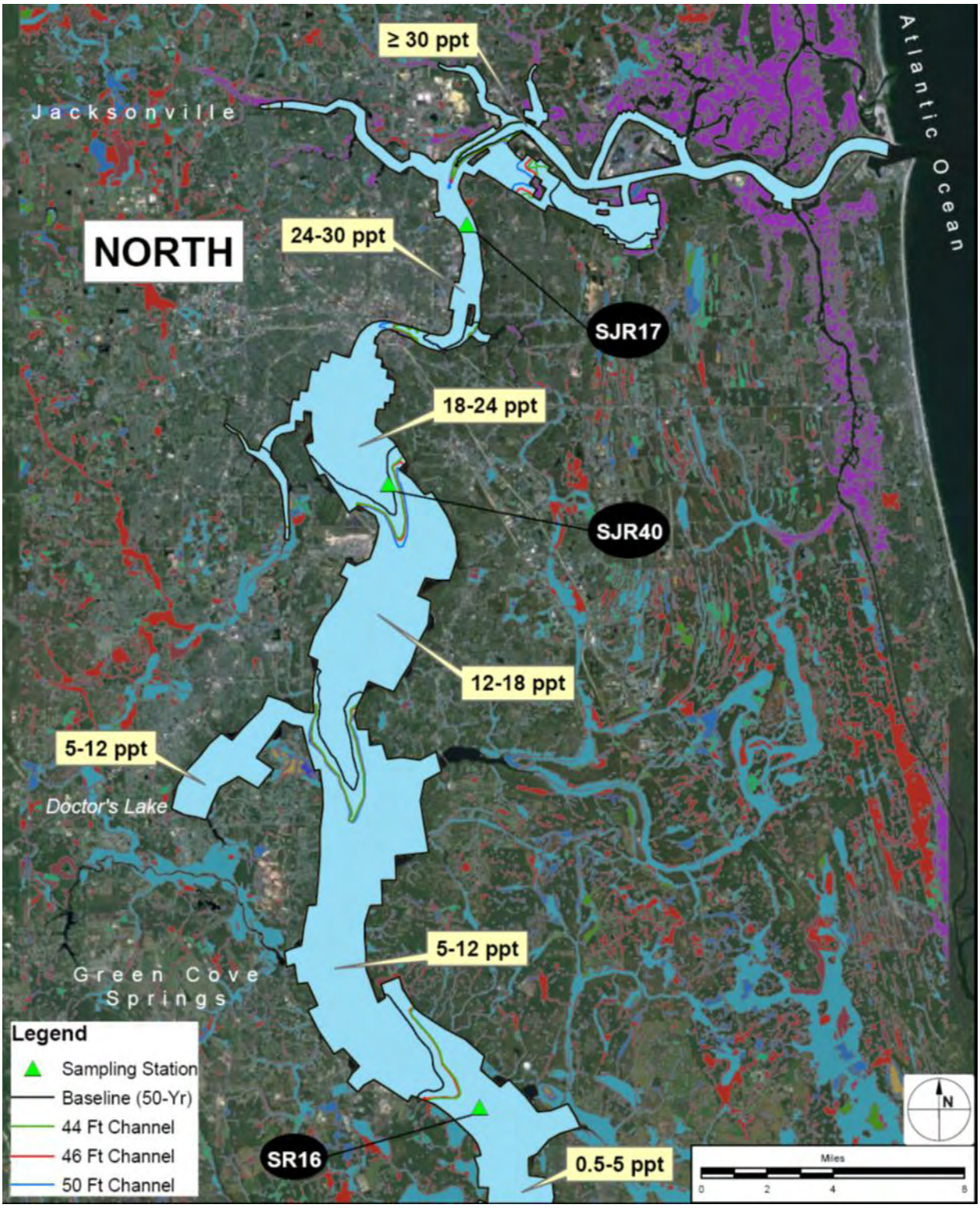


**Figure 5.6** 50-yr Horizon Maximum Water Column Salinity, LSJR North, 30-Day Moving Average: Baseline, 44-ft, 46-ft, and 50-ft Channels

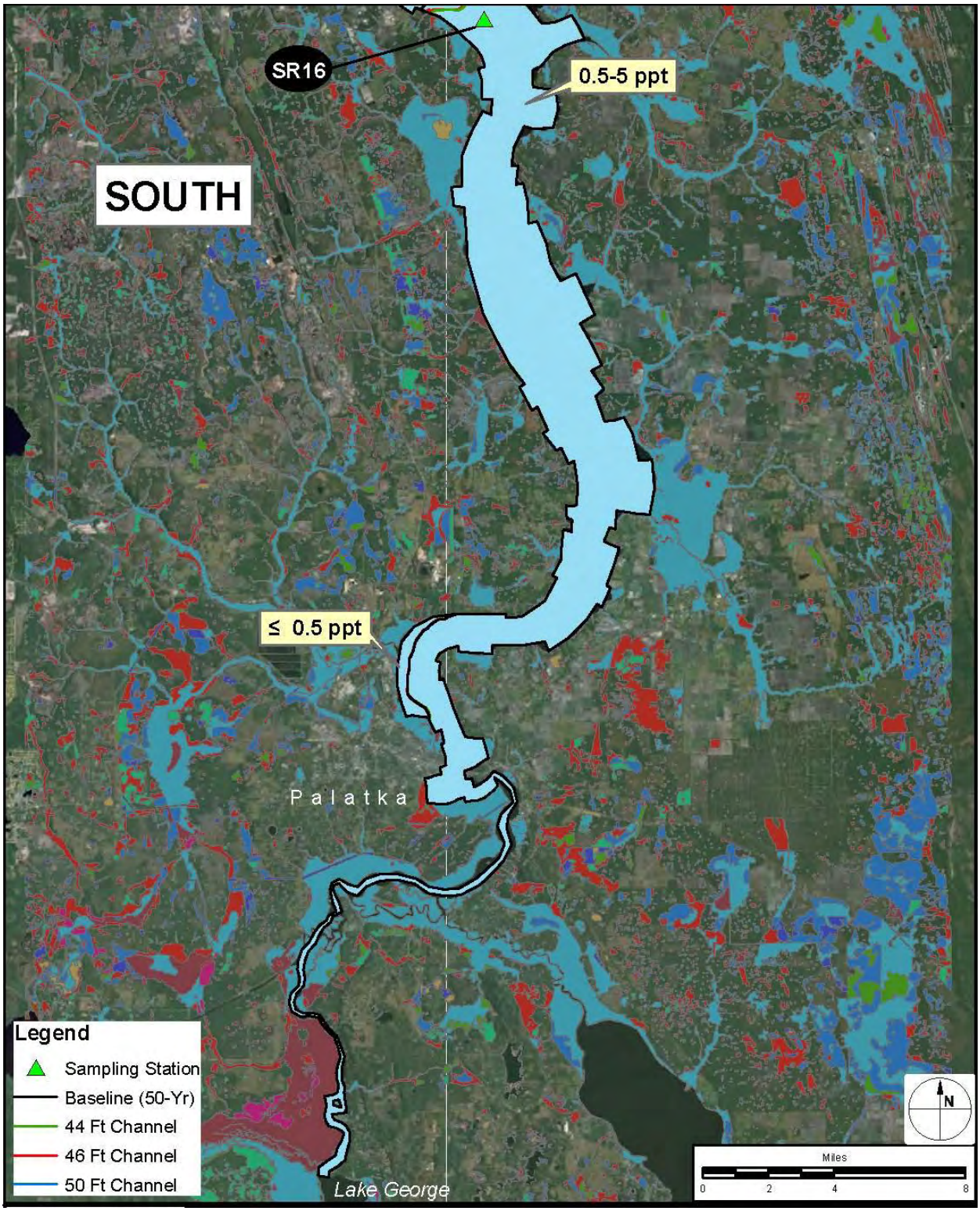


**Figure 5.7** 50-yr Horizon Maximum Water Column Salinity, LSJR South, 30-Day Moving Average: Baseline, 44-ft, 46-ft, and 50-ft Channels

# 6.0 BENTHIC MACROINVERTEBRATES

## 6.1 Introduction and Existing Conditions

Benthic macroinvertebrates (BMI) occupy an important place in the LSJR ecosystem, in the local fresh seafood economy, and in regional fishing recreation. Therefore, potential impact to this community as a result of proposed channel deepening requires analysis. This chapter presents results of analyses of channel changes that may affect BMI communities. The methods applied are those used by the SJRWMD in WSIS (2012). The interested reader should refer to Chapter 11 and Chapter 11 appendices of that report (Mattson et al.2011) to obtain an understanding of the BMI communities of the LSJR estuary.

Size and general body structure typically define BMI — invertebrate organisms retained by a mesh size of 200 to 500 μm (Stickney, 1984; Rosenberg and Resh, 1993). For this assessment, BMI will also include blue crabs (*Callinectes sapidus*) white shrimp, brown shrimp, and pink shrimp (*Litopenaeus setiferus, Farfantepenaeus aztecus*, and *Farfantepenaeus duorarum*), organisms that exceed size thresholds typically defining BMI. The importance of these species to the LSJR ecosystem and local economics warrants their inclusion in this assessment. Of the three shrimp species, white shrimp comprises by far the greatest portion of the shrimp population captured by commercial and recreational fishing efforts.

From a management perspective, BMI communities have provided biological indicators of water quality and integrity for decades (Gaufin, 1973; Rosenberg and Resh, 1993; Davis and Simon, 1995) and EPA has standardized protocols to sample BMI for this purpose. BMI have provided one means to assess habitat conditions, effects of hydrologic alteration, and water quality (e.g., Boon et al., 1992; Gore et al., 2001). A number of studies have correlated changes in salinity with changes in macrofauna abundance (e.g. Montagna and Kalke 1992, Montague and Ley 1993, Palmer at al. 2002), diversity (e.g. Mannino and Montagna 1997, Montagna et al. 2002), biomass (e.g. Rosenberg 1992, Kim and Montagna 2009) and community composition (e.g. Giberto et al. 2004, Mooraki et al. 2009, Strom and Thompson 2000). Applying available models of salinity-related community changes in the BMI community in the LSJR may provide a well-documented means of assessing effects of different channel deepening alternatives on the riverine BMI communities.

Deepening the Federal navigation channel (beyond its current 40-ft authorized depth) in the first 14 miles of the St. Johns River may elevate upstream salinities beyond those found under existing conditions. (See Chapter 1 and Chapter 8 for a full description of existing conditions as developed in the

EFDC salinity simulations for this project). Based on the WSIS study, elevated salinities that may impact the main stem natural communities are assumed to occur primarily upstream of the deepened channel, as the salinity in main river channel where the 40-ft channel occurs is already close to marine conditions.

Benthic macroinvertebrates transform primary production (live and detrital plant material) into animal biomass for use by higher trophic levels (Cummins et al., 2008). Estuarine and marine fishes use the BMI community as a key food source at a variety of life cycle stages. In addition to their role as primary consumers, shrimp (primarily white shrimp, *Litopenaeus setiferus*) and blue crab (*Callinectes sapidus*) provide a significant component of the local commercial seafood market. Recreational anglers also use traps and nets to capture these animals. Jacoby (2011) provides a synoptic review of the life histories of blue crab and the shrimp species listed above, including a discussion of the species' relationships between life stage, salinity, and habitat. Mattson (2012) provided a description of BMI communities in the St. Johns River, dividing the descriptions by WSIS river segment (See Chapter 1 Figure 1.2 for a WSIS river segment map). The river segments of interest for this report include Segments 1 – 3 (Mattson et al.2012: Figure 3.1), which comprise the main drainage channels for the LSJR watershed below Lake George.

Montagna et al. (2008, 2011), analyzed BMI data collected between 1974 and 1998 from 17 sampling stations in the LSJR estuary (downstream of Palatka, FL). The report provides detailed descriptions of the taxonomic composition of the various BMI communities, and statistical relationships of total abundance, taxon abundance, and salinity. Of the more than 545 species identified, 30 species comprised about 80% of the mean BMI abundance in the estuary. Abundance peaked at the lowest salinity sampled, and ranged from 250 / $m^2$ at Mill Cove, toward the mouth of the Estuary, to 12,000 per $m^2$ at a station approximately midway between the mouth of the river and the upstream-most sampling station near Palatka. The report applied multivariate analysis of the datasets under study to detail the species associations (defined by genera, family and phyla) at different salinity ranges, noting that eight "low salinity" communities occurred in mean salinities of 0.4 to 5.8 ppt (with one exception) and (with a single exception) nine high salinity communities occurred in waters of 13.6 ppt to 25.7 ppt salinity. The report includes details of salinity – abundance response models for the three parameter log normal model of salinity versus total abundance, 12 numerically dominant taxa, 30 numerically dominant species, and correlations between abundances and salinity for 17 dominant higher taxonomic categories.

Mattson et al. (2012) and referenced literature, in particular Montagna et al. (2008, 2011), provide detailed discussions of the BMI communities of the LSJR relevant to the channel deepening project. A

short list of the some of the main general findings of those documents includes the following (Montagna et al.2008, 2011; Mattson et al.2012).

- Sampling of BMI in the LSJR has yielded 1,063 species of freshwater, estuarine, and marine invertebrates. Dominant taxa (by number of species) in freshwater reaches include aquatic insects, mollusks, and oligochaete worms. In the estuarine portion of the river, mollusks, crustaceans, and polychaetes dominate the species composition.
- The LSJR has seen a wide variety of sampling efforts but no routine, systematic, long-term (≥ 10 years) program. Of the 31 sampling efforts identified, 11 reported sampling in the lower basin, including 2 basin-wide sampling efforts and 9 focused only on the LSJR. Mattson et al.(2012) concluded that those 9 efforts provided more data than available in the middle and upper basins of the river.
- Because salinity "affects benthic communities primarily because of salinity regime alternations," "managing the inflows into estuaries" should include preservation of natural salinity regimes (Mattson et al., 2012)
- Individual taxa often exhibit nonlinear responses to salinity and many taxa exhibit optimal salinity ranges. In addition, some display linear or curvilinear responses to salinity gradients.
- Critical BMI habitats in the LSJR include submerged vegetation (*Vallisneria americana*), which can tolerate "moderate levels of salinity" (exposure to salinity of 15 ppt or more for more than a day or so).
- Dissolved oxygen (DO) is an important factor in distribution of BMI. Taxa more tolerant of low DO (e.g., chironomids and oligochaetes) sometimes required up to 30 days of low DO before experiencing lethal effects. In estuaries, DO below 2 to 3 mg/L could have severe effects on benthic community structure and function.
- BMI are key components in the diets of many fish species important as recreational or commercial fisheries.
- Many members of the BMI community in the LSJR project area are generally adapted to a dynamic salinity regime. High salinity communities tend to be numerically dominated by members of the Cnidaria, Echinodermata, and Chordata phyla, with fewer individuals of the Insecta (phylum Arthropoda). Polychaete genera tend toward high salinity conditions, with some genera much more prevalent in high rather than low salinity conditions. However, some polychaete genera occur almost exclusively in high salinity communities.
- Regardless of the taxonomic level selected to represent community composition, BMI community composition show higher correlations to salinity than to other variables tested (DO, pH, and temperature).

DRAFT

- Nonmetric multidimensional scaling (MDS) analysis found that the dataset clustered in two main groups representing low salinity sites (0.4 ppt – 5.8 ppt) and higher salinity sites (13.6 ppt to 25.7 ppt). Regression of abundance (number of individuals per $m^2$) against salinity showed abundance peaking at a mean salinity of 0.4 ppt. Reduced abundance in the lower reaches of the estuary (river segments 1 and 2) likely occurs because of greater salinity variability and the related physiological stresses occurring there, as well as pollution from the urban environment.

The mouth of the St. Johns River and the associated marshes and open waters comprise part of the Timucuan Ecological and Historic Preserve (TIMU) a unit of the National Park System established in 1988. TIMU "encompasses 46,000 acres of salt marsh and coastal hammock habitat in addition to marine and brackish open waters...and contains the seaward confluence of the Nassau and St. Johns Rivers" (http://www.npca.org/parks/timucuan-ecological-and-historic-preserve.html). Those marshes associated with the St. Johns River include almost all of the estuarine (*Spartina alterniflora / Juncus romerianus* dominated) marshes within the ecological modeling study area. These marshes serve as nursery areas for a wide variety of marine and estuarine fishes and invertebrates, including species important to humans.

Hymel (2009) described the TIMU marshes as "heavily influenced by urban areas (City of Jacksonville), manufacturing (pulp and paper mills), petroleum storage, shipping (Port of Jacksonville; JAXPORT), military bases (Naval Station Mayport), power stations (Jacksonville Electric Authority), and recreational activities on the Nassau, Ft. George, and St. Johns rivers". She summarized benthic macroinvertebrate studies in TIMU and the nearby lower St. Johns River main channel by Long (2004), Landsberg et al. (2004), Anderson et al. (2005), and Evans et al. (2004). Those studies suggested that over the past 20 years the marsh has shifted from relatively low salinity pollution-sensitive to higher-salinity, pollution tolerant taxa (Long 2004). Evens et al. (2004) concluded that BMI communities in the river upstream of TIMU and within the City of Jacksonville (located near Bolles School, the Naval Air Station, Doctor's Lake, and Pirates Cove) consisted of low diversity, pollution tolerant associations. Clapboard Creek, Dunn's Creek, and Broward River BMI communities had moderate diversity with pollution tolerant species. Hymel (2009) also identified invasive species introduced by ships traveling through JAXPORT as an emerging concern for TIMU.

Gregory et al. (2011) reported water quality and sediment quality in the TIMU as generally "Good" and "Fair" respectively. Most of the lower quality findings related to excess phosphorus, nitrogen, and chlorophyll a in the water and nutrient rich sediments, as well as some sites with high levels of total organic carbon (TOC) in the sediments. He noted that the sites with elevated nutrient conditions tend to occur "in the more upstream reaches of the Nassau River and St. Johns River as well as inland

areas along Clapboard Creek." Fair and Poor sediment conditions "due to elevated TOC were generally observed in more inland and riverine areas of TIMU."

Wright et al. (2012) reported 2011 salinities at a water quality sampling station in Clapboard Creek (located within TIMU on the north side of the river slightly downstream of the JEA North Power Plant) ranging between about 11 and 35 ppt with the vast majority of the data between 25 ppt and 35 ppt.

### 6.2 Potential River Deepening Effects on Macroinvertebrates

If deepening the channel caused an upstream salinity shift of the baseline salinity gradient, this shift could cause an equivalent upstream shift in communities and taxa, to the extent of individual BMI taxon sensitivities to changes in salinity. Montagna et al. (2011: Table 5) found that for lower St. Johns River species, genera, families, and phyla tested, salinity generated the highest Spearman Correlation Coefficient of the variables salinity, temperature, pH, and dissolved oxygen. However, the research also found the communities sampled included two main clusters, each salinity tolerant within a fairly wide range. The results suggest that if upstream salinity shifts were to occur, estuarine and possibly marine salinity communities would expand to the detriment of freshwater BMI communities they would replace. That shift might occur as a gradient of community change along the new salinity gradient, as some species within the low salinity community have more tolerance than others for increased salinities. In addition to shifting communities upstream, the shift could move the optimum salinity range for some species away from the optimum (fixed) habitat for those species. However, the BMI species are generally characterized by small, very rapidly reproducing, very fecund species; BMI species are typically assumed to produce many more offspring than will ultimately survive in any case. For the LSJR, the large inter-annual variability in salinity gradients probably exerts a dominant effect on most BMI distributions. In addition, much of the estuarine portion of the river runs through the City of Jacksonville and urbanization has tended to reduce the acreage of key estuarine habitats such as marshes. Thus, salinity shifts within the urbanized area may not represent a significant change in available habitat. The high salinities reported in the TIMU marsh station in Clapboard Creek (located relatively near to adjacent uplands and away from the river main channel) may reflect general conditions in the marshes adjacent to the main channel. Again, salinity shifts in this area may be minor or insignificant, as the area appears to experience high salinities under most conditions most of the year.

*Vallisneria americana* (eelgrass) the primary freshwater submersed vegetation in the LSJR extends downriver to about river mile 25 (Chapter 3). Impacts to eelgrass, a habitat relatively high in BMI diversity, could occur if the salinity gradient were to shift upstream. The unvegetated benthic habitat that

accounts for most of the river bottom could also experience a shift in species composition with an upstream shift in the salinity gradient. Shifts from less to more saline conditions tend to reduce BMI diversity and total abundance (Montagna et al. 2011) However, eelgrass occurs only along the shorelines and thus covers a relatively small fraction of the total BMI habitat. Thus, unvegetated habitat would account for most of the standing stock or abundance reduction due to salinity changes.

## 6.3 BMI Analysis Methods

To assess impacts of altered LSJR salinity regimes on the BMI community, the analyses used in this study use, to the extent possible, the same methods as those SJRWMD used to assess impacts of upstream water withdrawals. SJRWMD described these methods in the WSIS (Mattson et al. 2012). The USACE and Taylor Engineering reviewed that WSIS chapter, related appendices, and referenced documents. The USACE project team concluded that most of the BMI analysis methods were as useful for assessing the effects of salinity changes as they were for the SJRWMD to assess potential changes in freshwater inflows to the estuary.

This BMI analysis compares the baseline condition to each alternative separately, followed by consideration of the relationship between different alternatives. The BMI effects assessment also considers the results of the Submerged Aquatic Vegetation analysis (SAV: Chapter 4 of this report) to identify potential effects on BMI of salinity-related impacts to SAV from channel deepening alternatives. Mattson et al. (2008) identified salinity as a primary variable in BMI community composition within SAV.

### *6.3.1 BMI Taxa Population and Community Abundance and Salinity*

Although many estuarine organisms generally have a wide salinity tolerance (from 0 to 30 psu - euryhaline), most are located within only a portion of their potential salinity range or have a distribution focused on a specific salinity range. Thus, salinity gradients play a major role in determining the distribution of estuarine organisms (Montagna et al. 2011). Secondary production of estuarine benthic macrofauna in particular is known to increase with increases in freshwater inflow and salinities that range 15 – 20 psu (Montagna and Kalke 1992). Salinity gradients also can act as barriers to predators and disease. Two important oyster predators in Gulf of Mexico estuaries, the southern oyster drill, *Thais haemastoma,* and the stone crab *Menippe mercenaria* are intolerant of sustained salinities below 15 psu (Menzel et al. 1957; MacKenzie 1977). Freshwater inflow, depending on the volume, can dilute or even eliminate infective *Perkinsus marinus* oyster disease particles in low salinity areas because disease

organisms prefer salinities above 25 psu (Mackin 1955; La Peyre et al. 2009). The timing of freshwater inflows is also important to estuarine organism abundance and distribution because the organisms have evolved over long periods to particular regimes of freshwater inflow and associated salinity conditions such that there are breaks in tolerances of various BMI below 15 psu, around 20 psu, and 25 psu (Montagna et al. 2002). To examine changes in space occupied by different salinity zones, this analysis applied SJRWMD salinity breakpoints of 0.5, 5, 12, 18, and 30 ppt salinity, and added an additional breakpoint at 24 ppt salinity. To help link consideration of spatial changes in salinities at specific locations probabilities of salinity durations considered at the three sites included 0.5, 1, 2, 3, 4, 5, 12, 18, 24, and 30 ppt. The additional salinity break points 1, 2, 3, 4, and 5 ppt provided more details about the changes at the upstream end of the LSJR estuarine salinity.

Baseline maximum daily bottom salinity day identified from 30-day, 60-day, and 90-day moving average values of daily salinity maxima provided the moving average (MA) day used to calculate salinity zones and areas. Appendix B (from Taylor Engineering, 2012) provides a detailed description of the moving average calculation process. The salinity calculations varied somewhat from the SJRWMD approach. Because the bottom layer lies closest to the sediments sampled for BMI abundance, we selected bottom layer salinity values to calculate BMI salinity zones, rather than using the maximum water column salinities as done in the WSIS. We selected an additive set of moving average periods for the BMI and Fish Assessments (Chapter 7) to provide the best opportunity for consideration of linkages between BMI and fish community changes. The SJRWMD WSIS study used 30-, 60-, and 120-day moving average periods.

GIS analysis transformed the model cell output data to salinity isohaline lines and polygons used to define salinity ranges (Table 6.1)

DRAFT

**Table 6.1** Salinity Breakpoints and Related Salinity Ranges for Salinity Area Estimates

| Salinity Breakpoint (ppt) | Salinity Zone Range (ppt) | Salinity Category |
|---|---|---|
| | x<0.5 | limnetic |
| 0.5 | 0.5 ≤x <5.0 | oligohaline |
| 5.0 | 5.0≤x<12.0 | low mesohaline |
| 12.0 | 12 ≤x <18.0 | high mesohaline |
| 18.0 | 18 ≤x <24.0 | low polyhaline |
| 24.0 | 24 ≤x <30.0 | high polyhaline |
| 30.0 | ≥X30.0 | euhaline |

GIS analysis calculated and mapped the area associated with each salinity zone (Table 6.1) for baseline and alternative scenarios. For the baseline scenario, the lowest salinity range (x<0.5 ppt) included the model upstream boundary cell just downstream of Lake George to the 0.5 ppt isohaline line downstream. The euhaline salinity range (≥30 ppt) comprised the space between the calculated 30 ppt isohaline line and the mouth of the river. The EFDC model grid predicting salinities extends into the offshore coastal shelf of the Atlantic Ocean; these cells did not enter into the calculation of salinity zones. The SJRWMD and USACE analyses were similar in this respect, with only slight differences associated with the upstream and river mouth terminus points for the analysis. SJRWMD (2012: Chapter 11) used a single zone for the salinity values between 18 ppt and 30 ppt and did not include the area greater than or equal to 30 ppt. This assessment separates the 18 ppt to 30 ppt salinity zone into 18 ppt – 24 ppt and 24 ppt – 30 ppt because many estuarine invertebrates have salinity optima between 18 ppt and 24 ppt salinity (Paul Montagna, personal communication, September 14, 2012). Changes in the location of the 18 – 24 ppt zone may reflect more or less high quality physical habitat space for estuarine species. The consideration of a ≥30 ppt zone, absent from the SJRWMD report, provided a more complete picture of the potential for upstream movement of ocean salinity conditions after channel deepening.

The mean and 95% confidence interval for each salinity zone area in the project baseline and alternative data sets provided a comparison tool to assess differences between years within moving average categories and salinity zones. This tool provided a possible means to assess differences between the baseline and each alternative.

The salinity zone area data provided the means to estimate changes in total BMI community abundance by salinity zone. Montagna et al. (2011) developed equations to estimate changes in total BMI community abundance with salinity in the LSJR. Mattson (2012) described a spreadsheet model of BMI abundance constructed with the equation

DRAFT

$$Y = ae^{\left[-0.5\left(\frac{ln\left(\frac{x}{X_c}\right)}{b}\right)^2\right]} \qquad \text{Equation 1}$$

Where Y = a biological characteristic (abundance)

X = salinity

a= maximum value of the biological characteristic

b = skewness or rate of change of the response as a function of salinity

$X_c$ = the peak response value on the salinity axis

ln = natural log function

e = exponential function

The BMI analysis reported here used the SJRWMD EXCEL spreadsheet version of this nonlinear model (Ed Lowe, SJRWMD, personal communication email, April 6, 2012) to calculate BMI community abundance estimates for each salinity zone area. The BMI density (number / $m^2$) for each salinity zone calculated using equation 1 above provided the base BMI density value against which to calculate density changes. The spreadsheet calculated a baseline BMI density. That baseline value was multiplied by the percent difference in area of each salinity zone (Table 6.1) in the baseline and alternatives to identify the change in density. The baseline value minus the density change value provided the density for the salinity zones of each alternative scenario. Impact assessment compared alternatives' effects on BMI density with respect to the baseline condition and the changes in the physical location of each salinity zone in each alternative.

Calculating the difference between baseline BMI density in each salinity zone and the BMI density in each salinity zone of each alternative yielded the changes in BMI community density (number of individuals per $m^2$) by scenario by salinity zone.

### *6.3.2 Partial Duration Frequency Analysis of Salinity*

Partial Duration Frequency Analysis (PDFA) of salinity in the LSJR (Mattson et al. 2012) detailed the changes in salinity level and duration at three locations within river segment 2 (see Figure 1.2, for river segment boundaries) which locations also served as sampling stations for BMI. This study performed PDFA at the same locations (Figure 6.1 PDFA Analysis Station Locations) to describe the extent and intensity of salinity changes occurring as a result of project alternatives. The USACE also selected these locations because a clear salinity – freshwater boundary for SAV occurred between the most upstream and downstream-most of the three stations. In addition, preliminary USACE salinity

modeling results suggest that many of the effects might occur within the river within the upstream and downstream boundaries.

Slater et al. (2011) provided a detailed mathematical description of PDFA that the interested reader should review to best understand this method. For this study, Taylor Engineering used the mathematical description found in that document to develop a spreadsheet model for PDFA analysis at the same locations used by SJRWMD (Table 6.2). The input salinity data included single cell maximum daily bottom salinities for the period of record used in the analysis (six years, 1995 – 2001 inclusive) at three locations.

**Table 6.2** Locations of Salinity Data Used for PDFA Analysis From Mattson Et al.(2012).

| Site | Modeled Station Name | Latitude | Longitude | River km (mile) |
|---|---|---|---|---|
| JAXSJR17 | JAXSJR17 | 30 deg 22.0 min | 81 deg 37.1 min | 29 (18.0) |
| JAXSJR40 | JAXSJR40 | 30 deg 15.1 min | 81 deg 39.1 min | 47 (29.2) |
| SJSR16 | SR16 | 29 deg 58.6 min | 81 deg 36.6 min | 81.7 (50.8) |

Frequency analysis estimates how often, on average, a given event will occur. For this analysis, "on average" meant annually. If annual series hydrologic data provide the data to generate the statistics, frequency analysis estimates the probability of a given hydrologic event happening in any given year (Slater et al., 2011). For salinity data used here, PDFA analyzes the data record (in this case the entire six years of simulation days) to identify what period (length of days) and number of times a given salinity was exceeded. The results are divided by the number of years to produce an annual exceedance probability. The return interval for the same exceedance was defined as basically the inverse of the annual probability. The Weibull plotting position formula was used to create frequency and return interval plots.

The PDFA analyses compared the probability of a given salinity level event compared to the baseline behavior to provide an understanding of the salinities at which changes salinity regimes occur at a location and to show differences between salinity durations of the baseline and a project alternative for the same salinity.

Assessment of water withdrawal effects on blue crab and shrimp populations employed a regression relationship between lagged inflow (the sum of SJRWMD discharge near Deland and the Ocklawaha River flow downstream of Kirkpatrick Dam), and crab and shrimp population data. While appropriate to assess water withdrawal effects, these regressions do not assess salinity effects. This report includes a summary of the last quarter century (1986 – 2011) of blue crab and white shrimp landings for

the five counties with borders on the LSJR (Nassau, Clay, Duval, St. Johns, and Putnam) as a means to scale the importance of these commercial fisheries. Note that due to restrictions on commercial shrimping methods in most of the LSJR, landings are associated almost completely with catches from the Atlantic Ocean. However, white shrimp (as well as brown shrimp and pink shrimp) conduct key parts of their life cycle in the LSJR estuary and are considered here for that reason.

USACE also considered the effects of salinity-based changes in SAV (principally eelgrass, *Vallisneria americana*) cover on BMI. This chapter will also include a review of potential effects of BMI from SAV changes identified in Chapter 4 of this report.

## 6.4 Results

### *6.4.1 Salinity Zones and BMI Community Abundance*

This analysis used the daily maximum bottom salinity values to calculate 30-day, 60-day, and 90-day moving average (MA) salinities for all cells in the simulation. The daily maximum salinity is the highest salinity in the hourly model output for each day. The highest MA day for each year in the baseline simulation provided the model salinity data to calculate salinity zones in the project area for each year. Initial comparison of the three MA datasets revealed that the 30-day MA dataset included the greatest changes between years. This is not surprising, as the longer MA time periods reduce variability in the resulting MA datasets. Thus, the 30-day MA results are used here to assess changes in salinity and potential impacts of those changes. Because of high inter-annual variability in the salinity zone areas (Figure 6.1) and because the maximum bottom salinities as calculated already represent a relatively extreme view of bottom salinity dynamics, we used the six year average of maximum salinities or a single year, 1999, to illustrate bottom salinity dynamics. The year 1999 was the first dry (low rainfall) year of three (1999, 2000, and 2001) drought years modeled of which 2001 was the driest.

Average annual baseline maximum bottom salinity zones (Figure 6.1: 6-year average 30-day MA salinity zones) show the general pattern reflected in all alternatives. At the downstream end of the estuary, the baseline maximum bottom salinity zone ≥30 ppt extended well into downtown Jacksonville. The Talleyrand Terminal stretch of the river saw maximum bottom salinities between 18 and 24 ppt. Maximum bottom salinities below 18 ppt did not occur until just downstream of Doctors Lake. While most of Doctors Lake remained in the 0.5 ppt – 5.0 ppt range, salinities in the main channel around Doctors Lake remained between 5 and 12 ppt. Salinities fell below 5.0 ppt near Green Cove Springs and below 0.5 ppt between Green Cove Springs and Palatka (Figure 6.1).

Considering inter-annual variation in baseline condition salinity zone areas (Figure 6.2), the greatest changes occurred in the salinity zone <0.5 ppt at the upstream end of the study area. The LSJR estuary study area salinities (zones of annual maximum 30-day average bottom salinity days for the years 1996 – 2001 inclusive) considered in this analysis never fell below 0.23. In very low rainfall years (1999 and 2001) the lowest salinity zone (<0.5 ppt) at the upstream end of the study area decreased significantly in area (from 43,137 acres in 1998 to 108 acres in 1999) and subsequently disappeared (from 18,988 acres in 2000 to no area in 2001). The greatest change in zone area for those years was associated with increases in the ≥0.5 – 4.99 ppt salinity zone area. The size of the other zones did not vary so dramatically (Figure 6.2), but in general, slight expansions of salinities 12 ppt and higher balanced reductions in the lower salinity zones areas.

A plan view of the shifts in salinity zones shows small changes in location when comparing the baseline, 46-ft, and 50-ft channel depth simulation salinity boundaries (Figures 6.3 and 6.4). Note that the figures do not include the 44-ft alternative boundaries. Those boundaries lie very close to and downstream of the 46-ft alternative boundaries and makes boundary distinctions very difficult.

Upstream shifts in salinity zones at the project 50-year horizon (Figure 6.5 Comparison of Baseline and 50-yr Baseline Horizon Salinity Zones, LSJR North and Figure 6.6, Comparison of Baseline and 50-yr Baseline Horizon Salinity Zones, LSJR South) are similarly small, as are shifts at the 50-yr horizon resulting from resulting from different channel depth alternatives. Note again in the 50-yr horizon alternative figures, the 44-ft alternative does not occur as it lies very close to and immediately downstream of the zones created by the 46-ft alternative).

DRAFT

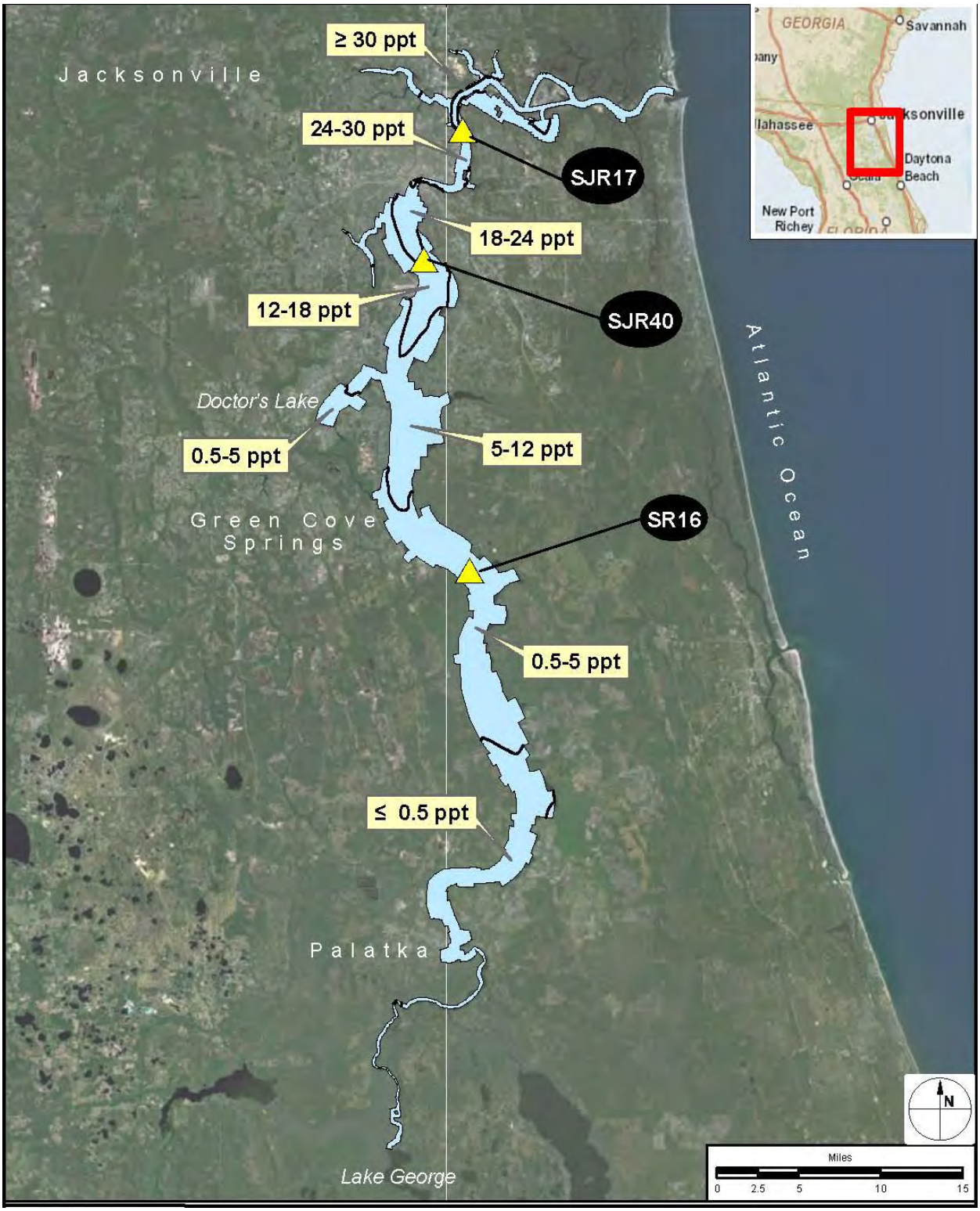


**Figure 6.1** Maximum Bottom Salinity, LSJR, 30-Day Moving Average, Baseline Simulation

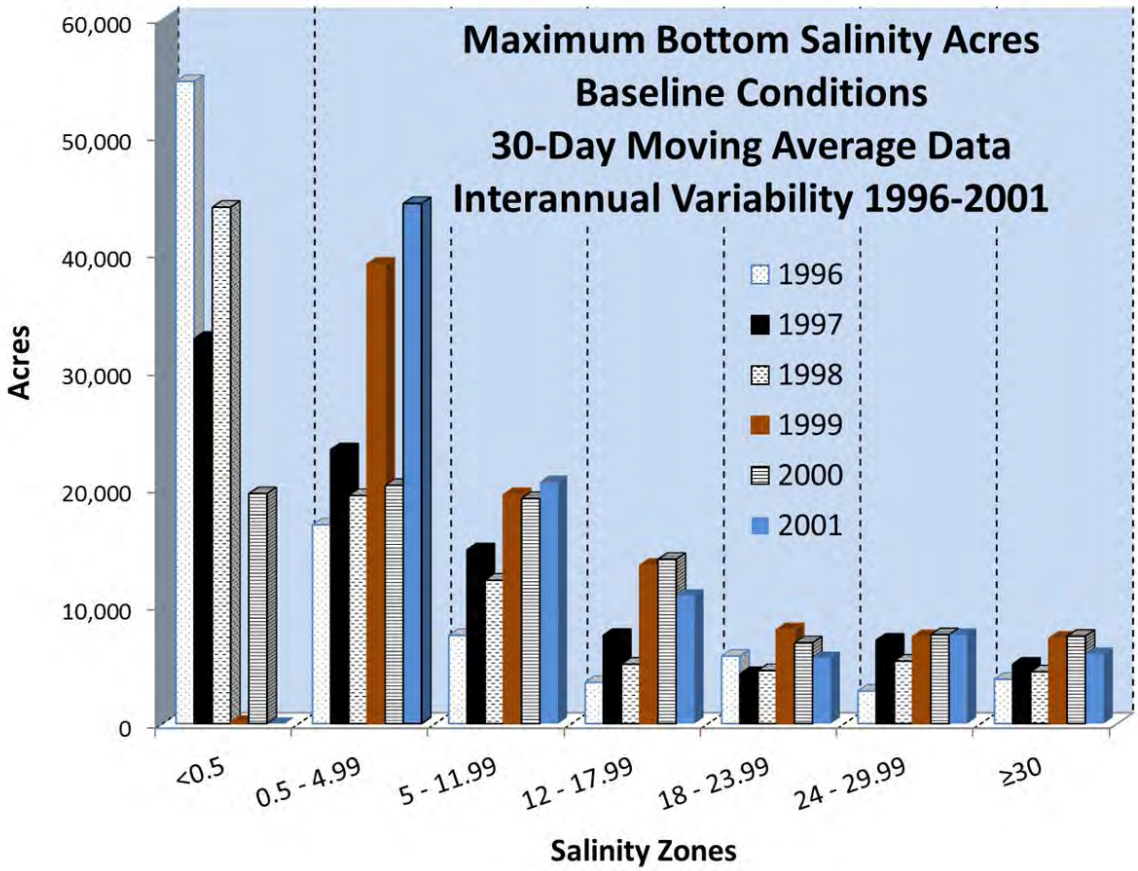


**Figure 6.2** Inter-annual Variability in Salinity Zones for the Baseline Conditions of the Simulation

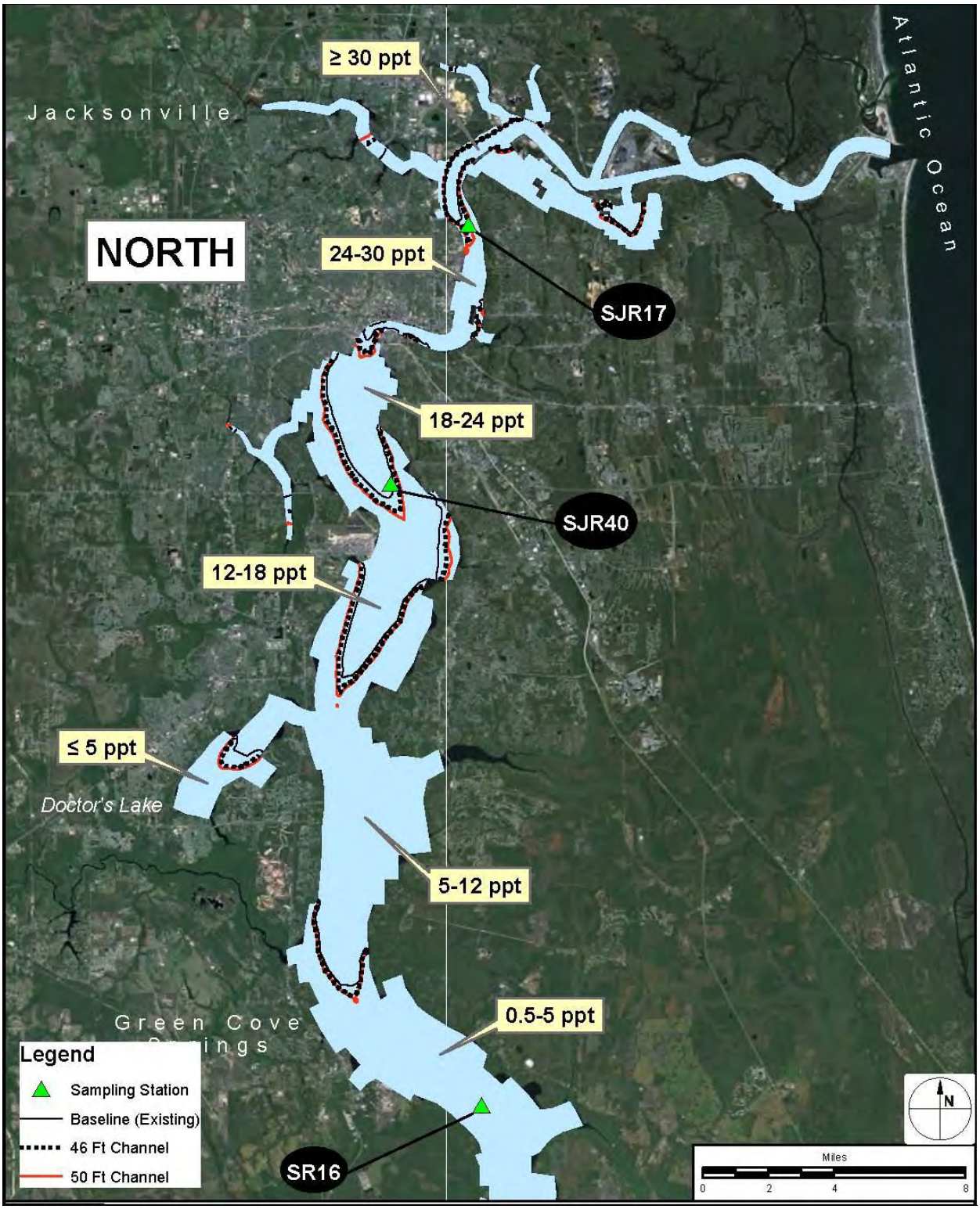


**Figure 6.3** Maximum Bottom Salinity, LSJR North, 30-Day Moving Average, Baseline, 46-ft and 50-ft Channels

**Figure 6.4** Maximum Bottom Salinity, LSJR South, 30-Day Moving Average, Baseline, 46-ft and 50-ft Channels

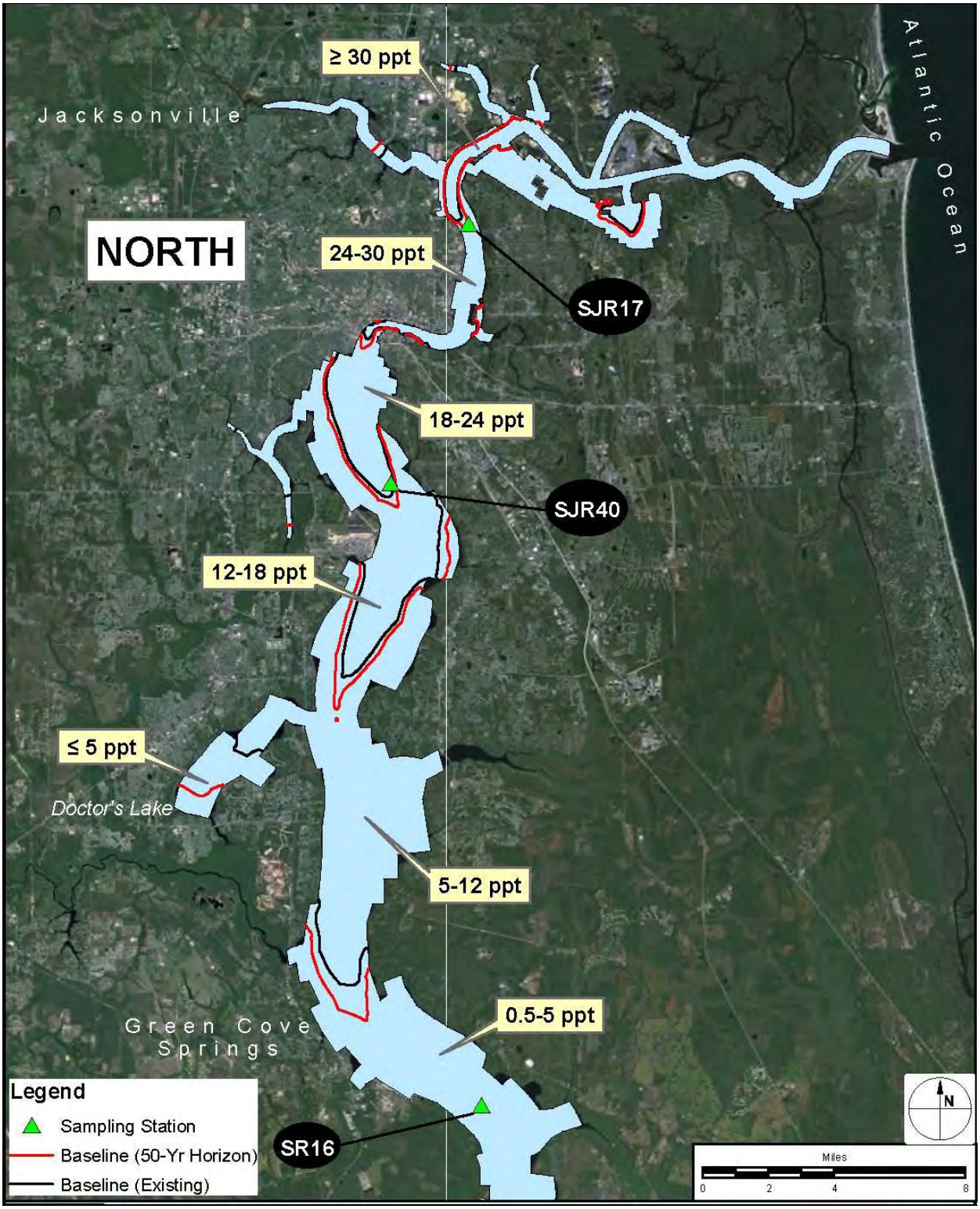


**Figure 6.5** Maximum Bottom Salinity, LSJR North, 30-Day Moving Average, Comparison: Baseline and 50-yr Horizon Baseline

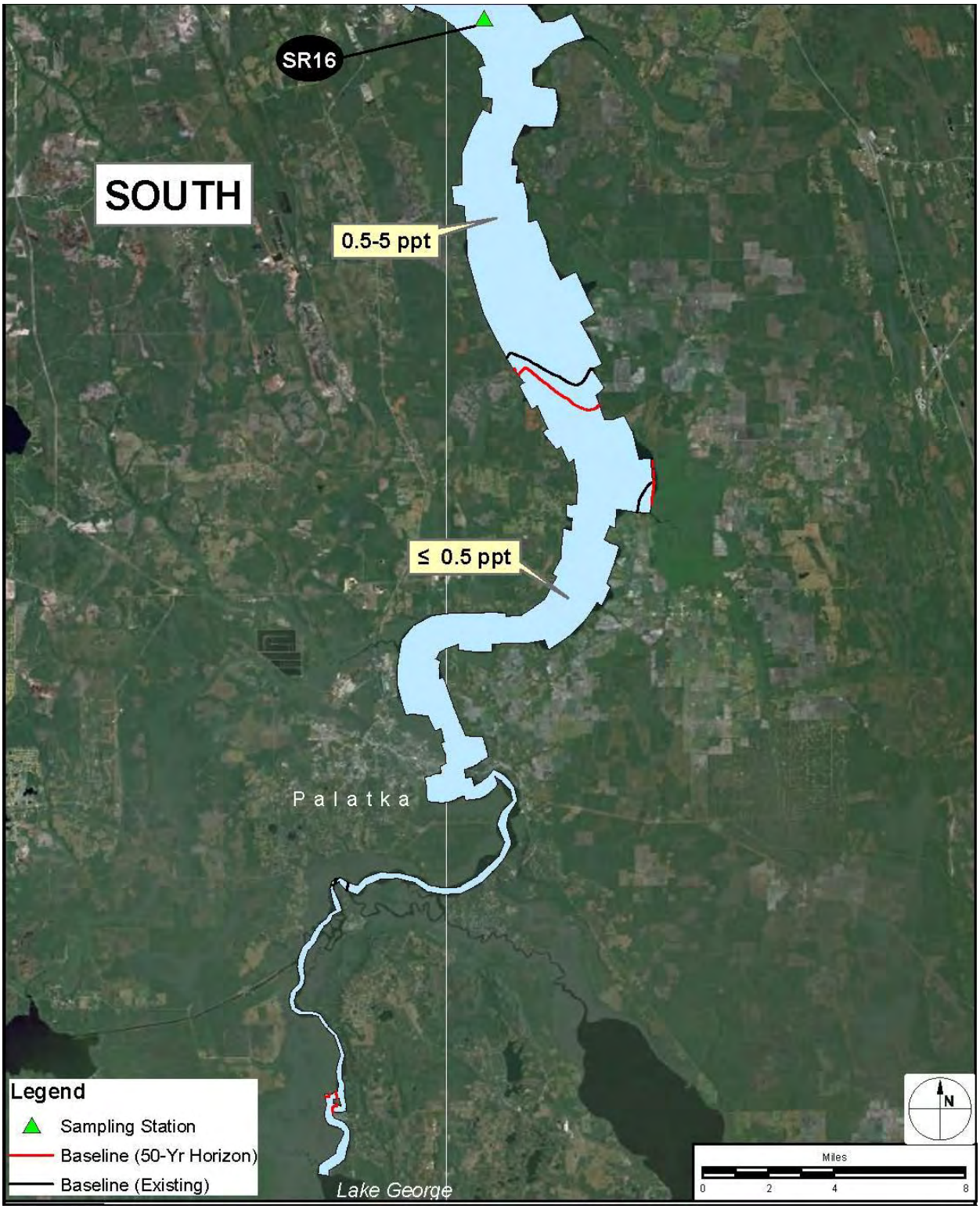


**Figure 6.6** Maximum Bottom Salinity, LSJR South, 30-Day Moving Average, Comparison: Baseline and 50-yr Horizon Baseline

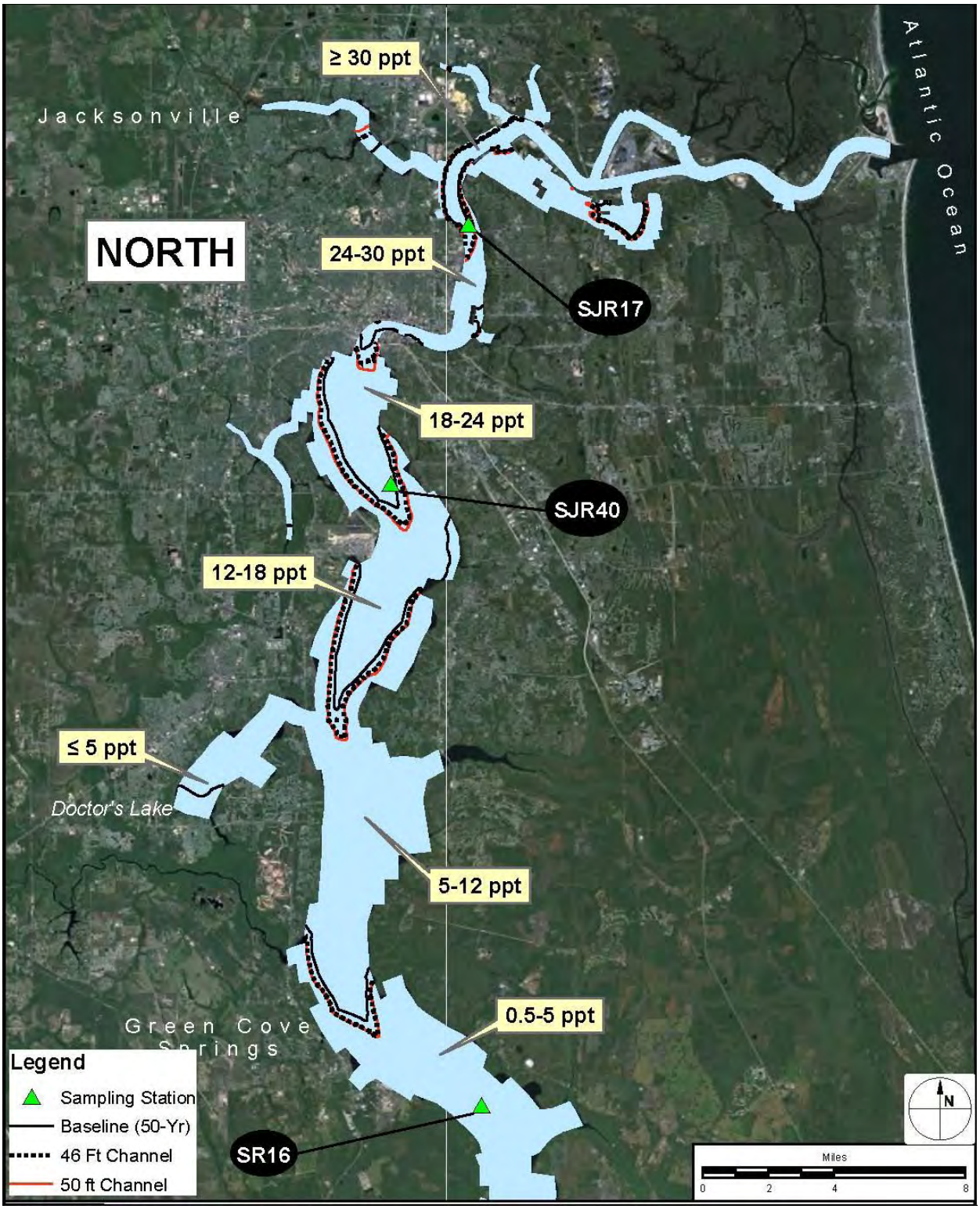


**Figure 6.7** Maximum Bottom Salinity, LSJR North, 30-Day Moving Average, 50-yr Horizon: Baseline, 46-ft and 50-ft Channels

**Figure 6.8** Maximum Bottom Salinity, LSJR South, 30-Day Moving Average, 50-yr Horizon: Baseline, 46-ft and 50-ft Channels

### *6.4.2 Changes in Salinity Zone Areas*

Each alternative reduces the area of the lowest salinity zone and generally distributes the area lost to the <0.5 ppt zone among the ≥0.5 to <24 ppt salinity zones (Figure 6.9). The ≥24 ppt – <30 ppt zone decreased in all channel deepening alternatives and all deepening alternatives increased the salinity zone ≥30 ppt. The physical structure of the river may explain what occurs in the ≥24 ppt – <30 ppt zone. The river narrows in the baseline ≥24 ppt – <30 ppt zone and the bottom shifts from relatively deep (> 30 ft deep) to a much more shallow condition (≤15 ft deep) near the upstream end of the section. This rapid elevation change and the narrowness of the river in that area may tend to minimize change in the middle of the ≥24 ppt – <30 ppt zone and the narrowness of the river may restrict mixing (and thus salinity changes) in that area compared to conditions at the upstream and downstream of that section of the river. The most dramatic percent increases in the 50-year horizon areas of the most saline bottom conditions occur in the downstream end of the river with salinities ≥30 ppt (Figure 6.9).

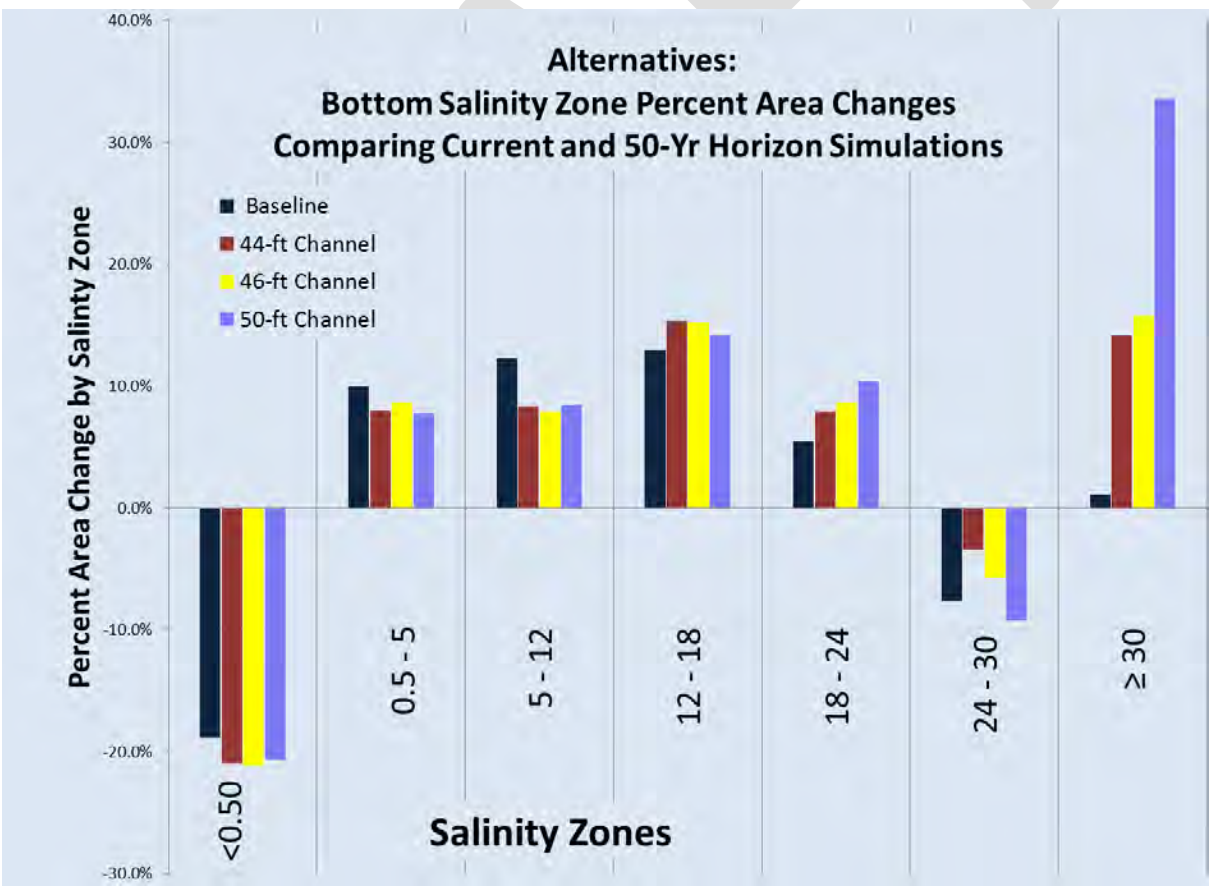


**Figure 6.9** Average Salinity Zone Percent Changes Comparing the Current Baseline to Each Alternative Considered at the 50-yr Horizon

### *6.4.3 Changes in BMI Densities*

A spreadsheet model of Equation 1 constructed by SJRWMD (Edgar Lowe, personal communication April 6, 2012), used the changes in area of each salinity zone with respect to the baseline area to calculate total BMI density changes by deepening alternative. The model calculated the percent change in area of a zone (negative or positive) multiplied by the baseline population density for that salinity range. The spreadsheet could also calculate total abundance of a salinity zone; as these calculations simply reflected the abundance changes as the new density times the change in area, this study does not report abundances.

Because changes in area formed the basis for changes in BMI density, only minor density changes occurred between alternatives and between current and 50-yr horizon conditions. The greatest density changes occurred along the estuary salinity gradient. Densities in the freshest portions of the project area averaged over 6,000 individuals / $m^2$. Moving toward the river mouth, densities fell by about 25% between the freshest zone and salinities of 0.5 ppt to 5 ppt. Densities fell by almost 50% after salinity increased above 5 ppt, and fell between about 30 and 40% with succeeding salinity zones up to 24 ppt. The two most saline zones had very similar densities (between about 500 and 700 individuals / $m^2$ (Figure 6.10).

Only relatively small maximum bottom salinity zone shifts in the river occurred due to deepening alternatives (Figures 6.4 and 6.5) ft to the effects of the 50-ft channel alternative (Figure 6.5) show that the most extreme change shifts the salinity zones relatively little. The figure shows the differences between the baseline and the deepest channel alternative salinity values for the maximum 30d moving average day values in the 1999 simulation. 1999 was chosen because it is the first very dry year of the simulation period.

### *6.4.4 Partial Duration Frequency Analysis of Salinity Behaviors*

Comparisons of salinity level durations at three points in the river (Figure 6.1: SJR17, SJR40, SR16) for alternative simulations provided another way to consider potential impacts of channel deepening on the BMI community. Comparisons of partial duration frequency analysis results (PDFA) for maximum 30d moving average bottom salinity demonstrates the differences in bottom salinity maxima at different locations and showed where salinity durations did not change.

DRAFT

The bottom layer of one simulation model cell provided the data for PDFA analysis of each of the three locations shown in Figure 6.1. The point farthest downstream, SJRMWD Station ID SJR17 showed little change in 30 ppt and 24 ppt salinity duration curves (Figures 6.11 and 6.12). The 50-yr Horizon 50-ft Channel alternative showed some increase in duration for low probability events

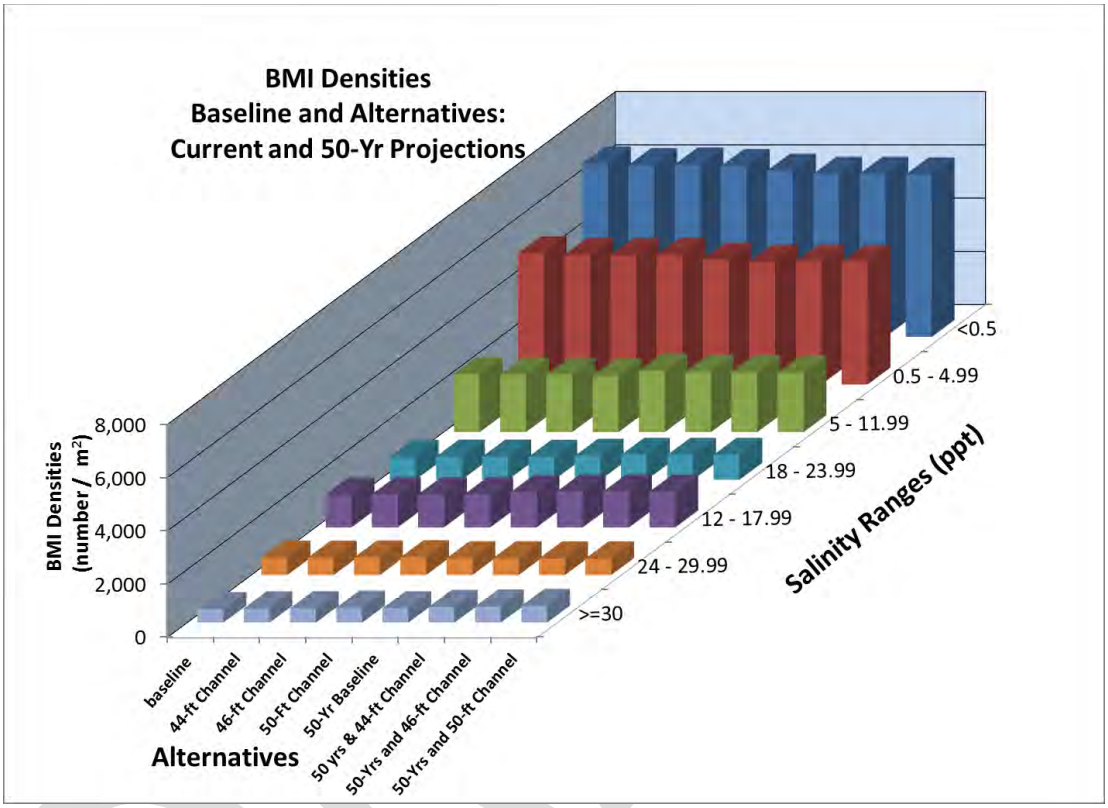


**Figure 6.10** Total BMI Densities for Baseline and Alternative Current Condition Simulations and 50-Yr Horizon Condition Simulations

At SJR17, Channel deepening alternatives did not affect salinity duration probabilities at the 30 ppt and 24 ppt salinity breaks (Figures 6.11 and 6.12). Deepening begins to affect duration of salinity events at 18 ppt (Figure 6.13, 6.14). Channel deepening increases the probability of relatively long-duration (50 – 350 d) salinity events 5% to 10% above the baseline condition. All "long-duration" events probabilities are relatively low (below 20% annual probability of occurrence). The simulations provided similar results for this site under the 50-yr horizon condition. At 12 ppt however, the 50-ft Channel alternative (both under current and 50-year horizon conditions caused clear changes in 12 ppt salinity events (Figure 6.15) with probabilities of between 15% and 30% changes of one year or longer increases in salinities compared to the baseline condition. The project did not appear to greatly affect tested salinity regimes lower than 12 ppt at SJR17.

Changes to salinity regimes at SJR40 (Figure 6.1) do not become apparent until the 1 ppt salinity level (Figure 6.16, 6.17, 6.18). At 5 ppt, all duration frequencies lie atop on another. At 1 ppt, Figure 5-15) each alternative has a distinct probability pattern, with changes beginning at low duration events with close to 40% annual probability. The several alternatives produce very distinct differences for events with 20% probabilities or less at durations of 50 or more days annually. The increase in event probability increases in regular order from baseline to 50-ft alternative, with 50-yr horizon conditions showing greater change than alternatives under current conditions. The differences span about 15% points all with less than 20% probability. At this location, the 0.5 ppt event salinity duration patterns (Figure 6-16) are very similar to the 1 ppt events. The 50-yr horizon 50-ft channel alternative increases salinity events more distinctly than do the other alternatives or the other alternatives compared to the baseline.

At the SR16 location, the upstream-most station of the three tested (Figure 6.1) some unusual salinity dynamics occur. At 5 ppt, the maximum salinity for which the baseline and deepened channel alternatives differ greatly, the baseline condition salinity duration probabilities are in reverse order for the 50-year horizon. This means that the baseline 50-yr horizon condition has the greatest durations at any particular probability, and the 44-ft alternative next in those terms, followed by the 46-ft and 50-ft alternatives in that order (Figure 6.19). A possible hydrodynamic reason for this occurs, if at this location in the river for these alternatives, the ebb tide is stronger (moves downstream more rapidly) for the alternatives than does the baseline condition. Therefore, salinity would tend to mix less and remain higher for longer periods for the baseline condition than for the channel deepening conditions.

Figures 6.20 through 6.24, display PDFA results for 4 ppt, 3 ppt, 2 ppt, 1 ppt, and 0.5 ppt salinities. The series shows the effects of this reversal shifting back to an expected pattern between 4 ppt and effects of channel alternatives at SR16, located most upstream of the three sites tested (Figure 6.1) occurred between 0.5 ppt and 2 ppt salinity. At 0.5 ppt salinity, the 50-ft horizon differences differentiate themselves clearly from the current condition set of alternatives, with greater probabilities of 0.5 ppt salinity events between 30 and 200 days.

DRAFT

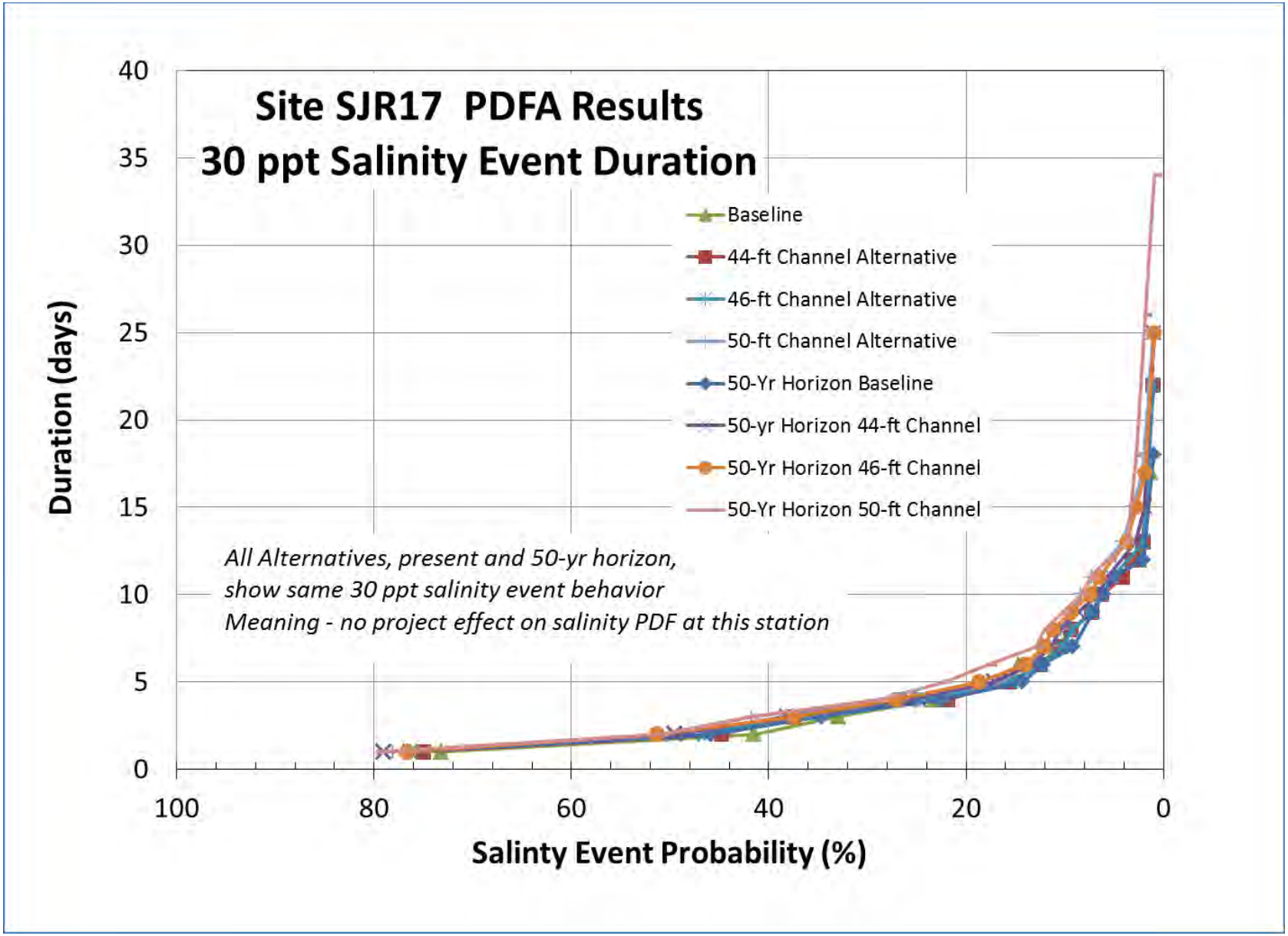


**Figure 6.11** Partial Duration Frequencies for Current and 50-yr Horizon Project Alternatives: 30ppt Salinity Duration Probabilities at Site SJR17

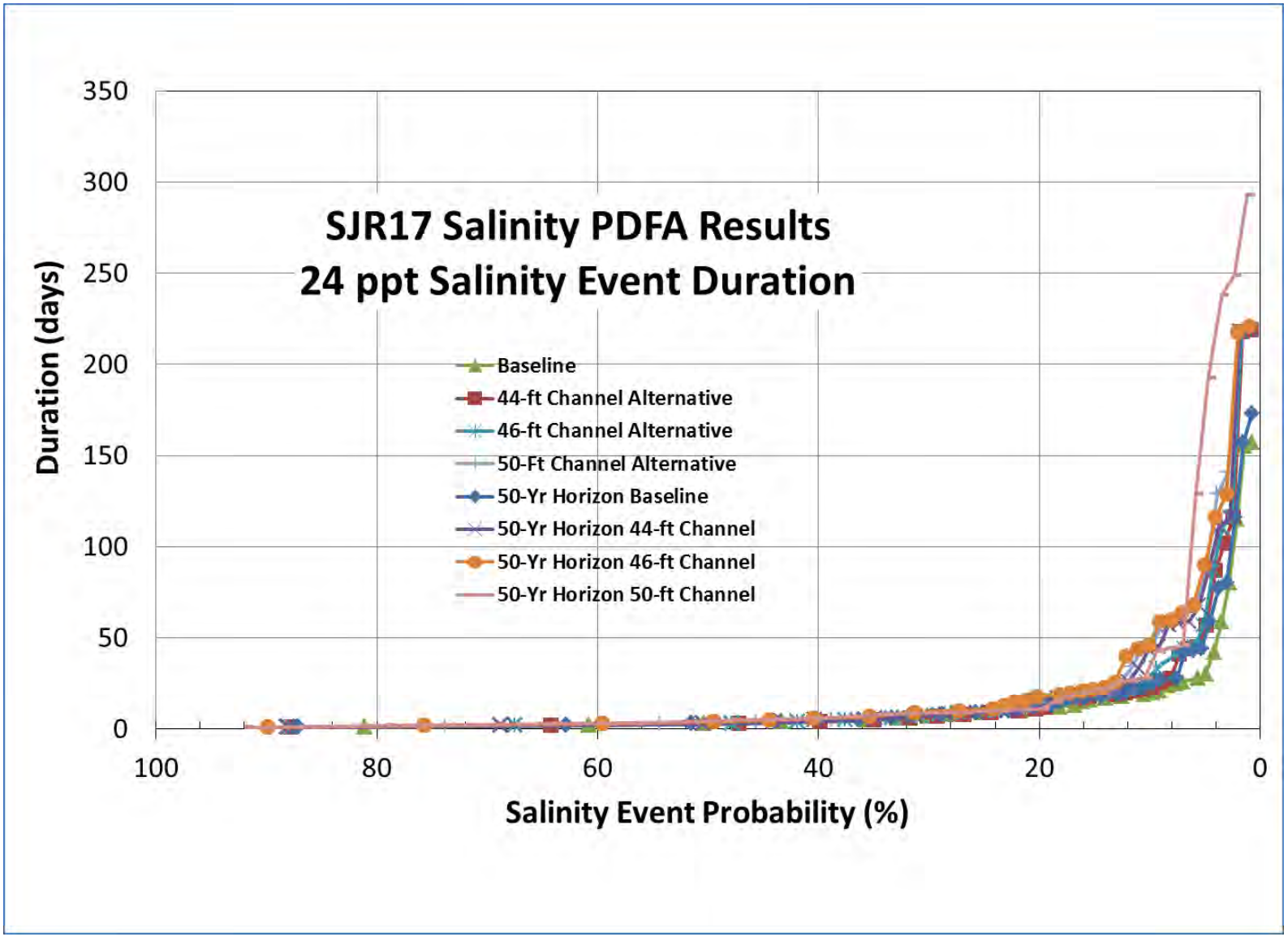


**Figure 6.12** Partial Duration Frequencies for Current and 50-yr Horizon Project Alternatives: 24 ppt Salinity Duration Probabilities at Site SJR17

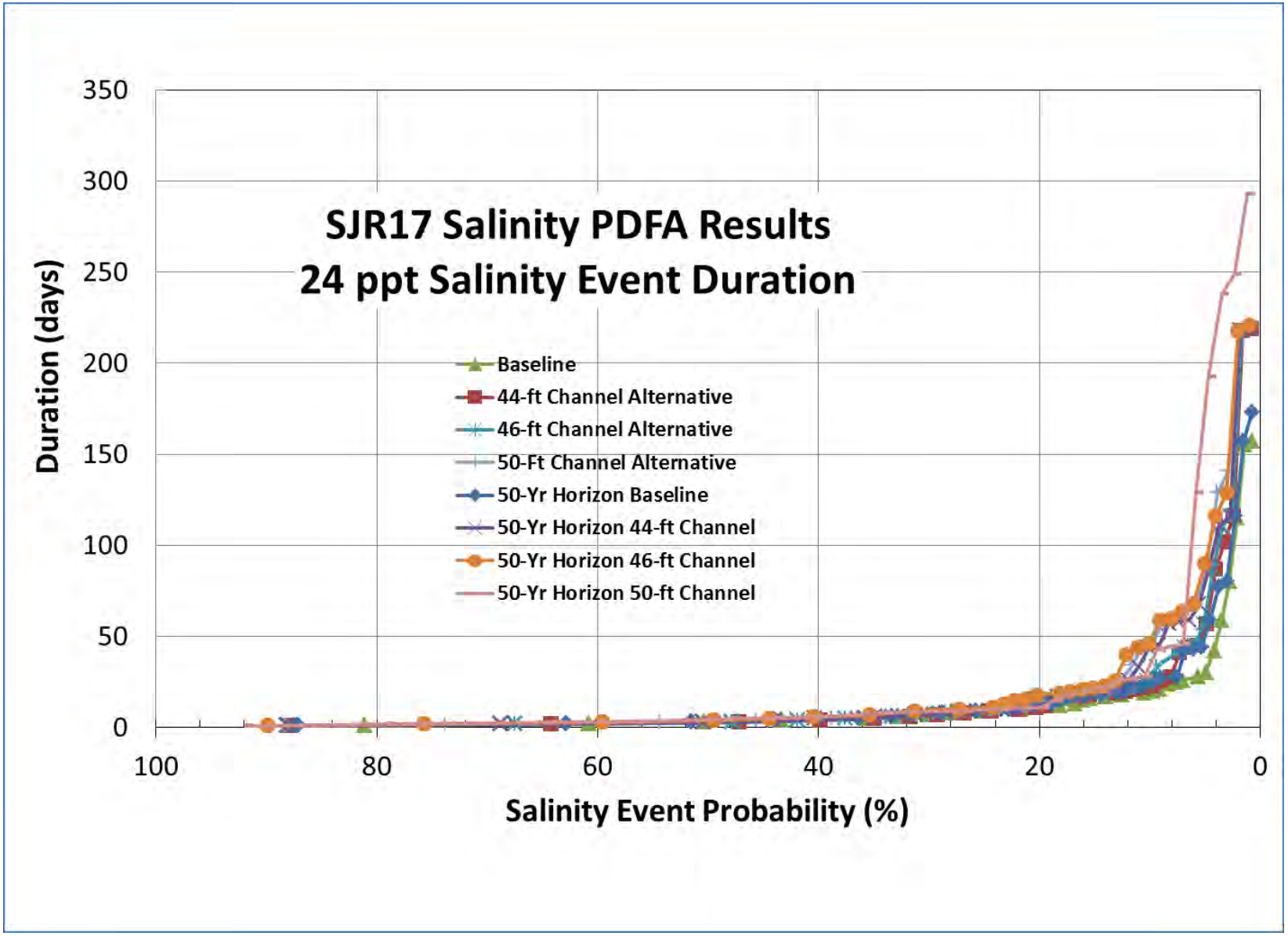


**Figure 6.13** Partial Duration Frequencies for Alternatives under Current Conditions: 18 ppt Salinity Duration Probabilities at Site SJR17

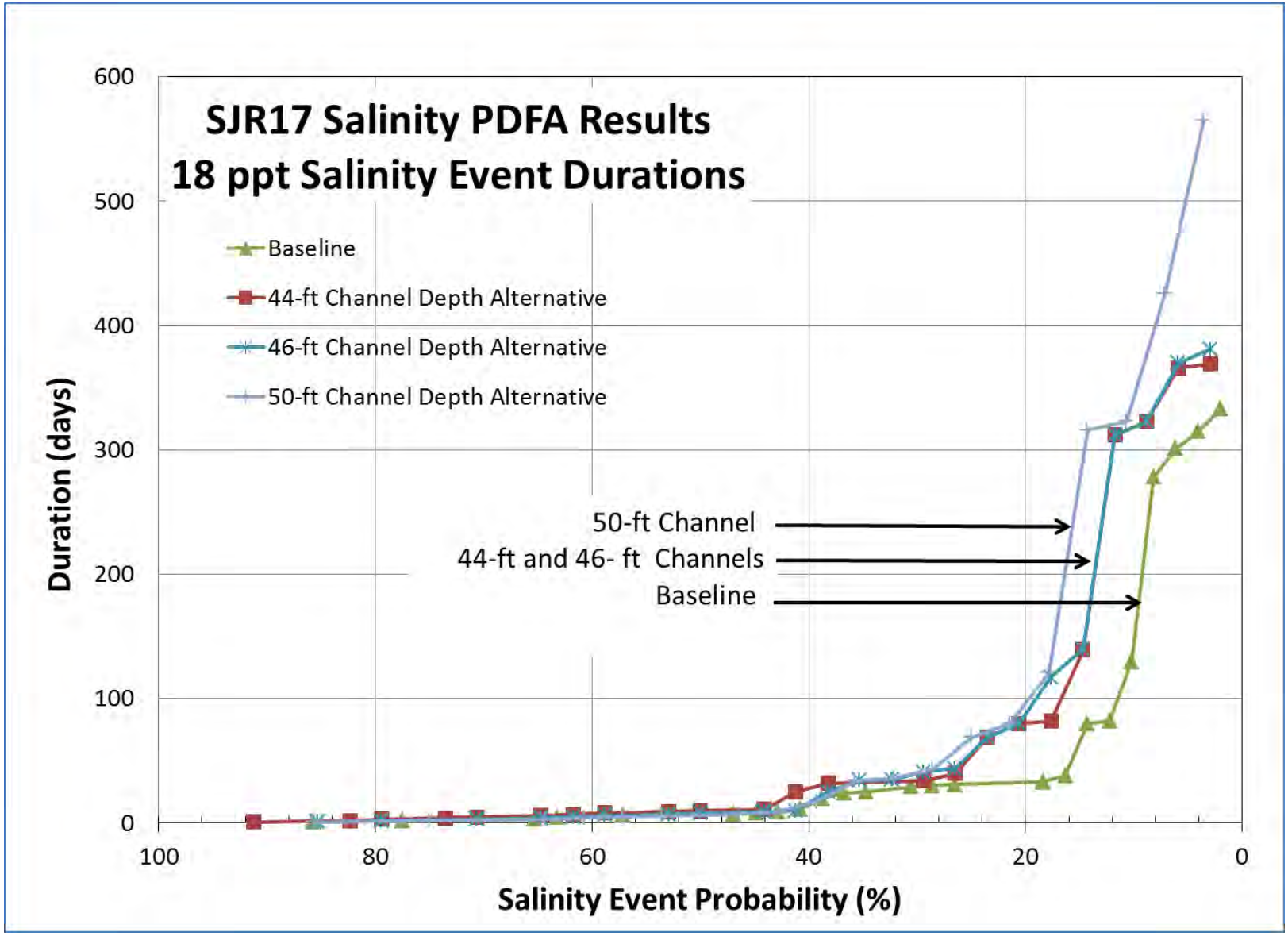


**Figure 6.14** Partial Duration Frequencies for the 50-yr Horizon: 18 ppt Salinity Duration Probabilities at Site SJR17

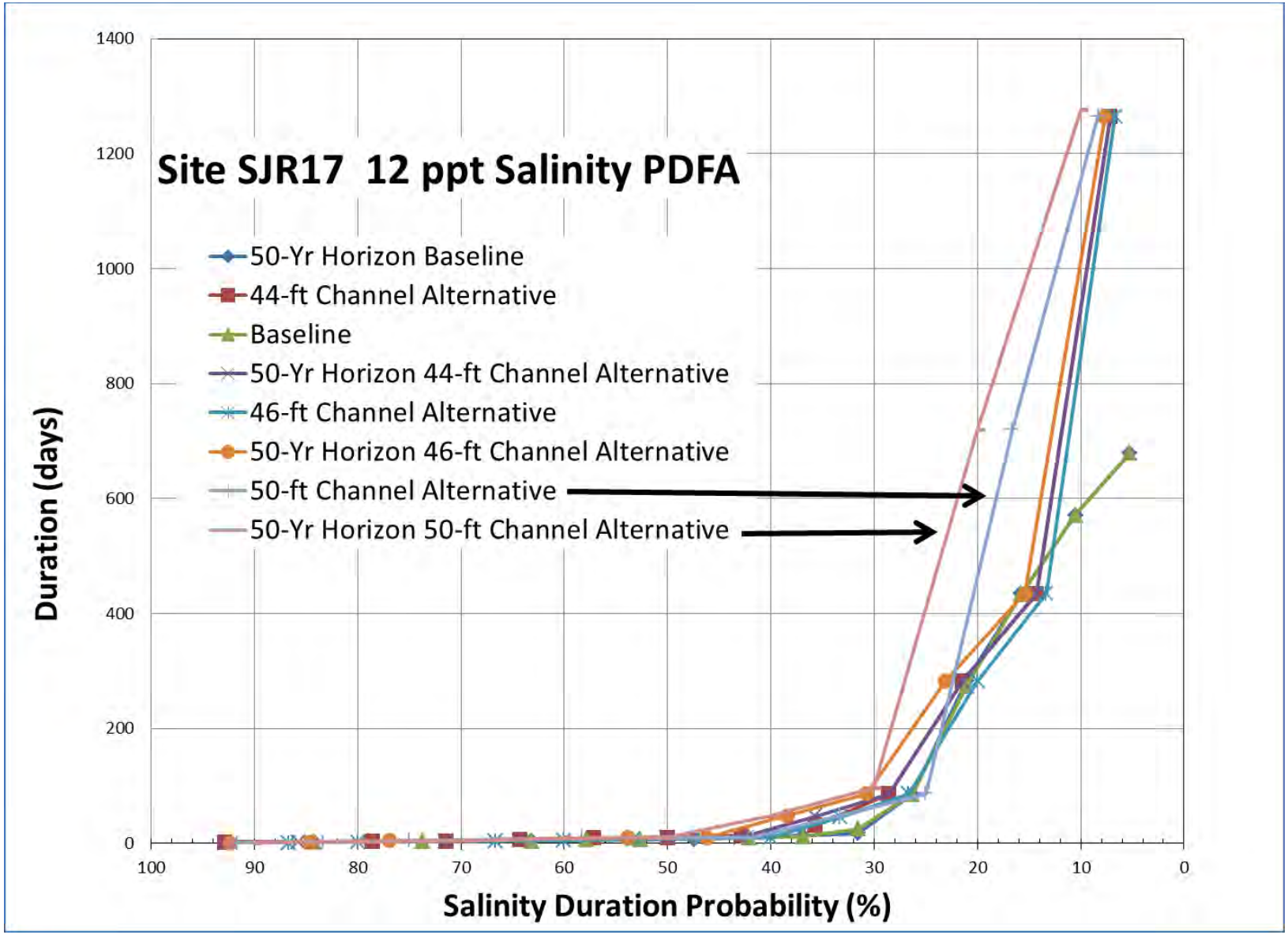


**Figure 6.15** Partial Duration Frequencies for Current and 50-yr Horizon Conditions: 12 ppt Salinity Duration Probabilities at Site SJR17

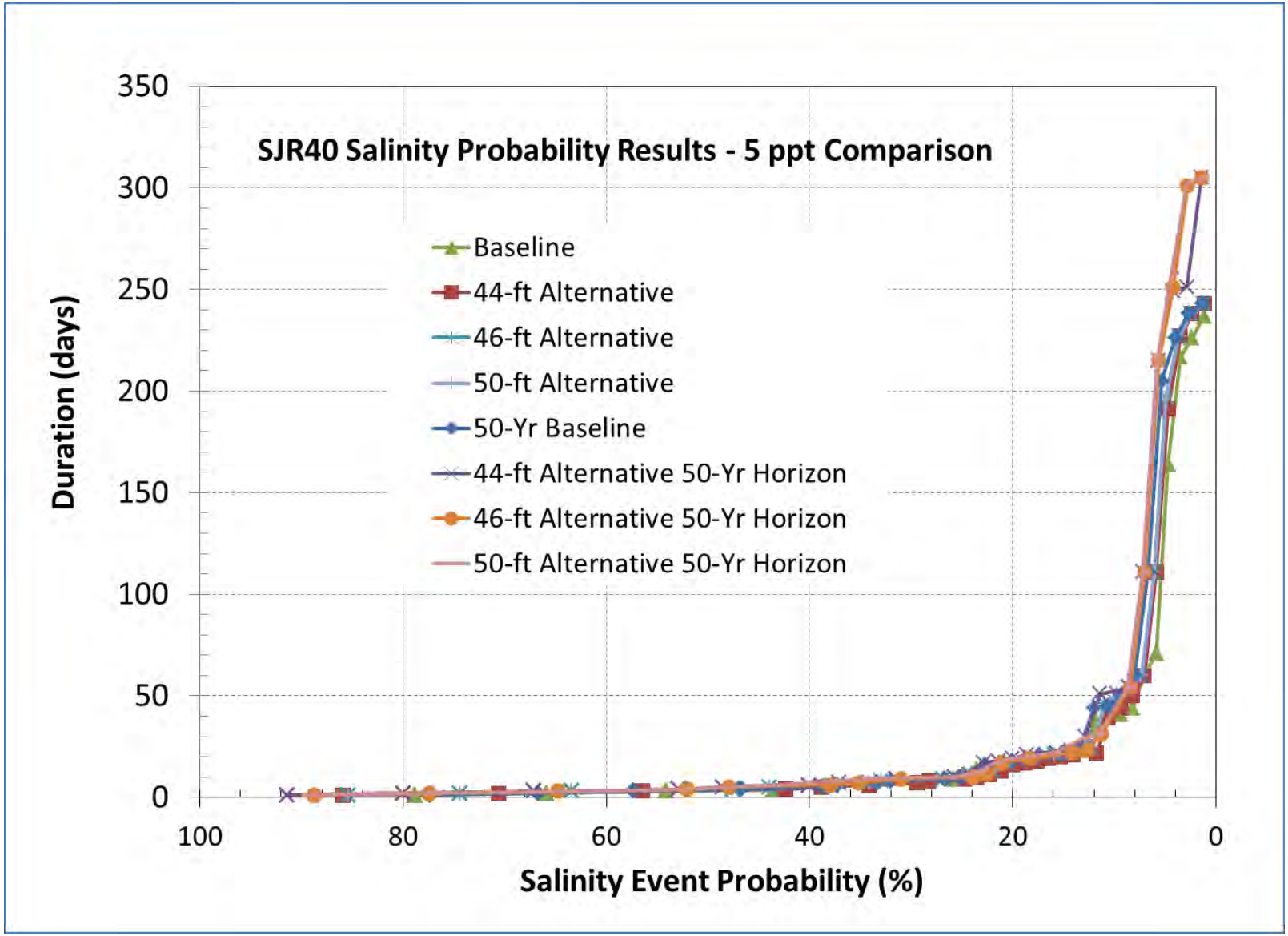


**Figure 6.16** Partial Duration Frequencies for Current and 50-yr Horizon Conditions: 12 ppt Salinity Duration Probabilities at Site SJR17

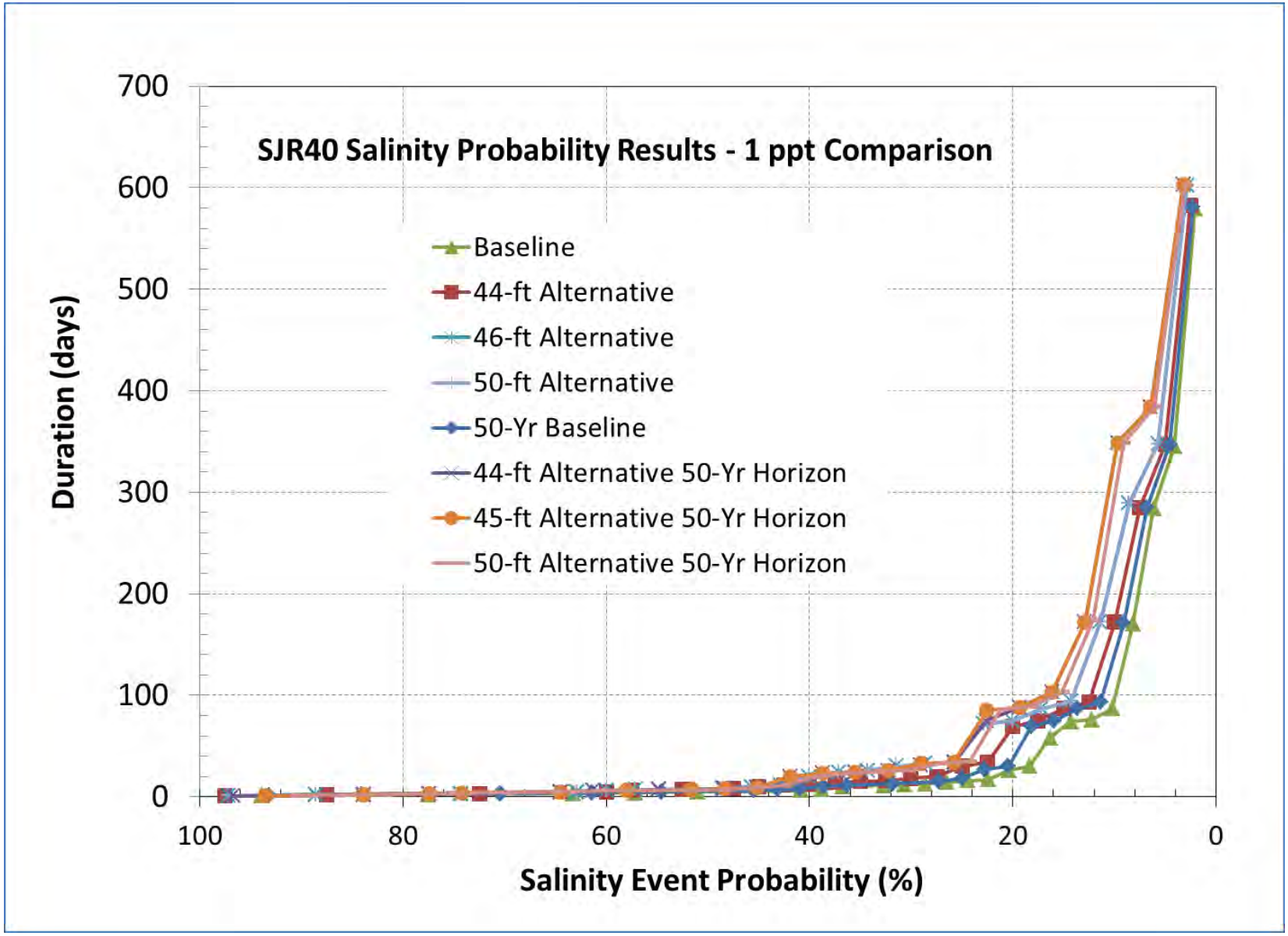


**Figure 6.17** Partial Duration Frequencies for 1 ppt Salinity at SJR 40.

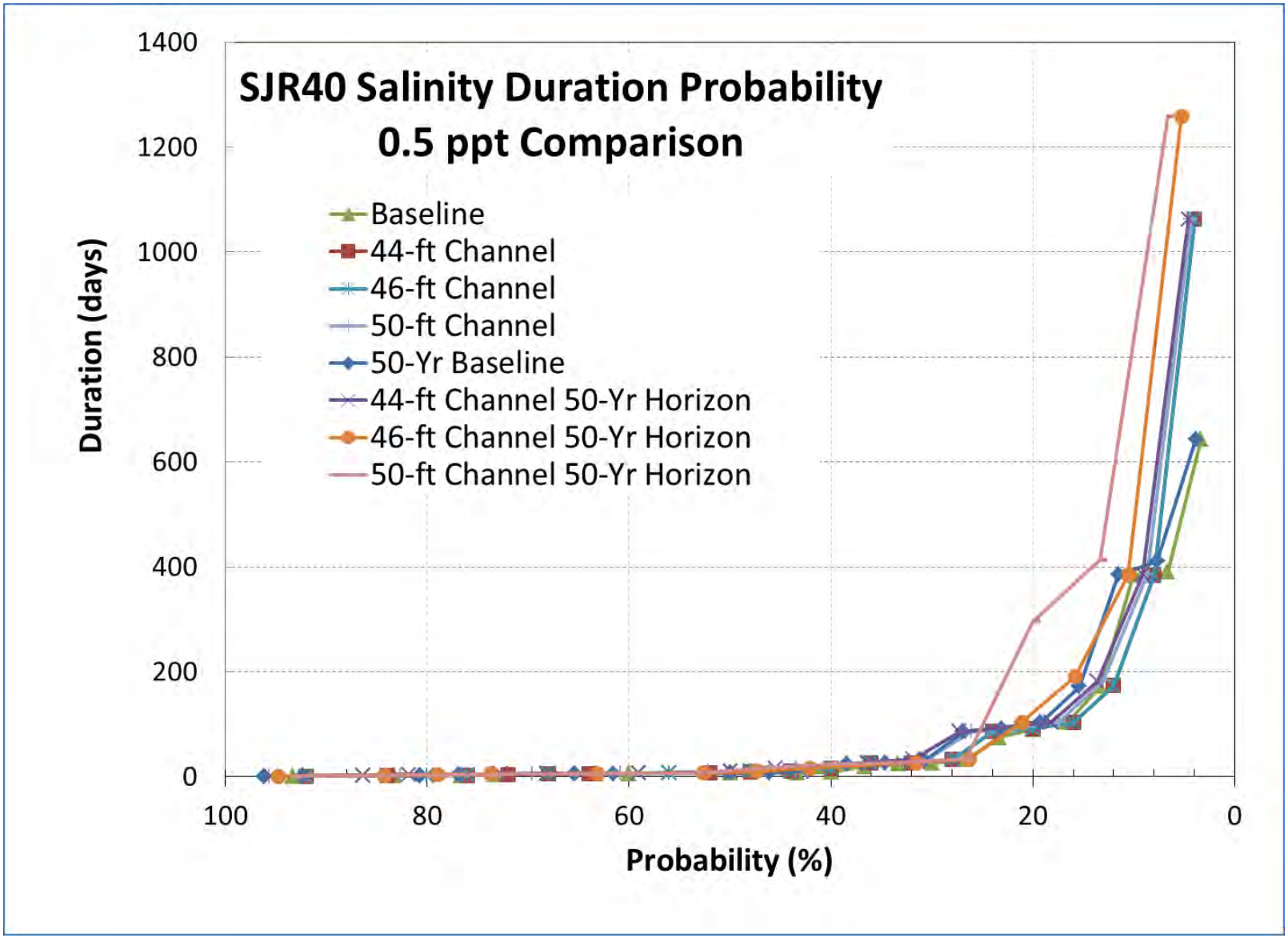


**Figure 6.18** Partial Duration Frequencies for 0.5 ppt Salinity at SJR 40.

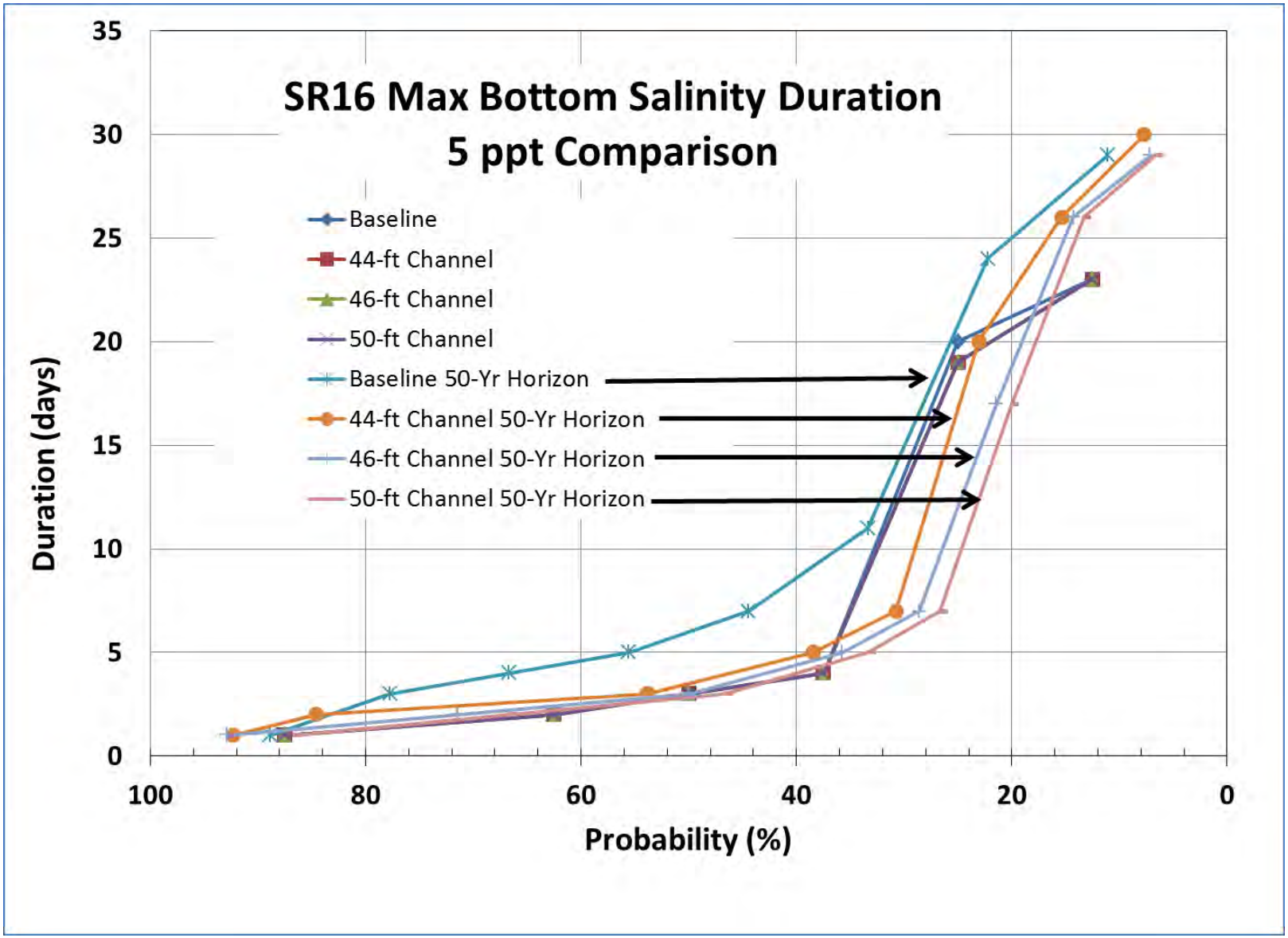


**Figure 6.19** Duration Frequencies for 5.0 ppt Salinity at SR16.

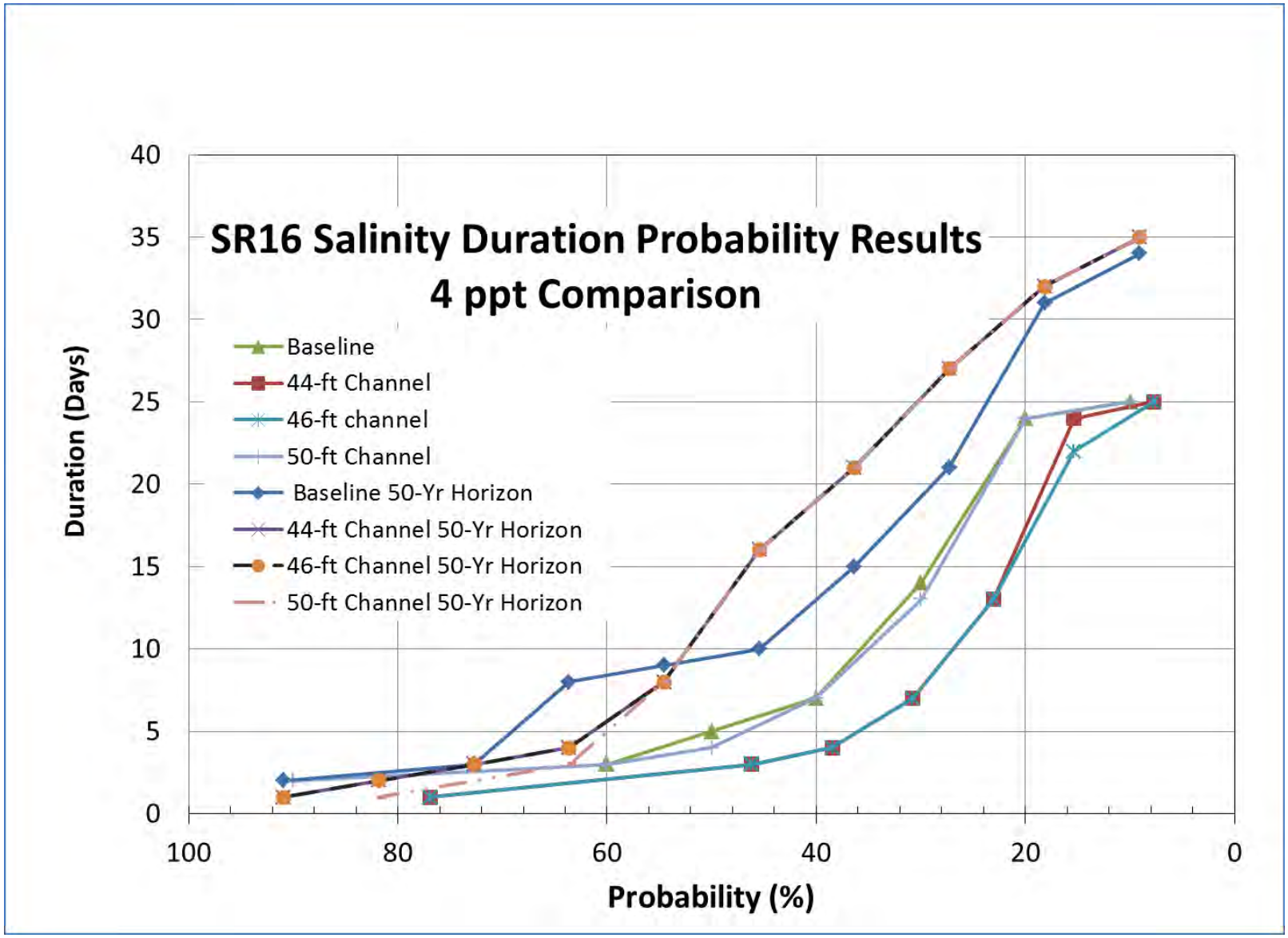


**Figure 6.20** Partial Duration Frequencies for 4.0 ppt Salinity at SR16.

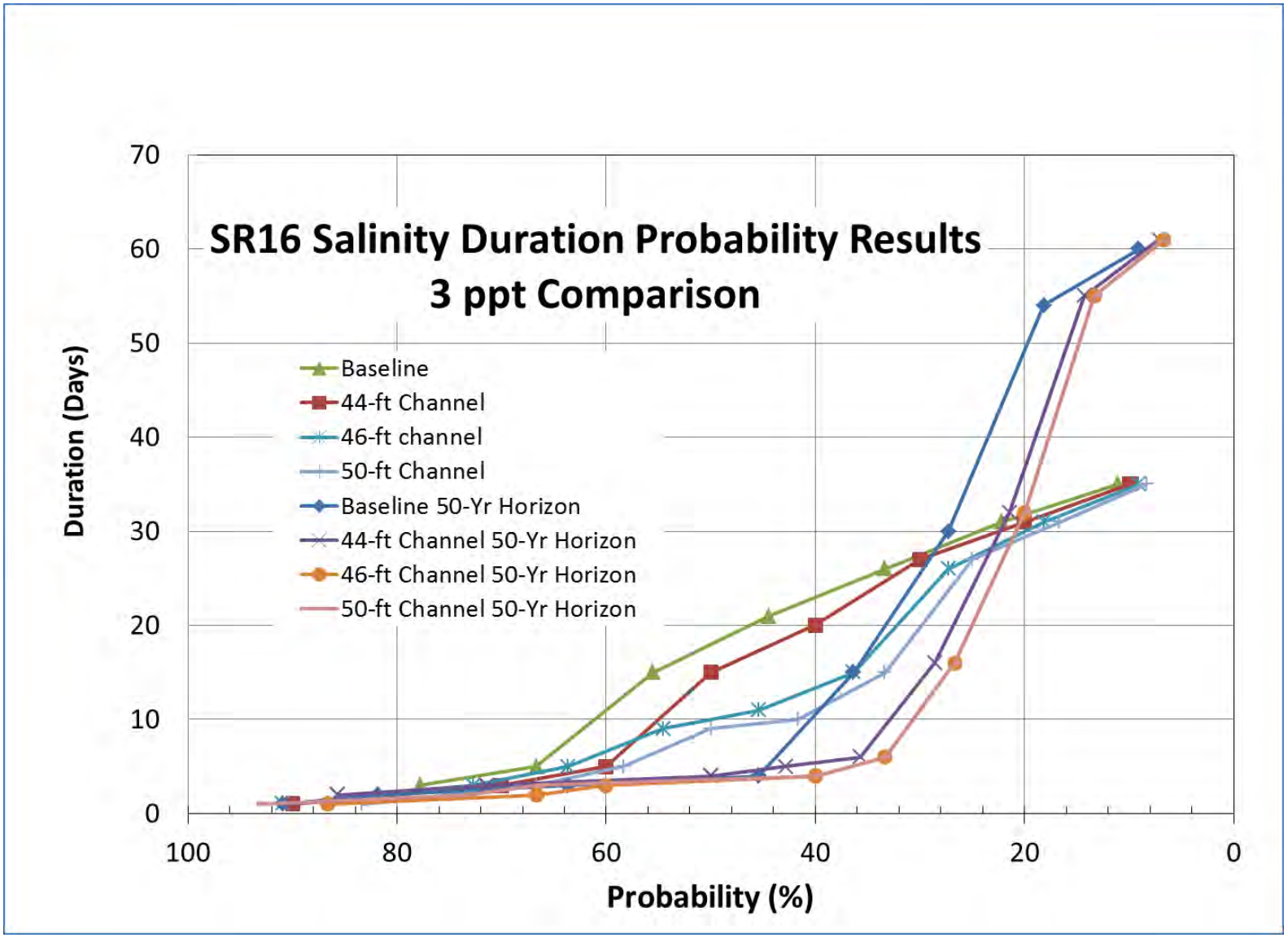


**Figure 6.21** Partial Duration Frequencies for 3.0 ppt Salinity at SR16.

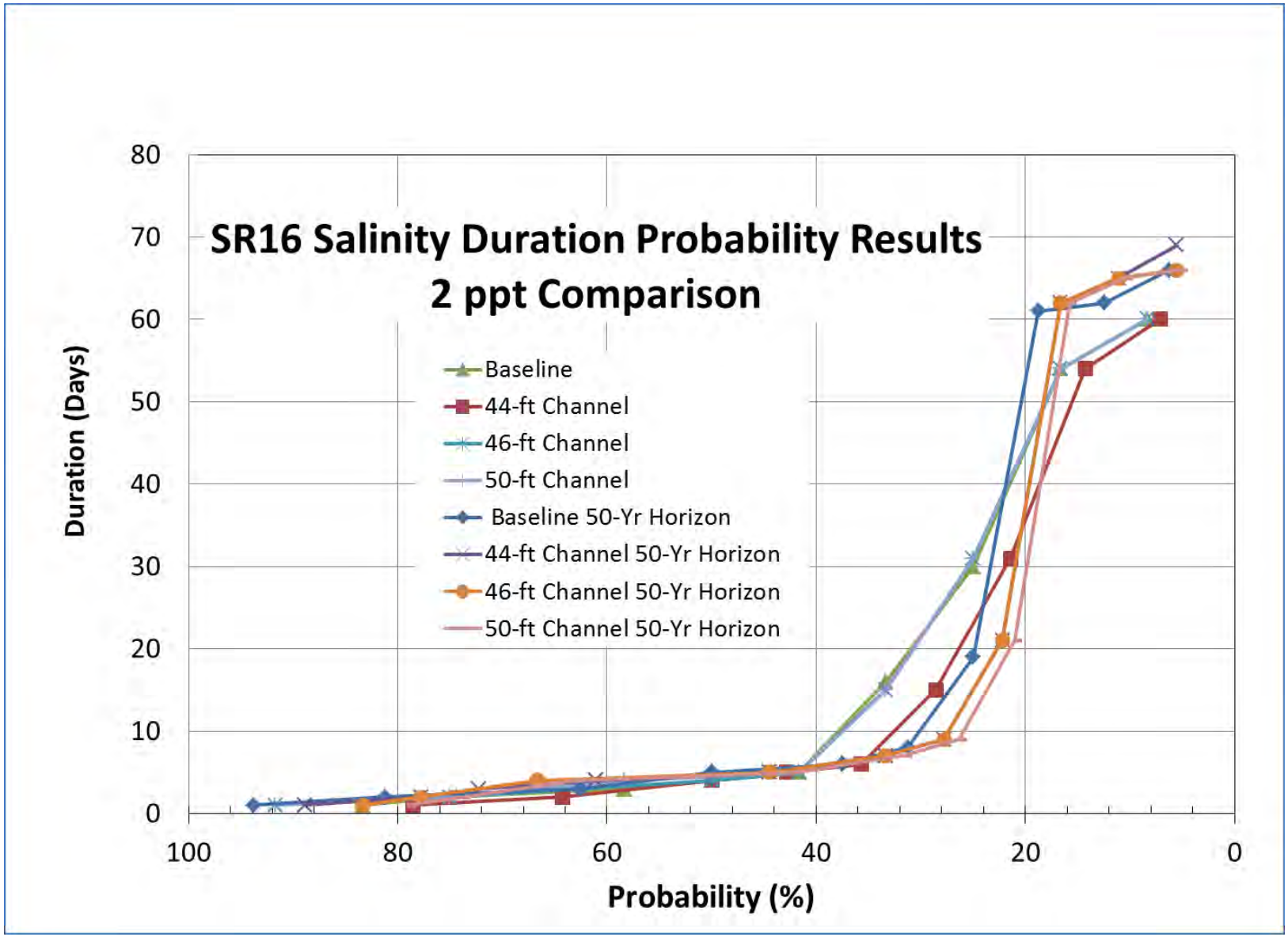


**Figure 6.22** Partial Duration Frequencies for 2.0 ppt Salinity at SR16

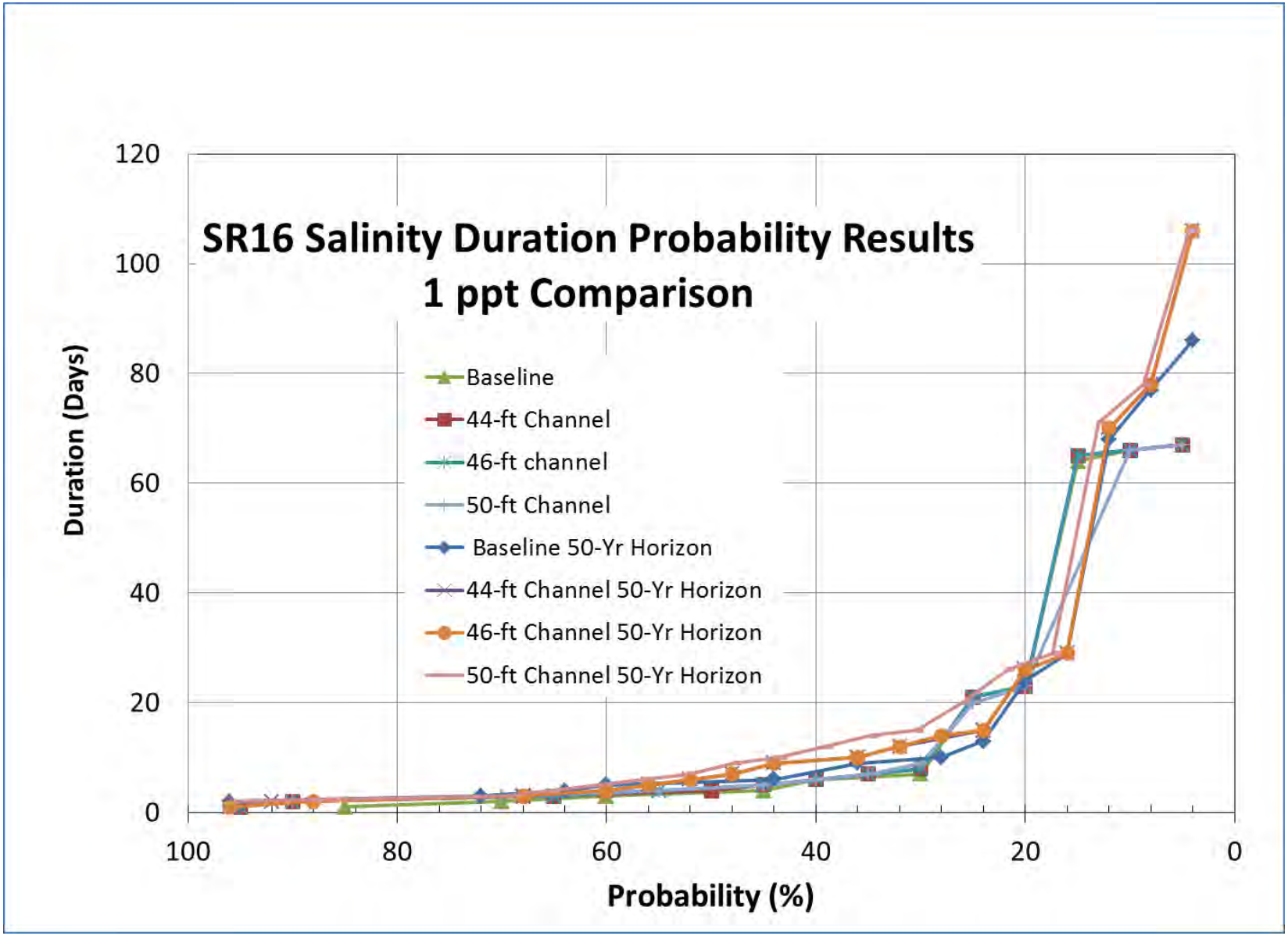


**Figure 6.23** Partial Duration Frequencies for 1.0 ppt Salinity at SR16

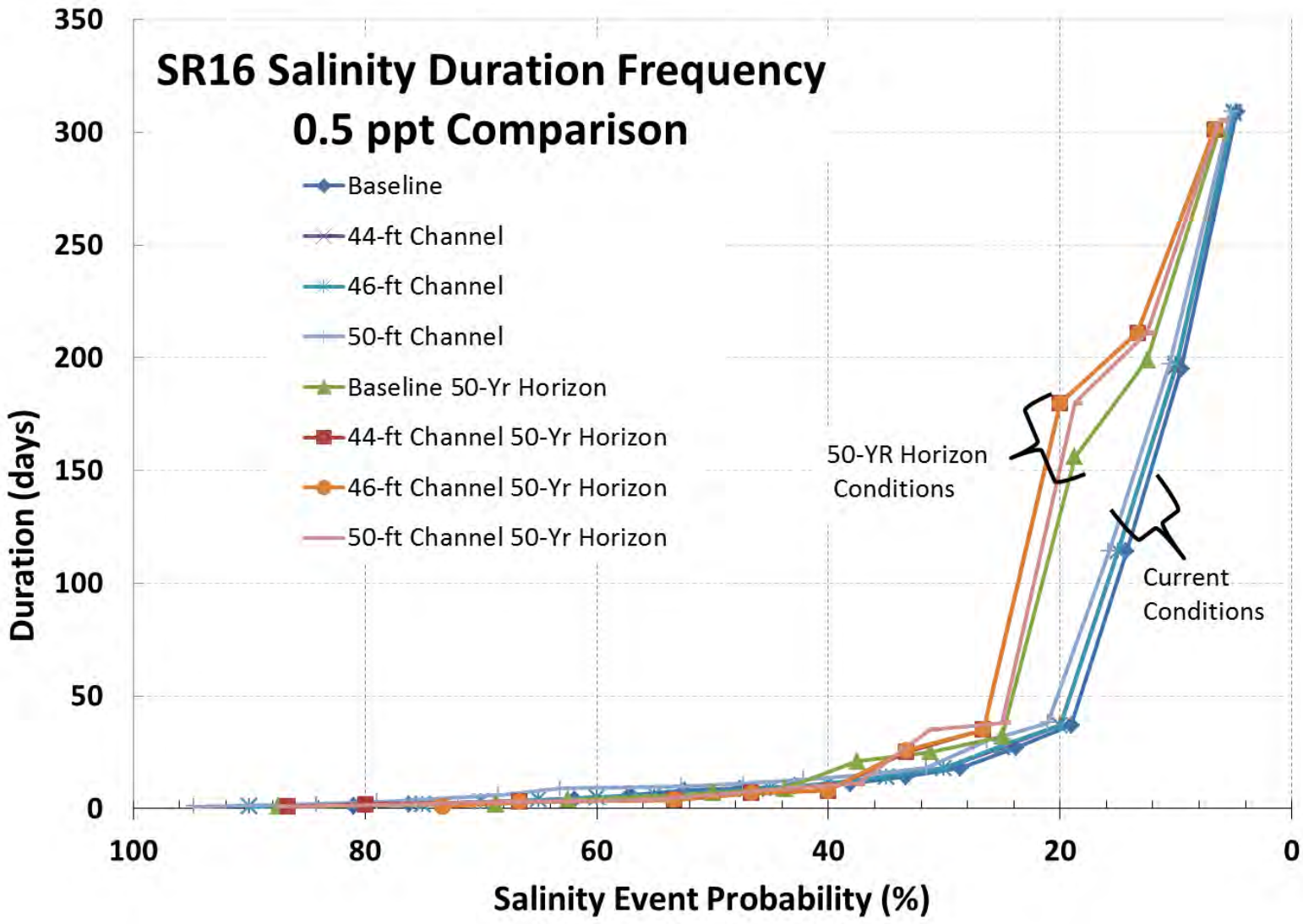


**Figure 6.24** Partial Duration Frequencies for 0.50 ppt Salinity at SR16

### *6.4.5 Effects of Salinity Changes on Commercially Important Species*

Harvest of blue crab (*Callinectes sapidus*) from the LSJR and shrimp (particularly white shrimp *Litopenaeus setiferus,* but also brown and pink shrimp) from the nearshore Atlantic waters (> one mile from shore by regulatory requirement) provide an important seafood harvest industry for the general project area. The LSJR estuary serves as an important component of the life cycle of these taxa. Consideration of proposed salinity changes on these commercially and recreationally important fisheries should evaluate the potential for channel deepening to affect the life history and production of these species.

**Blue crab**

The blue crab, *Callinectes sapidus*, has important ecological and economic functions in the LSJR estuary. Ecologically they are scavengers, processing a wide range of food items, including smaller and/or more sedentary prey (e.g., bivalve mollusks) and provide a common prey item in the diets of many estuarine fishes (Van Den Avyle and Fowler 1984). Blue crabs have provided for a major commercial fishery in the LSJR for decades, but the Florida Atlantic catch generally has been declining since the 1980s, and that statistic is reflected in landings for the five county area including Nassau, Duval, Clay, Putnam, and St. Johns counties (Figure 6.23). The landings of about 800,000 lbs of hardshell crabs, a relatively low landing year, had a value of about $1.04 million (Mattson et al., 2012). The population does undergo large oscillations "often related to extended years of drought when blue crab production is apparently low and wet years when blue crab production is apparently high" (Murphy et al., 2007) (Figure 6.22). Soft-shell crab landings and soft-shell production (by holding crabs in cages until they molt) have become more important in recent years (Figure 6.23) but still only account for a relatively small fraction of overall blue crab landings (http://myfwc.com/research/saltwater/crustaceans-marine-arthropods/blue-crabs/).

Sempsprott (2011) summarized blue crab life history and distribution literature, stating, "there is a strong relationship between blue crab survival and habitat quality," pointing to Apalachee Bay and Suwannee Sound/Waccasassa Bay, which have the highest blue crab production in Florida. These very open bays have large areas of tidal marsh and freshwater inflows that reduce salinities that would otherwise result in salinities more closely reflecting the salinities of the larger gulf waters. Guillory et al. (2001) cited alternation of freshwater flows (closely correlated with salinity) nutrient pollution and pesticide runoff as a major components of declines in south Florida blue crab populations.

**Effects of Predicted Changes in Salinity on Blue Crab**

Deepening of the Federal navigation channel in the first 14 miles of the river has the potential to affect blue crab populations in two ways: alteration of spatial and temporal salinity patterns and/or alteration of critical habitats (especially SAV) or food resources. Evaluation of the potential for effects also requires consideration of the complex life history of the species, with both planktonic (larval) and benthic (juvenile and adult) phases. Jacoby (2012) provided a detailed review of salinity effects on blue crabs that found literature indicating that many life stages of this crab exhibit a fairly wide degree of salinity tolerance, particularly juvenile and adult crabs, which are the main benthic life stages that occur within the river mouth in the lower river and estuary. Based on this review of the literature, in conjunction with the EFDC model-predicted salinity changes described above, salinity changes due to upstream water withdrawals will be unlikely to have an adverse impact on populations of blue crab in the St. Johns River. Minor upstream advances in salinity regimes do not greatly impact the total area of salinity zones, and upstream of Shands Bridge, the greatest potential channel depth produces only very minor increases in frequency and duration of salinity concentrations. For the 50-yr horizon scenarios, alternative-driven changes are similar in degree to the current condition changes, except that the baseline salinities will have slightly farther upstream.

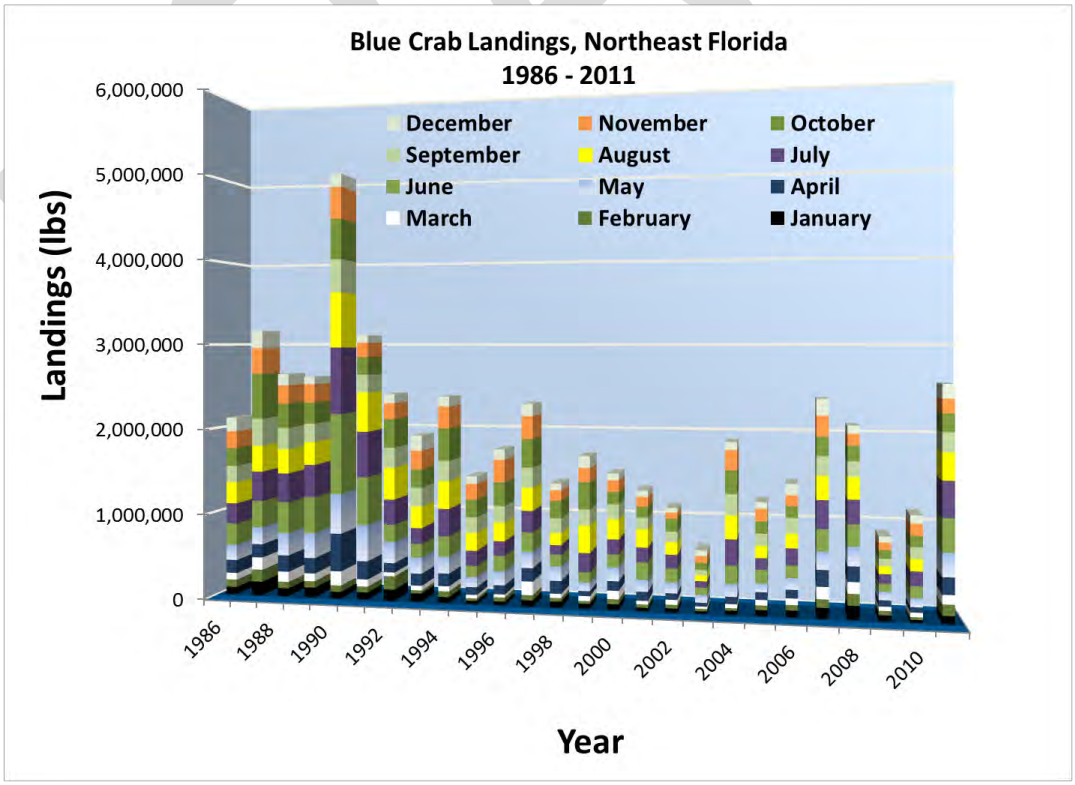


**Figure 6.25** Annual Blue Crab Landings from Five Northeast Florida Counties 1986 – 2011

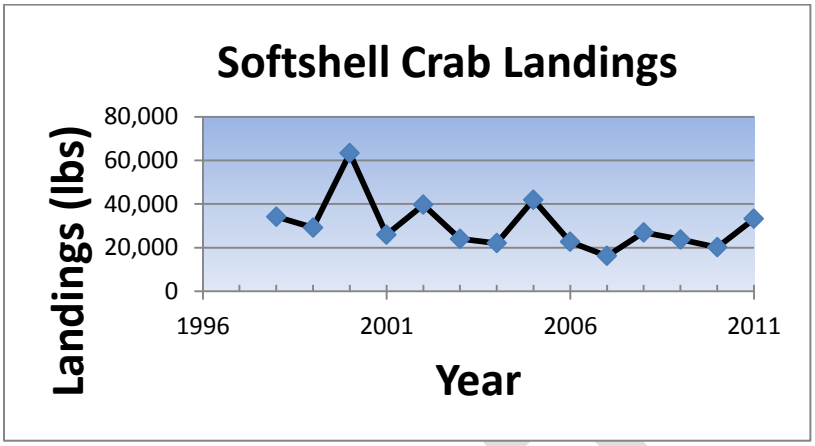


**Figure 6.26** Soft-shell Crab Landings 1998 – 2011, for Five-County Northeast Florida Region.

The WSIS study (SJRWMD, 2012: Mattson et al., 2012) evaluated the effects of water withdrawals in the middle and upper St. Johns River on the lower river and estuary. Mattson et al. (2012) concluded that for the "worst case" (greatest upstream withdrawal) scenario, blue crab abundance would increase. The WSIS analysis reaches conclusions opposite to other findings (see above) that extended drought periods (where less water flows down to the estuary) are correlated with decreased crab abundance. Mattson et al. also found that "increased freshwater inflows to the St. Johns River estuary (from the USJRB Projects and 2030 land use) result in reduced blue crab abundance…possibly due to downstream movement of areas of preferred salinity into areas of less-than-desirable habitat (downtown Jacksonville and the Port of Jacksonville). Imposition of withdrawals on these future conditions results in increased crab abundance (Table 4.16)." This conclusion counters findings of crab abundance analyses reported in Sempsrott (2011) and Murphy et al. (2007), where upstream, low salinity conditions are important for female crab reproductive processes, high salinity habitats are sought by juveniles and males, and high inflows are correlated with greater crab abundance in the Florida estuaries studied.

Impacts to SAV habitat from channel deepening (due to increased salinities) appears minor (Chapter 3), and the loss of habitat would not likely impact blue crab populations. The PDFA results for the downstream most site analyzed (SJR17 , above) suggested no changes in salinity regimes at 30 ppt salinity and only minimal changes at 24 ppt salinity, with clear changes due to the deepening alternatives at 18 ppt in that location. These results suggest that the marshes at the mouth of the river would experience only minor shifts in salinity events, maintaining the quality of those marshes, at least with respect to salinity regimes. The findings concerning changes in salinity regimes also suggests that the prey items for the blue crab would not greatly change either. Given the plasticity of the blue crab diet, it

appears that small episodic salinity changes would not likely impact the species abundance or biomass production.

**Shrimp**

White shrimp (*Litopenaeus setiferus*), brown shrimp (*Farfantepenaeus aztecus*), and pink shrimp (*Farfantepenaeus duorarum*) occur in the lower St. Johns River estuary. Of the three, white shrimp are by far the most abundant of the three in commercial landings, followed by brown shrimp and pink shrimp. These shrimp are generally abundant. As consumers of detrital material these species link primary and secondary production by their role as a major food item for many estuarine fishes (mostly sciaenids (e.g., red and black drum, spotted sea trout, croaker), which are also a target of recreational anglers.

Jacoby (2012) provides an overview of the distribution, life history, and ecology of the three penaeid shrimp species and detailed discussion of habitat preferences including (among others) sediment, vegetation, and salinity. He noted that the three shrimp species in nauplii through postlarval stages are tolerant of a wide range of salinities and salinity with optima near marine conditions. Laboratory experiments have shown that larvae can be successfully reared at a range of salinities between 18 – 34 ppt (Perez-Farfante 1969). Juvenile white shrimp in particular has a salinity optimum of less than 10 psu; the other two species are more broadly tolerant as juveniles. As they enter maturity, white and brown shrimp have very broad salinity optima; pink shrimp prefer salinities above 25 psu.

Commercial shrimpers in the St. Johns estuary and primarily in the nearshore Atlantic outside the mouth of the river harvest penaeid shrimp both for food and for recreational fishing bait. Commercial landings of white shrimp in the five-county northeast Florida area associated with the lower St. Johns River (Nassau, Duval, Clay, St. Johns, and Volusia) for the period 1986 through 2011 (Figure 6-24) shows shrimp landings in the general project area have increased relatively steadily over the past decade. Brown and pink shrimp landings have not been nearly so consistent (Figure 6-25). The Shrimp alliance estimated that northeast Florida landings between 2005 and 2008 were worth between $1.97 and $2.09 / lb of live shrimp, which would have a total market value of about $6,000,000 to $10,000,000 in those years. The majority (if not all) of the shrimp landings in the five-county area are assumed to come from populations supported by the St. Johns River estuary. (http://www.shrimpalliance.com/new/downloads/RequestforCertificationforNEFloridaasFiled.pdf)

Recreational fishing (primarily with a cast-net) for shrimp also has many practitioners in the LSJR during the late summer (Mattson et al., 2012). The landings from this recreational sector are not quantified in Florida, but surveys in other southeastern states suggests it could be substantial (Muncy, 1984).

FWC has estimated that the shrimp harvest is at or beyond the maximum sustainable and are suggesting that a larger minimum harvest size might help sustain or improve the value of the fishery (http://myfwc.com/media/195867/penaeid_shrimps.pdf). In the same article, the authors noted that the white shrimp harvests were most abundant in and adjacent to areas with extensive estuarine marshes. "White shrimp were landed mostly in Nassau, Duval, St. Johns, Brevard, and Dade counties on the Atlantic coast and Franklin County in the panhandle region of the Gulf in areas adjacent to extensive saltwater marshes and high freshwater run-off."

**Effects of Predicted Changes in Salinity on Shrimp Species**

Changes in salinity zones and salinity duration probabilities do not appear to have changed sufficiently in the mainstem LSJR to impact the penaeid shrimp populations. Assuming that salinities in the river main channel are relatively well reflected in the adjacent estuarine marshes near the mouth of the river and in Mill Cove, none of the proposed alternatives would appear to have significant impacts on blue crab or shrimp populations.

DRAFT

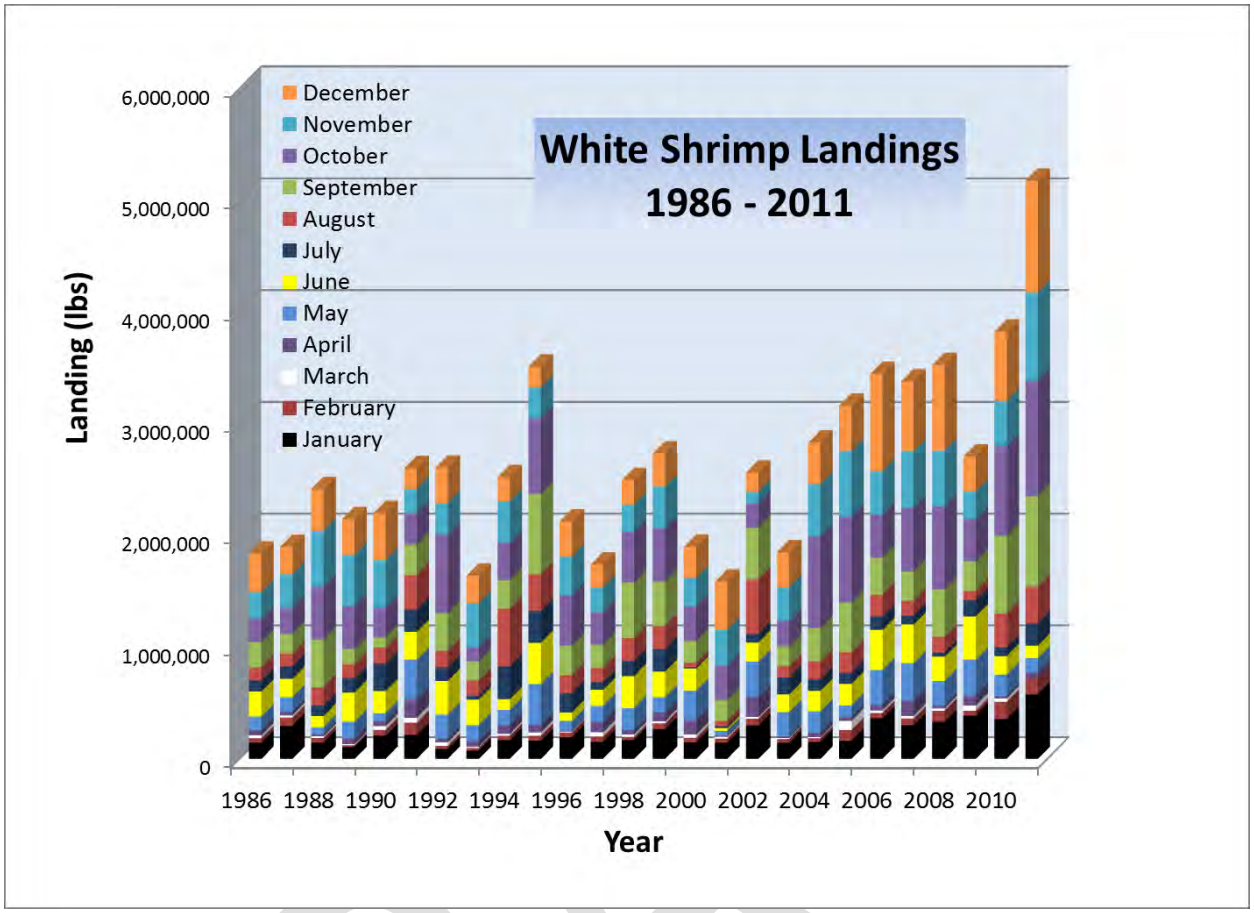


**Figure 6.27** White Shrimp Landings Recorded by Florida Fish and Wildlife Conservation Commission. Monthly, 1986 – 2011

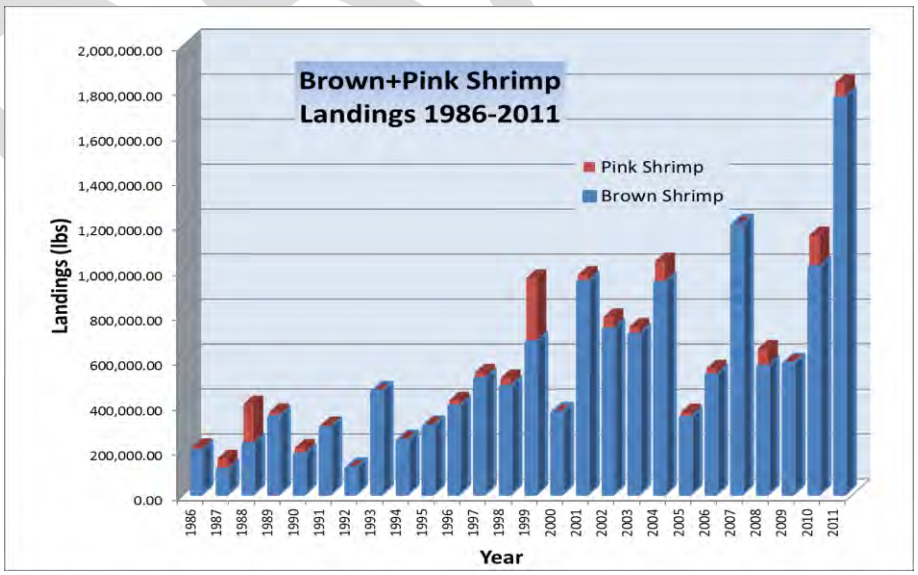


**Figure 6.28** Brown and Pink Shrimp Landings Recorded by Florida Fish and Wildlife Conservation Commission. Monthly, 1986 – 2011

### *6.4.6 Potential Effects of Channel on Estuarine Benthic Communities*

This chapter used the understanding of LSJR BMI communities developed in Mattson et al. (2012) and methods used to assess effects of water withdrawal on potential changes in BMI communities described in that same document, to assess changes in BMI communities due to a deepened Federal navigation channel in the first 13 miles of the LSJR. The methods applicable to this study suggested that only minor changes to the BMI community would occur, even for the deepest (50-ft) channel examined as an alternative in this report. The greatest changes in the river occur as a result of inter-annual variability in salinity. The effects identified by calculating salinity zones, both visually in the river and by comparing acreage, indicated that the shifts occurred as small upstream movements in the salinity boundaries. This becomes significant only when the changes affect SAV, which is an important habitat for BMI, although only in a small fraction of the river bottom cross section upstream of the Acosta Bridge. The conclusion reached by Mattson et al. regarding estuarine BMI community impacts from water withdrawal scenarios is equally applicable to channel deepening alternatives "because overall benthic community abundance was highest in the lowest salinity zones and because many of the benthic taxa and taxa groups examined by Montagna et al. (2011) exhibited peak abundance at or below 5 ppt, we maintain that loss of low salinity habitat (< 5 ppt) due to water withdrawals would be the principal concern for estuarine benthic communities."

Modeling indicated that the greatest changes in salinity occurred in the 0.5 ppt zone (the most upstream portion of the study area) as a result of inter-annual variation in salinity regimes. In dry years 1999 and 2000 the salinity increased above 0.5 ppt throughout the project study area (from just below Lake George to the river mouth). PDFA demonstrated that The greatest changes in salinity with the conditions created by different potential channel depths occurred upstream of Station SJR17, which occurs slightly upstream of the mouth of Mill Cove, for salinities around 18 ppt. Moving upriver, salinity affects ended at Station SR16, located near Shands Bridge, at the 0.5 ppt salinity level. Comparison of the most disparate conditions, current baseline and the 50-yr horizon alternatives, suggested the following:

- Inter-annual variability was a greater source of variability in terms of benthic salinity zones than were any of the alternatives.
- PDFA suggested that above about 18 ppt and downstream of Station SJR17, salinity dynamics were not greatly affected by the alternatives tested.
- Changes in salinity dynamics would most likely affect those BMIs in areas with background salinities less than 5 ppt, and within those areas, those with SAV.

- Location of salinity zones shifted only slightly upstream, regardless of alternative or time period considered.
- Percent habitat area losses of bottom habitat in the less than 0.5 ppt range generally distributed themselves over the salinity zones between 0.5 ppt and 18 ppt.
- The 18 -24 ppt salinity zone lost area in each comparison (baseline to 50-yr horizon 44-ft, 46-ft, and 50-ft salinity zones). This likely occurred because of the river morphology (narrow width and presence of a depth sill in that area, centered around the Tallyrand Terminal)
- Considering the comparison that should yield the greatest changes (baseline to 50-yr horizon alternatives) the ≥30 ppt salinity zone expanded the most compared to the other zones of the 50-yr horizon alternatives (>30 percent increase). All other percent changes, positive or negative, remained less than about 20%.
- The analyses performed did not suggest that project alternatives would impact commercially important invertebrates (blue crab and shrimp).

### *6.4.7 Uncertainties*

The quantitative relationships between salinity and benthic communities and populations developed by Montagna et al. (2008, 2011) for the LSJR benthic communities and populations, provided a solid basis on which to interpret the salinity trends identified in the analyses described in this chapter. The biological trends in the river also fall well within the generally recognized influence of salinity gradients on benthic macroinvertebrates. The sources of uncertainty for the BMI community except for the commercially important species are the same as those recognized by Mattson et al. (2012) "Most sources of uncertainty are from limitations on the data collected from a segment (e.g., segment 1 [the downstream most end of the river] had relatively little existing data), or from the moderate levels of certainty associated with the predictive models. Overall, the levels of uncertainty associated with assessment of effects of benthic communities of the lower river and estuary are low to medium due to the development of moderately strong predictive models, strong supporting evidence from the literature, and good understanding of mechanisms".

No direct analysis of effect of salinity on shrimp or blue crabs was available, as the WSIS used inflow as the independent variable to assess changes in center of abundance for those species. Thus, the level of uncertainty with respect to the commercial species is high. Further, the EFDC model used to predict salinities functioned only within the mainstem; the model did not include the salinity dynamics of the tributaries or the estuarine marshes at the mouth of the river. While the mainstem salinity changes occurred upstream of the deepening area, potential changes in the tributaries upstream of the deepening

project and in the marshes adjacent to the deepening project could not be assessed with the available models.

### 6.5 Recommendations

While most of the WSIS methods were implemented for this analysis, analysis of potential effects of salinity changes in the tributaries and marshes was not available with the EFDC model. In addition, the assessment of commercially important BMI species, implemented in the WSIS using freshwater inflows, was not applicable for assessment of salinity effects. Therefore, we recommend additional assessment of salinity changes to better understand potential effects of channel deepening on the BMI community. This work would necessarily include additional salinity modeling with a tool with a grid that included more of the tributary lengths and with programming to simulate marsh wetting and drying behaviors. Additional analysis of FIM data to examine salinity related behaviors of commercially important macroinvertebrates (if successful) combined with salinity modeling could provide useful insight into salinity effects on those populations.

DRAFT

# 7.0 PHYTOPLANKTON

The District's plankton working group for the WSIS evaluated potential effects of water withdrawal on plankton communities and dissolved oxygen. Coveney et al. (2012) describe the working group's plankton evaluation and development of the plankton empirical regression models and mechanistic models. This chapter reviews and summarizes the Coveney et al. (2012) empirical models and identifies the models' applicability for evaluation of effects of the Jacksonville Harbor deepening project. Chapter 8 discusses mechanistic model (EFDC/ICM-CEQUAL) development for evaluation of chlorophyll and dissolved oxygen.

Coveney et al. (2012) determined that the most important potential effects of water withdrawal on plankton communities relate to potential alteration of phytoplankton blooms. Algal blooms are common in the St. Johns River. Cyanobacteria dominate blooms in the freshwater part of the river; dinoflagellates in brackish parts. Potential adverse effects of algal blooms include increased dominance by toxic dinoflagellate species downstream and increased cyanobacterial bloom activity upstream, additional N loading from $N_2$-fixing cyanobacteria, altered phytoplankton community composition and increased amount of cyanobacterial toxins, dissolved oxygen depletion (with concomitant effects on fish populations), and changes in zooplankton community structure and reduction in fish production. The working group focused its attention on evaluation of these effects in River Segments 2 – 4, which encompass the lower freshwater and upper brackish water parts of the river.

The WSIS phytoplankton working group assessed the potential adverse effects of algal blooms with four bloom metrics and developed measurable variables associated with each metric. The four metrics and associated variables were:

1. Marine algal blooms as measured by maximum annual dinoflagellate biovolume
2. Change in N load as measured by annual mass of N added by $N_2$ fixation
3. Freshwater bloom magnitude as measured by maximum annual bloom chl-a and dissolved oxygen concentrations
4. Freshwater bloom duration as measured by duration of longest annual bloom.

## 7.1 WSIS Plankton Empirical Models

The plankton working group determined that the primary hydrologic variable governing algal bloom dynamics is water residence time. The group used the output from EFDC model simulations of river hydrology and phytoplankton characteristics from field collections to develop a series of empirical

regression models allowing evaluation of the four algal metrics. The regression models tested 42 derived water age values as independent variables and the field measured phytoplankton bloom metrics as dependent variables. Field collections for phytoplankton data occurred at SJRWMD stations MP72, DTL, SRP, FP44, SJP, and PA32.

The EFDC model provided "water age" (i.e., residence time) data, defined as the "the average time that water resided in the model domain before reaching a specific site (model grid cell)". The model calculated water age in model cells at 30-second time intervals. Low water age values for the first three months of model simulations ("spin-up") precluded use of the results from that time period. The water age results for each cell corresponding to the phytoplankton data collection stations were processed to derive several different water age values as independent variables for the regression equations.

The working group derived water age variables for a series of five-quarter periods, each period beginning with the last quarter of a calendar year (quarter "A") and extending through the four quarters ("B", "C", "D", "E") of the following calendar year. Within each five-quarter period, the group derived minimum, maximum, and mean water age values for each of seven time periods (April - October, April – August, and quarters A, B, C, D, and E). The group also used the inverse of each derived variable as independent variables in the regression calculations.

The regression modeling resulted in a set of eight regression models addressing the four bloom metrics in River Segments 2 and 3 (Coveney et al., 2012). Six of the regression models are relevant to the river segments included in the Jacksonville Harbor deepening ecological modeling study area:

1. Dinoflagellate biovolume in Segment 2 (Regression A)
2. $N_2$-fixation in Segment 3 (Regression B)
3. Freshwater maximum Chl-a in Segment 2 (Regression C, applicable only in Doctors Lake; not in main stem)
4. Freshwater maximum Chl-a in Segment 3 (Regression D)
5. Freshwater bloom duration in Segment 2 (Regression F, applicable only in Doctors Lake; not in main stem)
6. Freshwater bloom duration in Segment 3 (Regression G)

Note that none of the WSIS phytoplankton models are applicable in River Segment 1.

The regression models require differing sets of water age input variables. Table 7.1 shows the variable set required for the six models.

**Table 7.1** Input Variables For The Phytoplankton Empirical Regression Models (required variable indicated by "✓")

| | Time Period | | | | | | |
|---|---|---|---|---|---|---|---|
| **Variable** | **A** | **B** | **C** | **D** | **E** | **April - August** | **April - October** |
| Mean Water Age | ✓ | | | ✓ | | ✓ | |
| Minimum Water Age | | | | ✓ | | | |
| Maximum Water Age | ✓ | | ✓ | | ✓ | | ✓ |
| Inverse Mean Water Age | ✓ | ✓ | ✓ | | ✓ | | ✓ |
| Inverse Minimum Water Age | | | ✓ | ✓ | | | ✓ |
| Inverse Maximum Water Age | ✓ | | | | ✓ | | |

The methods applied by SJRWMD for assessment of phytoplankton are applicable in Segment 2 and Segment 3. The SJRWMD WSIS did not develop phytoplankton assessment methodology for Segment 1.

## 7.2 Application of the Phytoplankton Model for Jacksonville Harbor Deepening GRR-2 Ecological Effects Evaluation

The EFDC model outputs water age values for each layer of each model cell at one-hour time intervals. We post-processed the output data to produce vertically averaged daily water age values for the four cells corresponding to the SJRWMD phytoplankton sampling stations (Figure 7.1). From the daily water age values, we calculated the derived water age variables identified in Table 7.1. We set up spreadsheet models to apply the six applicable phytoplankton regressions described in Appendix 8.C of Coveney et al. (2012).

## 7.3 Results

The calculation of phytoplankton metrics with the regression equations produced some unexpected results. These results, some of which are illustrated in Figures 7.2 – 7.5, indicate that the regression models should not be used to evaluate the effects of Jacksonville Harbor deepening.

Figure 7.2 shows marine algal bloom (i.e., algal biomass) results from the Doctors Lake station in River Segment 2. The range of values generated from the regression equation appears reasonable in comparison to the distribution of values shown in the fit diagnostics for this equation in Coveney et al. (2012). Generally, annual variation in biomass appears greater than differences between the baseline and channel deepening alternatives.

Figure 7.3 shows nitrogen fixation for the Racy Point station in River Segment 3. The predicted data for 1998 appear unusually high and exceed observed and predicted values shown in the fit diagnostics. Again, the annual variation in predicted values exceeds the variation among the baseline and project alternatives.

Figure 7.4 shows results from the freshwater maximum chlorophyll-a regression at Racy Point in River Segment 3. As with the prior examples, annual variation exceeded variation among the simulated alternatives. Additionally, this model generated clearly unrealistic results with several of the simulations generating negative values for chlorophyll-a.

Figure 7.5 shows regression model results for freshwater bloom duration at Doctors Lake in River Segment 2. This model in some cases predicted algal blooms of negative duration, another unlikely occurrence in the river.

The results of the phytoplankton regression models are inconclusive regarding possible effects of Jacksonville Harbor deepening on phytoplankton communities. Some of the models produce apparently unreasonable results, which call into question the results from any of the regressions. Based on discussion and comments from SJRWMD staff, we believe that the regression models may function well only with data from the specific EFDC model used for the WSIS evaluation. The EFDC model modifications discussed in Chapter 2 and in Taylor (2012) may have resulted in minor variations in water age output values that were nonetheless sufficient to render the regression equations invalid for use with the Jacksonville Harbor Deepening GRR-2 ecological evaluation. This issue could perhaps be resolved through development of new regression equations based on the results of the Jacksonville Harbor Deepening GRR-2 EFDC model and the SJRWMD phytoplankton data set. However, such effort could require considerable time and with uncertainty of successful application.

DRAFT

### 7.4 Recommendations

Given these issues with application of the WSIS phytoplankton models, the best path for assessing potential harbor deepening impacts on phytoplankton communities lies with the CE-QUAL-ICM model under development and discussed separately in this report. The CE-QUAL-ICM model will include simulation of chlorophyll-a concentrations which will allow separate assessment of both magnitude and duration of phytoplankton blooms.

DRAFT

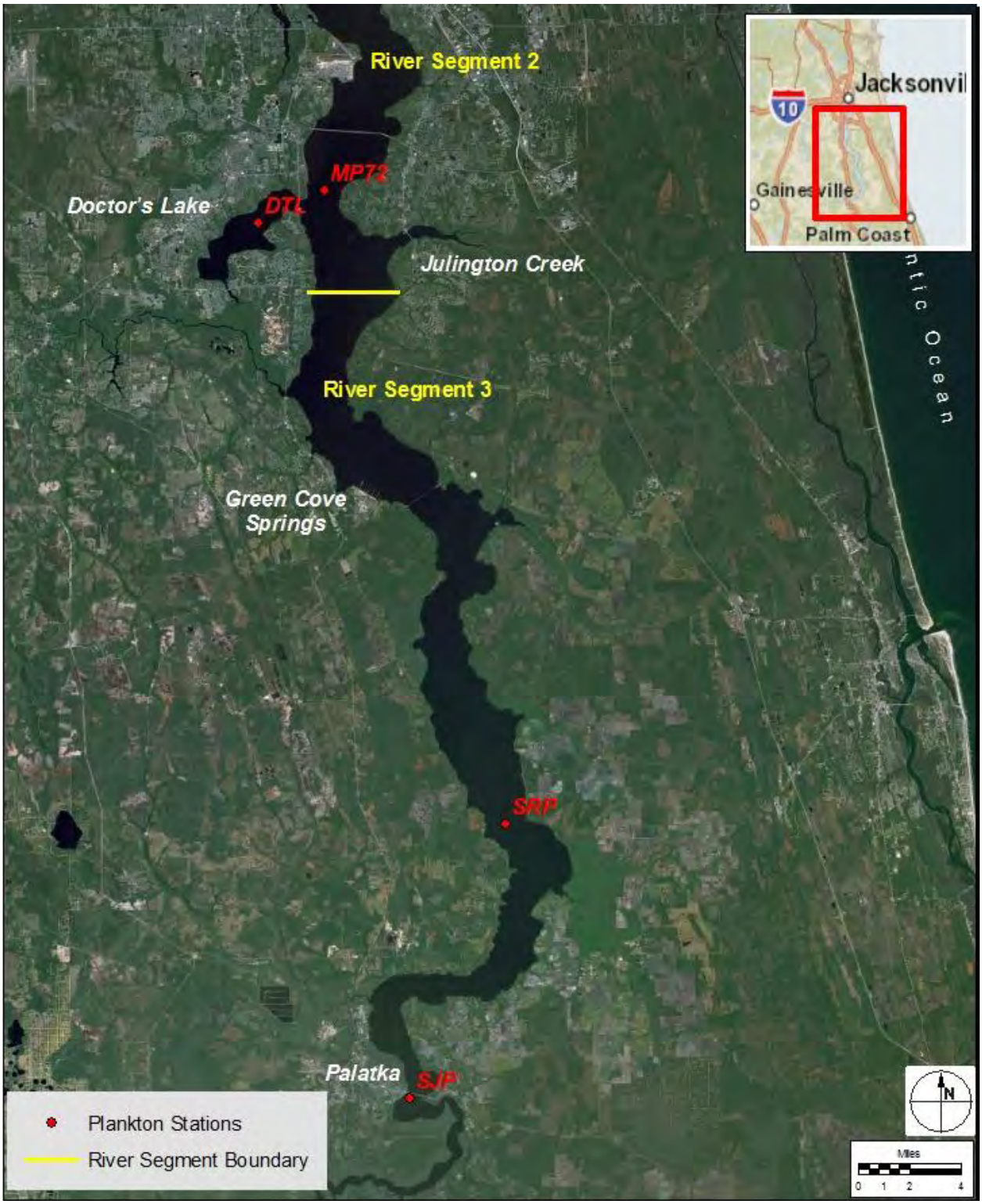


**Figure 7.1** Phytoplankton Sampling Stations

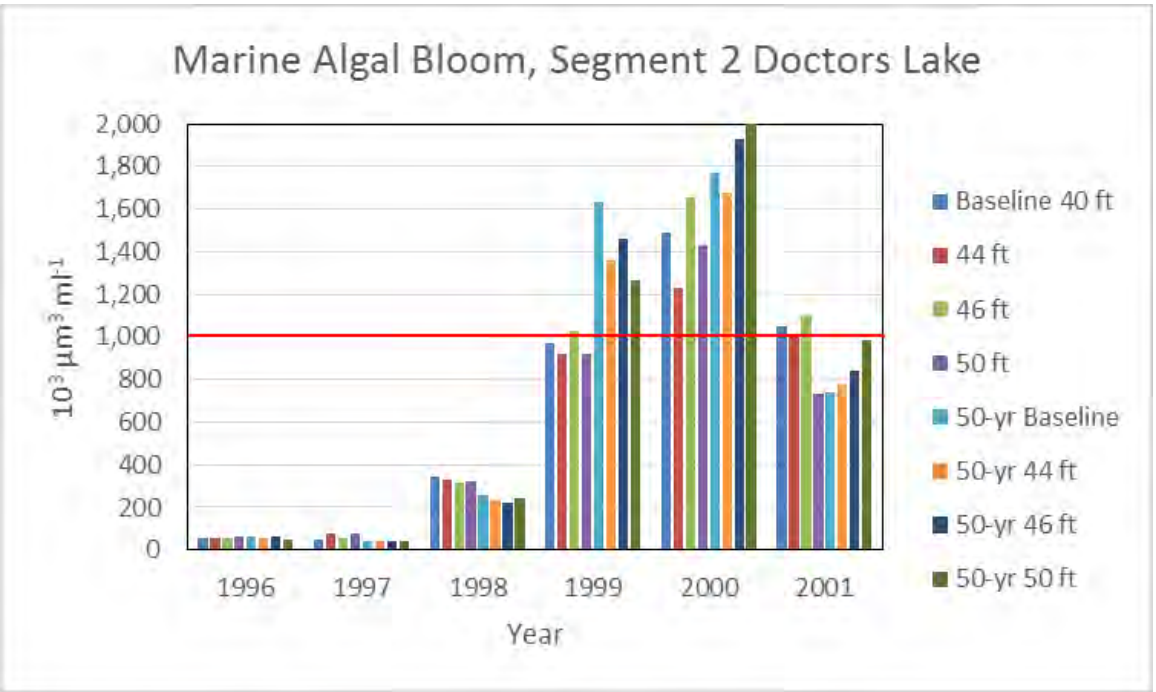


**Figure 7.2** Regression Results — Marine Algal Bloom, Segment 2, Doctors Lake.

Horizontal Red Line Indicates 1,000 X 103 µm3 ml-1 Effects Threshold

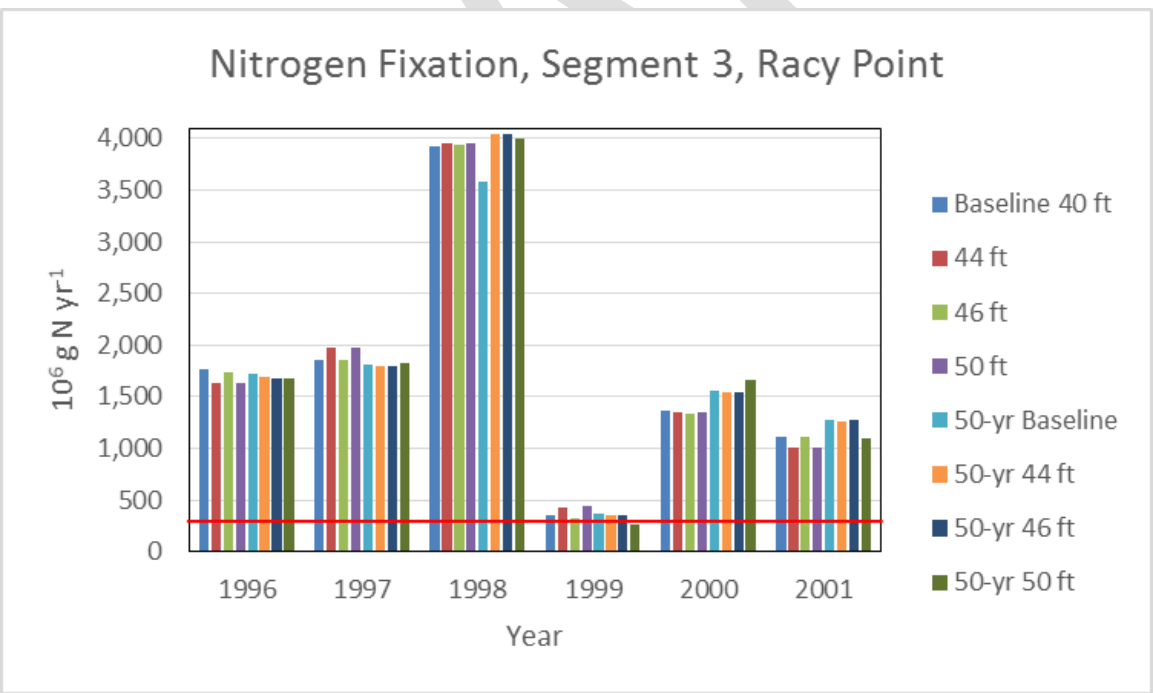


**Figure 7.3** Regression Results — Nitrogen Fixation, Segment 3, Racy Point.

Horizontal Red Line Indicates 308 X $10^6$ G N $Yr^{-1}$ Effects Threshold

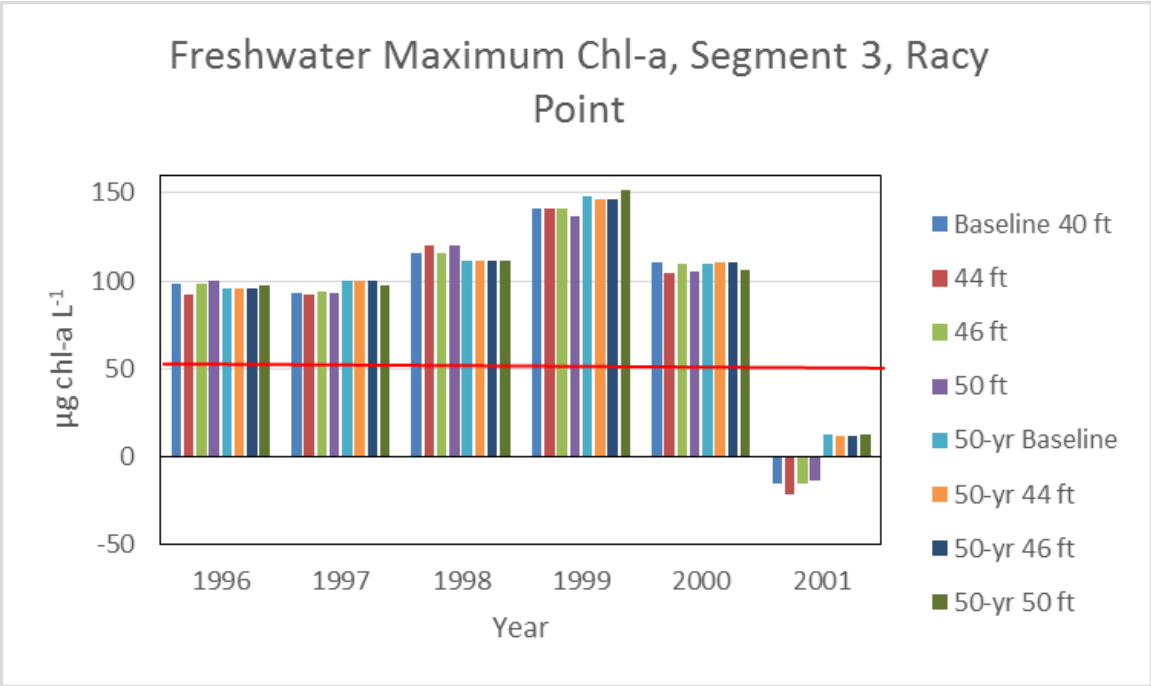


**Figure 7.4** Regression Results — Freshwater Maximum Chl-A, Segment 3, Racy Point. Horizontal Red Line Indicates 50 µg Chl-A $L^{-1}$ Effects Threshold

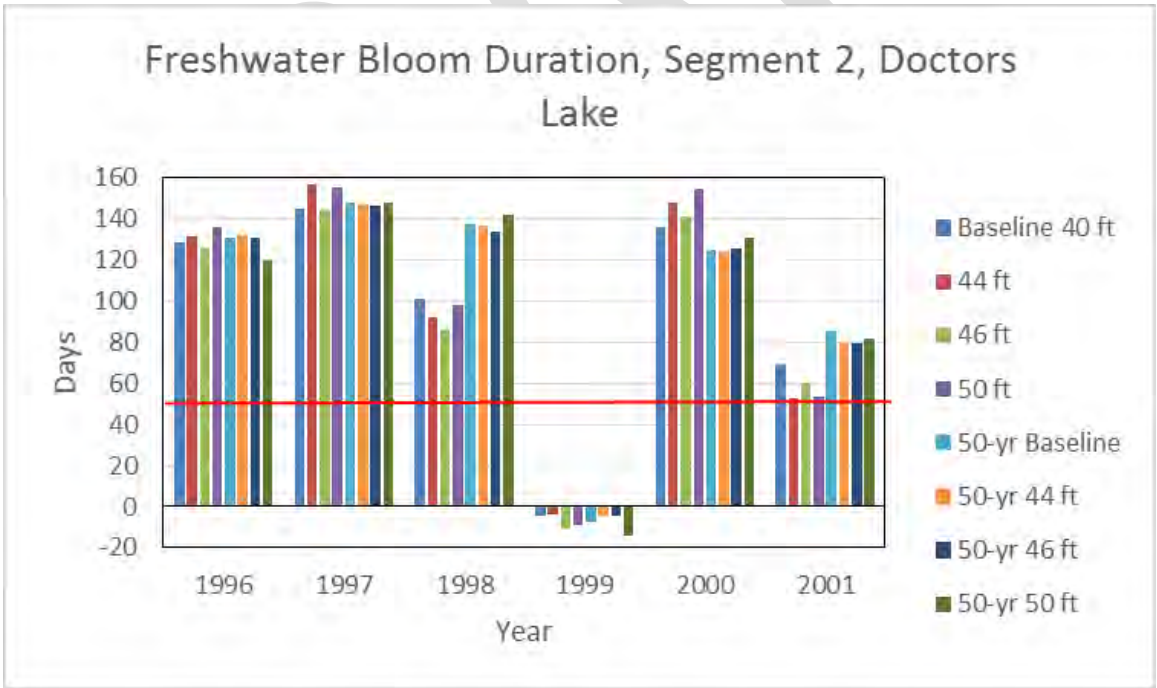


**Figure 7.5** Regression Results — Freshwater Bloom Duration, Segment 2, Doctors Lake. Horizontal Red Line Indicates 50 Days Effects Threshold

# 8.0 WATER QUALITY

## 8.1 WSIS Water Quality Model

The District's phytoplankton working group for the WSIS evaluated potential effects of water withdrawal on chlorophyll a and dissolved oxygen with the CE-QUAL-ICM mechanistic model (Coveney et al. 2012). This chapter summarizes the Coveney et al. (2012) CE-QUAL-ICM modeling effort and identifies the models' applicability for evaluation of effects of the Jacksonville Harbor deepening project.

The WSIS study group used the CE-QUAL-ICM numerical water quality model to examine the effects of water withdrawal on chlorophyll a in River Segment 3. The WSIS CE-QUAL-ICM model was a modified version of a model originally developed by the SJRWMD for setting total maximum daily loads (TMDL) in the LSJR. The EFDC model provided hydrodynamic input for the CE-QUAL-ICM model. Coveney et al. (2012) describe the WSIS modifications to the original TMDL version of the model and the WSIS simulation conditions for the EFDC/CE-QUAL-ICM model system. Although the model tended to overpredict chlorophyll a concentrations relative to measured values, the WSIS group concluded that the EFDC/CE-QUAL-ICM model was useful for evaluation of chlorophyll concentration changes in response to hydrology changes.

## 8.2 Jacksonville Harbor Deepening GRR-2 Water Quality Model

For the Jacksonville Harbor Deepening GRR-2 ecological study, the USACE elected to apply the TMDL versions of the EFDC hydrodynamic and CE-QUAL-ICM water quality models. The objective in using the TMDL versions was to allow evaluation of both chlorophyll a and dissolved oxygen in the LSJR, a task for which the TMDL version appeared better suited because of its emphasis on simulating dissolved oxygen in River Segments 1, 2, and 3. Similar to the EFDC model mesh modifications described earlier, we modified the TMDL CE-QUAL-ICM model mesh to allow definition of river bathymetry following harbor deepening.

Appendix C describes development and application of the TMDL version of the EFDC hydrodynamic model to generate the hydrologic data for CE-QUAL-ICM. Appendix D describes calibration and verification of the TMDL version of the CE-QUAL-ICM model.

DRAFT

As described in Appendix D, we successfully calibrated and verified the TMDL version of the CE-QUAL-ICM model with the modified mesh and a pre-project bathymetry similar to that used by the SJRWMD. However, when we attempted simulations with the model bathymetry modified to reflect USACE baseline bathymetry and the dredged river channel, the CE-QUAL-ICM model suffered temporally and spatially localized instability issues which caused it to crash. We are currently working to identify the cause of the instability and develop recommendations to correct the problem.

DRAFT

## 9.0 REFERENCES


Anderson, S. M., C. Katin, and W. R. Wise. 2005. *Assessment of Coastal Water Resources and Watershed Conditions at Timucuan Ecological and Historic Preserve (FLORIDA)*. National Park Service, Water Resources Division.Fort Collins, CO 80525.

Bass, D. G., and D. T. Cox. 1985. River habitat and fishery resources of Florida. Pages 121-187 *in* W. J. Seaman, editor. Florida Aquatic Habitat and Fishery Resources Florida Chapter of the American Fisheries Society.

Boon, P. J. P. Calow, and G. E. Petts (eds.). 1992. *River Conservation and Management*. J. Wiley and Sons, New York, NY.

Brody, R.W. 1994. Vol. 6 of the lower St. Johns River Basin reconnaissance: biological resources. Technical Publication SJ94-2. Palatka, Fla.: St. Johns River Water Management District.

Burgess, G. H., and R. Franz. 1978. Zoogeography of the aquatic fauna of the St. Johns River system with comments on adjacent peninsular faunas. American Midland Naturalist 100(1):160-170

Coveney, M.F., Hendrickson, J.C., Marzolf, E. R., Fulton, R. S., Di, J. J., Neubauer, C.P., Dobberfuhl, D.R., Hall, G.B., Paerl, H. W., and Phlips, E. J. 2012. *Chapter 8. Plankton*. St. Johns River Water Supply Impact Study. Technical Publication No. SJ2012-1. SJRWMD, Palatka, FL.

Cox, D. T., E. D. Vosatka, G. Horel, R. Eisenhauer, H. L. Moody, W. K. Bradley, L. L. Connor, and R. L. Smith. 1980. St. Johns fishery resources: study I ecological aspects of the fishery. Florida Game and Fresh Water Fish Commission, 1979-1980 Federal Aid in Chapter 12 Fish St. Johns River Water Management District 12-95 Sport Fish Restoration Annual Progress Report for Dingell-Johnson Project F-33-4, Tallahassee, Florida.

Davis, W. S. and T. P. Simon. 1995. *Biological Assessment and Criteria. Tools for Water Resource Planning and Decision Making*. CRC Press, Boca Raton, FL.

DeMort, C. L. 1990. The St. Johns River system. Pages 97-120 in R. J. Livingston, editor. The rivers of Florida, volume Ecological studies 83. Springer-Verlag New York, Inc., New York, NY.


DRAFT

Dobberfuhl, D., Chamberlain, B., Hall, S., Jacoby, C., Mattson, R., Morris, L., Slater , J., Moore, K., Virnstein, B. 2012. *Chapter 9. Submerged Aquatic Vegetation.* St. Johns River Water Supply Impact Study. Technical Publication No. SJ2012-1. SJRWMD, Palatka, FL.

Eilefson, E. and M. Young. Benthic Macroinvertebrate and Sediment Composition Monitoring In The Restored Nisqually Estuary. Accessed at: *www.nisquallyestuary.org/benthic.doc*

Evans, D.L., D. G. Strom, J. Higman, E. Hughes, E. A. Hoover, and L. M. Line. 2004. *An Evaluation of Benthic Macroinvertebrate Data from 20 Surface Water Sites Within The Lower St. Johns River Basin, 2002-2003*. Special Publication SJ2004-SP241, St. Johns River Water Management District, Palatka, Florida, 110 pp.

Gaufin, A. R. 1973. Use of aquatic invertebrates in the assessment of water quality. Pp. 96-116 IN: J. Cairns, Jr. and K. L. Dickson (eds.), Biological Methods for the Assessment of Water Quality, American Society for Testing and Materials. ASTM Special Technical Publication 528. Philadelphia, PA.

Giberto D.A, C.S. Bremec, E.M. Acha and H. Mianzan. 2004. Large-scale spatial patterns of benthic assemblages in the SW Atlantic: the Rio de la Plata estuary and adjacent shelf waters. Estuarine Coastal and Shelf Science 61: 1-13.

Gore, J. A., J. B. Layzer, and J. Mead. 2001. Macroinvertebrate instream flow studies after 20 years: a role in stream management and restoration. Regulated Rivers: Research and Management 17: 527-542.

Gregory, M. Brian, J.C. DeVivo, P. H. Flournoy, and K. A. Smith. 2011. Assessment of estuarine water and sediment quality at Timucuan Ecological and Historic Preserve, 2008. Natural Resource Data Series NPS/SECN/NRDS—2011/134. National Park Service, Fort Collins, Colorado

Holder, J., R. Hyle, and E. Lundy. 2006. Annual performance report fiscal year 2005-2006 Lower St. Johns River resource development. Florida Fish and Wildlife Conservation Commission Fish and Wildlife Research Institute. DeLeon Springs, Florida.

Hymel, S. N. 2009. Inventory of marine and estuarine benthic macroinvertebrates for nine Southeast Coast Network parks. Natural Resource Report NPS/SECN/NRR—2009/121. National Park Service, Fort Collins, Colorado. July 2009.

DRAFT

Jacoby, Charles J. 2012. Potential Effects of Water Withdrawals on Blue Crabs, White Shrimp, Brown Shrimp, and Pink Shrimp. Appendix 11-H in SJRWMD Water Supply Impact Study.by St. Johns River Water Management District, Palatka Florida. 2012

Johnson, M. R., and F. F. J. Snelson. 1996. Reproductive life history of the Atlantic stingray, Dasyatis sabina (Pisces Dasyatidae), in the freshwater St. Johns River, Florida. Bulletin of Marine Science 59(1):74-88.

Kim H.C. and P.A. Montagna. 2009. Implications of Colorado River (Texas, USA) freshwater inflow to benthic ecosystem dynamics: A modeling study. Estuarine Coastal and Shelf Science 83: 491-504.

Kinser, P., Fox, S., Keenan, L., Ceric, A., Baird, F., Sucsy, P., Wise, W., Montague, C. 2012. *Chapter 10 Wetland Vegetation*. St. Johns River Water Supply Impact Study. Technical Publication No. SJ2012-1. SJRWMD, Palatka, FL.

La Peyre Megan K., Bryan Gossman, and Jerome F. La Peyre. 2009. Defining Optimal Freshwater Flow for Oyster Production: Effects of Freshet Rate and Magnitude of Change and Duration on Eastern Oysters and Perkinsus marinus Infection Estuaries and Coasts (2009) 32:522–534

Landsberg, J. A., K. A. Steidinger, D. F. Millie, C. Tomas, P. Tester, P. Carlson, W. Litaker, B. Mahmoudi, R. Rose, O. Schofield, C. Cooksey, and M. B. Neely. 2004. Intensive monitoring for Pfiesteria and Pfiesteria-like organisms in the St. Johns River. Florida Fish and Wildlife Conservation Commission, Fish and Wildlife Research Institute, St. Petersburg, Florida.

Long, J. M. 2004. Analysis of long-term benthic invertebrate sampling data: Sisters Creek, Timucuan Ecological and Historic Preserve. Southeast Region, National Park Service.

MacDonald, T.C., J. Solomon, C.B. Guenther, R.B. Brodie, and R.H. McMichael, Jr. 2009. Assessment of Relationships Between Freshwater Inflow and Populations of Fish and Selected Macroinvertebrates in the Lower St. Johns River, Florida. Florida Fish and Wildlife Conservation Commission, Fish and Wildlife Research Institute. St. Petersburg, FL

DRAFT

MacKenzie, Clyde L. Jr. 1977. Development of an Aquacultural Program for Rehabilitation of Damaged Oyster Reefs in Mississippi.Marine Fisheries Review 39(8):1-13. Marine Fisheries Review Paper 1259 August 1977.

Mackin, J. G. 1956. Dermocystidium marinum and salinity. Proc. Nat. Shellfish. Ass., 46, 116–133.

Mannino, A. and Montagna, P.A.: 1997, 'Small-scale Spatial Variability of Macrobenthic Community Structure', Estuaries 20: 159-173.

Mattson, R. A., K. W. Cummins, R. W. Merritt, P. A. Montagna, T. Palmer, J. Mace, J. Slater, and C. Jacoby. 2012. Chapter 11. Benthic Macroinvertebrates. St. Johns River Water Supply Impact Study. Technical Publication No. SJ2012-1. SJRWMD, Palatka, FL.

McLane, W. M. 1955. The fishes of the St. Johns River system. Doctoral dissertation. University of Florida, Gainesville, Florida.

Menzel, R. Winston, Neil C. Hulings. and Ralph R. Hathaway. 1957. Causes of depletion of oysters in St. Vincent Bay, Apalachicola Bay, Florida. Proceedings of the National Shellfisheries Association 48:66-71 August 1957.

Merritt, R. W., J. R. Wallace, M. J. Higgins, M. K. Alexander, M. B. Berg, W. T. Morgan, K. W. Cummins, and B. Vandeneeden. 1996. Procedures for the functional analysis of invertebrate communities of the Kissimmee River-floodplain ecosystem. Fla. Scientist 59(4): 216-249.

Merritt, R. W., K. W. Cummins, and M. B. Berg (eds.). 2008. An introduction to the aquatic insects of North America (4th edition). Kendall/Hunt Publ. Co., Dubuque, IA

Merritt, R. W., K. W. Cummins, M. B. Berg, J. A. Novak, M. J. Higgins, K. J. Wessell, and J. L. Lessard. 2002. Development and application of a macroinvertebrate functional-group approach in the bioassessment of remnant river oxbows in southwest Florida. J. North American Benthological Soc. 21(2): 290-310.

Montagna, P.A. and R.D. Kalke. 1992. The Effect of Freshwater Inflow on Meiofaunal and Macrofaunal Populations in the Guadalupe and Nueces Estuaries, Texas. Estuaries 15:307-326.

Montagna, P.A. and R.D. Kalke. 1995. Ecology of Infaunal Mollusca in south Texas estuaries. American Malacological Bulletin, 11:163-175.

DRAFT

Montagna, P.A., E.D. Estevez, T.A. Palmer, and M.S. Flannery. 2008a. Meta-analysis of the relationship between salinity and molluscs in tidal river estuaries of southwest Florida, U.S.A. American Malacological Bulletin 24: 101-115.

Montagna, P.A., R.D. Kalke, and C. Ritter. 2002. Effect of restored freshwater inflow on macrofauna and meiofauna in upper Rincon Bayou, Texas, USA. Estuaries 25:1436-1447.

Montagna, P.A., T.A. Palmer, and J.B. Pollack. 2008b. St. Johns Estuary: Estuarine Benthic Macroinvertebrates, Phase 1 Final Report. Report Submitted to: St. Johns River Water Management District.

Montagna, P.A., T.A. Palmer, and J.B. Pollack. 2011. St. Johns Estuary: Estuarine Benthic Macroinvertebrates Phase 2. A final report submitted to the St. Johns River Water Management District, Harte Research Institute for Gulf of Mexico Studies Texas A&M University – Corpus Christi, Corpus Christi, Texas, 49 pp.

Montagna, Paul A., Terry A. Palmer, and Jennifer B. Pollack. 2008. St. Johns Estuary: Estuarine Benthic Macroinvertebrates. Phase 1 Final Report. Submitted to: St. Johns River Water Management District P.O. Box 1429 Palatka, Florida 32178 October 16, 2008.

Montague C.L. and Ley J.A. 1993. Title: a possible effect of salinity fluctuation on abundance of benthic vegetation and associated fauna in northeastern Florida Bay. Estuaries 16: 703-717.

Montague, C. L., and J. A. Ley. 1993. A possible effect of salinity fluctuation on abundance of benthic vegetation and associated fauna in northeastern Florida Bay. Estuaries 16:703-717.

Mooraki N, A.E. Sari, M.Soltani and T. Valinassab. 2009. Spatial distribution and assemblage structure of macrobenthos in a tidal creek in relation to industrial activities International Journal of Environmental Science and Technology 6: 651-662.

Murphy, Michael D., Anne L. McMillen-Jackson, and Behzad Mahmoudi. 2007. A stock assessment for blue crab, *Callinectes sapidus*, in Florida waters Report to the Florida Fish and Wildlife Commission Division of Marine Fisheries Management In House Report 2007-006. Florida Fish and Wildlife Conservation Commission Fish and Wildlife Research Institute St. Petersburg, Florida. June 22, 2007

DRAFT

Palmer, T.A., P.A. Montagna, and R.D. Kalke. 2002. Downstream effects of restored freshwater inflow to Rincon Bayou, Nueces Delta, Texas, USA. Estuaries 25:1448-1456.

Perez-Farfante, I. 1969. Western Atlantic shrimps of the genus Penaeus. U.S. Fish Wildlife Service Fisheries Bulletin 67(3):461-591.

Rosenberg, D. M. and V. H. Resh. 1993. Freshwater Biomonitoring and Benthic Macroinvertebrates. Chapman and Hall, New York, NY.

Sempsrott, M. 2011. Florida's Commercial Blue Crab (Callinectes sapidus) Managing Harvest with output controls Oregon State University Capstone Project – FW 506 03/08/2011. Accessed at: http://fw.oregonstate.edu/pdfs/FL_BlueCrabFishery_Sempsrott.pdf

St. Johns River Water Management District (SJRWMD). 2012. *St. Johns River Water Supply Impact Study.* Technical Publication No. SJ2012-1. SJRWMD, Palatka, FL.

Stickney, R. R. 1984. Estuarine Ecology of the Southeastern Unites States and Gulf of Mexico. Texas A&M University Press, College Station, TX.

Strom, Douglas and Mark Thompson. 2000. Biological Implications of Stable Salinity Gradients within the Context of the St. Lucie Estuary, Florida. Florida Department of Environmental Protection Southeast District Water Quality Program November 1, 2000.

Tagatz, M. E. 1968. Fishes of the St. Johns River, Florida. Quarterly Journal Florida Academy of Science 30:25-50.

Taylor Engineering, Inc. (Taylor). 2012. *EFDC Salinity Modeling for Jacksonville Harbor GRR-2 Deepening Project, Phase 2*. Draft report prepared for USACE Jacksonville District. Taylor Engineering, Inc., Jacksonville, FL.

Taylor Engineering, Inc. (Taylor). 2011. *EFDC Salinity Modeling for Jacksonville Harbor GRR-2 Deepening Project Phase I Draft Report*, Jacksonville, FL.

Van Den Avyle, M. J. and D. L. Fowler. 1984. Species Profiles: Life Histories and Environmental Requirements of Coastal Fishes and Invertebrates (South Atlantic) – Blue Crab. U.S. Fish and Wildlife Service Report FWS/OBS-82/11.19. U.S. Army Corps of Engineers Report TR EL-82-4.

DRAFT

Wright, W., M. B. Gregory and A. Rinehart. 2012. Fixed-station water quality monitoring at Timucuan Ecological and Historic Preserve: 2011 data summary. Natural Resource Data Series NPS/SECN/NRDS—2012/393. National Park Service, Fort Collins, Colorado

DRAFT

# APPENDIX A

## Calculation of Moving Average Salinities for Fish Analyses

An Appendix to:

Ecological Modeling for Jacksonville Harbor Deepening GRR-2

March 2013

## Appendix A

## Calculation of Moving Average Salinities for Fish Analyses

The fish model evaluates the potential effects of channel deepening on the spatial coverage of five salinity habitat blocks communities in Lower St. Johns River (Figure 1). Periods of maximum average salinity (30-, 60-, and 90-day) determined from baseline and alternative scenarios by year provided basis for fish model. Periods of maximum average for the baseline scenario were determined by examining running daily and vertical averages of basin-wide salinity. The post-processing follows the following steps.

1. List the required cells in EFDC.inp.
2. Run the program ECO_XXX.exe. The program will
    a. Extract the hourly salinity data of all layers at each cell. Calculate the vertical average value and save the results to SALT_TS.txt.
    b. Using the file SALT_TS.txt, calculate the daily average salinity value at each cell. Save the results to SALT_DAILY.txt.
    c. Calculate basin wide mean salinity using the daily average salinity value at each cell and store that data to a temporary file.
    d. Calculate the 30-day moving average salinity at each cell and basin wide mean 30-day moving average salinity. Save the resulting dataset in SALT_MEAN_30.txt. The date of each year is determined at the baseline condition, not necessarily the date with highest basin wide mean moving average values for the other scenarios.
    e. Within each year of mean 30-day moving average values, determine the date with the highest basin-wide mean 30-day moving average salinity. From file SALT_MEAN_30.txt extract the basin-wide cell data for the day in each year with the highest basin-wide 30-day moving average salinity. Store the daily average salinity data for that day in each year to SALT_30_MAX.txt. Stored data will include the day date, and the salinity value.
    f. Repeat step (d) and (e) for 60-day and 90-day moving average. The date of each year is determined at the baseline condition, not necessarily the date with highest basin wide mean moving average values for the other scenarios. Data will be saved in SALT_60_MAX.txt and SALT_90_MAX.txt.

**Figure 1** Complete Model grid cells for Wetland, Fish, and BMI Analyses

# APPENDIX B

## Benthic Macroinvertebrates (BMI) Moving Average Salinity Calculations

An Appendix to:

Ecological Modeling for Jacksonville Harbor Deepening GRR-2

March 2013

## Appendix B

## Benthic Macroinvertebrates (BMI) Moving Average Salinity Calculations

Assessment of changes in total benthic populations requires salinity zone area changes. In turn, assessment of changes in salinity zone areas requires output similar to the fish model. Calculated periods of maximum average salinity (30-, 60-, and 90-day) determined from baseline and alternative scenarios by year provided basis for BMI. Periods of maximum average for the baseline scenario were determined by examining running daily averages of basin-wide bottom salinity. Additionally, BMI partial duration frequency analysis modeling required daily maximum bottom salinities at three specified locations (Table 1).

The ECO_XXX.exe post-processing follows the following steps.

1. List the required cells in EFDC.inp.
2. Run the program ECO_XXX.exe. The program will
    a. Extract the bottom layer hourly salinity data and save the results to SALT_TS.txt.
    b. Determine the daily Max salinity value at each cell and save the results to SALT_DAILYMAX.TXT.
    c. Calculate basin wide mean salinity based on the daily max value at each cell.
    d. Calculate 30-day moving average salinity at each cell and basin wide mean 30-day moving average salinity (SALT_MEAN_30.TXT).
    e. Determine the date of each year with the highest basin wide mean 30-day moving average salinity and save the 30-days moving average salinity of each cell for that day to SALT_30_MAX.TXT. The date of each year is determined at the baseline condition, not necessarily the date with highest basin wide mean moving average values for the other scenarios.
    f. Repeat step (d) and (e) for 60-day and 90-day moving average. The date of each year is determined at the baseline condition, not necessarily the date with highest basin wide mean moving average values for the other scenarios. Data will be saved to SALT_60_MAX.TXT and SALT_90_MAX.TXT.

The post-processor program for daily maximum bottom salinity files for three separate cells follows the following steps.

1. Extract the bottom layer hourly salinity data and save the results at SALT_TS.txt.

2. Determine the daily maximum salinity value of each cell and save the results to SALT_DAILYMAX.txt.

**Table 1** Post-Processing Stations for BMI Model

| Station | State Plane Florida East NAD 83 | |
|---|---|---|
| | X (ft) | Y (ft) |
| JAXSJR17 | 460987.5 | 2193911.0 |
| JAXSJR40 | 448481.8 | 2152256.5 |
| SJSR16 | 463032.3 | 2052159.3 |

# APPENDIX C

## EFDC Hydrodynamic Modeling for Water Quality Model Input for the Jacksonville Harbor GRR-2 Deepening Project

An Appendix to:

Ecological Modeling for Jacksonville Harbor Deepening GRR-2

March 2013

# EFDC Hydrodynamic Modeling for Water Quality Model Input for the Jacksonville Harbor GRR-2 Deepening Project

**Draft Report**

Prepared for

U.S. Army Corps of Engineers, Jacksonville District
Jacksonville, Florida

by

Taylor Engineering, Inc.
10151 Deerwood Park Blvd.
Bldg. 300, Ste. 300
Jacksonville, Florida 32256
(904) 731-7040

C2012-010

March 2013

DRAFT

## EXECUTIVE SUMMARY

The Jacksonville Harbor General Re-evaluation Study Project Management Plan (PMP) provides a plan to identify solutions to improve navigation in federally-maintained channels in the St. Johns River and to evaluate the impacts of these solutions. One of the solutions identified in the plan is modification of the federal navigation channel. The U.S. Army Corps of Engineers, Jacksonville District (USACE-SAJ), as part of its General Re-evaluation Study to improve Jacksonville Harbor navigation, is assessing the effects of potential channel modifications on the general circulation, salinity, ecology, and water quality in the St. Johns River. For the water quality modeling, the USACE-SAJ chose to use the Integrated Compartment Model (CE-QUAL-ICM) with hydraulics input supplied by the Environmental Fluid Dynamics Code (EFDC). This study describes the setup, mesh refinement, and validation of the EFDC hydrodynamic and salinity model (USACE model) that will provide input information to the CE-QUAL-ICM water quality model.

Taylor Engineering, Inc. refined an existing St. Johns River Water Management District EFDC model mesh in and near the navigation channel to develop the USACE model mesh and allow description of bathymetries of potential channel changes for the Jacksonville Harbor Deepening Project. The mesh refinement increased horizontal cells across the navigation channel from one to three from the river mouth to Mile 20.

Taylor Engineering then calibrated and verified the USACE model with monitoring data of water level and salinity collected during 1997 and 1998. The overall good agreement between simulated and observed water levels and salinity demonstrates the capability of the USACE model to reasonably simulate these processes in the Lower St. Johns River. Based on the model calibration and verification results, the USACE model is suitable for predicting hydrodynamic and salinity in the Lower St. Johns River and for producing CE-QUAL-ICM input hydraulic information.

DRAFT

**TABLE OF CONTENTS**

**EXECUTIVE SUMMARY** ..... **i**
**LIST OF FIGURES** ..... **iii**
**LIST OF TABLES** ..... **iv**
**1.0 INTRODUCTION** ..... **1**
**2.0 STUDY AREA** ..... **2**
**2.1 Project Area** ..... **3**
**2.2 St. Johns River Basin** ..... **4**
**2.3 Lower St. Johns River Area** ..... **4**
**3.0 EFDC MODEL DESCRIPTION AND LOWER ST. JOHNS RIVER EFDC SALINITY MODEL SETUP** ..... **7**
**3.1 Model Description** ..... **7**
**3.2 Model Setup** ..... **7**
*3.2.1 Model Domain* ..... *7*
*3.2.2 Boundary Conditions* ..... *8*
3.2.2.1 Ocean Water Level and Salinity ..... 8
3.2.2.2 Lateral Discharge and Salinity ..... 8
3.2.2.3 Meteorology: Rainfall, Evaporation, and Wind ..... 12
**3.3 Model Mesh Refinement** ..... **14**
**4.0 VALIDATION OF USACE HYDRODYNAMIC AND SALINITY MODEL** ..... **17**
**4.1 Model Calibration Methodology** ..... **17**
**4.2 Hydrodynamic Model Parameters** ..... **18**
**4.3 USACE Model Calibration** ..... **19**
*4.3.1 Water Surface Level Calibration* ..... *19*
*4.3.2 Salinity Calibration* ..... *25*
**4.4 USACE Model Verification** ..... **31**
*4.4.1 Water Level Verification* ..... *31*
*4.4.2 Salinity Verification* ..... *34*
**5.0 SUMMARY AND CONCLUSIONS** ..... **39**
**REFERENCES** ..... **40**

**APPENDIX A Governing Hydrodynamic**

DRAFT

## LIST OF FIGURES


**Figure 1.1** Jacksonville Harbor Segments (Source: USACE-SAJ) ..... 1

**Figure 2.1** Study Area ..... 2

**Figure 2.2** St. Johns River Federal Navigation Channel Mile Markers and Authorized Depths (Source: USACE-SAJ) ..... 3

**Figure 2.3** Major Tributary Basins and Sub-Basins of the St. Johns River Basin ..... 5

**Figure 3.1** 2001 SJRWMD EFDC Model Mesh on Google Earth Image ..... 9

**Figure 3.2** Locations of Stations with Observed Rainfall, Evaporation and Wind Data ..... 13

**Figure 3.3** SJRWMD EFDC Model Mesh in the Navigation Channel from River Mile 10 to 20 ..... 15

**Figure 3.4** USACE Model Updated Mesh with Three Elements in the Navigation Channel from River Mile 10 to 20 ..... 16

**Figure 4.1** Locations of Water Level Stations ..... 20

**Figure 4.2** Locations of Salinity Stations ..... 21

**Figure 4.3** EFDC Model Bottom Roughness Height ..... 22

**Figure 4.4** Comparison of Computed and Observed Water Levels during a Portion of the Calibration Period (Long Branch) ..... 23

**Figure 4.5** Comparison of Computed and Observed Water Levels during a Portion of the Calibration Period (Main Street Bridge) ..... 23

**Figure 4.6** Comparison of Computed and Observed Water Levels during a Portion of the Calibration Period (Buckman Bridge) ..... 24

**Figure 4.7** Comparison of Computed and Observed Water Levels during a Portion of the Calibration Period (Shands Bridge Station) ..... 24

**Figure 4.8** Comparison of Computed and Observed Salinity during a Portion of the Calibration Period (Dames Point) ..... 27

**Figure 4.9** Comparison of Computed and Observed Salinity during a Portion of the Calibration Period (Acosta Bridge) ..... 28

**Figure 4.10** Comparison of Computed and Observed Salinity during a Portion of the Calibration Period (Buckman Bridge) ..... 29

**Figure 4.11** Comparison of Computed and Observed Salinity during a Portion of the Calibration Period (Shands Bridge) ..... 30

**Figure 4.12** Comparison of Computed and Observed Water Level during a Portion of the Verification Period (Long Branch) ..... 32


DRAFT

**Figure 4.13** Comparison of Computed and Observed Water Level during a Portion of the Verification Period (Main Street Bridge) ..... 32
**Figure 4.14** Comparison of Computed and Observed Water Level during a Portion of the Verification Period (Buckman Bridge) ..... 33
**Figure 4.15** Comparison of Computed and Observed Water Level during a Portion of the Verification Period (Shands Bridge) ..... 33
**Figure 4.16** Comparison of Computed and Observed Salinity during a Portion of the Verification Period (Dames Point) ..... 35
**Figure 4.17** Comparison of Computed and Observed Salinity during a Portion of the Verification Period (Acosta Bridge) ..... 36
**Figure 4.18** Comparison of Computed and Observed Salinity during a Portion of the Verification Period (Buckman Bridge) ..... 37
**Figure 4.19** Comparison of Computed and Observed Salinity during a Portion of the Verification Period (Shands Bridge) ..... 38

## LIST OF TABLES

**Table 3.1** Model Lateral Inflows and Locations (NAD83 State Plane Florida East) ..... 10
**Table 3.2** Model Stations with Observed Rainfall, Evaporation and Wind Data in the Lower St. Johns River Basin ..... 12
**Table 4.1** Model Calibration Statistics for Water Level in 1997 ..... 25
**Table 4.2** Model Calibration Statistics for Salinity in 1997 ..... 26
**Table 4.3** Model Verification Statistics for Water Level in 1998 ..... 31
**Table 4.4** Model Verification Statistics for Salinity in 1998 ..... 34

DRAFT

## 1.0 INTRODUCTION

The Jacksonville Harbor, as described by the U.S. Army Corps of Engineers, Jacksonville District (USACE-SAJ), includes the first 20 river miles from the St. Johns River mouth in the Atlantic Ocean. The harbor consists of three segments (Figure 1.1) namely (a) Segment 1 — from the entrance channel to River Mile 14 — has an authorized existing depth of 40 ft, (b) Segment 2 — from River Mile 14 to River Mile 20 — has an authorized depth of 40 feet, and (c) Segment 3 (West Blount Island Channel) has an existing authorized depth of 38 feet.

**Figure 1.1** Jacksonville Harbor Segments (Source: USACE-SAJ)

The Jacksonville Harbor General Re-evaluation Study Project Management Plan (PMP) provides a plan to identify solutions to improve navigation in federally-maintained channels in the St. Johns River and to evaluate the impacts of these solutions. One of the solutions identified in the plan is modification of the federal navigation channel. The USACE-SAJ, as part of its General Re-evaluation Study to improve Jacksonville Harbor navigation, is assessing the effects of potential channel modifications on the general circulation, salinity, ecology, and water quality in the St Johns River. For the water quality modeling, the USACE-SAJ chose to use the Integrated Compartment Model (CE-QUAL-ICM) with hydraulics input supplied by the Environmental Fluid Dynamics Code (EFDC).

This report describes the EFDC model setup, validation, and model output to provide input data to the CE-QUAL-ICM. Following this introduction, Chapter 2 describes the study area. Chapter 3 describes the EFDC model setup. Chapter 4 describes EFDC model calibration and verification. Chapter 5 provides a summary and conclusions.

DRAFT

## 2.0 STUDY AREA

The study area encompasses the lower (northern) 90 mi of the St. Johns River from its mouth near Mayport to Buffalo Bluff. The study area includes portions of the Atlantic Ocean, the Lower St. Johns River, Chicopit Bay, White Shells Bay, Mill Cove, major river tributaries, and sections of the Atlantic Intracoastal Waterway (AIWW). Figure 2.1 shows a map of the study area. As described in the following paragraphs, the project area extends only to the first 20 miles of the St. Johns River (i.e., Segments 1, 2, and 3 of Jacksonville Harbor).

**Figure 2.1** Study Area

Tides, winds, and freshwater flows from upstream and tributaries mainly influence the river flow in the study area. Semi-diurnal tide propagates from the Atlantic Ocean and reaches up to Buffalo Bluff. Measured data shows salinity is highest in the project area, lowest from Green Cove south to Palatka, and increases south of Palatka as the ground water inflows contain salts and calcium.

## 2.1 Project Area

The proposed Federal navigation channel deepening project area stretches from just east of mouth of the St Johns River to mile-marker 20. Along this stretch of the river, the navigation channel width ranges 400 – 1,200 ft. Figure 2.2 shows the main Federal channel mile markers, authorized channel depths, and dredged material sites. The USACE-SAJ plans to evaluate the impacts of dredging portions of this stretch for depths that range 40 – 50 ft. Although channel deepening considerations extend only up to around the Talleyrand Terminal (Mile 20), the USACE-SAJ would like to assess the extent of the channel deepening impacts at river areas located further upstream. Thus, the study area includes most of the Lower St. Johns River.

**Figure 2.2** St. Johns River Federal Navigation Channel Mile Markers and Authorized Depths (Source: USACE-SAJ)

## 2.2 St. Johns River Basin

The St. Johns River, spanning 310 miles (mi), is the longest river in Florida. The St. Johns River drainage basin encompasses over 8,840 square miles (sq. mi) spread across 16 counties (Sucsy and Morris, 2002). A slow-moving water body with very mild slope, the St. Johns River drops an average 0.1 foot per mile (ft/mi) (Toth, 1993). The mild slope of the river allows tidal effects to extend at least 106 mi from the river mouth in Duval County to Lake George in Volusia County. Periods of reverse flow, when the daily net discharge moves upstream, extend the upstream movement of salt as well as upstream dispersal of pollutants entering the river.

The St. Johns River Water Management District (SJRWMD) manages and divides the basin into three sub-basins — Upper, Middle, and Lower St. Johns River. The Upper St. Johns River sub-basin extends from the headwaters of the St. Johns River in Okeechobee and Indian River Counties to the confluence of Econlockhatchee River in Seminole County. The Middle St. Johns River sub-basin extends from Lake Harney (Seminole and Volusia Counties) to the confluence of the Ocklawaha River near Welaka. The Lower St. Johns River sub-basin extends from the confluence of the Ocklawaha River to the river mouth at the Atlantic Ocean in Duval County (http://www.protectingourwater.org/watersheds/map). In addition, to these three sub-basins, the Lake George and Ocklawaha River Basins also drain into the St. Johns River (Figure 2.3). Located in the Lower St. Johns River, the Jacksonville Harbor main shipping channel, a 23-mi stretch of the river, extends from the river mouth to the Jacksonville Port Authority (JAXPORT) Talleyrand Marine Terminal just north of downtown Jacksonville. The incoming ocean tide acts as a nearly pure progressive shallow-water wave over the lower 31 mi, from the river mouth to Jacksonville (Sucsy and Morris, 2002).

## 2.3 Lower St. Johns River Area

The Lower St. Johns River receives 42% of its total annual freshwater flow from sources upstream of Astor. The surrounding local watersheds of the Lower St. Johns River encompass 2,300 sq. mi, about 27% of the total watershed area (Sucsy and Morris, 2002). The main tributaries of the Lower St. Johns River include Black Creek, Deep Creek, Sixmile Creek, Etonia Creek, Julington Creek, McCullough Creek, Arlington River, Broward River, Dunns Creek, Ortega River, Trout River, and Atlantic Intracoastal Waterway.

DRAFT

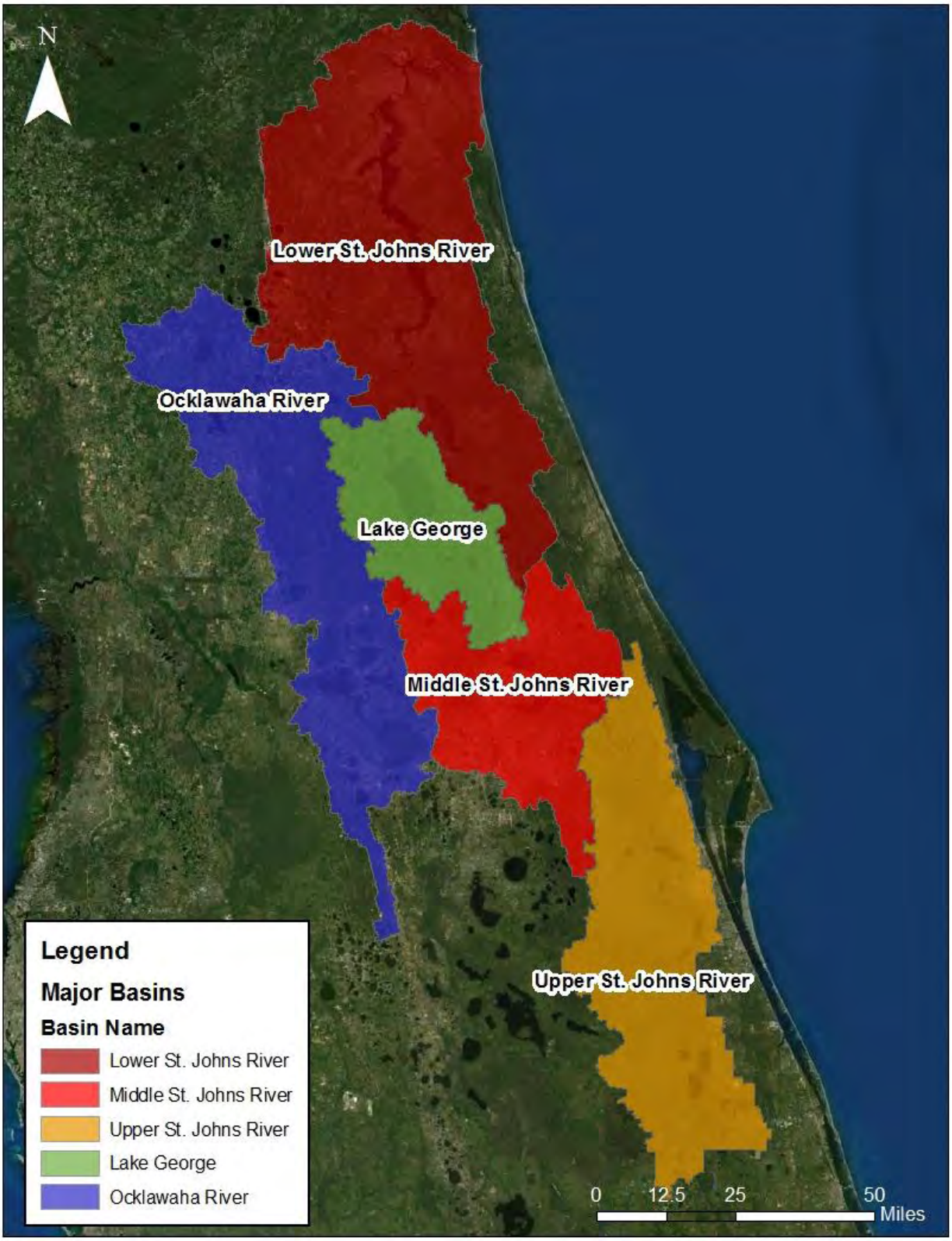


**Figure 2.3** Major Tributary Basins and Sub-Basins of the St. Johns River Basin

In the Lower St. Johns River, three major factors govern the upstream extent of salinity: net freshwater discharge entering the upper estuary through Astor, subtidal variability of ocean water levels, and wind. Salinity data provided by SJRWMD showed the salinity front reached an area between Buckman Bridge (river mile 35) and Shands Bridge (river mile 47). Moderate levels of salinity intrusion rarely reached Shands Bridge. Although a water quality monitoring station located about 4.3 mi upstream of Shands Bridge recorded salinity at 5 practical salinity units (psu, approximately equal to 5 ppt) during May 1994, neither a theoretical maximum nor probability of the extent of upstream salinity intrusion has been determined (Sucsy and Morris, 2002).

Between the river mouth and downtown Jacksonville, highly variable salinity ranges from completely fresh conditions to near ocean levels. At the Acosta Bridge near downtown Jacksonville, salinity ranges from completely fresh conditions due to high river discharges to 28 psu during dry conditions. At Dames Point, farther downstream near Blount Island, salinity ranges from 0.4 to 34.9 psu (Sucsy and Morris, 2002).

DRAFT

# 3.0 EFDC MODEL DESCRIPTION AND LOWER ST. JOHNS RIVER EFDC SALINITY MODEL SETUP

## 3.1 Model Description

This study employed the Environmental Fluid Dynamics Code (EFDC), the three-dimensional (3-D) numerical model developed by John Hamrick (1996). A public domain modeling package, EFDC simulates multidimensional flow, transport, and biochemical processes in surface water systems including lakes, rivers, estuaries, reservoirs, wetlands, and coastal regions. This model, currently maintained by Tetra Tech with support from the U.S. Environmental Protection Agency (USEPA), has a history of extensive use in the United States (e.g., Wool et al., 2003; Sucsy and Morris, 2002; Jin et al., 2000; and Hamrick et. al, 1995). More recently, the SJRWMD St. Johns River Water Supply Impact Study (2011) presents the completed application of the model to quantify the effects of water withdrawals on hydrodynamics throughout the St. Johns River. The EFDC model has undergone extensive tests, documentation, and applications in more than 200 modeling studies worldwide by research institutions, governmental agencies, and consulting organizations (Hamrick, 2011).

The hydrodynamic model, based on the 3-D shallow water equations of motion, includes dynamically coupled salinity and temperature transport. The physics of the EFDC model, and many aspects of the computational scheme, are similar to the widely used Blumberg-Mellor model, which later became Princeton Ocean Model (Blumberg and Mellor, 1987). The EFDC model employs a curvilinear-orthogonal horizontal grid, and a stretched or sigma vertical coordinate. In addition to hydrodynamic, salinity, and temperature transport simulation capabilities, EFDC can also simulate cohesive and non-cohesive sediment transport, near-field and far-field discharge dilution from multiple sources, eutrophication processes, transport and fate of toxic contaminants in the water and sediment phases, and transport and fate of various life stages of finfish and shellfish (USEPA, 2007). Appendix A describes the governing equations of the EFDC model.

## 3.2 Model Setup

### *3.2.1 Model Domain*

The model applied for this study originated from the Lower St. Johns River Hydrodynamic Model developed by the SJRWMD, hereinafter the 2001 SJRWMD EFDC model. The SJRWMD calibrated and verified the 2001 SJRWMD EFDC model with data from a three-year period (1996 – 1998).

The SJRWMD applied the 2001 model on its St. Johns River total maximum daily load study for the Lower St. Johns River (FDEP, 2008).

The 2001 SJRWMD EFDC model domain covers the Lower St. Johns River (LSJR) from Buffalo Bluff to the Atlantic Ocean (Figure 3.1). The model domain comprises 2,210 curvilinear horizontal water cells with the model variables (water surface elevation, velocity, temperature, salinity, etc.) calculated within each cell over the model simulation period. Each horizontal cell comprises six equally divided layers in the vertical direction. Thus, six equally stretched layers compose the model's vertical dimension. A 13-sq. mi sponge area (directly upstream of Buffalo Bluff) was applied at the upstream model boundary to prevent tide through Buffalo Bluff from being artificially reflected back into the model domain. The sponge comprises 72 model grids cells with a uniform depth.

### *3.2.2 Boundary Conditions*

Boundary conditions used for model forcing include ocean water level, ocean salinity, lateral discharge and salinity, wind, rainfall, and evaporation. Ocean water level and salinity define the seaward (downstream) open ocean boundary. Notably, the SJRWMD provided the 2001 SJRWMD EFDC model with the temperature variable switched off which means the model does not include the effect of temperature changes in the model simulations. Model boundary conditions span a period that allows the model to run for the 1995 through 1999 period. The USACE-SAJ scope of work states the SJRWMD processed and quality-assured the boundary conditions data.

#### 3.2.2.1 Ocean Water Level and Salinity

Nineteen cells form the open ocean boundary along the eastern side of the LSJR grid. Ocean water level provides the forcing function along the open ocean boundary. SJRWMD provided a time-series of hourly water surface elevation — vertical displacements above or below the mean tide level. During the simulation years, ocean water levels — dominated by semidiurnal tides — ranged from -5.05 to +4.17 ft NAVD. Ocean salinity was set along the open ocean boundary at a temporally constant value varying linearly from a surface value of 35 ppt to a bottom value of 36 ppt.

#### 3.2.2.2 Lateral Discharge and Salinity

The model applied discharge and salinity along the western boundary of the sponge area (Sucsy and Morris, 2002). In addition, SJRWMD specified tributary discharges at 64 locations in the model

domain (Table 3.2). SJRWMD provided a time series of daily discharge for each location using observed data, simulated data, or a combination of both

**Figure 3.1** 2001 SJRWMD EFDC Model Mesh on Google Earth Image

**Table 3.1** Model Lateral Inflows and Locations (NAD83 State Plane Florida East)

| Lateral Inflows Boundary Condition | X (ft) | Y (ft) |
|---|---|---|
| St. Johns River | 425539.67 | 1902656.62 |
| St. Johns River | 425722.23 | 1904435.44 |
| St. Johns River | 425868.17 | 1906432.51 |
| St. Johns River | 426048.07 | 1908614.19 |
| St. Johns River | 426297.49 | 1910832.79 |
| St. Johns River | 426582.41 | 1912820.83 |
| St. Johns River | 426810.20 | 1914523.35 |
| St. Johns River | 426955.42 | 1916229.14 |
| St. Johns River | 427053.57 | 1918035.86 |
| St. Johns River | 427165.98 | 1920048.52 |
| St. Johns River | 427327.82 | 1922191.63 |
| St. Johns River | 427511.61 | 1924319.16 |
| Dunns Creek | 455348.06 | 1910509.49 |
| Mill Branch | 466615.81 | 1928984.40 |
| Rice Creek | 450104.24 | 1949997.12 |
| Dog Branch | 474876.37 | 1952067.17 |
| Mason Branch | 476031.52 | 1966300.16 |
| Deep Creek | 489117.05 | 1974670.75 |
| Moccasin Branch | 489285.14 | 1979060.36 |
| McCullough Creek | 486629.33 | 1983146.39 |
| Cedar Creek | 470250.97 | 1991466.17 |
| Tocoi Creek | 477510.74 | 2008921.20 |
| Clarkes Creek | 458925.66 | 2023680.16 |
| Sixmile Creek | 477269.70 | 2049535.33 |
| Orange Grove | 453991.12 | 2065804.00 |
| Governors Creek | 439226.43 | 2062975.80 |
| Black Creek | 432518.23 | 2076275.94 |
| Cunningham Creek | 453359.56 | 2094937.93 |
| Swimming Pen Creek | 418959.58 | 2100026.64 |
| Doctors Lake West | 418274.28 | 2106754.65 |
| Lucy Branch | 421571.41 | 2110939.14 |
| Doctors Lake East | 427285.50 | 2110686.42 |
| Ortega River | 432164.14 | 2144438.04 |
| Cedar River | 422475.41 | 2161624.81 |
| Trout River | 428165.05 | 2212869.17 |
| Broward River | 457177.09 | 2219288.70 |
| Dunn Creek | 471908.03 | 2219223.07 |
| Gin House Creek | 490084.30 | 2190398.51 |
| Pottsburg Creek | 463995.67 | 2175585.41 |
| Julington Creek | 455230.18 | 2107035.22 |

DRAFT

| Lateral Inflows Boundary Condition | X (ft) | Y (ft) |
|---|---|---|
| Moccasin Creek | 451338.04 | 1952918.88 |
| Unnamed Creek | 462971.91 | 2007281.90 |
| Kendall Creek | 458757.03 | 2062917.51 |
| Kentucky Branch | 443714.31 | 2080596.61 |
| Peters Branch | 438203.72 | 2098564.51 |
| Durbin Creek | 455230.18 | 2107035.22 |
| Flora Branch | 455230.18 | 2107035.22 |
| Cormorant Creek | 455230.18 | 2107035.22 |
| Unnamed Creek | 447332.49 | 2164850.96 |
| Christopher Bran | 455873.36 | 2148858.01 |
| New Rose Creek | 450293.53 | 2155946.21 |
| Craig Creek | 449161.46 | 2168394.65 |
| Miller Creek | 457190.95 | 2174014.99 |
| Unnamed Creek | 467281.61 | 2200353.48 |
| Unnamed Creek | 470536.08 | 2198283.39 |
| New Castle Creek | 473000.93 | 2196637.49 |
| Jones Creek | 487035.37 | 2190359.12 |
| Cow Head Creek | 488583.12 | 2190261.49 |
| Unnamed Creek | 501852.36 | 2202000.21 |
| Mt. Pleasant Creek | 510748.41 | 2196420.04 |
| Drummond Creek | 463477.42 | 2208340.93 |
| Moncrief Creek | 447873.17 | 2204805.44 |
| Ribault River | 444027.44 | 2208898.03 |
| Block House Creek | 439425.83 | 2212888.87 |
| West Branch | 434011.43 | 2213032.45 |
| Hogan Creek | 451733.48 | 2177325.66 |
| Long Branch | 456381.22 | 2195605.31 |
| McCoy Creek | 445479.11 | 2177725.24 |
| Big Fishweir Creek | 433340.10 | 2165048.70 |
| Williamson Creek | 423147.60 | 2161094.77 |
| Butcher Pen Creek | 425615.52 | 2158247.68 |
| Fishing Creek | 428166.62 | 2156624.76 |
| Unnamed Creek | 441738.10 | 2138528.06 |
| Orange Park Slou | 437114.53 | 2119464.00 |
| Goodbys Creek | 457851.25 | 2138658.51 |
| Deep Bottom Creek | 451529.48 | 2125721.86 |

DRAFT

3.2.2.3 Meteorology: Rainfall, Evaporation, and Wind

The model applied spatially-uniform rainfall from SJRWMD's network of eight local stations to account for precipitation that fell into the model domain (Table 3.2 and Figure 3.2). An area-weight spatial interpolation computed the spatially-uniform rainfall (Sucsy and Morris, 2002). The model also accounted for daily river evaporation based on pan evaporation data obtained from a National Oceanic and Atmospheric Administration (NOAA) pan station in Gainesville, Florida (Table 3.2 and Figure 3.2). The SJRWMD used a pan correction factor of 0.78 to adjust the observed pan evaporation data to river evaporation (Sucsy and Morris, 2002). The model applied a spatially-uniform wind field from hourly wind observation data at Jacksonville Naval Air Station (Table 3.2 and Figure 3.2) to account for wind shear on the river's water surface. The SJRWMD selected this wind station given its close proximity to the mainstream of the St. Johns River and location in an open area with no evidence of directional blocking (Sucsy and Morris, 2002).

**Table 3.2** Model Stations with Observed Rainfall, Evaporation and Wind Data in the Lower St. Johns River Basin

| Data Type | Agency | Location | Longitude | Latitude |
|---|---|---|---|---|
| Evaporation | NOAA | Gainesville WNW | 82° 30′ 00″ | 29° 41′ 00″ |
| Wind | NOAA | Naval Air Station | 81° 40′ 29″ | 30° 14′ 03″ |
| Rain | SJRWMD | Palatka | 81° 41′ 39″ | 29° 39′ 51″ |
| Rain | SJRWMD | Reid Farms | 81° 29′ 12″ | 29° 41′ 26″ |
| Rain | SJRWMD | Bostwick | 81° 39′ 41″ | 29° 44′ 07″ |
| Rain | SJRWMD | Elkton | 81° 26′ 38″ | 29° 46′ 30″ |
| Rain | SJRWMD | Molasses Junction | 81° 29′ 59″ | 29° 50′ 45″ |
| Rain | SJRWMD | Green Cove Sprngs | 81° 33′ 01″ | 30° 00′ 29″ |
| Rain | SJRWMD | Mandarin Lift | 81° 34′ 49″ | 30° 10′ 19″ |
| Rain | SJRWMD | Jacksonville | 81° 39′ 43″ | 30° 20′ 36″ |

DRAFT

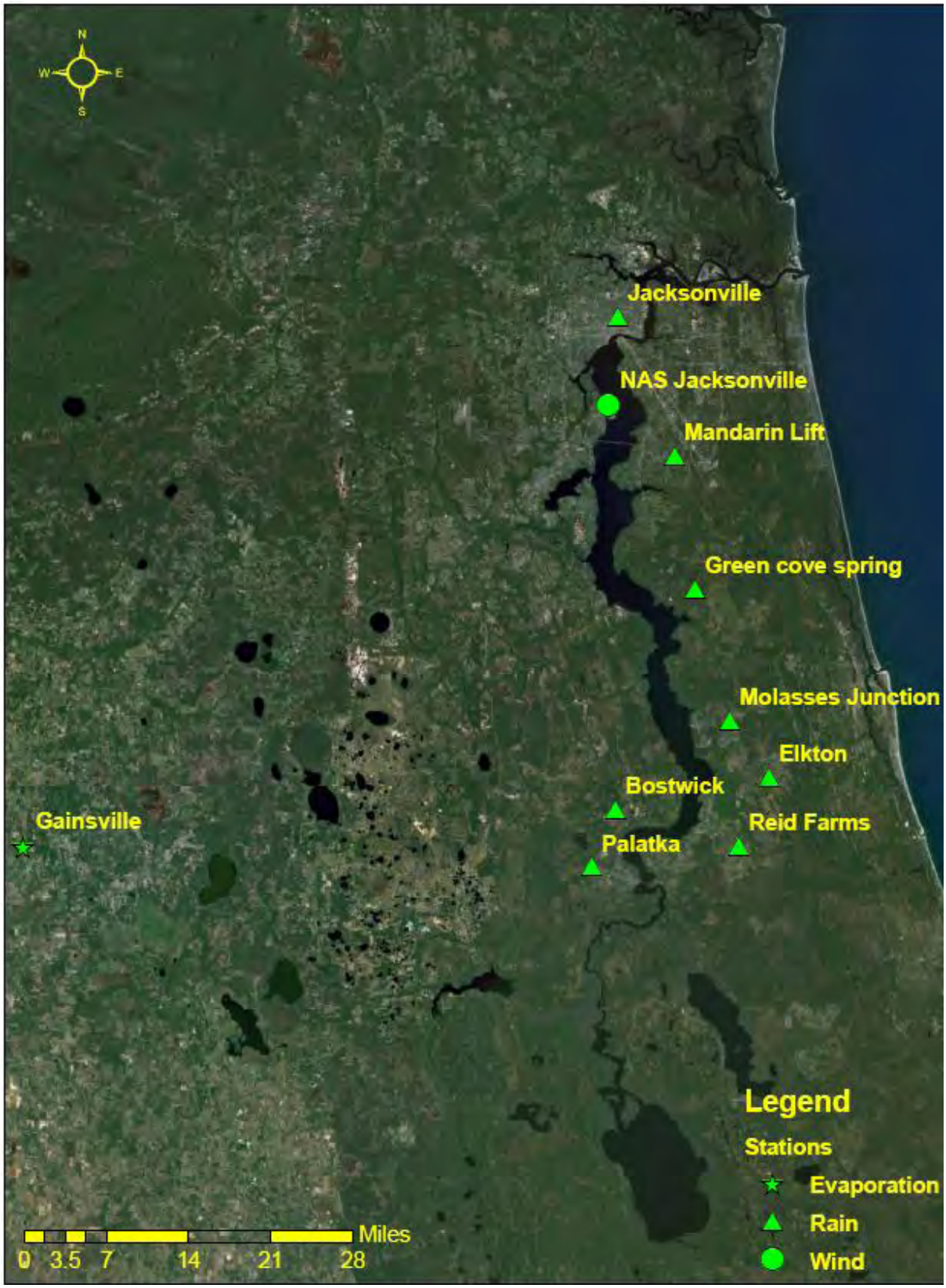


**Figure 3.2** Locations of Stations with Observed Rainfall, Evaporation and Wind Data

### 3.3 Model Mesh Refinement

The SJRWMD EFDC model provides limited resolution inside and near the channel (Figure 3.3). Ideally, the model would simulate continuous, longitudinal unidirectional flow through the deep channel as much as possible. Achieving these ends first required two adjustments to the model mesh — realigning the model's single element in the navigation channel and splitting the single element to multiple elements. Representing the trapezoidal channel accurately required at least three cross-channel elements (Figure 3.4). Multiple cells inside and near the channel from the river mouth to River Mile 20 provide better description of model bathymetry for various potential dredging templates for the Jacksonville Harbor Deepening Project.

While at least three elements are required to accurately represent the navigation channel modifications, more than three elements require additional computation time with potentially negligible improved accuracy. Notably, the cells inside the channel are much smaller than their adjacent cells outside the channel. The differing element sizes increase the numerical instability of the model, which then requires longer computing time to arrive at a suitable numerical solution. An investigation of the 2001 model with four channel elements showed no appreciable increase in model accuracy, but showed a significant increase in model instability and computation time. After mesh refinement, the updated Jacksonville Harbor EFDC model (hereinafter referred to as the USACE model) comprises six vertical layers and 2,707 horizontal cells with lengths varying between 113 ft and 6,545 ft.

DRAFT

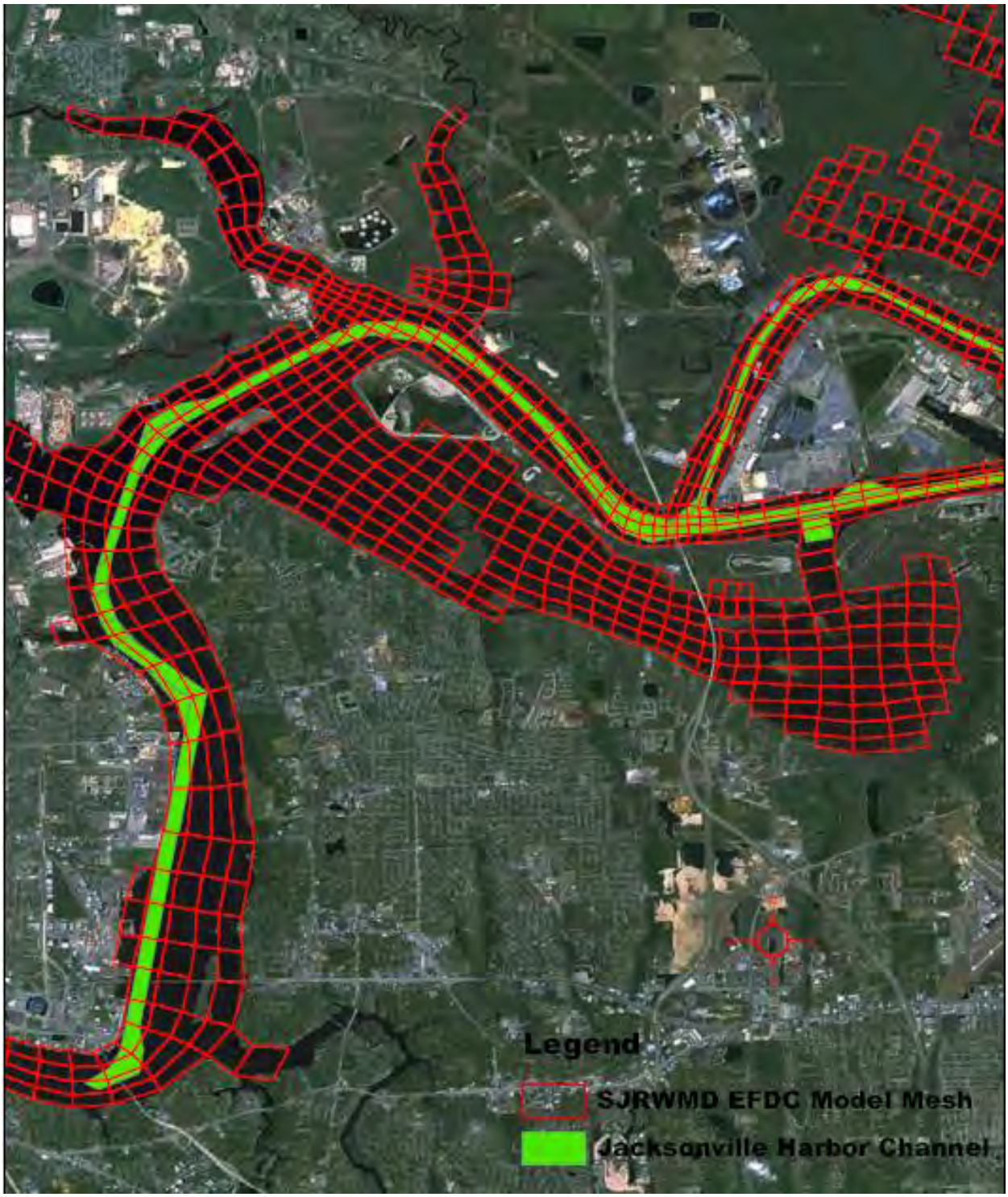


**Figure 3.3** SJRWMD EFDC Model Mesh in the Navigation Channel from River Mile 10 to 20

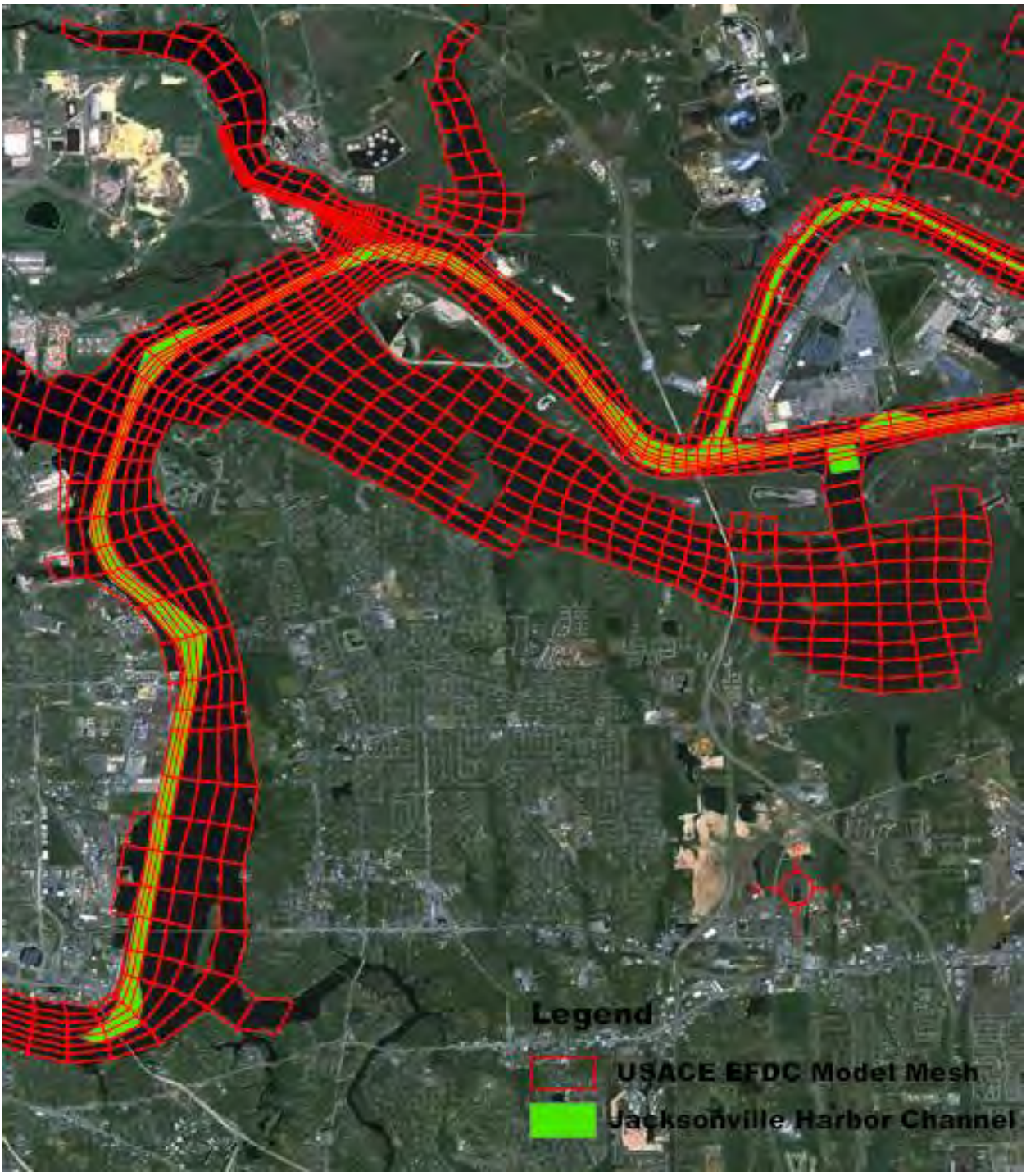


**Figure 3.4** USACE Model Updated Mesh with Three Elements in the Navigation Channel from River Mile 10 to 20

# 4.0 VALIDATION OF USACE HYDRODYNAMIC AND SALINITY MODEL

Validation of the USACE model provides confidence the model accurately simulates its intended parameters and conditions. Model validation comprises two components — calibration and verification. Calibration fine-tunes a model to improve predictions of simulated conditions for a specific study domain and period of record. In general, the calibration process is an iterative procedure to select model parameters that improve the accuracy of model outputs, such that model results provide the best comparison with field measured data. Model verification involves model application and comparison of the model results with an independent set of data (not used for model calibration) to make sure that the calibrated model's good performance extends beyond the calibration period. Once calibrated and verified, a numerical model can serve as a reliable tool to simulate changes in modeled processes (e.g., water level and salinity) in the model domain. This chapter describes the calibration and verification of the Jacksonville Harbor EFDC model and the results of the model calibration and verification simulations.

## 4.1 Model Calibration Methodology

Calibration of the St. Johns River USACE model included qualitative and quantitative comparisons of model results with field-measured data. Qualitative comparisons consisted of visual inspections of model results with the data via comparisons of time series plots and spatial graphics of water level and salinity. Visual inspections determined whether the model could reproduce field-measured data in time and space. In contrast, quantitative comparisons used statistical analyses to measure accuracy of model results compared with the data. For the quantitative evaluations of model calibration and verification, this study applied the RMSE and correlation statistical calculations. The RMSE measures the size of the discrepancies between model-calculated and field-measured values and provides an indication of model prediction accuracy. The correlation coefficient measures the tendency of the model-calculated and observed values to vary together linearly.

The comparisons of model results began with comparisons of water levels followed by comparisons with salinity concentration data. Each of these two parameters has its own importance in judging the success of the model calibration. Calibration with water levels improves confidence that the modeling process properly simulates parameters relevant to the driving transport mechanisms such as flow volume and velocity, bed friction, tidal phasing, and hydraulic boundary conditions. A good calibration with salinity concentration improves confidence that the model properly simulates advection-dispersion processes.

DRAFT

### 4.2 Hydrodynamic Model Parameters

Frequently adjusted parameters in EFDC modeling setup and calibration include bottom friction, such as the bottom roughness height, and the horizontal momentum diffusion coefficient.

Adjustments to bottom roughness height usually occur before adjustments of horizontal momentum diffusion coefficient during hydrodynamic model calibration. Bottom roughness differs from a friction coefficient because it corresponds to the logarithmic boundary layer roughness height in meters. The solution of momentum equations requires a bottom stress $\tau_b$

$$\tau_b = \rho u_*^2 = c_b \rho U^2 \tag{4.1}$$

where $u_*$ is the friction or shear velocity , $c_b$ is the bottom stress coefficient (friction coefficient), and U is the flow velocity at the bottom layer. Applying a logarithmic distribution of velocity profile between the solid bottom and the middle of the bottom cell layer provides the bottom stress coefficient:

$$c_b = \kappa^2 [\ln(\frac{H}{2z_0^*})]^{-2} \tag{4.2}$$

where $z_0^*$ is the dimensional bottom roughness height , $\kappa$ is von Karman constant, and H is the height of the bottom layer.

The SJRWMD optimized the bottom roughness height in the model to minimize the difference between observed and simulated harmonic tide given the importance of tidal dynamics to circulation and mixing in this area. Grid cells were grouped into different segments within which bottom roughness was optimized and varied from 6.56 x $10^{-4}$ to 7.22 x $10^{-1}$ ft.

The horizontal momentum diffusion coefficient is pre-specified or calculated with the Smagorinsky formula:

$$A_H = C\Delta x \Delta y [(\frac{\partial u}{\partial x})^2 + (\frac{\partial v}{\partial y})^2 + \frac{1}{2}(\frac{\partial u}{\partial y} + \frac{\partial v}{\partial x})^2]^{1/2} \tag{4.3}$$

where $C$ is the horizontal mixing constant, and $\Delta x$ and $\Delta y$ are the model grid size in x and y horizontal directions. The Smagorinsky formula links the numerical model's horizontal mixing to current shear and model grid size.

DRAFT

## 4.3 USACE Model Calibration

The USACE-SAJ selected 1997 as the USACE model one-year calibration period. Calibration consisted of comparisons of model-calculated and measured water levels at four stations — Long Branch, Main Street Bridge, Buckman Bridge, and Shands Bridge (Figure 4.1) and comparisons of model-calculated and measured salinity at four stations — Dames Point, Acosta Bridge, Buckman Bridge, and Shands Bridge (Figure 4.2).

The abovementioned stations provide continuous records of measured water level or salinity. The SJRWMD provided all the measured water level and salinity hourly data collected during 1995 – 1999 in cooperation with the Florida Department of Environmental Protection (FDEP) and the U.S. Geological Survey (USGS). For water level data, the FDEP measures water level at six-minute intervals at the water level stations. Salinity data came from the USGS, which monitors salinity at hourly intervals at the salinity stations in the Lower St. Johns River. This salinity network began in the early 1995 as a joint effort between USGS and SJRWMD to provide continuous salinity data for the TMDL modeling study.

The calibrated model yielded a horizontal momentum diffusion coefficient with Smagorinsky formula horizontal mixing constant ($C$) equal to 0.01and Figure 4.3 shows the final calibrated bottom roughness height. The following sections describe the final calibration and verification results.

### *4.3.1 Water Surface Level Calibration*

Comparisons of simulated and measured hourly water levels at the four water level stations along the Lower St. Johns River provided the means to evaluate model performance of the USACE model during the water level calibration period. Figure 4.4 – Figure 4.7 show the comparison plots and Table 4.1 provides the root mean square errors (RMSE) and correlation coefficients of simulated and measured hourly water levels for each of the water surface stations for the one-year calibration period. To discern tidal periods in the plot, a one-month period from each calibration condition was selected to show the observed and simulated time-series of water level. The graphs show that semidiurnal tides dominate water levels although lower frequency variability occurs, especially during the dry season, when the influence from freshwater inflow weakens. Figure 4.6 (Buckman Bridge) and Figure 4.7 (Shands Bridge) indicate times when the model lateral inflows were likely larger than actual inflows and caused the model to overestimate water level by 0.25 ft. Overall, the comparisons show good agreement between the measured and simulated water surface level. RMSE equal less than 0.31 ft and the correlation coefficient R is greater than 0.92 at all stations. The correlation coefficient generally decreases from downstream to upstream.

**Figure 4.1** Locations of Water Level Stations

**Figure 4.2** Locations of Salinity Stations

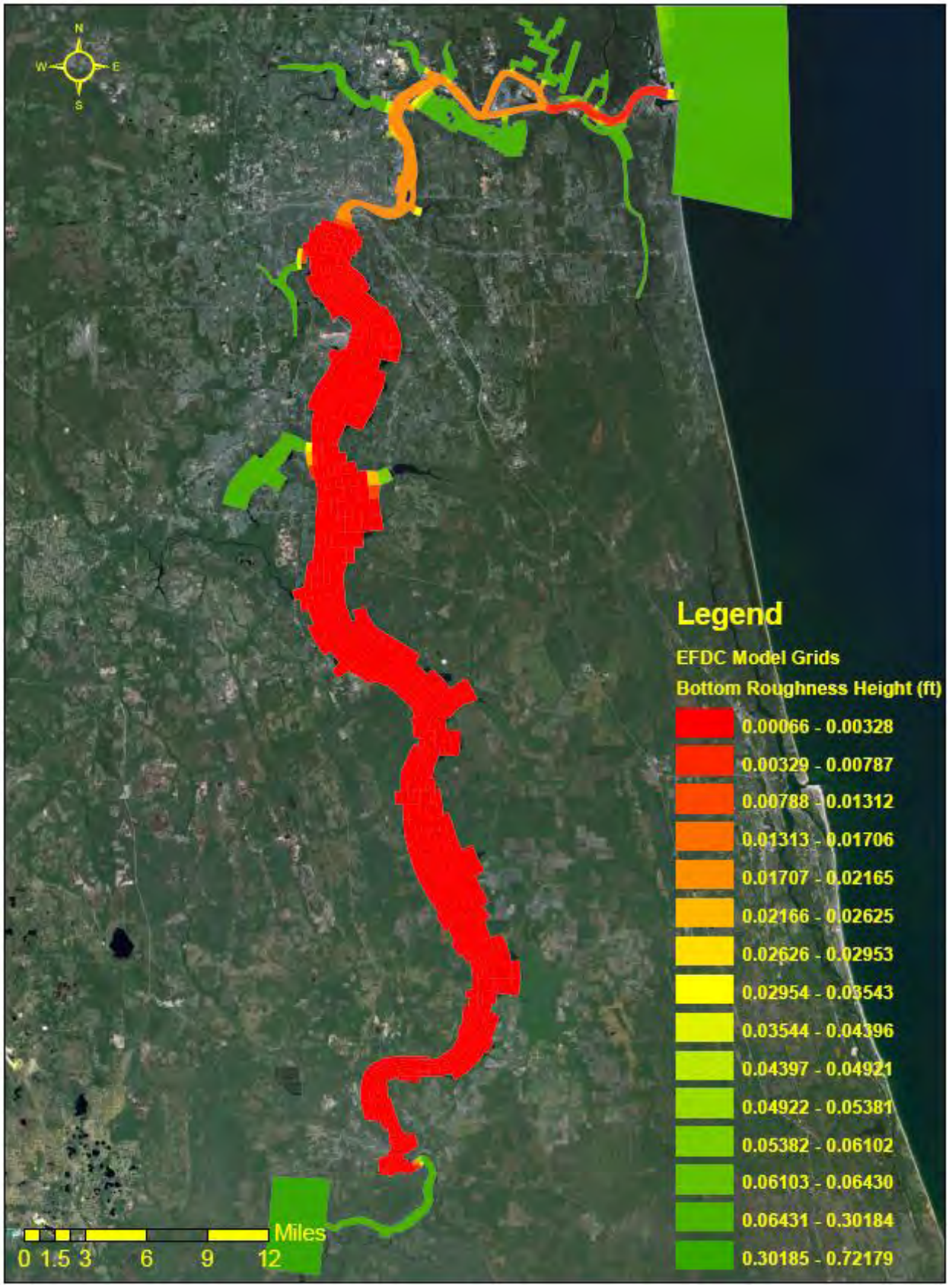


**Figure 4.3** EFDC Model Bottom Roughness Height

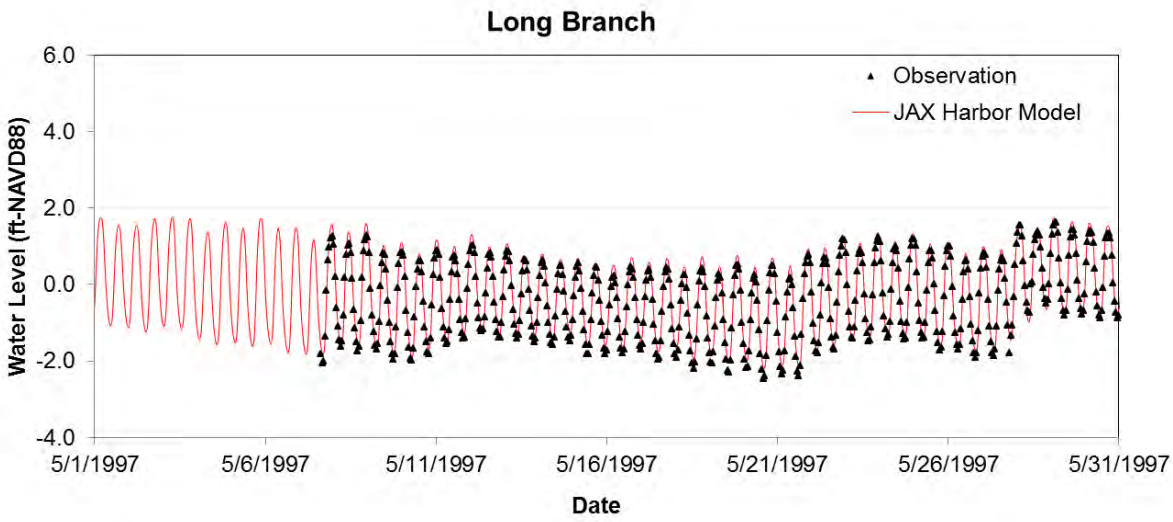


**Figure 4.4** Comparison of Computed and Observed Water Levels during a Portion of the Calibration Period (Long Branch)

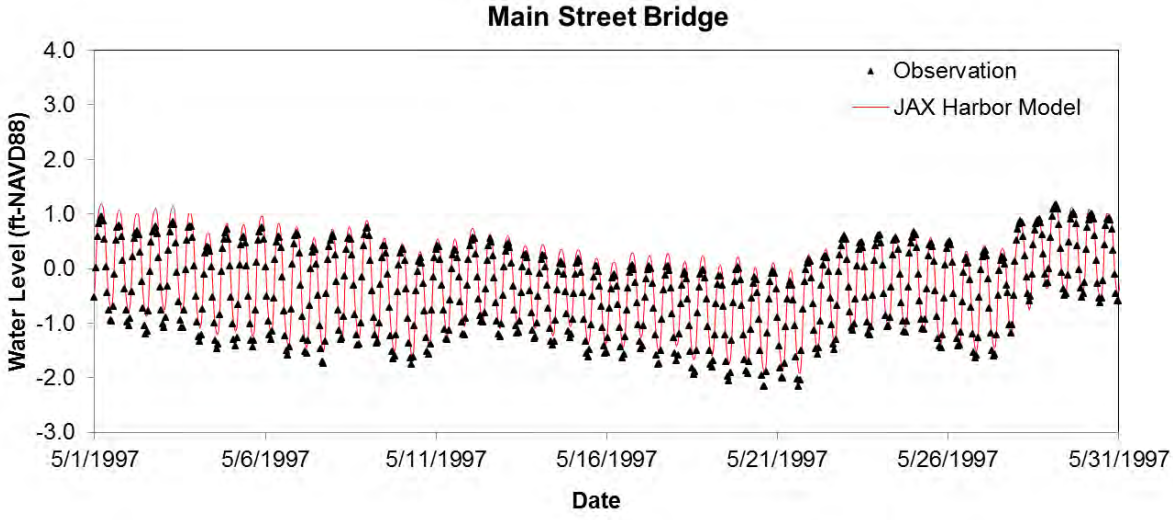


**Figure 4.5** Comparison of Computed and Observed Water Levels during a Portion of the Calibration Period (Main Street Bridge)

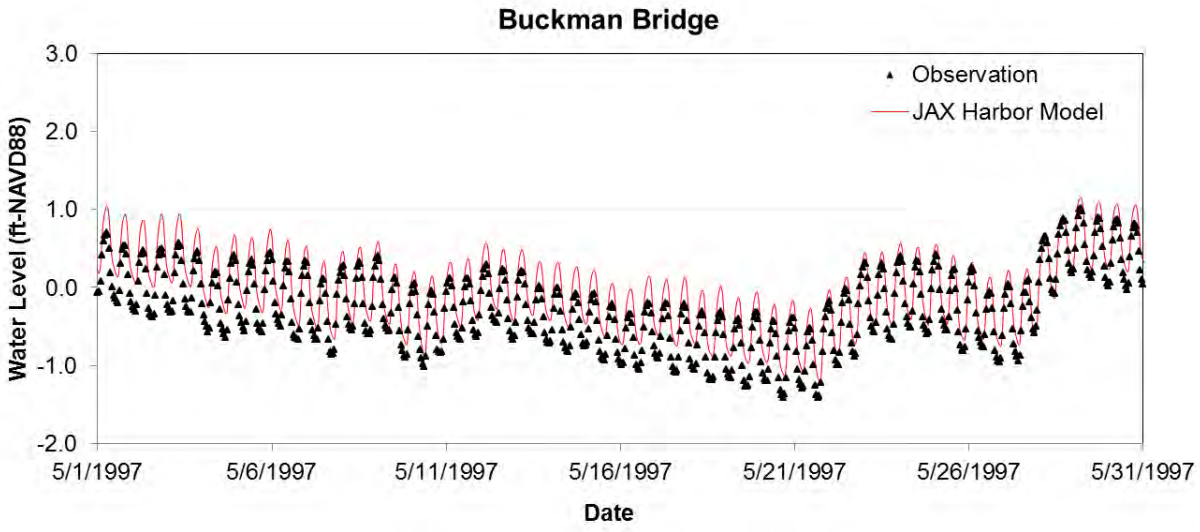


**Figure 4.6** Comparison of Computed and Observed Water Levels during a Portion of the Calibration Period (Buckman Bridge)

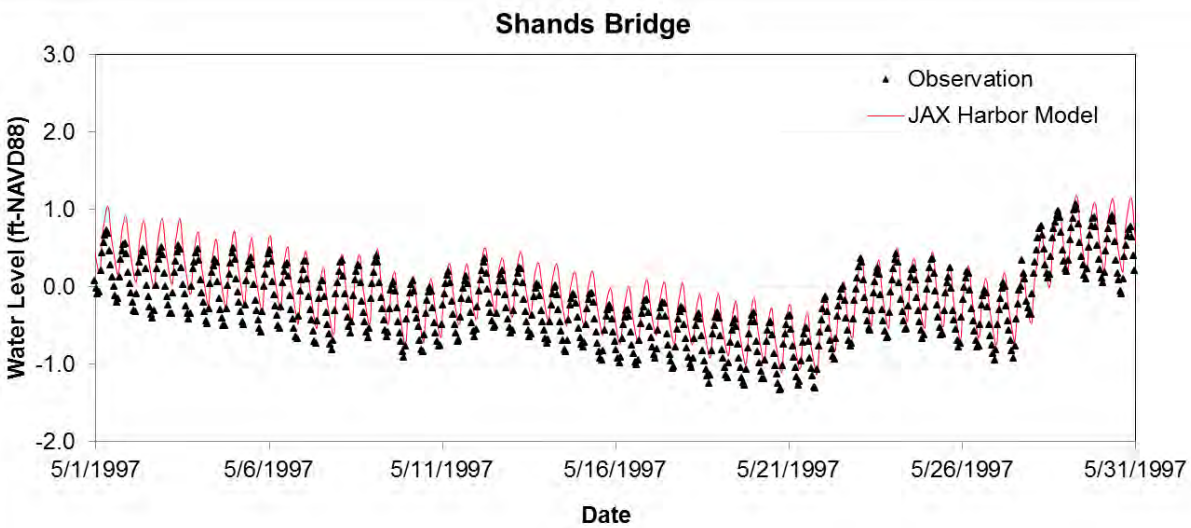


**Figure 4.7** Comparison of Computed and Observed Water Levels during a Portion of the Calibration Period (Shands Bridge Station)

**Table 4.1** Model Calibration Statistics for Water Level in 1997

| Station / Parameters | Long Branch Station | Main Street Bridge | Buckman Bridge | Shands Bridge |
|---|---|---|---|---|
| Correlation Coefficient, R | 0.988 | 0.983 | 0.965 | 0.929 |
| Root Mean Square Error, RMSE (ft) | 0.213 | 0.204 | 0.265 | 0.301 |

### *4.3.2 Salinity Calibration*

As a conservative constituent, salinity provides a means to assess the integration of all forces that drive the transport, circulation, and mixing processes. Additionally, salinity is a critical factor affecting the marine environment in estuaries. Thus, accurate simulation of salinity is critical to this study as the USACE model will serve to evaluate the response of salinity transport to channel deepening. Comparisons of observed and simulated hourly salinity at four stations (Dames Point, Acosta Bridge, Buckman Bridge, and Shands Bridge) along the Lower St. Johns River provide the means to evaluate model performance during the salinity calibration period.

Table 4.2 provides statistical comparisons of simulated and measured hourly salinity. The table provides the RMSE and correlation coefficient at each station. The salinity correlation coefficient is above 0.83 at Dames Point, Acosta Bridge, and Buckman Bridge and above 0.68 at Shands Bridge. Very low tidal influence and slight horizontal gradients of salinity from larger freshwater flows led to the smaller correlation coefficient at Shands Bridge. Notably, simulating low salinities at locations far away from the source (ocean) is very difficult. The range of the RMSE — 0.06 ppt (Shands Bridge) to 3.74 ppt (Dames Point) — was influenced by persistently low salinity at Shands Bridge and highly variable and large salinity at Dames Point.

Figure 4.9 – Figure 4.13 show the comparison plot of a month (chosen to discern tidal variability in plots) for the calibration period. The plots of hourly salinity illustrate the high correlation of salinity variability with tide for stations downstream of Buckman Bridge. During certain dry periods, both Shands Bridge and Buckman Bridge salinity follow a tidal signature. The signature follows the tide's semi-diurnal frequency as well as the neap to spring cycles. For example, Figure 4.10 shows the daily salinity range at Buckman fell to about 1 ppt during the week of May 22, 1997 but exceeded 5 ppt during the



DRAFT

week of May 29, 1997. In contrast, essentially no tidal signature is apparent in the salinity range at Shands Bridge. Inaccurate estimates of freshwater flows can also account for the isolated poor comparison of modeled salinity to data. Overall, visual observation of figures and examination of the statistical results show generally good agreement between the measured and simulated salinity.

**Table 4.2** Model Calibration Statistics for Salinity in 1997

| Station / Parameters | Dames Point | Acosta Bridge | Buckman Bridge | Shands Bridge |
|---|---|---|---|---|
| **Surface** | | | | |
| Correlation Coefficient, R | 0.893 | 0.901 | 0.836 | 0.686 |
| Root Mean Square Error, RMSE (ppt) | 2.856 | 2.130 | 1.086 | 0.065 |
| **Bottom** | | | | |
| Correlation Coefficient, R | 0.875 | 0.888 | 0.883 | 0.691 |
| Root Mean Square Error, RMSE (ppt) | 3.738 | 2.517 | 1.735 | 0.064 |

DRAFT

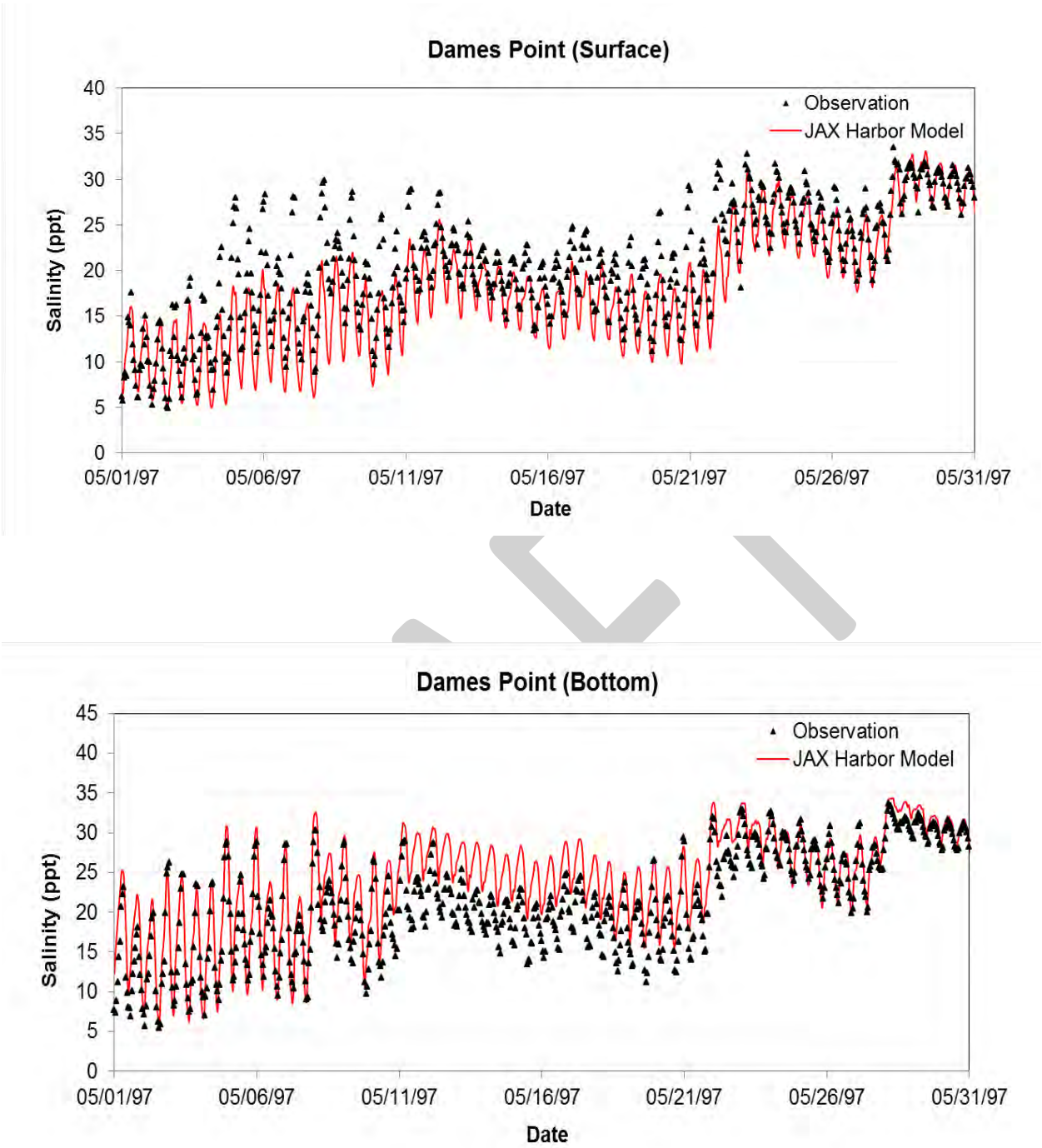


**Figure 4.8** Comparison of Computed and Observed Salinity during a Portion of the Calibration Period (Dames Point)

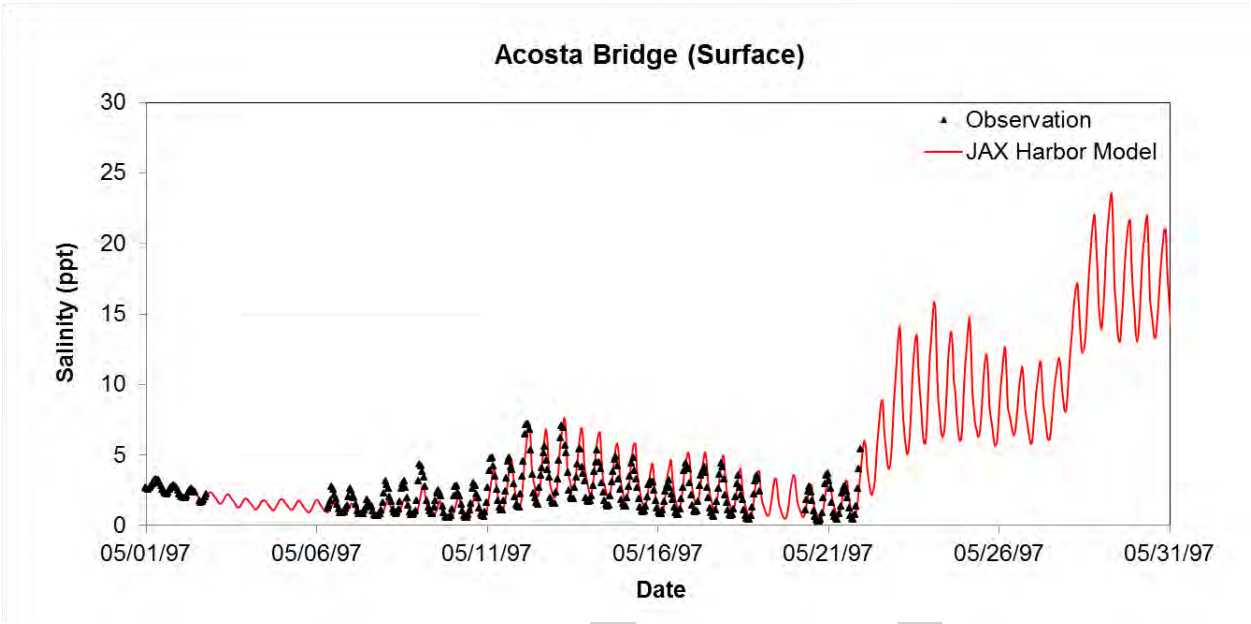


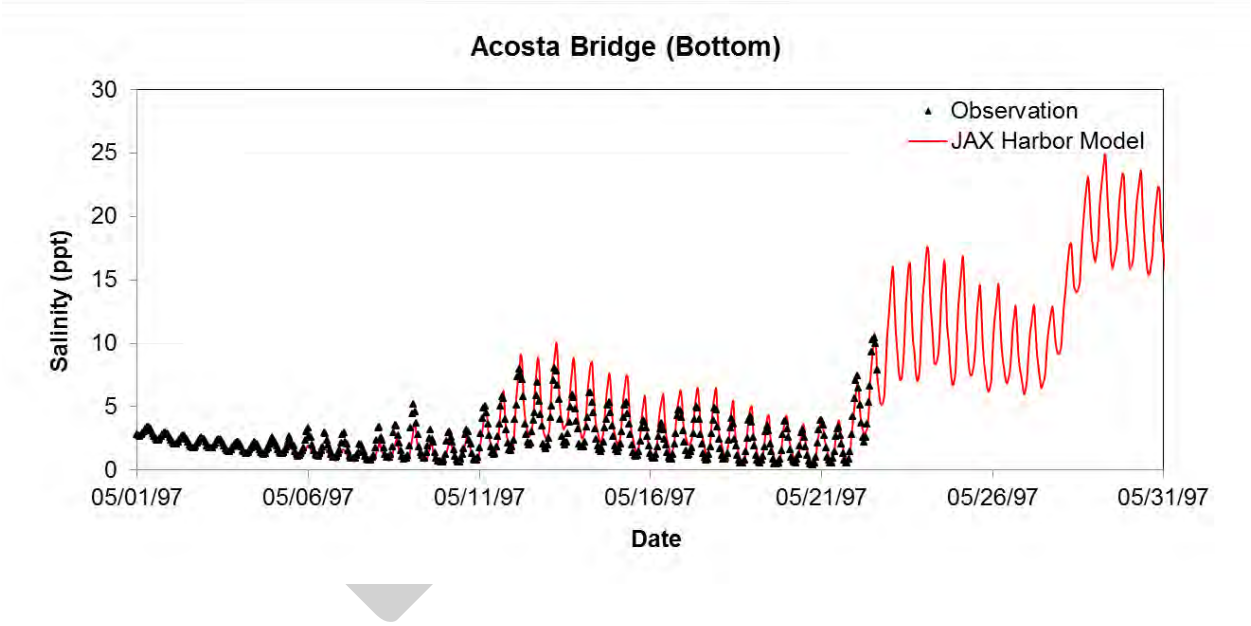


**Figure 4.9** Comparison of Computed and Observed Salinity during a Portion of the Calibration Period (Acosta Bridge)

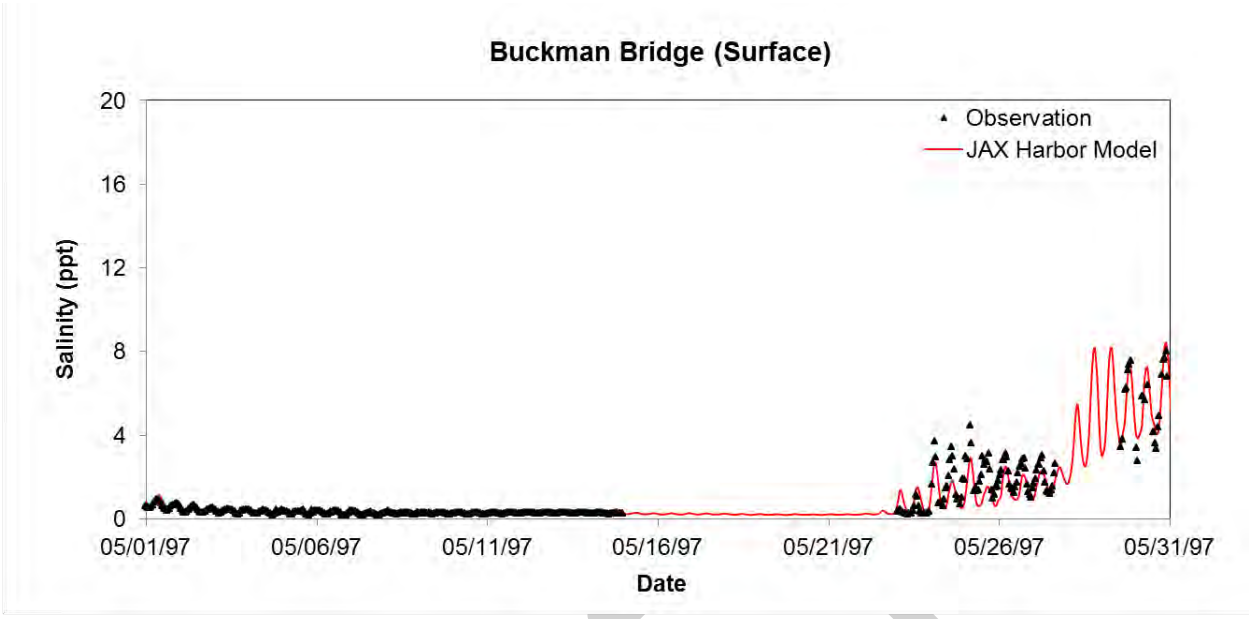


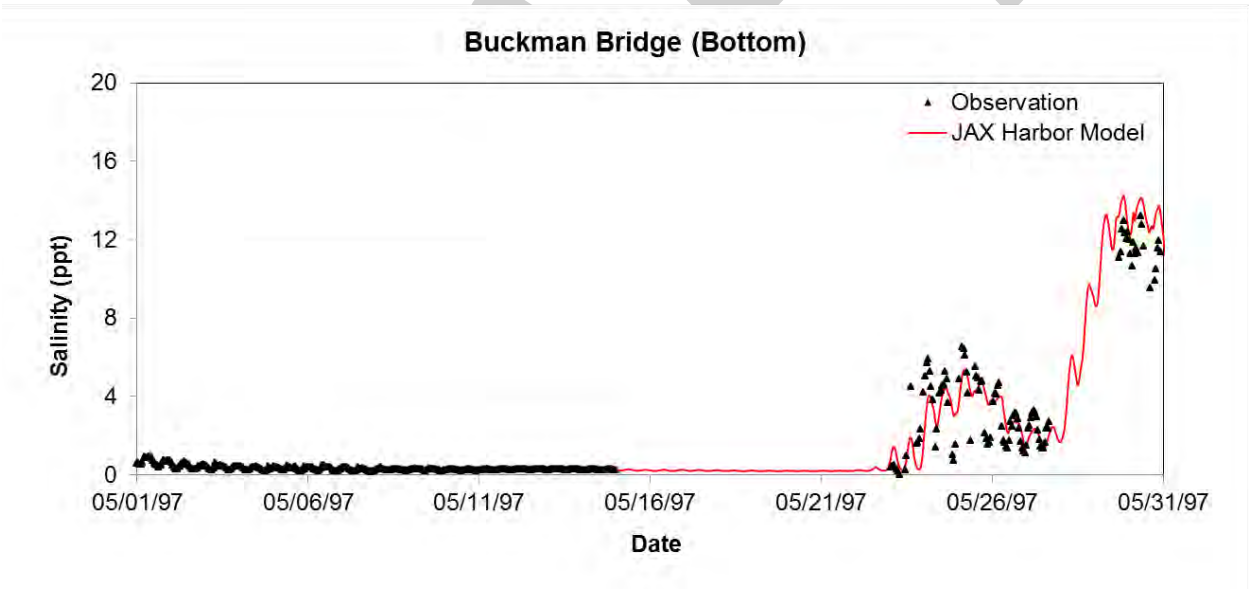


**Figure 4.10** Comparison of Computed and Observed Salinity during a Portion of the Calibration Period (Buckman Bridge)

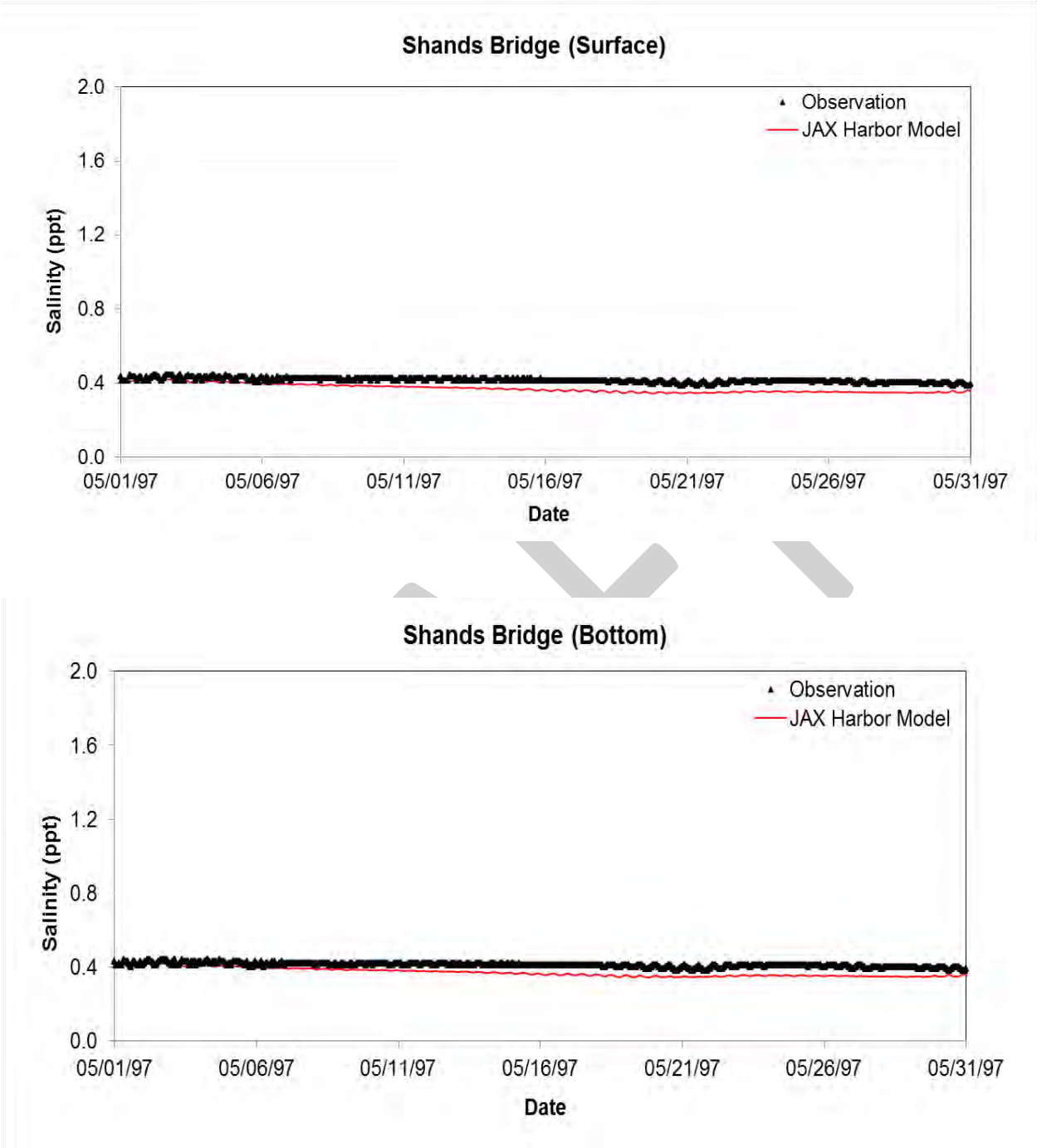


**Figure 4.11** Comparison of Computed and Observed Salinity during a Portion of the Calibration Period (Shands Bridge)

## 4.4 USACE Model Verification

Model verification ensures that the model's calibrated parameters also apply for other data sets (i.e., data sets outside the calibration period). Model verification applied the same model parameters determined during model calibration. The USACE-SAJ selected 1998 as the one-year model verification period. The following sections present graphical and statistical comparisons of model predictions to observed data for water level and salinity for the verification period.

### *4.4.1 Water Level Verification*

Simulated and measured hourly water levels were compared at the four water level stations along the Lower St. Johns River. Similar to comparisons during model calibration, the comparisons show overall good agreement between the measured and simulated water surface level for both wet and dry conditions. Table 4.3 presents the statistics of water levels for measured and simulated data for the verification stations. Overall, RMSE equals less than 0.31 ft, and the correlation coefficient R is greater than 0.95 at all stations. Figure 4.12 through Figure 4.15 show the graphical comparisons between the measured and simulated values for a 30-day period. Notably, Figure 4.12 shows a different period than those for the other figures because water level data is not available for the same period as in the other figures. Although the model overestimates water levels by 0.3 ft at Buckman Bridge and Shands Bridge, the tide ranges match very well. Lateral inflow inputs likely provided larger inflows that resulted in the overestimation of the water level. Generally, excellent agreement between measured and simulated data occurs at all stations.

**Table 4.3** Model Verification Statistics for Water Level in 1998

| Station / Parameters | Long Branch Station | Main St. Bridge | Buckman Bridge | Shands Bridge |
|---|---|---|---|---|
| Correlation Coefficient, R | 0.988 | 0.976 | 0.965 | 0.952 |
| Root Mean Square Error, RMSE (ft) | 0.259 | 0.245 | 0.291 | 0.306 |

DRAFT

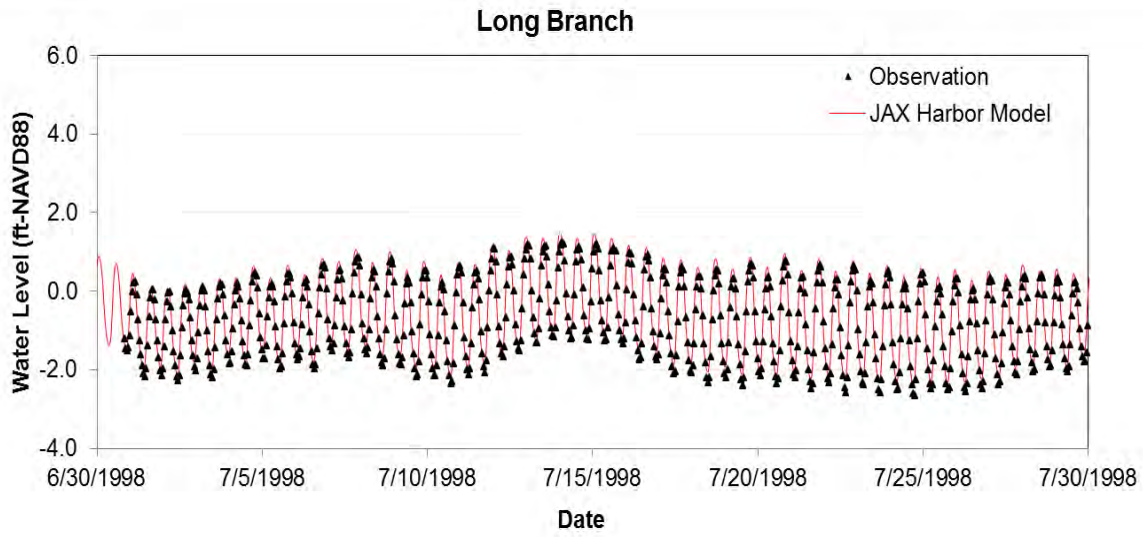


**Figure 4.12** Comparison of Computed and Observed Water Level during a Portion of the Verification Period (Long Branch)

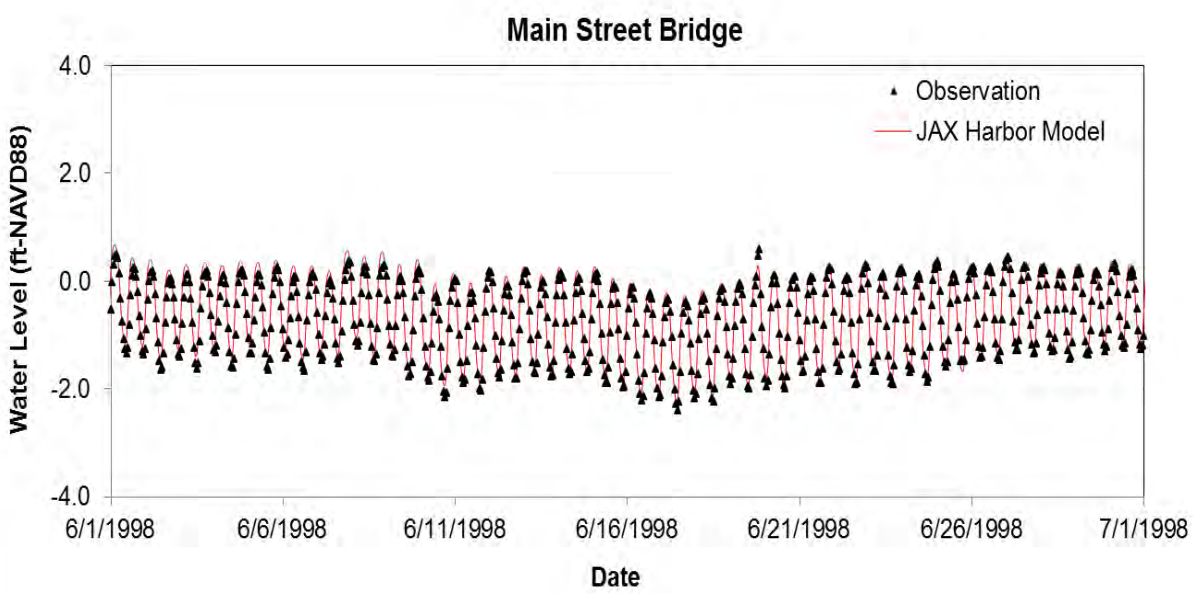


**Figure 4.13** Comparison of Computed and Observed Water Level during a Portion of the Verification Period (Main Street Bridge)

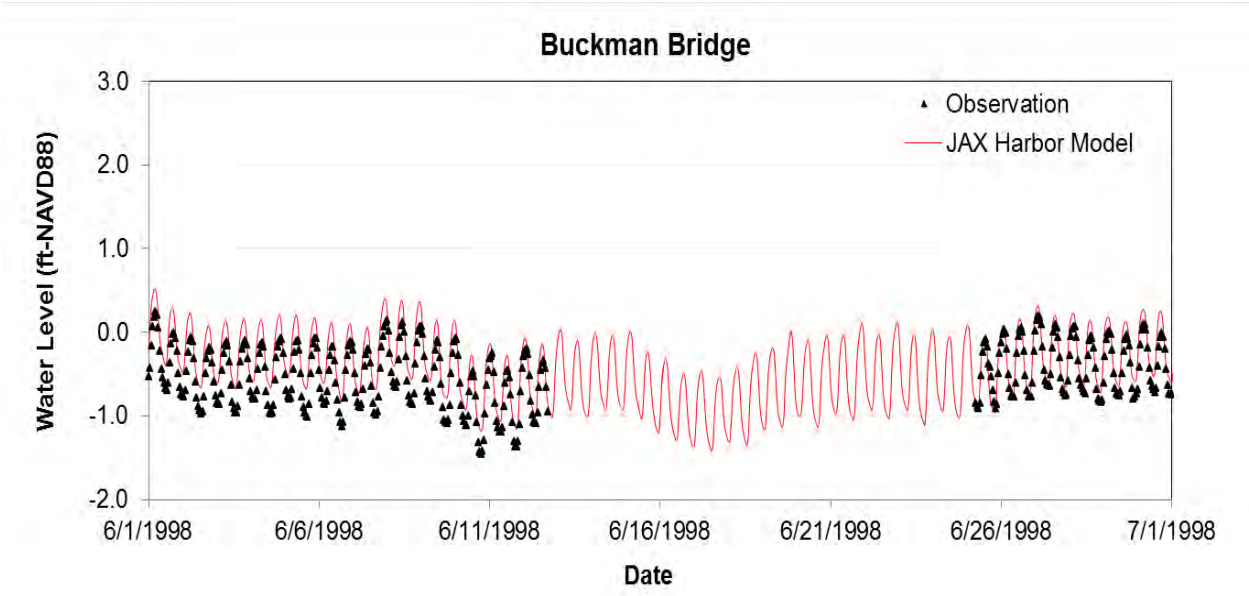


**Figure 4.14** Comparison of Computed and Observed Water Level during a Portion of the Verification Period (Buckman Bridge)

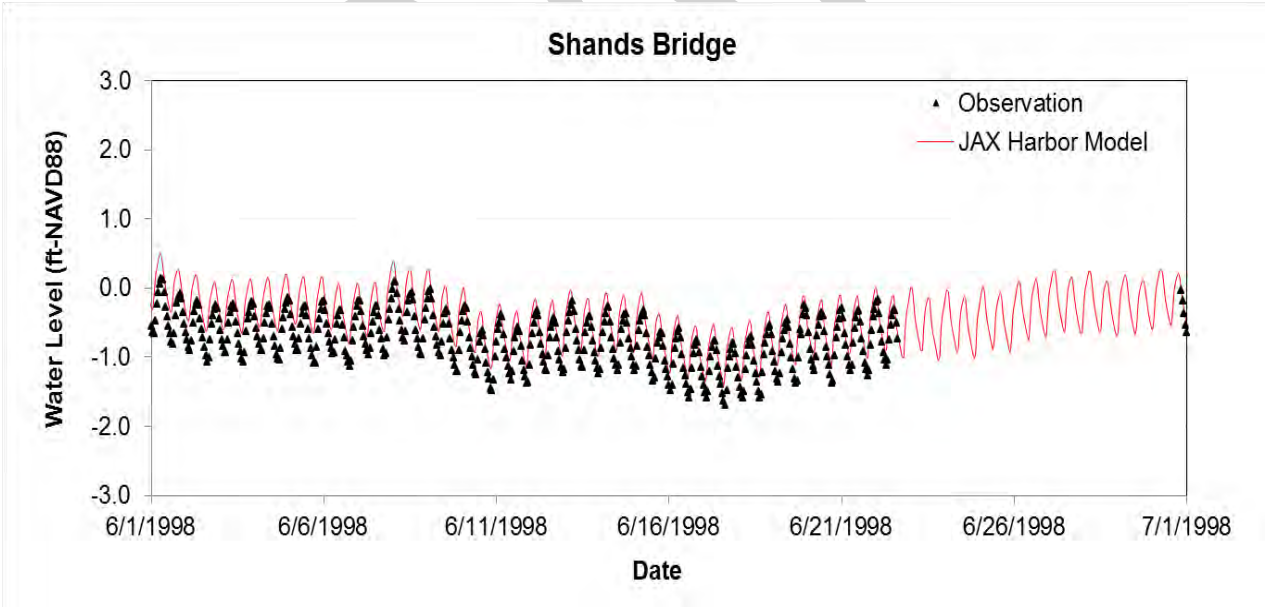


**Figure 4.15** Comparison of Computed and Observed Water Level during a Portion of the Verification Period (Shands Bridge)

### *4.4.2 Salinity Verification*

Table 4.4 shows salinity statistics for measured and simulated data. Overall, results compare well with the observation data with RMSE less than 1.2 ppt except at Dames Point (where salinity was high and varied over a wide range) and correlation coefficient R greater than 0.8 at these all stations. Figure 4.16 through Figure 4.19 present comparisons of measured and simulated salinities for a one-month period. The model captures the salinity intrusion on the Lower St Johns River relatively well. During the verification period, the model underestimates the salinity at Dames Point and Acosta Bridge although the simulated ranges compare very well. Evidently, the model applied too much freshwater inflow. Notably, the freshwater inflow is an unadjustable model input (provided by SJRWMD), which Taylor Engineering recognizes as a limitation beyond the scope of this study. Overall, the comparisons show that the model used in this study captures the general distribution of salinity along the Lower St. Johns River, and appears sufficiently calibrated and verified to evaluate hydrodynamic and salinity in the Lower St. Johns River and to provide CE-QUAL-ICM input hydraulic information.

**Table 4.4** Model Verification Statistics for Salinity in 1998

| Station / Parameters | Dames Point | Acosta Bridge | Buckman Bridge | Shands Bridge |
|---|---|---|---|---|
| **Surface** | | | | |
| Correlation Coefficient, R | 0.948 | 0.974 | 0.794 | 0.979 |
| Root Mean Square Error, RMSE (ppt) | 2.407 | 1.202 | 0.860 | 0.023 |
| **Bottom** | | | | |
| Correlation Coefficient, R | 0.881 | 0.974 | 0.852 | 0.979 |
| Root Mean Square Error, RMSE (ppt) | 3.927 | 1.023 | 0.788 | 0.022 |

DRAFT

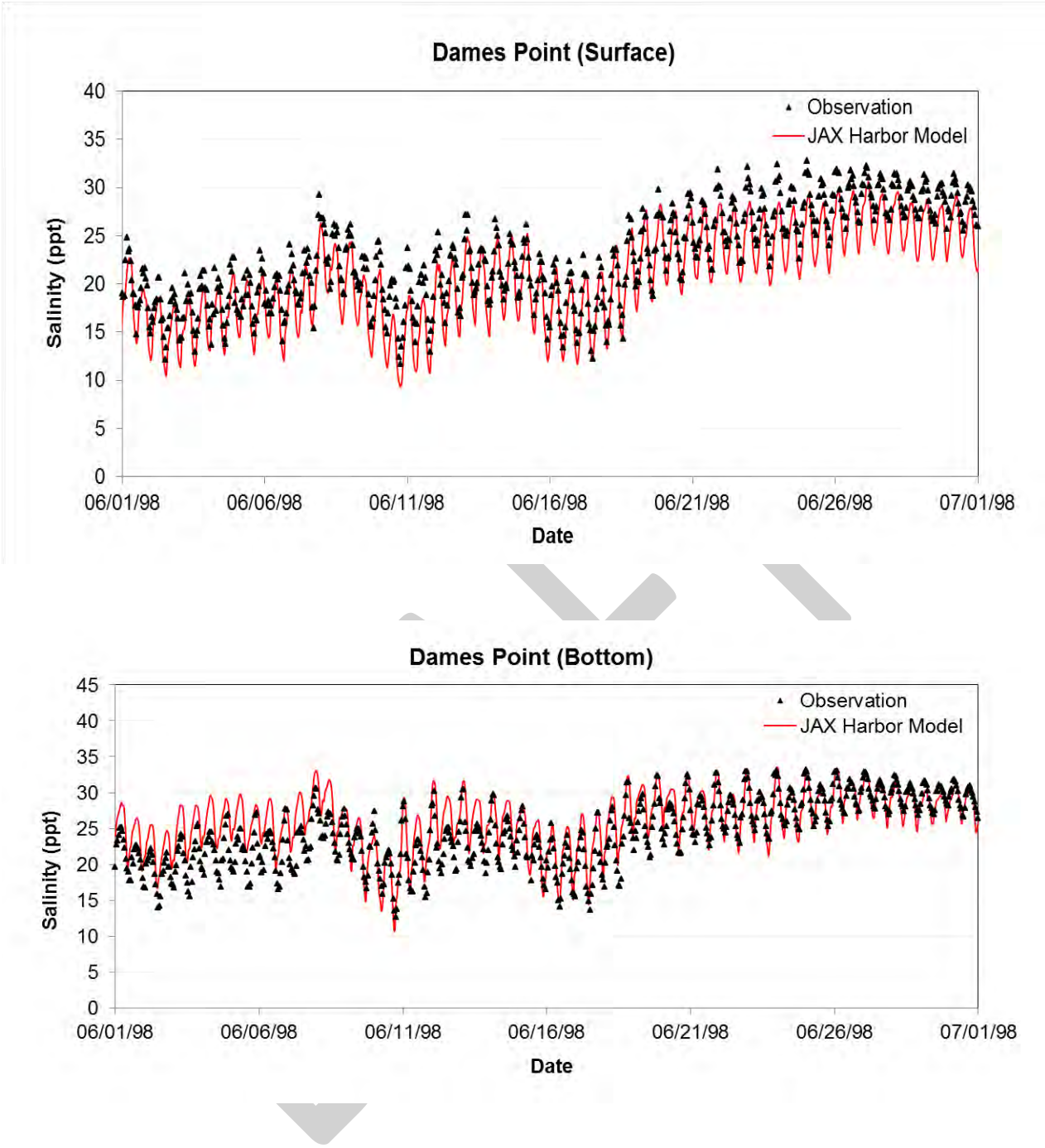


**Figure 4.16** Comparison of Computed and Observed Salinity during a Portion of the Verification Period (Dames Point)

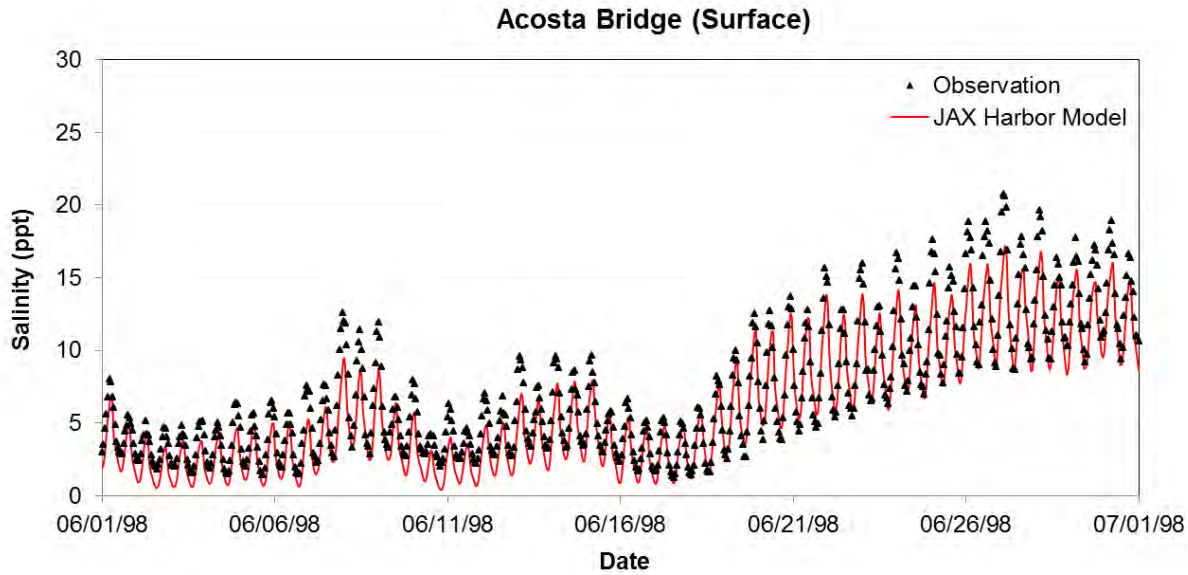


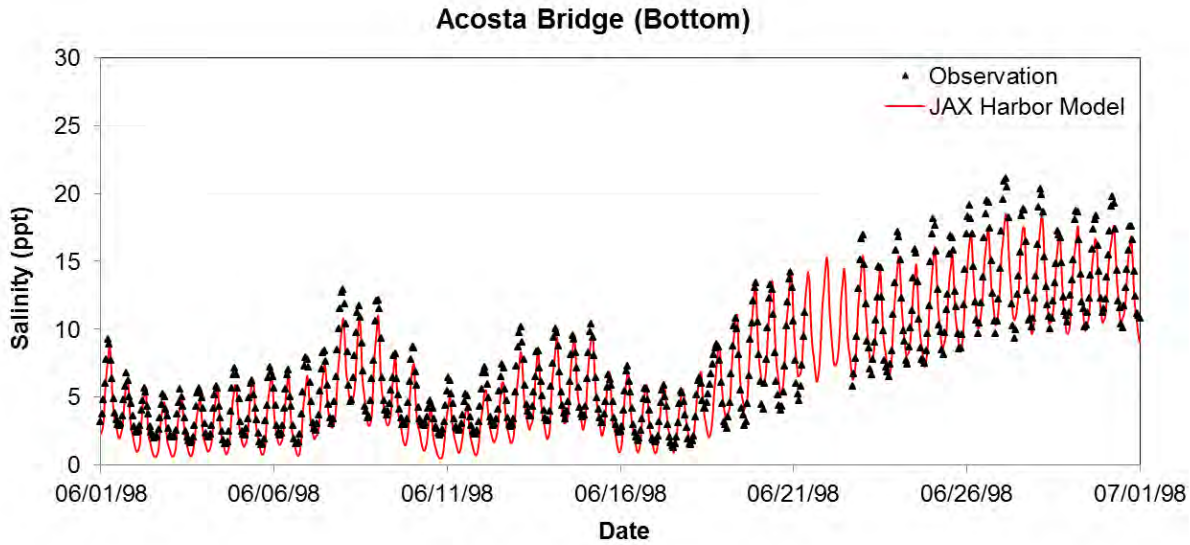


**Figure 4.17** Comparison of Computed and Observed Salinity during a Portion of the Verification Period (Acosta Bridge)

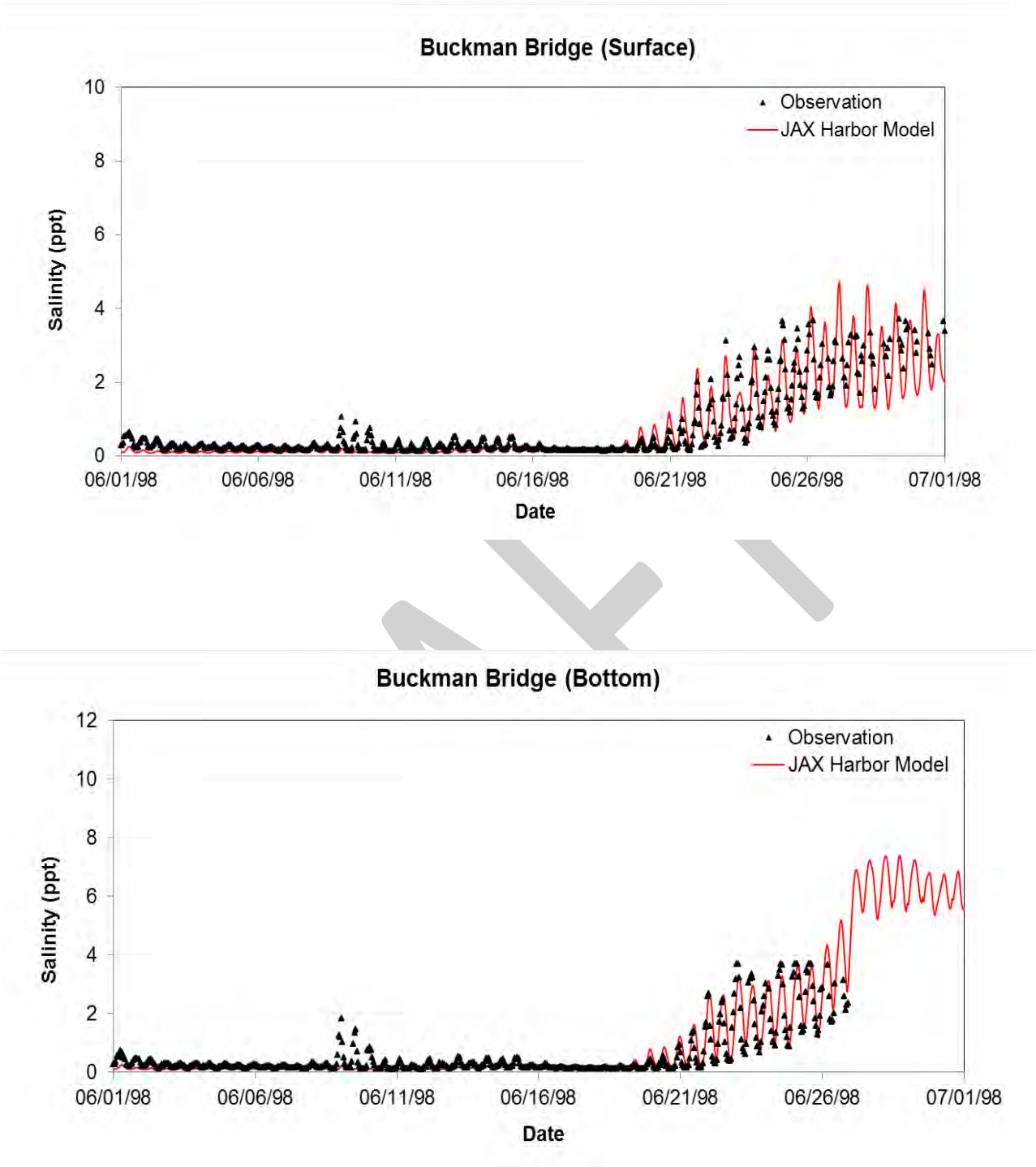


**Figure 4.18** Comparison of Computed and Observed Salinity during a Portion of the Verification Period (Buckman Bridge)

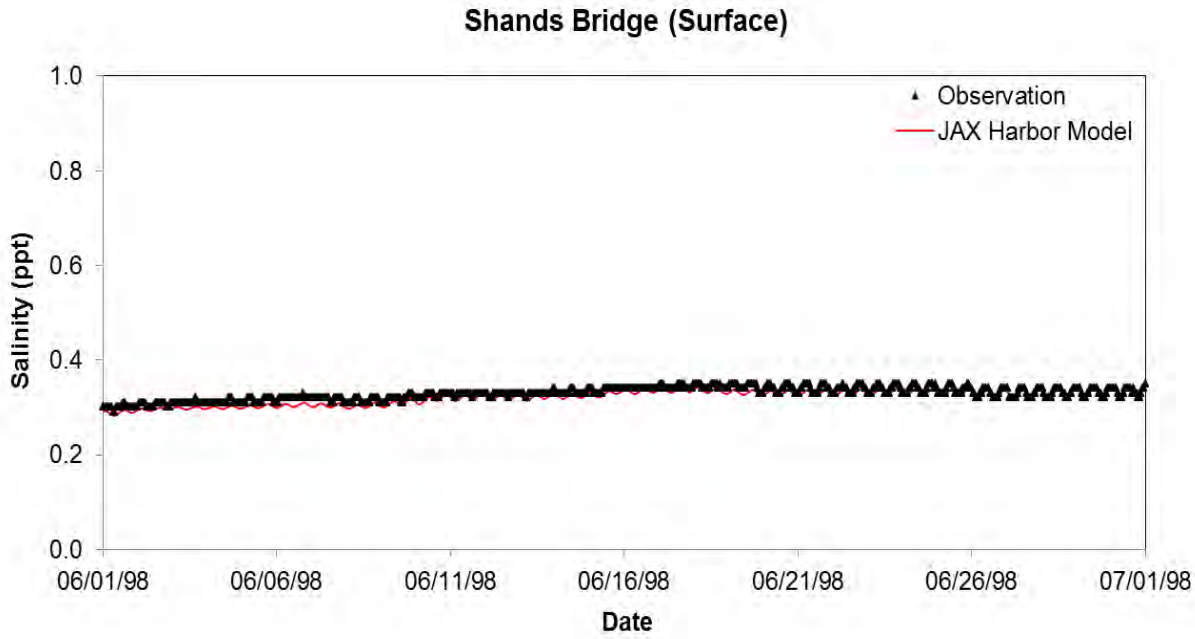


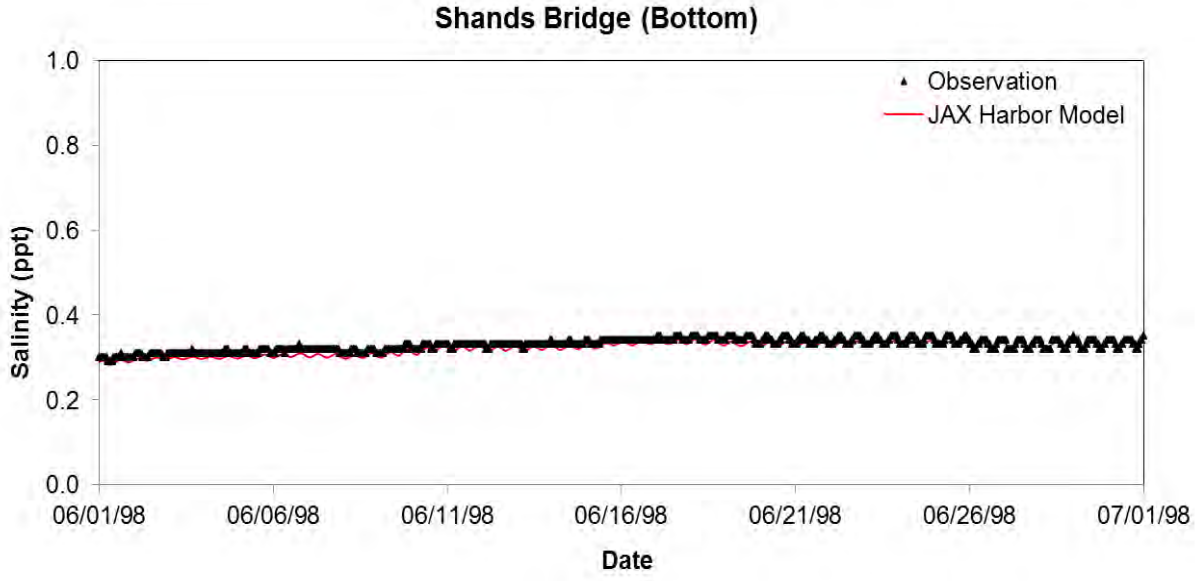


**Figure 4.19** Comparison of Computed and Observed Salinity during a Portion of the Verification Period (Shands Bridge)

## 5.0 SUMMARY AND CONCLUSIONS

This study describes the setup, mesh refinement, and validation of the USACE hydrodynamic and salinity model that will provide input information to the CE-QUAL-ICM water quality model. The USACE-SAJ plans to use the CE-QUAL-ICM to assess direct impacts to water quality of navigation channel modifications for the Jacksonville Harbor Deepening.

The original St. Johns River Water Management District EFDC mesh was refined in and near the navigation channel to develop the USACE model mesh and allow description of bathymetries of potential channel changes for the Jacksonville Harbor Deepening Project. The mesh refinement increased horizontal cells across the navigation channel from one to three from the river mouth to Mile 20. Taylor Engineering calibrated and verified the USACE model with monitoring data of water level and salinity collected during 1997 and 1998. The overall good agreement between simulated and observed water levels and salinity demonstrates the capability of the USACE model to reasonably simulate these processes in the Lower St. Johns River. Based on the calibration and verification results, the USACE model is suitable for predicting hydrodynamics and salinity in the Lower St. Johns River and for producing CE-QUAL-ICM input hydraulic information.

DRAFT

## REFERENCES


Blumberg, A. F., and Mellor, G. L. 1987. "A Description of a Three-dimensional Coastal Ocean Circulation Model." In: *Three-Dimensional Coastal Ocean Models, Coastal and Estuarine Science, Vol. 4.* (Heaps, N. S., ed.) American Geophysical Union, pp. 1-19.

Clark, T., and Hall, W. 1991. Multi-domain Simulations of the Time Dependent Navier-Stokes Equations: Benchmark Error Analysis of Some Nesting Procedures. *J. Comp. Phys*., 92, 456-481.

Hamrick, J. M., Kuo, A. Y., and Shen, J. 1995. Mixing and dilution of the Surrey Nuclear Power Plant cooling water discharge into the James River. a report to Virginia Power Company, The College of William and Mary, Virginia Institute of Marine Science, Gloucester Point, VA, 76 pp.

Hamrick, J.M. 1996. User's Manual for the Environmental Fluid Dynamics Computer Code. Special Report No. 331 in *Applied Marine Science and Ocean Engineering*. Department of Physical Sciences, School of Marine Science, Virginia Institute of Marine Science, The College of William and Mary. Gloucester Point, VA.

Hamrick, J.M. 2011. Twenty Years of Estuary and Coastal Modeling with the Environmental Fluid Dynamic Code. (Presentation). *12th International Conference on Estuarine and Coastal Modeling.* Nov 7-9, St. Augustine, FL.

Mellor, G, L., (1991). An Equation of State for Numerical Models of Oceans and Estuaries. *J. Atoms. Oceanic Tech*, 8, 609-611.

Jin, K. R., J. M. Hamrick, and T. S. Tisdale, 2000: Application of a three-dimensional hydrodynamic model for Lake Okeechobee, *Journal of Hydraulic Engineering*, 106, 758-772.

St. Johns River Water Management District (SJRWMD). 2011. St. Johns River Water Supply Impact Study, Publication No. SJ2012-1, Palatka, FL.

Sucsy, P. and Morris, F. 2002. "Calibration of a Three-Dimensional Circulation and Mixing Model of Lower St. Johns River." (Memorandum draft). St. Johns River Water Management District, Palatka, FL.

Toth, D. J. 1993. Volume 1 of the Lower St. Johns River Basin Reconnaissance: Hydrogeology. Tech. Rept. SJ93-7. St. Johns River Water Management District, Palatka, FL.

U.S. Environmental Protection Agency, 2007. *National Management Measures to Control Nonpoint Source Pollution from Hydromodification.* EPA 841-B-07-002, U.S. Environmental Protection Agency, Washington, D.C.

Wool, T. A., S. R. Davie, and H. N. Rodriguez, 2003: Development of three-dimensional hydrodynamic and water quality models to support TMDL decision process for the Neuse River estuary, North Carolina. *Journal of Water Resources Planning and Management*, 129, 295-306.


DRAFT

# APPENDIX A

## Governing Hydrodynamic

DRAFT

The computational schemes in the EFDC model are equivalent to the widely used Princeton Ocean Model (POM) by Blumberg and Mellor (1987) in many aspects. The EFDC model uses sigma vertical coordinate and curvilinear orthogonal horizontal coordinates. The EFDC model solves the 3-D, vertically hydrostatic, free surface, turbulent averaged equations of motions for a variable density fluid. Dynamically coupled transport equations for turbulent kinetic energy, turbulent length scale, salinity, and temperature are also solved.

To provide uniform resolution in the vertical, a time variable stretching transformation is applied. The stretching is given by

$$z = (z^* + h)/(\zeta + h) \tag{A.1}$$

where * denotes the original physical vertical coordinates and $h$ and $\zeta$ are the physical vertical coordinates of the bottom topography and the free surface respectively. This so called "sigma" coordinate allows smooth representation of the bathymetry and same order of accuracy in shallow and deep waters.

In sigma coordinate, transforming the vertically hydrostatic boundary layer form of the turbulent equations of motion and utilizing the Boussinesq approximation for variable density results in the momentum and continuity equations and the transport equations for salinity and temperature, in the following form (John Hamrick ,1996):

$$\begin{aligned}&\partial_t(mHu) + \partial_x(m_y Huu) + \partial_y(m_x Hvu) + \partial_z(mwu) - (mf + v\partial_x m_y - u\partial_y m_x)Hv \\ &= -m_y H\partial_x(g\zeta + P) - m_y(\partial_x h - z\partial_x H)\partial_z P + \partial_z(mH^{-1}A_v\partial_z u) + Q_u\end{aligned} \tag{A.2}$$

$$\begin{aligned}&\partial_t(mHv) + \partial_x(m_y Huv) + \partial_y(m_x Hvv) + \partial_z(mwv) - (mf + v\partial_x m_y - u\partial_y m_x)Hu \\ &= -m_x H\partial_y(g\zeta + P) - m_x(\partial_y h - z\partial_y H)\partial_z P + \partial_z(mH^{-1}A_v\partial_z v) + Q_v\end{aligned} \tag{A.3}$$

$$\partial_z P = -gH(\rho - \rho_0)\rho_0^{-1} = -gHb \tag{A.4}$$

$$\partial_t(m\zeta) + \partial_x(m_y Hu) + \partial_y(m_x Hv) + \partial_z(mw) = 0 \tag{A.5}$$

$$\partial_t(m\zeta) + \partial_x\left(m_y H\int_0^1 u\,dz\right) + \partial_y\left(m_x H\int_0^1 v\,dz\right) = 0 \tag{A.6}$$

$$\rho = \rho(P, S, T) \tag{A.7}$$

$$\partial_t(mHS) + \partial_x(m_y HuS) + \partial_y(m_x HvS) + \partial_z(mwS) = \partial_z(mH^{-1}A_b\partial_z S) + Q_S \tag{A.8}$$

$$\partial_t(mHT) + \partial_x(m_y HuT) + \partial_y(m_x HvT) + \partial_z(mwT) = \partial_z(mH^{-1}A_b\partial_z T) + Q_T \tag{A.9}$$

DRAFT

In the above equations, u and v are the horizontal velocity components in the curvilinear, orthogonal coordinates x and y, $m_x$ and $m_y$ are the square roots of the diagonal components of the metric tensor, $m = m_x m_y$ is the Jacobian or square root of the metric tensor determinant. The vertical velocity, with physical units, in the stretched, dimensionless vertical coordinate z is w, and is related to the physical vertical velocity w* by:

$$w = w^* - z(\partial_t \zeta + u m_{x-1} \partial_x \zeta + v m_{y-1} \partial_y \zeta) + (1-z)(u m_{x-1} \partial_x h + v m_{y-1} \partial_y h) \qquad \text{(A.10)}$$

The total depth, $H = \zeta + h$, is the sum of the depth below and the free surface displacement relative to the undisturbed physical vertical coordinate origin, z* = 0. The pressure p is the physical pressure in excess of the reference density hydrostatic pressure, $\rho_0 g H(1-z)$, divided by the reference density $\rho_0$ . In the momentum equations (Equations A.2 and A.3), f is the Coriolis parameter, $A_v$ is the vertical turbulent or eddy viscosity, and $Q_u$ and $Q_v$ are momentum source-sink terms which will be later modeled as subgrid scale horizontal diffusion. The density $\rho_0$, is in general a function of temperature, T, and salinity or water vapor, S, in hydrospheric and atmospheric flows respectively and can be a weak function of pressure, consistent with the incompressible continuity equation under the anelastic approximation (Mellor, 1991, Clark and Hall, 1991). The buoyancy, b, is defined in Equation (A.4) as the normalized deviation of density from the reference value. The continuity equation (Equation A.5) has been integrated with respect to z over the interval (0,1) to produce the depth integrated continuity equation (Equation A.6) using the vertical boundary conditions, w = 0, at z = (0,1), which follows from the kinematic conditions and equation (Equation A.10). In the transport equations for salinity and temperature equations (Equations A.8 and A.9) the source and sink terms, $Q_S$ and $Q_T$ include subgrid scale horizontal diffusion and thermal sources and sinks, while $A_b$ is the vertical turbulent diffusivity.

DRAFT

# APPENDIX D

## Application of CE-QUAL-ICM to the Jacksonville Harbor GRR-2 Deepening Project in the Lower St. Johns River

An Appendix to:

Ecological Modeling for Jacksonville Harbor Deepening GRR-2

March 2013

# Application of CE-QUAL-ICM to the Jacksonville Harbor GRR-2 Deepening Project in the Lower St. Johns River

**Tasks 2.2 & 2.3 Report**

**Computational Hydraulics and Transport, LLC**

## Introduction

The U.S. Army Engineer District, Jacksonville (CESAJ), requires an assessment of the impacts of deepening of the navigation channel within the Lower St. Johns River (LSJR). The hydrodynamic model EFDC is being used with the U.S. Army Corps of Engineers Integrated Compartment water quality Model CE-QUAL-ICM (ICM for short) to assess the impacts on water quality.

The ICM model is a three dimensional (3D) eutrophication and water quality model that was initially developed for application on Chesapeake Bay (Cerco and Cole 1995). Since the initial development in the late 1980's and early 1990's, many refinements and additions to the model have been made, including those done for the LSJR (Tillman et al. 2004). The model computes and reports concentrations, mass transport, kinetics transformations, and mass balances for 36 water quality state variables including dissolved oxygen, physical properties, and multiple forms of algae, zooplankton, carbon, nitrogen, phosphorus, and silica. ICM includes the ability to activate or deactivate model features, diagnostic output, and volumetric and mass balances. Each state variable may be individually activated or deactivated. ICM is generally recognized as one of the most comprehensive 3D eutrophication and water quality models in the world. In addition to its application to Chesapeake Bay and the LSJR, it has also been applied to Lower Green Bay (Mark et al. 1993), New York Bight (Hall and Dortch 1994), San Juan Bay/Estuary (Bunch et al. 2000), Florida Bay (Cerco et al. 2000), Mississippi Sound (Dortch et al. 2007), and many other sites. The model has also been incorporated into other models, such as EFDC. Most ICM modeling studies have been aimed at improving water quality via nutrient and sediment reductions.

ICM uses an unstructured grid, finite volume modeling approach, within which mass is absolutely conserved as long as the hydrodynamics used to drive the model are volume conservative. Its unstructured grid feature enables it to be linked to output from various hydrodynamic models, including CH3D and EFDC. As it relies on other model's solutions to provide the hydrodynamic forces that transport water quality variables, the ICM water quality simulations reduce computational overhead because the hydrodynamics can be saved and used repeatedly without having to rerun the hydrodynamic model.

ICM was used by the St. Johns River Water Management District (SJRWMD) for assessing total maximum daily loads (TMDLs) (Sucsy and Hendrickson 2003). Since the model had been previously set up, calibrated, and validated for the LSJR TMDLs, it was the logical choice for examining the impacts of the Jacksonville Harbor GRR-2 Deepening Project. The TMDL version of the model used for in the LSJR simulates 28 water quality state variables as listed below:

1. Temperature [T] (°C)
2. Salinity [S]
3. Inorganic Suspended Solids [ISS]
4. Algal Group 1 (cyanobacteria, or blue green algae)
5. Algal Group 2 (freshwater diatoms)
6. Algal Group 3 (marine diatoms and other marine algae)
7. Labile Dissolved Organic Carbon [LDOC]
8. Refractory Dissolved Organic Carbon [RDOC]
9. Labile Particulate Organic Carbon [LPOC]
10. Refractory Particulate Organic Carbon [RPOC]
11. Ammonium nitrogen [NH4]
12. Nitrite+Nitrate nitrogen [Nox]
13. Labile Dissolved Organic Nitrogen [LDON]
14. Refractory Dissolved Organic Nitrogen [RDON]
15. Labile Particulate Organic Nitrogen [LPON]
16. Refractory Particulate Organic Nitrogen [RPON]
17. Total Inorganic Phosphorus (TIP)
18. Labile Dissolved Organic Phosphorus [LDOP]
19. Refractory Dissolved Organic Phosphorus [RDOP]
20. Labile Particulate Organic Phosphorus [LPOP]
21. Refractory Particulate Organic Phosphorus [RPOP]
22. Chemical Oxygen Demand [COD]
23. Dissolved Oxygen [DO]
24. Particulate Biogenic Silica [PSi]
25. Dissolved Available Silica [DSi]
26. Algal (internal) Phosphorus Group1
27. Algal (internal) Phosphorus Group 2
28. Algal (internal) Phosphorus Group 3

The ICM TMDL version of the code was provided by the SJRWMD and was recompiled using an Intel Fortran compiler on a desktop computer.

CESAJ funded a contract with Taylor Engineering to conduct the numerical modeling of the impacts of navigation channel deepening on water quality. Computational Hydraulics and Transport (CHT), which is a subcontractor to Taylor Engineering, is providing assistance on the water quality modeling portion of the study. This report provides the results of CHT Tasks 2.2 and 2.3, which is to conduct ICM set up, sensitivity analysis for the revised, refined grid being

used to model the impacts of the deeper channel, to conduct ICM calibration as necessary, and validate the model. This report provides the results of Tasks 2.2 and 2.3.

## Objective

The objective of Task 2.2 was to set up and test the performance of ICM over two years using the refined grid and report the results. The two-year period test will evaluate model stability and robustness in anticipation of two-year periods of model production simulations. The objective of Task 2.3 was to conduct ICM calibration/validation and report the results.

## Approach

The SJRWMD TMDL grid for the ICM model did not provide sufficient detail to simulate the effects of proposed Jacksonville Harbor deepening. Therefore, the model grid was refined to allow simulation of the bathymetric changes that would occur with channel deepening. This report refers to the original SJRWMD grid as the coarse grid. The revised grid is referred to as the refined grid.

There were several steps required prior to performance testing on the refined grid being used to assess channel deepening. The first step was to recompile ICM on the computer being used for the water quality simulations. The compiler that was used was the Intel visual Fortran Composer XE 2011. The recompiled model was executed on a CHT computer for a year of simulation time using the original, coarser grid that was used for the TMDL model, and results were compared with output provided by the SJRWMD as obtained from a run on their computer. The comparison showed that the recompiled model was accurately reproducing the results provided by the SJRWMD.

The second step was to run ICM using the original, coarser, TMDL grid for three years using the same inputs as used by the SJRWMD for their TMDL study. The three years of EFDC hydrodynamics that were developed for the coarser grid were provided to CHT by the SJRWMD along with the initial condition files they had developed from their model spin-up. These files were necessary for running with ICM to produce baseline water quality output for comparing the revised, refined-grid model to ensure that the solutions were similar and had not deteriorated. Additionally, the hydrodynamic linkage files were provided to the ICM for its execution. The three years that were simulated included 1996, 1997, and 1998. These three years had to be simulated one at a time since the SJRWMD TMDL version of ICM does not allow continuous multi-year simulations. As established by the SJRWMD, each year started on December 1 of the previous year rather than January 1 of the year. The year 1996 was considered a model spin-up year to help establish proper initial conditions. The years 1997 and 1998 were used for performance evaluations. The final results of these runs constituted the baseline conditions on the coarser grid, which were used to assess performance of the ICM on the refine grid. The coarser-grid ICM results are not shown in this report since the focus of this report is on performance of the refine-grid model. However, it is noted that the coarser grid results were visually identical to those presented in the SJRWMD TMDL report (Sucsy and Hendrickson 2003).

After these first two steps, the ICM was deemed ready for setup on the refine grid. This step required substantial modifications to the ICM input files for loadings and boundary conditions. Due to the unstructured grid feature of the ICM, any grid changes result in modifications to the grid mapping files and revisions to the loading and boundary files to adapt to the new grid map. Refined-grid setup also required providing the refined-grid hydrodynamics and associated linkage files. Taylor Engineering developed the refined-grid hydrodynamics. After revising the ICM inputs files, the model was run through a mass balance test to ensure that all the input file changes had been correctly performed. After passing this test, the ICM was deemed ready for operation on the refine grid.

ICM was run multiple times for the three study years with the refined-grid input files and hydrodynamics to make sure that the model was sufficiently spun-up for initial conditions in the sediment compartments, which can require on the order of 5 to 10 years. This was accomplished by starting each year with initial conditions that were obtained from the final sediment conditions of the previous year's output. Three spin-up cycles of the three years were run (i.e., 9 years of simulation), which resulted in adequate spin-up of initial sediment conditions. Following spin-up, the model was applied to 1997 and 1998 again to evaluate performance as described in the next section.

## ICM Performance on Refined Grid

Seven stations (Fulton Point, Talleyrand, Piney Point, Mandarin, Picolata, Racy Point, and Palatka) were selected for evaluating the ICM for the present study. These stations essentially cover the entire reach of the LSJR (see Figure 1). The model results were plotted versus time in days for the two study years (1997 – 1998) and for each water quality state variable for which there were observed data to compare against. These plots were generated for results from the original, coarser-grid model and the refine-grid model, and the two sets of plots were compared. Additionally, statistical comparisons (using statistics presented later below) were made between the two results (i.e., coarser- and refine-grid models). Both types of comparisons (plots and statistics) showed results generated with the refine-grid model were essentially the same or slightly better, compared to those generated with the original, coarser-grid model. These comparisons are not presented here since plots and statistics with the refined-grid model resulting from the calibration task are presented herein. The plots and statistics before and after the calibration task are nearly the same, so there was no need to present approximately the same results twice. Additionally, error statistics for the coarser-grid model (without calibration refinement) and refined-grid model (following calibration refinement) are presented later below.

There are minor differences in model-computed water quality when comparing the original coarser-grid model and the refined-grid model results. Dissolved oxygen (DO) and chlorophyll *a* (*Chl a*) are the two water quality constituents of the most interest, so comparisons of the two models were conducted for these two constituents. Figures 2 and 3 compare DO at Talleyrand for the two models (i.e., coarser and refined grid). Figure 2 is a standard plot of concentration that shows that the two model results are very close. Figure 3 is a deviation plot of concentration (i.e., refined- minus coarser-grid concentrations), which provides a more detailed examination of any concentration differences. Figure 3 shows that although there are some slight differences, overall, the two results for DO are quite close. Figures 4 and 5 provide the

same type of plots for *Chl a* at Racy Point. The same observational comments made for DO can be made for *Chl a*. These two stations were selected because of their location. Downstream stations are more pertinent for DO, while upstream stations are more relevant for *Chl a*. As can be seen from these figures, there are only very minor differences in DO and *Chl a*. These differences are attributed to slight differences in the hydrodynamics computed with the coarser and refined grids since all other inputs were the same for ICM. The differences in DO and *Chl-a* for the coarser- and refined-grid models are within the accuracy of most observations. Such minor differences confirm that the refined-grid model is performing as well as the coarser-grid model.

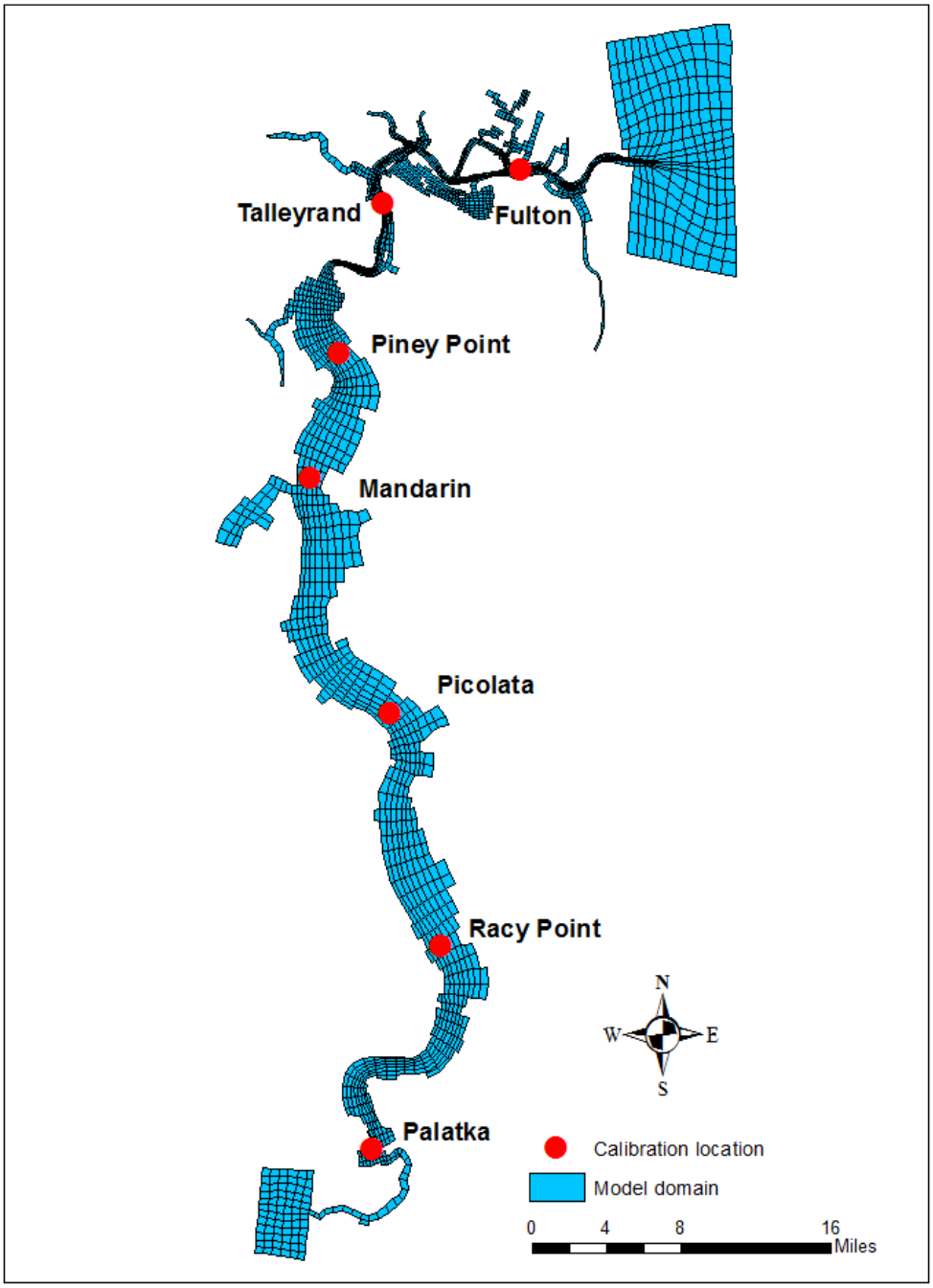

**Figure 1. Water quality observation station locations**

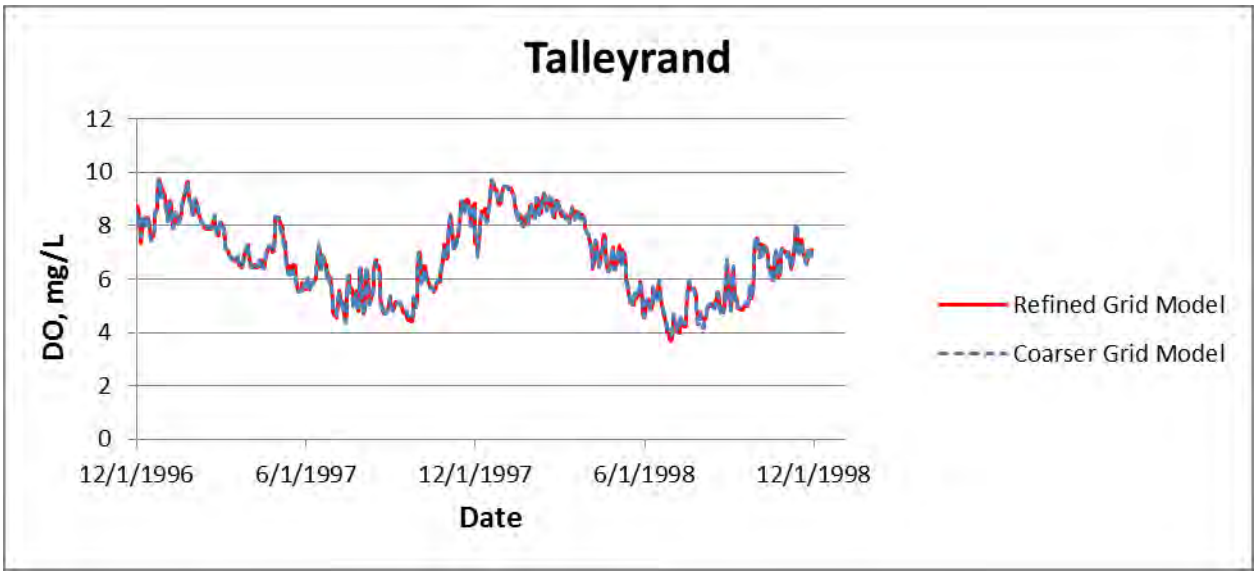


**Figure 2. Comparison of DO for refined- and coarser-grid models at Talleyrand**

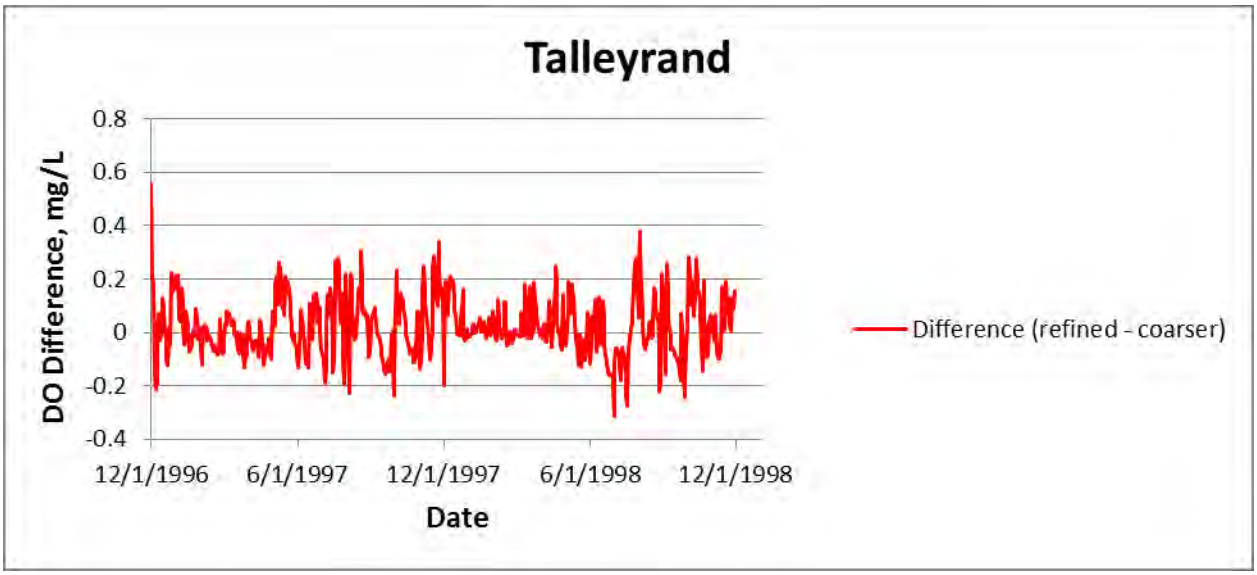


**Figure 3. Deviation plot of DO for refined- and coarser-grid models at Talleyrand**

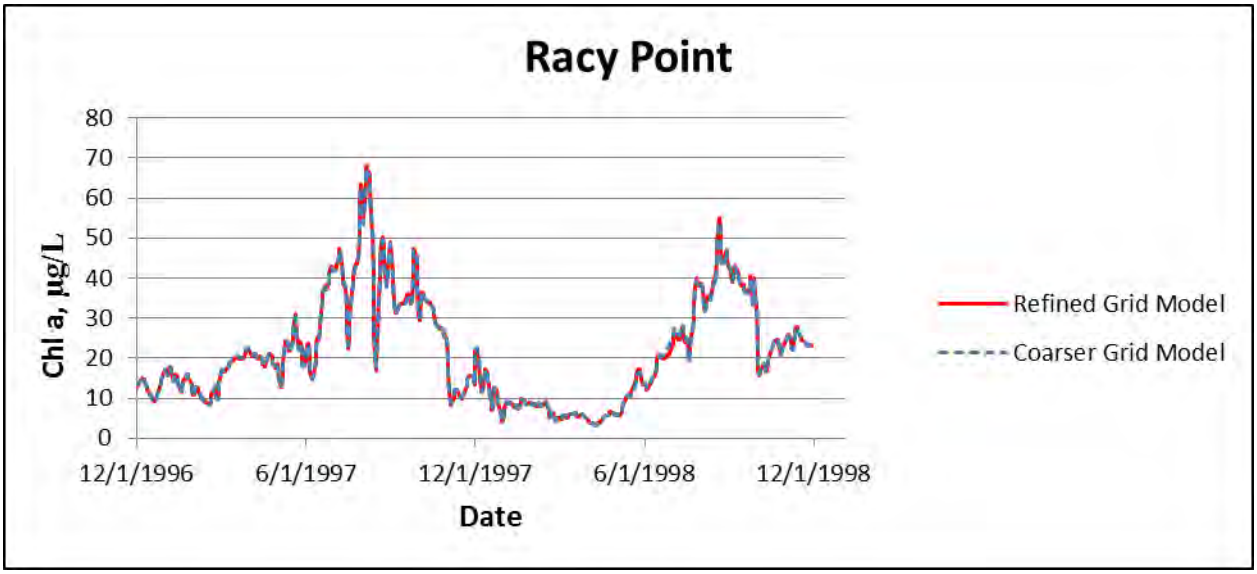


**Figure 4. Comparison of *Chl a* for refined- and coarser-grid models at Racy Point**

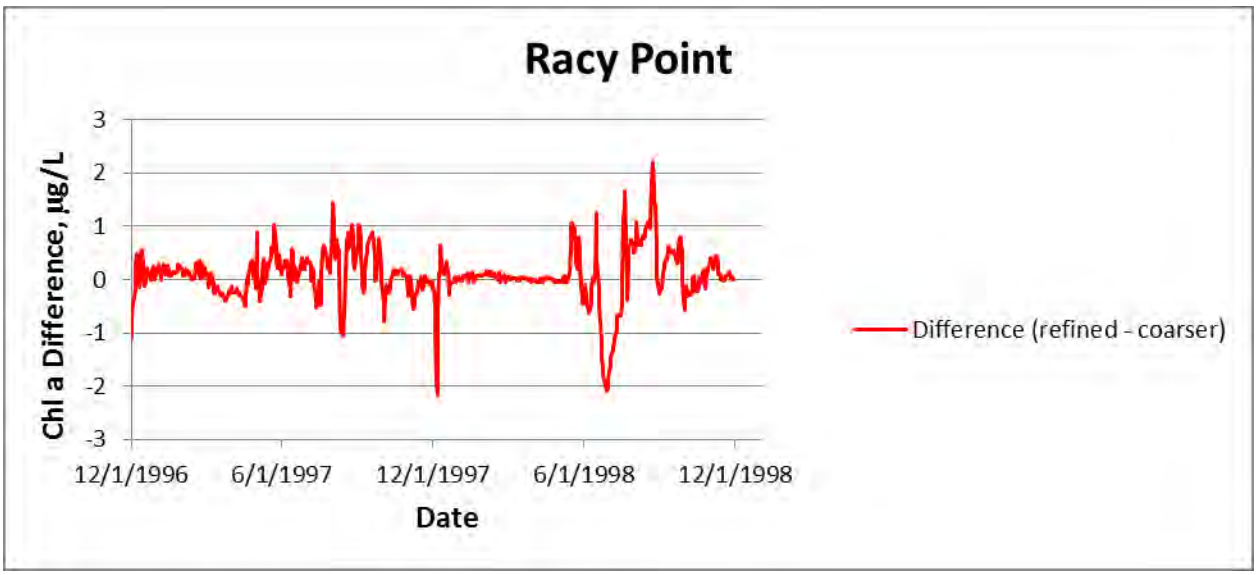


**Figure 5. Deviation plot of *Chl a* for refined- and coarser-grid models at Racy Point**

## Calibration/Validation

The model calibration task was initiated following confirmation that the refined-grid model was performing comparable to or better than the coarser-grid model. The year 1996 was used for spin-up, 1997 was used for calibration, and 1998 was used for validation. Each year was run sequentially using output from the previous year as input for the following year. There were no

model adjustments between each year. For these reasons, the period 1997 – 1998 can be thought of as concurrent calibration/validation.

All adjustable model input parameters (kinetic rates, stoichiometry, reference temperatures, organic splitting fractions, etc.) were reviewed and compared with the TMDL report as well as values used in ICM by Tillman et al. (2004) for calibration to the LSJR. All inputs were found to be reasonable and within expected bounds. There were no parameters that were considered erroneous or out of expected bounds.

It is recognized that some model errors are caused by inaccurate nutrient and organic carbon loadings and/or boundary conditions. There were no attempts to adjust loadings or boundary conditions as such actions would have been well beyond the scope of this study. A great amount of effort would be required to attempt to improve loadings and boundary conditions beyond those established by the SJRWMD as they are the most knowledgeable experts of the St. Johns River system and devoted considerable effort to establishing the loadings and boundary conditions for the TMDL model.

There were two model processes that were turned off in the TMDL and Tillman model that required investigation. These included sorption partitioning of dissolved inorganic phosphorus (DIP, mg/L or g/m$^3$) to inorganic suspended solids (ISS, mg/L or g/m$^3$) and nitrogen fixation of blue green algae. Simulations were conducted to evaluate the effects of activating these two processes. The sorption of dissolved available silica (DSi) to ISS was also turned off (partitioning set to zero), but this process was not activated since DSi adsorption to ISS is expected to be relatively minor.

The partitioning distribution coefficient for DIP adsorption to ISS, $K_d$, was set to zero for the TMDL model, where $K_d$ (m$^3$/g) is defined as $\nu$/DIP, and $\nu$ is the adsorbed inorganic phosphorus concentration (g/g) of suspended sediment. The particulate inorganic phosphorus concentration (PIP, mg/L or g/m$^3$) is computed from

$$PIP = \nu\ ISS = K_d\ ISS\ DIP = \frac{K_d\ ISS}{1 + K_d\ ISS} TIP \qquad (1)$$

where TIP is the total inorganic phosphorus concentration (mg/L or g/m$^3$), which is the state variable being solved by the model. The ICM was run on the refined grid with $K_d$ for inorganic phosphorus set to 0.006 m$^3$/g (6,000 L/kg), and results were compared to the baseline ICM results, which correspond to the TMDL model (i.e., $K_d$ = 0.0) run on the refined grid. This value of $K_d$ is recommended based on previous modeling experience[1] and falls within the range of expected values based on a previous literature review (Dortch and Gerald 1995).

Including sorption of DIP had the effect of decreasing DIP concentrations in the lower part of the river, which improved agreement with observed data. There was very little change in DIP for the middle and upper portions of the river where model agreement with observed data was already much better than for the lower river. Prediction of dissolved oxygen (DO) and

[1] Personal communication with Dr. Carl Cerco, May 2012, Environmental Laboratory, U.S. Army Engineer Research and Development Center, Vicksburg, MS

chlorophyll a (*Chl-a*) changed very little with DIP sorption activated. It was concluded that sorption portioning of inorganic phosphorus should be included in the model with a value of 0.006 $m^3/g$.

The ICM was run again with inorganic phosphorus sorption activated as discussed above and also with nitrogen (N) fixation for blue green algae activated. Turning on N fixation affected dissolved inorganic nitrogen (DIN) very little, but it increased *Chl a* concentrations substantially for most stations, especially the upstream stations, causing a degradation in model accuracy for *Chl-a*. Given the degradation of accuracy with N fixation, it was decided that N fixation should remain off in the final calibrated model. All other calibration parameters were set according to the TMDL model and are described in the TMDL report (Sucsy and Hendrickson 2003).

## Final Model Results

The final model results are plotted as time series of concentration during 1997 - 1998 at the seven stations shown in Figure 1. These time series plots are shown Figures 6 and 7 for model-predicted dissolved oxygen (DO) and chlorophyll *a* (*Chl a*), respectively, using the refined grid and with the final calibration with DIP sorption activated. The results for 1997 represent the calibration year, whereas 1998 represents the validation year. The same model parameters were used for both years. Appendix A presents the plots for the other water quality variables, which include: temperature, salinity, total nitrogen (TN), dissolved inorganic nitrogen (DIN, or Nox + $NH_4$), total phosphorus (TP), dissolved inorganic phosphorus (DIP), dissolved available silica (DSi), and total organic carbon (TOC). Observed data are included on the plots for comparison with the model. The plotted model results are daily averages and depth averages for all layers of model output, for each constituent, and for each station, whereas the observed data were collected at various depths and times throughout the day for each station and date collected. Thus, there can be more than one observed value on a given date, for a given station, and for a given water quality constituent. For these reasons, the observed values can vary about the model result for a particular date and station.

The results in Figures 6 and 7 and Appendix A indicate that the refined model performs well overall for all water quality constituents, capturing temporal and spatial trends. Model results compare closer to observed data for temperature, salinity, and DO than for nutrients. The greatest differences in model versus observed data occurs for DIN and DIP for the lower reaches of the river. Some of these differences could be caused by inaccuracies in nutrient loadings to the river. Additionally, there may be more variation in dissolved nutrient concentrations observed at different depths on a given date due to more vertical stratification in the lower river. Model-computed DO and *Chl-a* show good agreement with observed data throughout the river. Overall, the model results for the refined model are very close visually to those obtained with the TMDL model, which are shown in the TMDL report prepared by the SJRWMD. Statistical statements of model accuracy are discussed below.

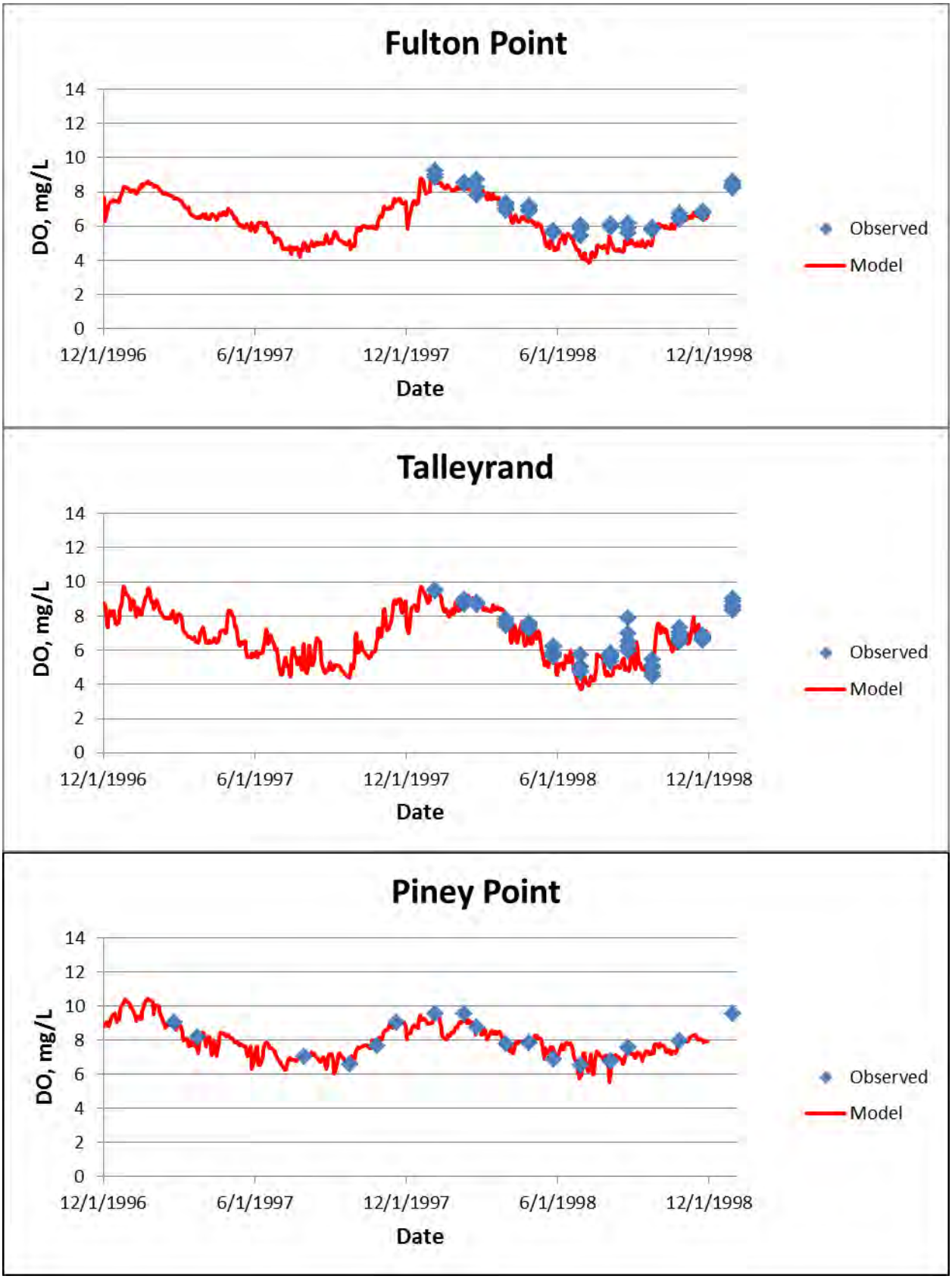
Fulton Point
DO, mg/L
14
12
10
8
6
4
2
0
12/1/1996
6/1/1997
12/1/1997
6/1/1998
12/1/1998
Date
Observed
Model
Talleyrand
DO, mg/L
14
12
10
8
6
4
2
0
12/1/1996
6/1/1997
12/1/1997
6/1/1998
12/1/1998
Date
Observed
Model
Piney Point
DO, mg/L
14
12
10
8
6
4
2
0
12/1/1996
6/1/1997
12/1/1997
6/1/1998
12/1/1998
Date
Observed
Model

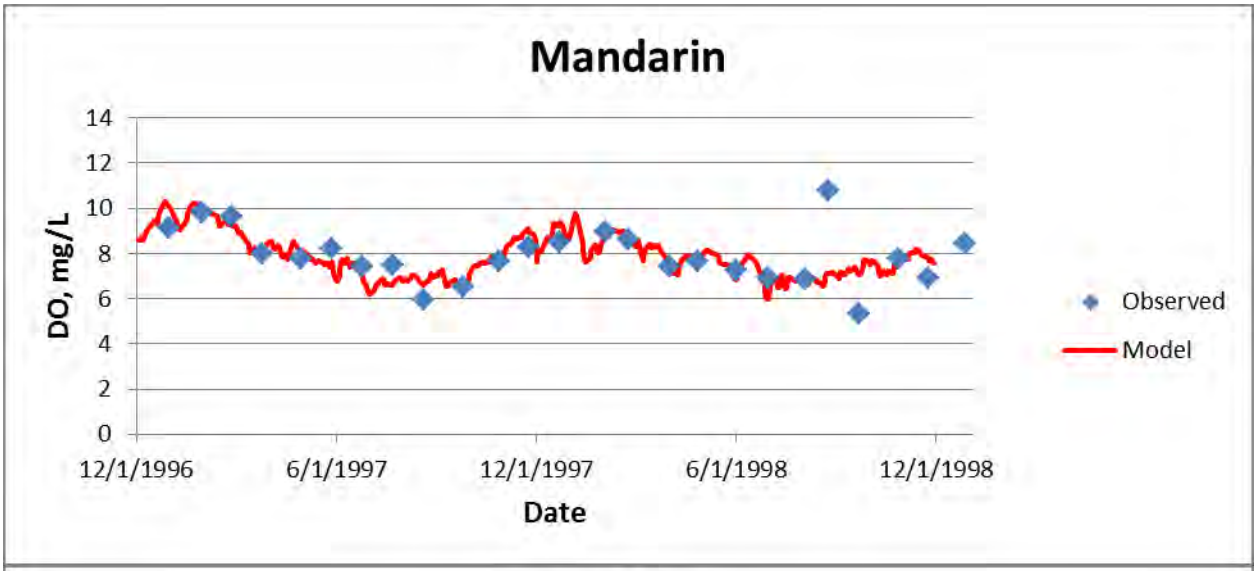
Mandarin
DO, mg/L
14
12
10
8
6
4
2
0
12/1/1996
6/1/1997
12/1/1997
6/1/1998
12/1/1998
Date
Observed
Model

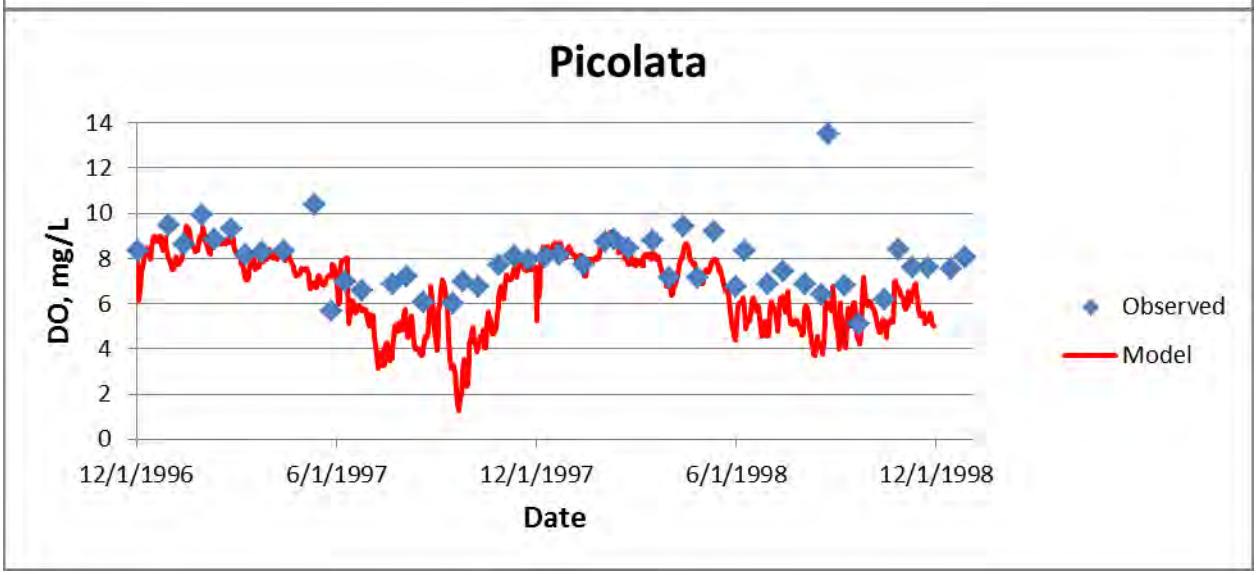
Picolata
DO, mg/L
14
12
10
8
6
4
2
0
12/1/1996
6/1/1997
12/1/1997
6/1/1998
12/1/1998
Date
Observed
Model

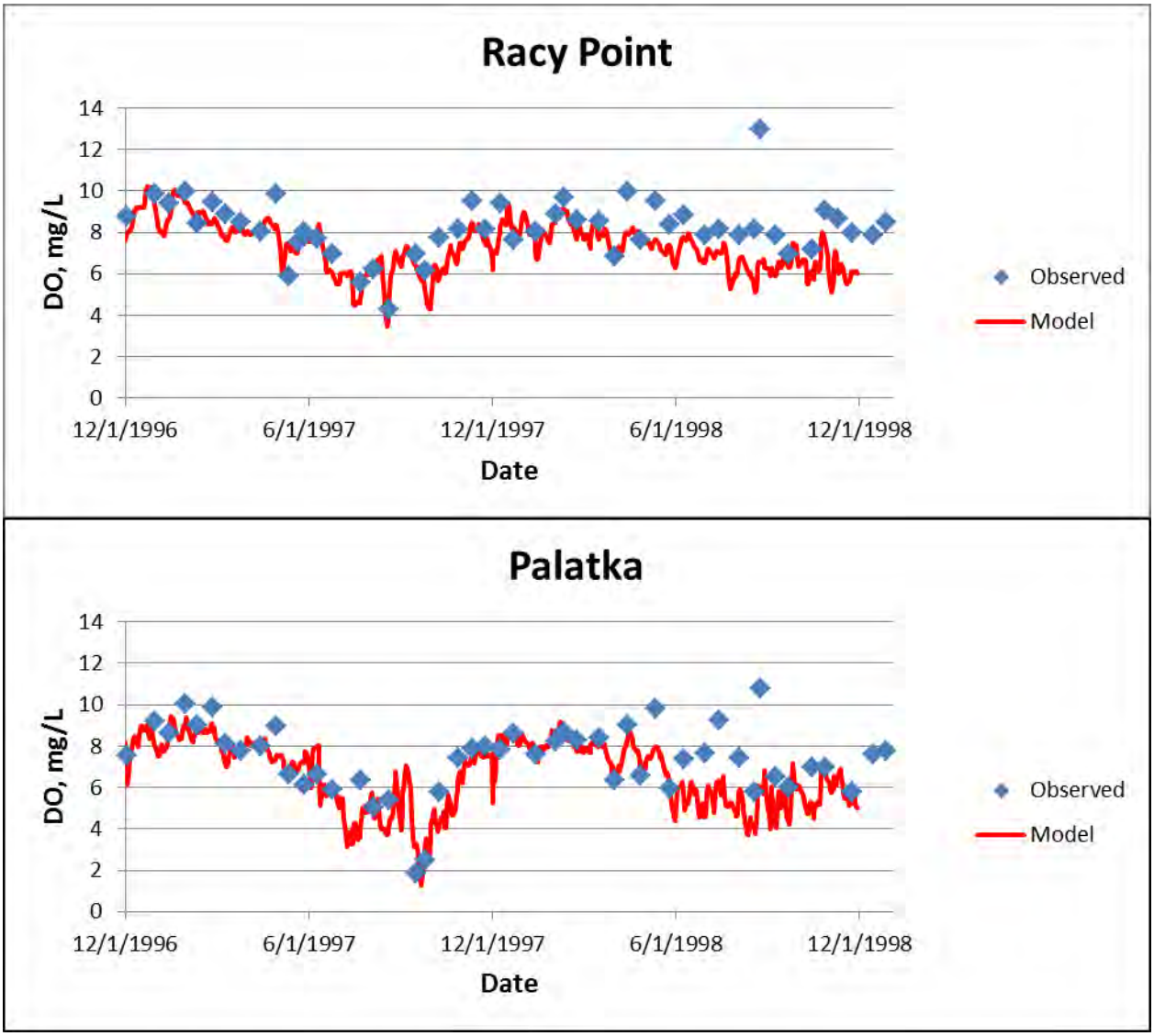


**Figure 6. Observed and depth-averaged, model-computed DO for seven stations**

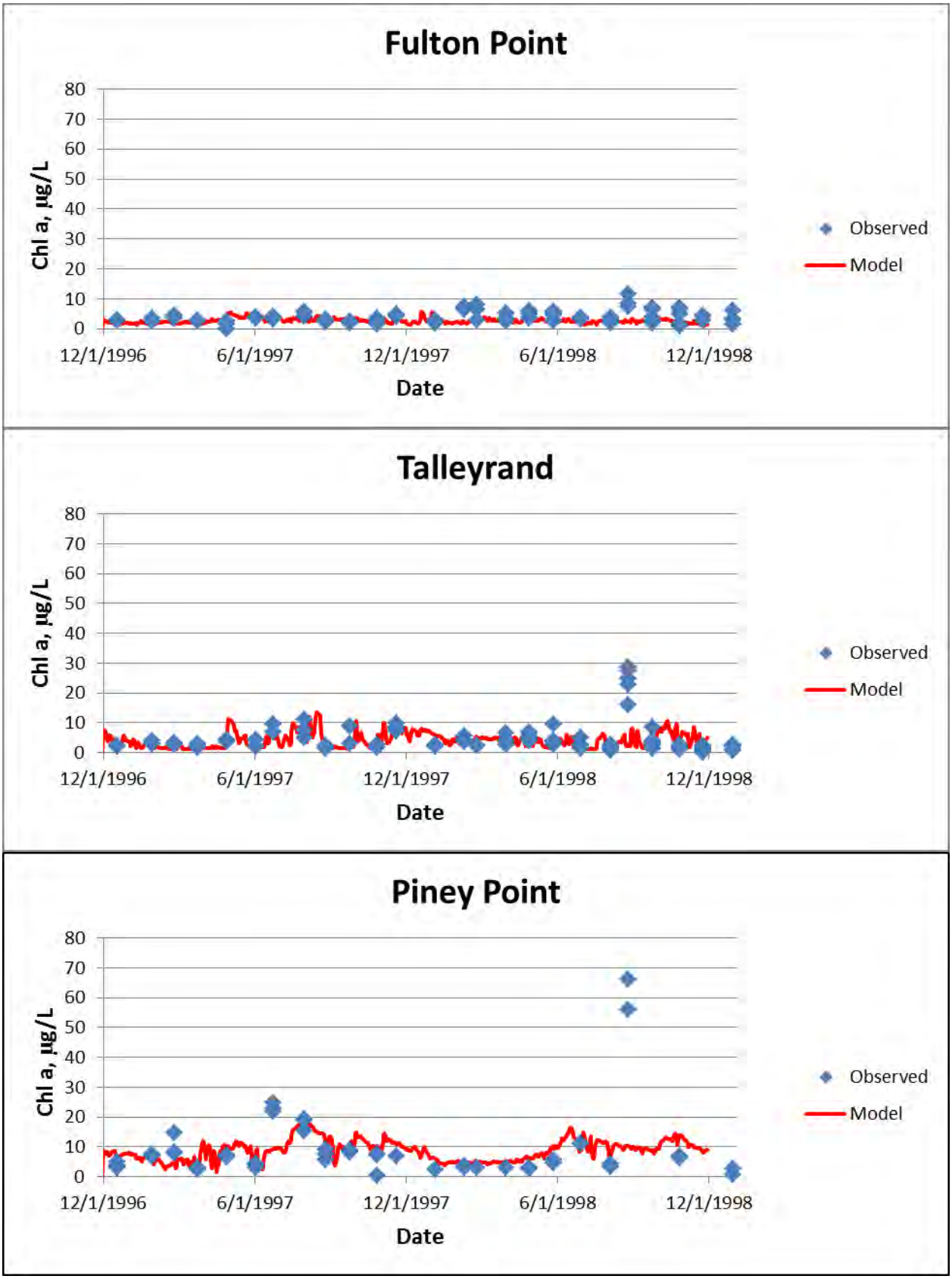
Fulton Point
Chl a, µg/L
80
70
60
50
40
30
20
10
0
12/1/1996
6/1/1997
12/1/1997
6/1/1998
12/1/1998
Date
Observed
Model
Talleyrand
Chl a, µg/L
80
70
60
50
40
30
20
10
0
12/1/1996
6/1/1997
12/1/1997
6/1/1998
12/1/1998
Date
Observed
Model
Piney Point
Chl a, µg/L
80
70
60
50
40
30
20
10
0
12/1/1996
6/1/1997
12/1/1997
6/1/1998
12/1/1998
Date
Observed
Model

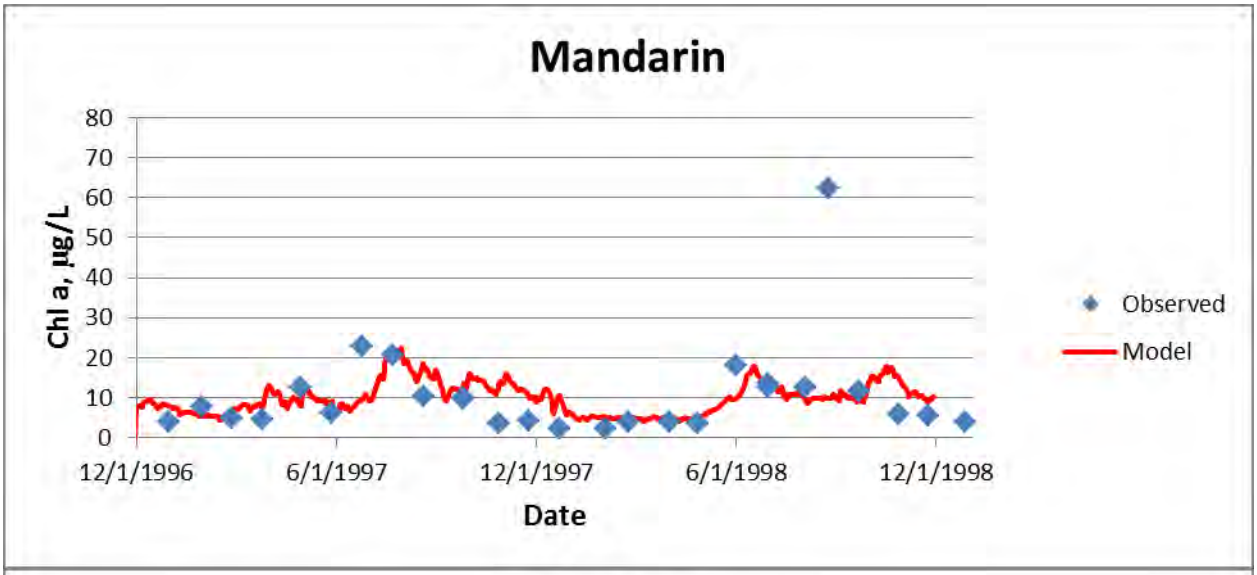
Mandarin
Chl a, µg/L
80
70
60
50
40
30
20
10
0
12/1/1996
6/1/1997
12/1/1997
6/1/1998
12/1/1998
Date
Observed
Model

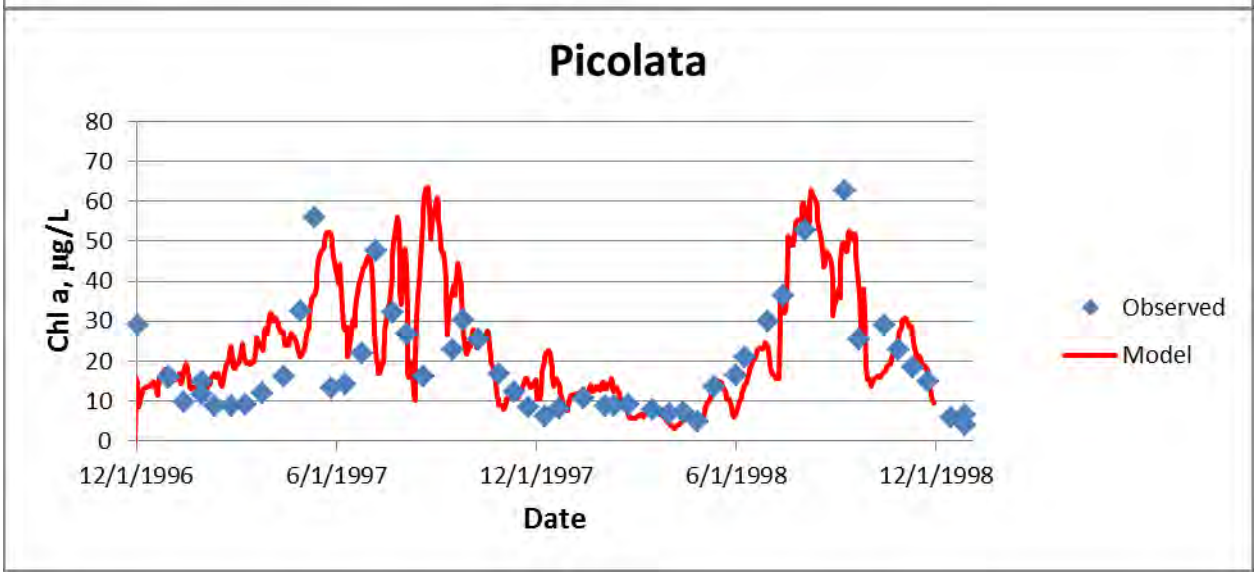
Picolata
Chl a, µg/L
80
70
60
50
40
30
20
10
0
12/1/1996
6/1/1997
12/1/1997
6/1/1998
12/1/1998
Date
Observed
Model

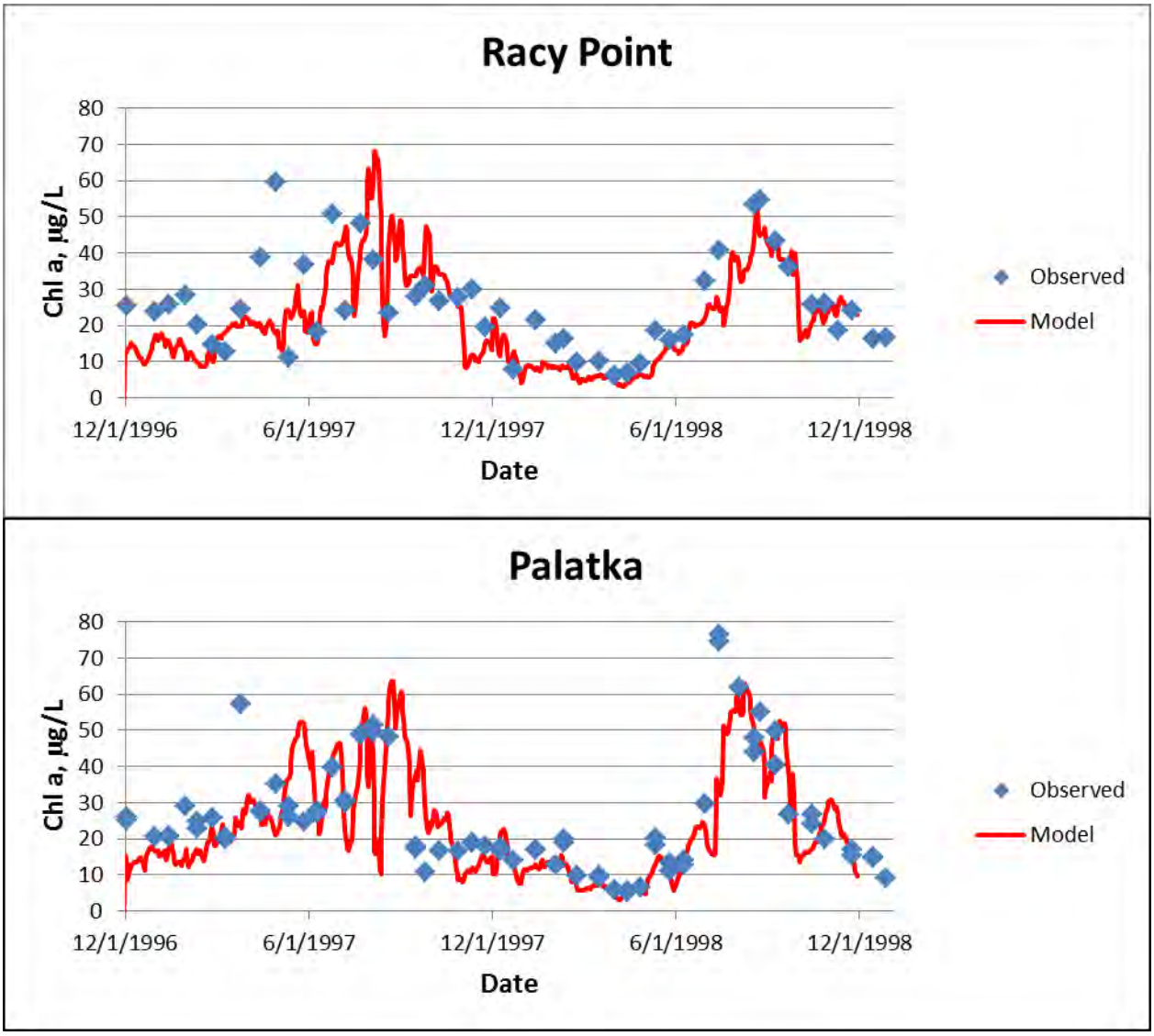


**Figure 7. Observed and depth-averaged, model-computed *Chl a* for seven stations**

Error statistics were also used to help evaluate model performance. The error statistics that were used included, relative error (RE), root mean squared error (RMSE), and the linear, least squares best fit statistics, which included the coefficient of determination ($R^2$), the slope of the fit, and the intercept of the fit. A perfect fit would have an $R^2$ and slope of 1.0 with an intercept of 0.0. The RE, RMSE, and $R^2$ were computed as follows,

$$RE = \frac{\sum_{i}^{n} |O_i - M_i|}{\sum_{i}^{n} O_i} \qquad (2)$$

$$RMSE = \sqrt{\frac{\sum_{i}^{n}\left(O_i - M_i\right)^2}{n}} \quad (3)$$

$$R^2 = \frac{\left[\sum_{i}^{n}\left(O_i - \bar{O}\right)\left(M_i - \bar{M}\right)\right]^2}{\sum_{i}^{n}\left(O_i - \bar{O}\right)^2 \sum_{i}^{n}\left(M_i - \bar{M}\right)^2} \quad (4)$$

where,

$O_i$ = observed value for a given station and date
$M_i$ = model-computed valued for a given station and date corresponding to the same station and date with observed data
$\bar{O}$ = mean of all observed values
$\bar{M}$ = mean of all model-computed values corresponding to stations and dates with observed data
n = total number of observed values

Each of the above statistics is compared in Table 1 for DO, for all stations and dates combined, and for the coarser-grid model results (without any recalibration) and refined-grid model results (following recalibration). It is noted again that all model results were depth averaged for each station and date, whereas observed values are for different depths. Overall, the error statistics are fairly good and similar to the accuracy reported for other water quality model studies (Arhonditsis and Brett 2004). The refined-grid ICM is slightly more accurate for DO than the coarser-grid ICM. This slight improvement in DO is attributed to the refined grid rather than calibration refinement since the calibration refinement had essentially no impact on DO.

The RE and RMSE for DO and the refined grid can be compared with the same two statistics reported for DO by Tillman et al. (2004) for combined 1997 and 1998 for all stations, which was RE = 9.43 and RMSE = 1.04 mg/L. Thus, the present, refined-grid model has accuracy similar to the Tillman et al. (2004) ICM model of the LSJR.

**Table 1. DO Error statistics for coarser- and refined-grid model results for all stations and dates (1997 – 1998)**

| Statistic | Coarser-Grid Model (no recalibration) | Refined-Grid Model (following calibration refinement) |
|---|---|---|
| RE, % | 10.56 | 10.22 |
| RMSE, mg/L | 1.13 | 1.11 |
| $R^2$ | 0.61 | 0.61 |
| Slope | 0.80 | 0.79 |
| Intercept, mg/L | 0.93 | 1.04 |

The same statistical comparisons performed for DO were also performed for *Chl a* and are shown in Table 2. These statistics are nearly identical for the two grids indicating that the

refined-grid model produces results comparable to those obtained with the coarser-grid model even after the calibration refinement for the refined-grid model. The statistics for *Chl a* reported by Tillman et al. (2004) were RE = 46.8 and RMSE = 10.21 μg/L. Thus, the accuracy for *Chl-a* of the present refined model is slightly better than the Tillman et al. (2004) version based on the RE values.

It is noted that Tillman et al. (2004) calculated their model statistics based on model-computed surface, mid-depth, and bottom values compared with observations near those locations. Thus, the Tillman et al. (2004) error statistics can be different from those presented here since for the present study depth-averaged model values were compared with the values for all depths for a given date and station.

**Table 2. *Chl a* Error statistics for coarser- and refined-grid model results for all stations and dates (1997 – 1998)**

| Statistic | Coarser-Grid Model (no recalibration) | Refined-Grid Model (following calibration refinement) |
|---|---|---|
| RE, % | 42.04 | 42.28 |
| RMSE, μg/L | 11.51 | 11.49 |
| $R^2$ | 0.50 | 0.50 |
| Slope | 0.51 | 0.51 |
| Intercept, μg/L | 3.75 | 3.87 |

The linear best fit plots for predicted versus observed DO and *Chl a* for the refined-grid ICM are shown in Figures 8 and 9, respectively. These plots indicate a reasonably good correlation of predictions with observations, although the correlation is much better for DO than for *Chl a*, which is normally the case.

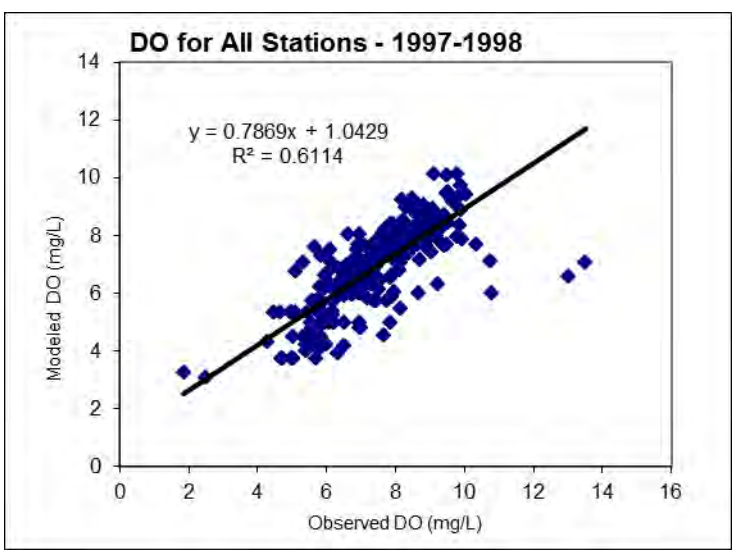


**Figure 8. Computed versus observed DO using the refined grid for all stations and dates during 1997 – 1998 following calibration**

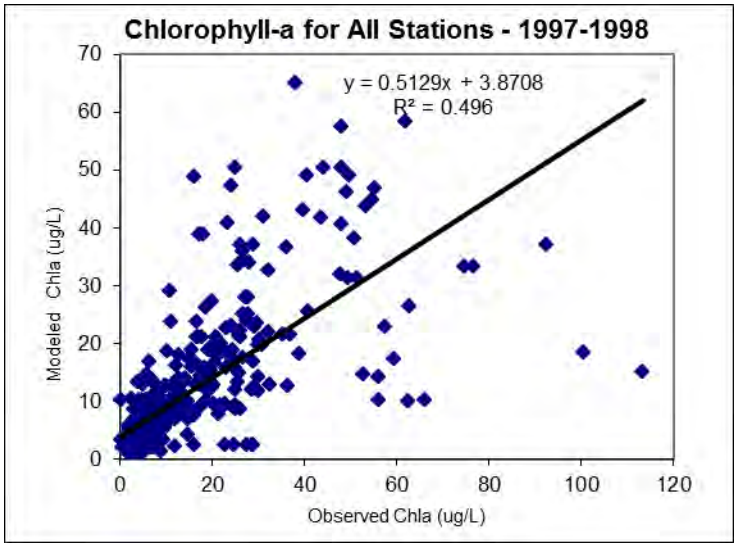


**Figure 9. Computed versus observed *Chl a* using the refined grid for all stations and dates during 1997 – 1998 following calibration**

The DO primary error statistics are also reported by year and by station as shown in Tables 3 and 4 for the refined and coarser grids, respectively. Similarly, the *Chl-a* error statistics are reported by year and by station as shown in Tables 5 and 6 for the refined and coarser grids, respectively. These tables show how well the model performs at each station and each of the two years. The model is the most accurate for DO at Piney Point and the least accurate at Racy Point or Palatka for both grids. The $R^2$ indicates that the model accuracy for *Chl-a* is much greater for the upstream stations than the downstream stations. The RE and RMSE are affected by the magnitude of constituent concentration, which varies greatly for *Chl-a* from the river mouth to the headwaters. So care should be exercised in using those two statistics to evaluate accuracy for *Chl a*. These tables show that results for the two grids are similar by station and year.

**Table 3. DO error statistics by model calibration and validation years and by station for the refined grid**

| Station | Model Calibration (1997) | | | Model Validation (1998) | | |
|---|---|---|---|---|---|---|
| | RE, % | RMSE, mg/L | $R^2$ | RE, % | RMSE, mg/L | $R^2$ |
| Fulton | ND | ND | ND | 12.14 | 1.37 | 0.26 |
| Talleyrand | ND | ND | ND | 8.37 | 0.81 | 0.84 |
| Piney Point | 3.6 | 0.42 | 0.83 | 4.08 | 0.42 | 0.9 |
| Mandarin | 5.82 | 0.53 | 0.95 | 10.17 | 1.20 | 0.76 |
| Picolata | 7.18 | 0.76 | 0.94 | 10.41 | 1.52 | 0.14 |
| Racy Point | 9.7 | 0.86 | 0.94 | 16.97 | 1.91 | 0.08 |
| Palatka | 12.68 | 1.08 | 0.77 | 16.12 | 1.69 | 0.32 |

ND = no data available

**Table 4. DO error statistics by model calibration and validation years and by station for the original, coarser grid**

| Station | Model Calibration (1997) | | | Model Validation (1998) | | |
|---|---|---|---|---|---|---|
| | RE, % | RMSE, mg/L | $R^2$ | RE, % | RMSE, mg/L | $R^2$ |
| Fulton | ND | ND | ND | 13.79 | 1.42 | 0.26 |
| Talleyrand | ND | ND | ND | 8.58 | 0.84 | 0.84 |
| Piney Point | 3.98 | 0.44 | 0.81 | 4.53 | 0.48 | 0.89 |
| Mandarin | 5.90 | 0.53 | 0.95 | 9.99 | 1.19 | 0.76 |
| Picolata | 7.24 | 0.76 | 0.94 | 10.31 | 1.51 | 0.15 |
| Racy Point | 9.68 | 0.86 | 0.94 | 16.79 | 1.89 | 0.08 |
| Palatka | 12.67 | 1.09 | 0.76 | 16.26 | 1.70 | 0.33 |

**Table 5. *Chl-a* error statistics by model calibration and validation years and by station for the refined grid**

| Station | Model Calibration (1997) | | | Model Validation (1998) | | |
|---|---|---|---|---|---|---|
| | RE, % | RMSE, µg/L | $R^2$ | RE, % | RMSE, µg/L | $R^2$ |
| Fulton | 31.75 | 1.21 | 0.10 | 50.21 | 2.82 | 0 |
| Talleyrand | 44.01 | 2.69 | 0.48 | 69.49 | 7.20 | 0.01 |
| Piney Point | 44.01 | 5.25 | 0.31 | 78.18 | 17.36 | 0.14 |
| Mandarin | 50.64 | 5.87 | 0.20 | 61.31 | 15.21 | 0.06 |
| Picolata | 38.82 | 12.73 | 0.17 | 56.31 | 29.01 | 0.26 |
| Racy Point | 44.15 | 14.58 | 0.29 | 30.63 | 13.34 | 0.67 |
| Palatka | 35.67 | 12.74 | 0.18 | 23.99 | 10.88 | 0.70 |

**Table 6. *Chl-a* error statistics by model calibration and validation years and by station for the original, coarser grid**

| Station | Model Calibration (1997) | | | Model Validation (1998) | | |
|---|---|---|---|---|---|---|
| | RE, % | RMSE, µg/L | $R^2$ | RE, % | RMSE, µg/L | $R^2$ |
| Fulton | 31.07 | 1.22 | 0.12 | 48.79 | 2.84 | 0 |
| Talleyrand | 42.23 | 2.61 | 0.42 | 68.51 | 7.25 | 0.02 |
| Piney Point | 44.08 | 5.27 | 0.30 | 77.64 | 17.20 | 0.18 |
| Mandarin | 47.86 | 5.68 | 0.22 | 59.48 | 15.15 | 0.06 |
| Picolata | 38.93 | 12.68 | 0.18 | 56.40 | 29.07 | 0.26 |
| Racy Point | 43.84 | 14.47 | 0.29 | 30.62 | 13.47 | 0.67 |
| Palatka | 35.43 | 12.68 | 0.18 | 24.72 | 11.21 | 0.69 |

## Conclusions

The efforts conducted within Task 2.2 showed that the coarser-grid model of the present study produces results that are virtually the same as the SJRWMD TMDL model. The refined-grid ICM was found to yield about the same water quality results as the coarser-grid model. There were slight differences that can be attributed to differences in the computed hydrodynamics for the two grids. The performance of the refined-grid ICM was found to be essentially the same as or slightly better than that of the coarser-grid model. Based upon this agreement, the refined-

grid ICM was successfully verified as operationally acceptable for performing the remaining modeling tasks of this project.

The only calibration change recommended for the ICM is to activate sorption partitioning of inorganic phosphorus to inorganic suspended solids. This should be accomplished by setting the partitioning distribution coefficient for inorganic phosphorus to 0.006 $m^3/g$. This change slightly improved the prediction of DIP in the lower part of the river, but it had essentially no effect on DO and *Chl a*. With this change, the ICM is ready for application on the refined grid to assess future project conditions. The accuracy of the present refined model is comparable to that of the original TMDL model with a slight improvement in accuracy for DO that is attributed to transport on the refined grid.

## References


Arhonditsis, G.B., and Brett, M.T. 2004. "Evaluation of the Current State of Mechanistic Aquatic Biogeochemical Modeling," *Mar. Ecol. Prog. Ser.*, 271, 13-26.

Bunch, B. W., Cerco, C. F., Dortch, M. S., Johnson, B. H., and Kim, K. W. 2000. "Hydrodynamic and Water Quality Model Study of San Juan Bay Estuary," ERDC TR-00-1, U.S. Army Engineer Research and Development Center, Vicksburg, MS.

Cerco, C.F., and Cole, T. 1995. "User Guide to the CE-QUAL-ICM Three-Dimensional Eutrophication Model, Release Version 1.0," Technical Report EL-95-15, U.S. Army Engineer Waterways Experiment Station, Vicksburg, MS.

Cerco, C. F., Bunch, B. W., Teeter, A. M., and Dortch, M. S. 2000. "Water Quality Model of Florida Bay," Report no. ERDC/EL TR-00-10, US Army Engineer Research and Development Center, Vicksburg, MS.

Dortch, M. S., and Gerald, J. A. 1995. "Screening-Level Model for Estimating Pollutant Removal by Wetlands," Technical Report WRP-CP-9, U.S. Army Engineer Waterways Experiment Station, Vicksburg, MS.

Dortch, M.S., Zakikhani, M., Noel, M.R., and Kim, S.C. 2007. "Application of a Water Quality Model to Mississippi Sound to Evaluate Impacts of Freshwater Diversions," ERDC/EL TR-07-20, U.S. Army Engineer Research and Development Center, Vicksburg, MS.

Hall, R. W., and Dortch, M. S. 1994. "New York Bight Study, Report 2: Feasibility Study of the Development and Application of a General Water Quality Model of the New York Bight," Technical Report CERC-94-4, U.S. Army Engineer Waterways Experiment Station, Vicksburg, MS.

Mark, D. L., Scheffner, N. W., Butler, H. L., Bunch, B. W., and Dortch, M. S. 1993. "Hydrodynamic and Water Quality Modeling of Lower Green Bay, Wisconsin," Technical Report, CERC-93-16, U.S. Army Engineer Waterways Experiment Station, Vicksburg, MS.

Sucsy, P., and Hendrickson, J. 2003. "Calculation of Nutrient Reduction Goals for the Lower St. Johns River by Application of CE-QUAL-ICM, a Mechanistic Water Quality Model," Department of Water Resources, St. Johns River Water Management District, Palatka, FL.

Tillman, D.H., Cerco, C.R., Noel, M.R., Martin, J.L., and Hamrick, J. 2004. "Three-Dimensional Eutrophication Model of the Lower St. Johns River, Florida," ERDC/EL TR-04-13, U.S. Army Engineer Research and Development Center, Vicksburg, MS.

# APPENDIX A

## Observed and Model-Computed Water Quality for Seven Stations

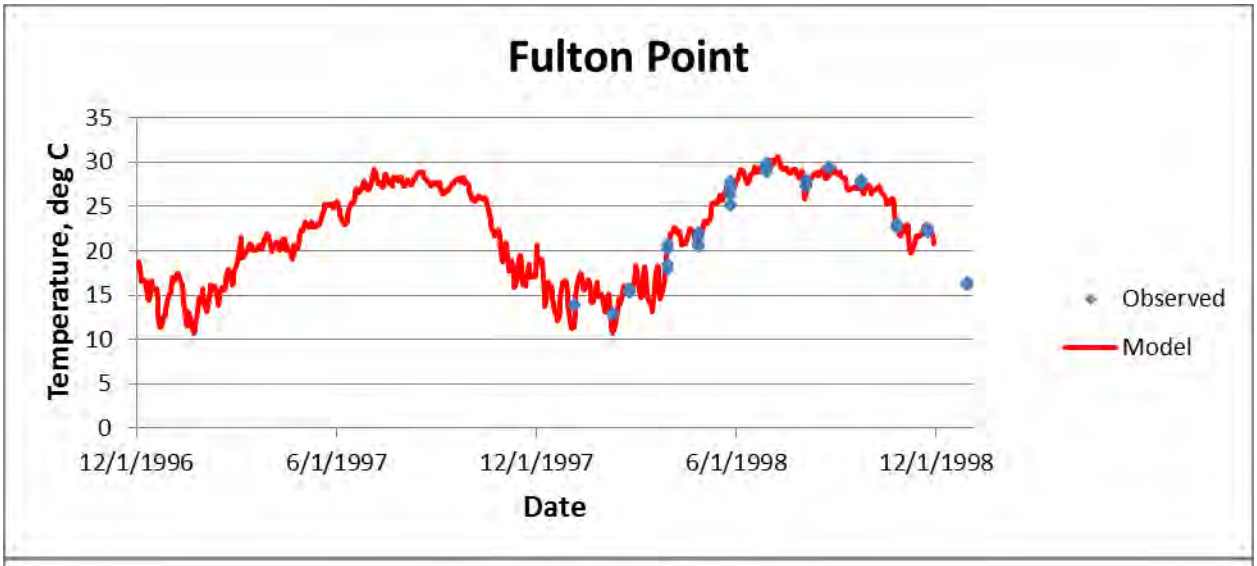
Fulton Point
Temperature, deg C
35
30
25
20
15
10
5
0
12/1/1996
6/1/1997
12/1/1997
6/1/1998
12/1/1998
Date
Observed
Model

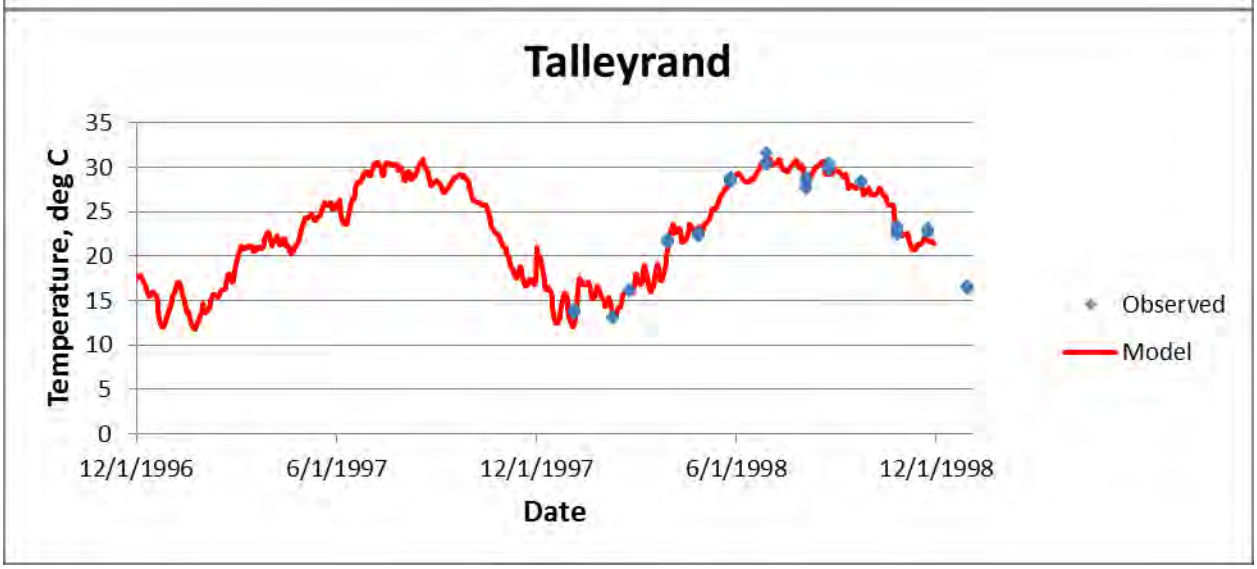
Talleyrand
Temperature, deg C
35
30
25
20
15
10
5
0
12/1/1996
6/1/1997
12/1/1997
6/1/1998
12/1/1998
Date
Observed
Model

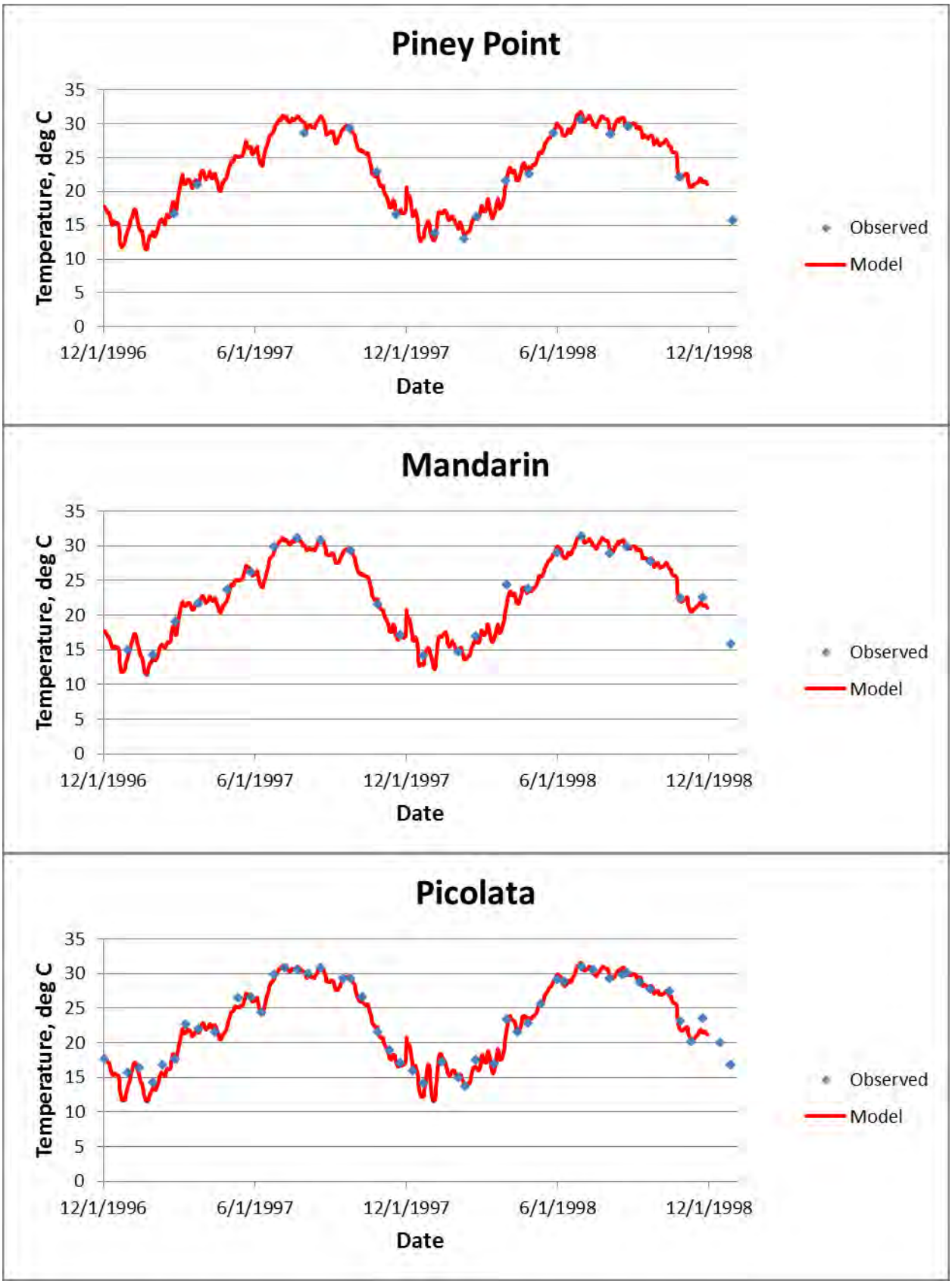
Piney Point
Temperature, deg C
35
30
25
20
15
10
5
0
12/1/1996
6/1/1997
12/1/1997
6/1/1998
12/1/1998
Date
Observed
Model
Mandarin
Temperature, deg C
35
30
25
20
15
10
5
0
12/1/1996
6/1/1997
12/1/1997
6/1/1998
12/1/1998
Date
Observed
Model
Picolata
Temperature, deg C
35
30
25
20
15
10
5
0
12/1/1996
6/1/1997
12/1/1997
6/1/1998
12/1/1998
Date
Observed
Model

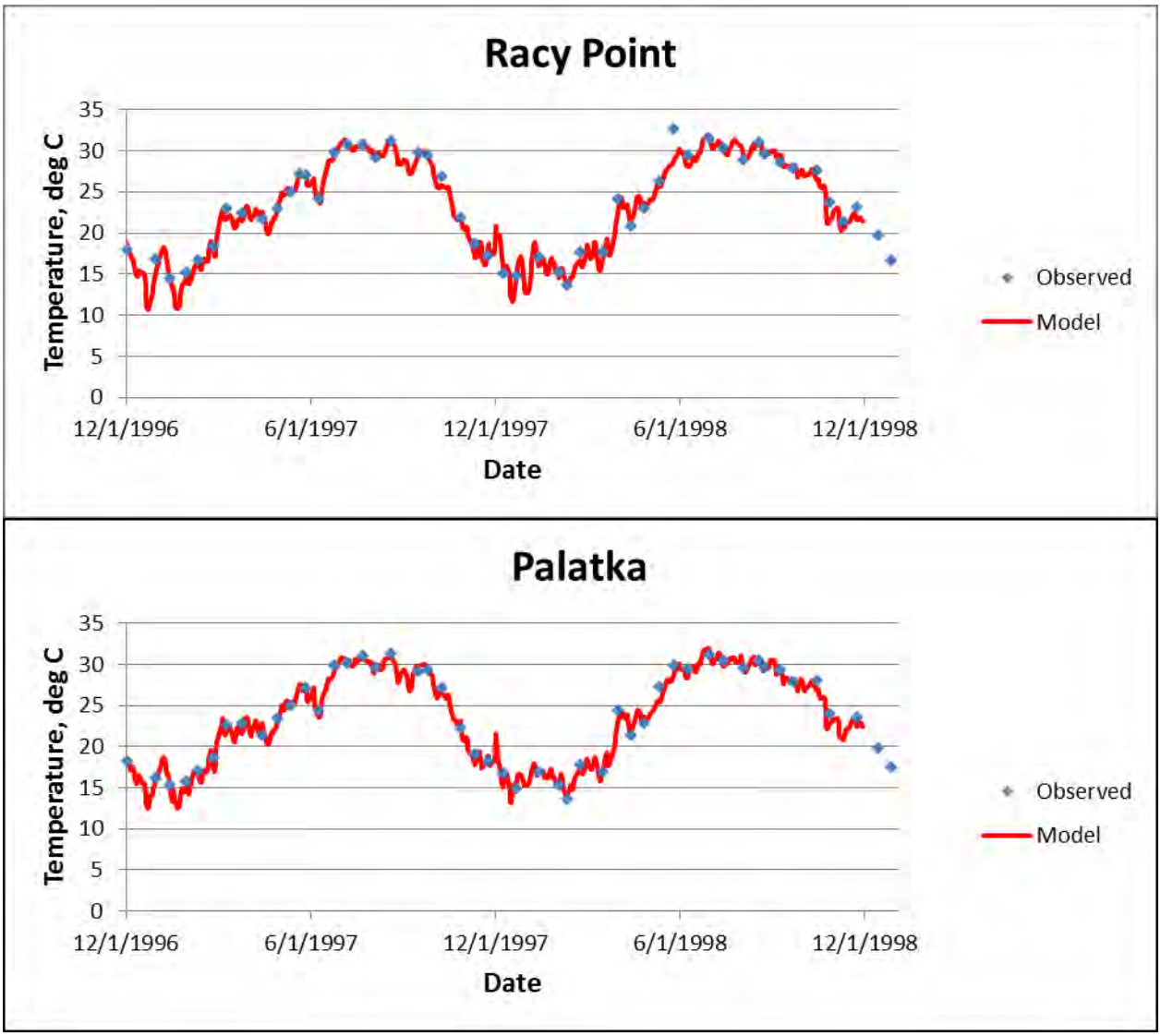


**Figure A1. Observed and depth-averaged, model-computed temperature for seven stations**

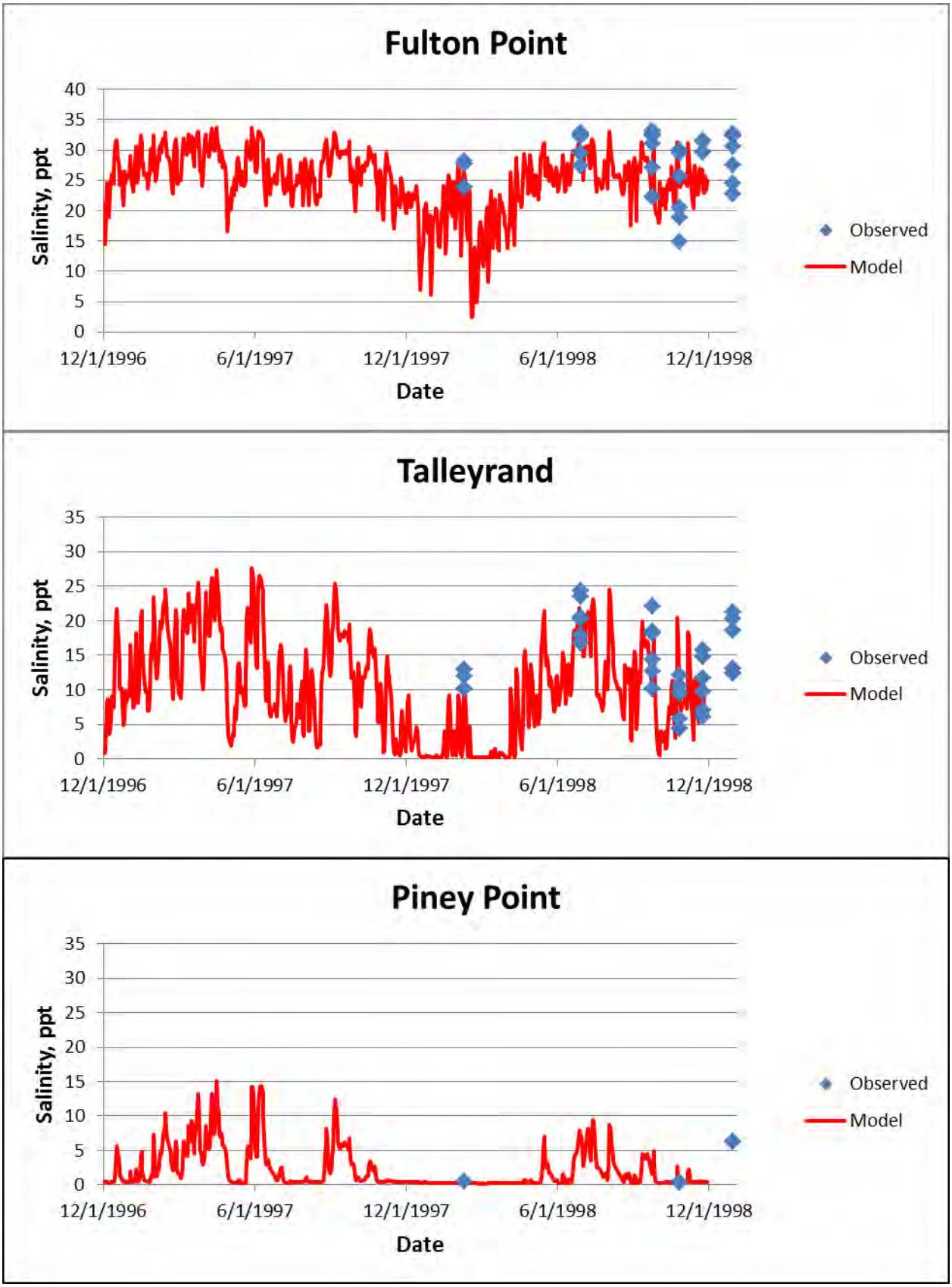
Fulton Point
Salinity, ppt
40
35
30
25
20
15
10
5
0
12/1/1996
6/1/1997
12/1/1997
6/1/1998
12/1/1998
Date
Observed
Model
Talleyrand
Salinity, ppt
35
30
25
20
15
10
5
0
12/1/1996
6/1/1997
12/1/1997
6/1/1998
12/1/1998
Date
Observed
Model
Piney Point
Salinity, ppt
35
30
25
20
15
10
5
0
12/1/1996
6/1/1997
12/1/1997
6/1/1998
12/1/1998
Date
Observed
Model

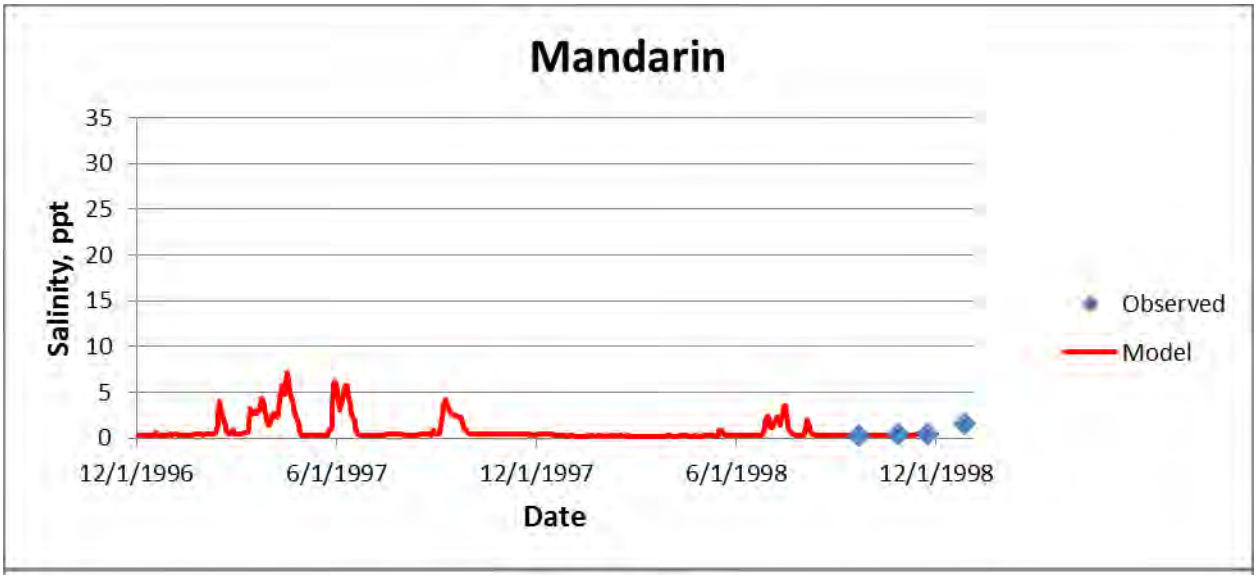
Mandarin
Salinity, ppt
35
30
25
20
15
10
5
0
12/1/1996
6/1/1997
12/1/1997
6/1/1998
12/1/1998
Date
Observed
Model

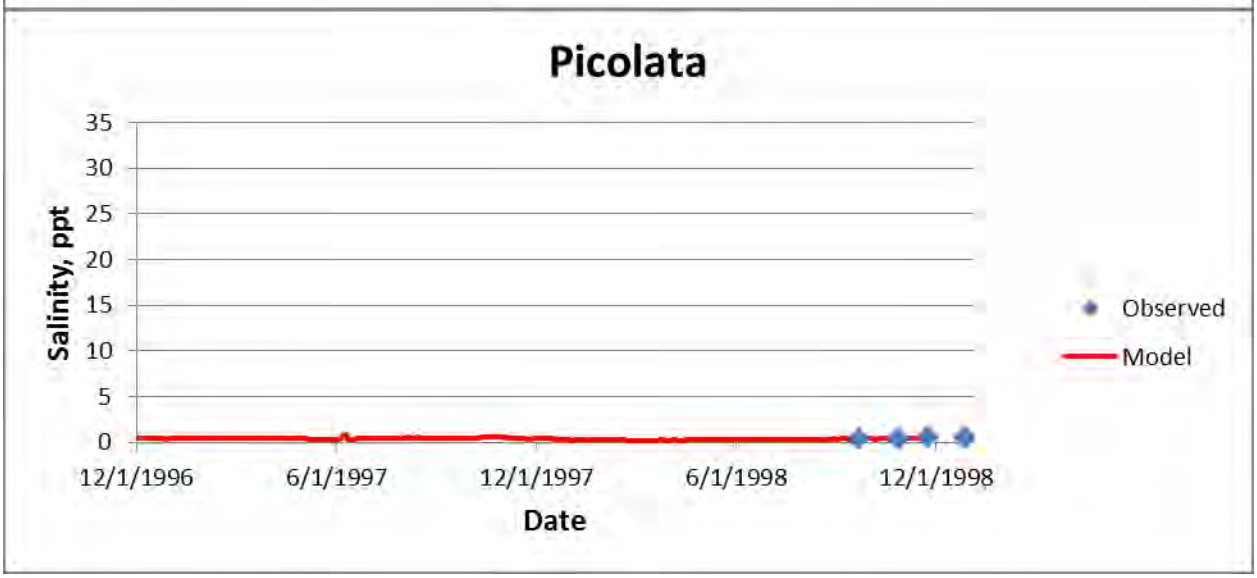
Picolata
Salinity, ppt
35
30
25
20
15
10
5
0
12/1/1996
6/1/1997
12/1/1997
6/1/1998
12/1/1998
Date
Observed
Model

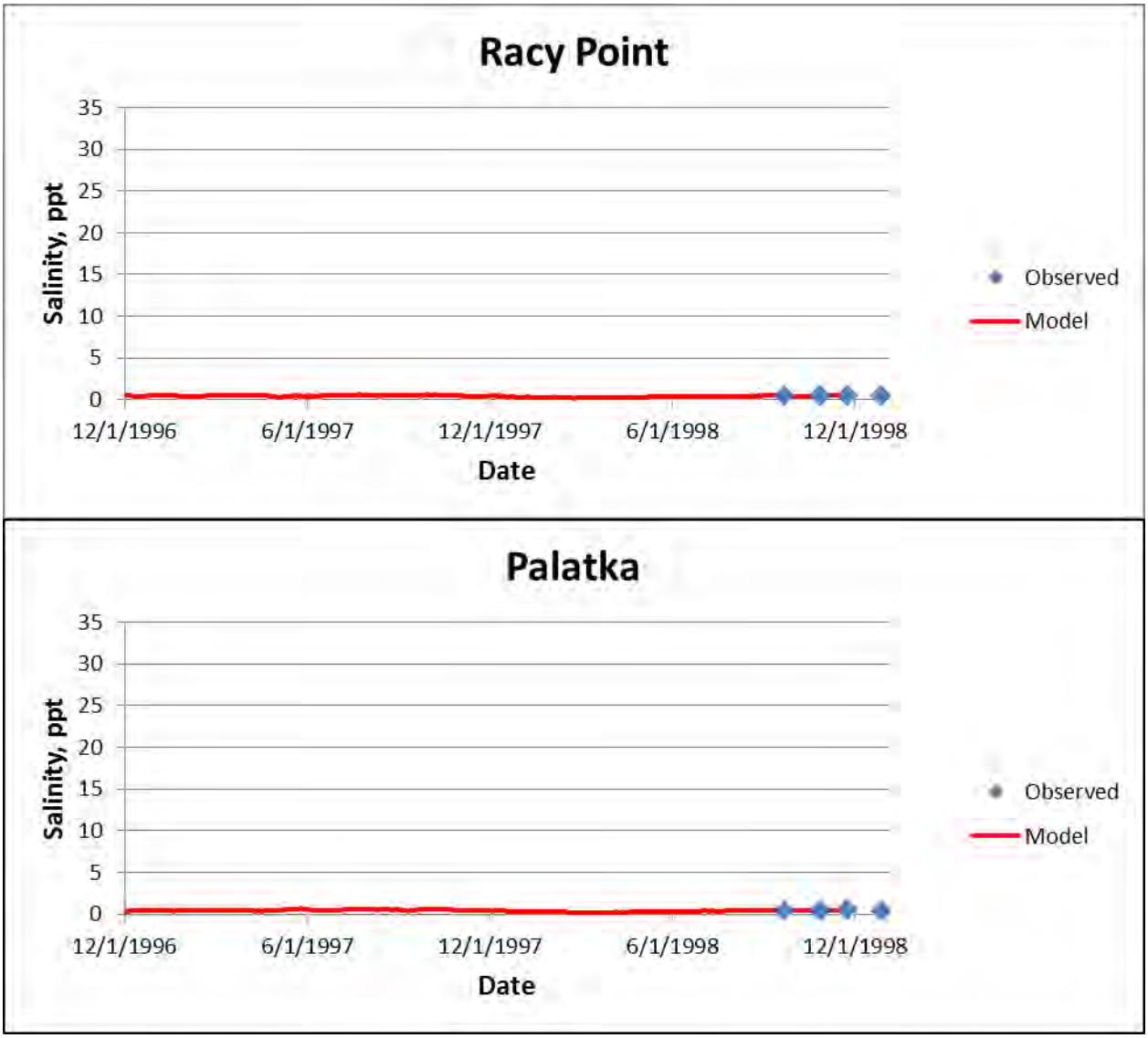


**Figure A2. Observed and depth-averaged, model-computed salinity for seven stations**

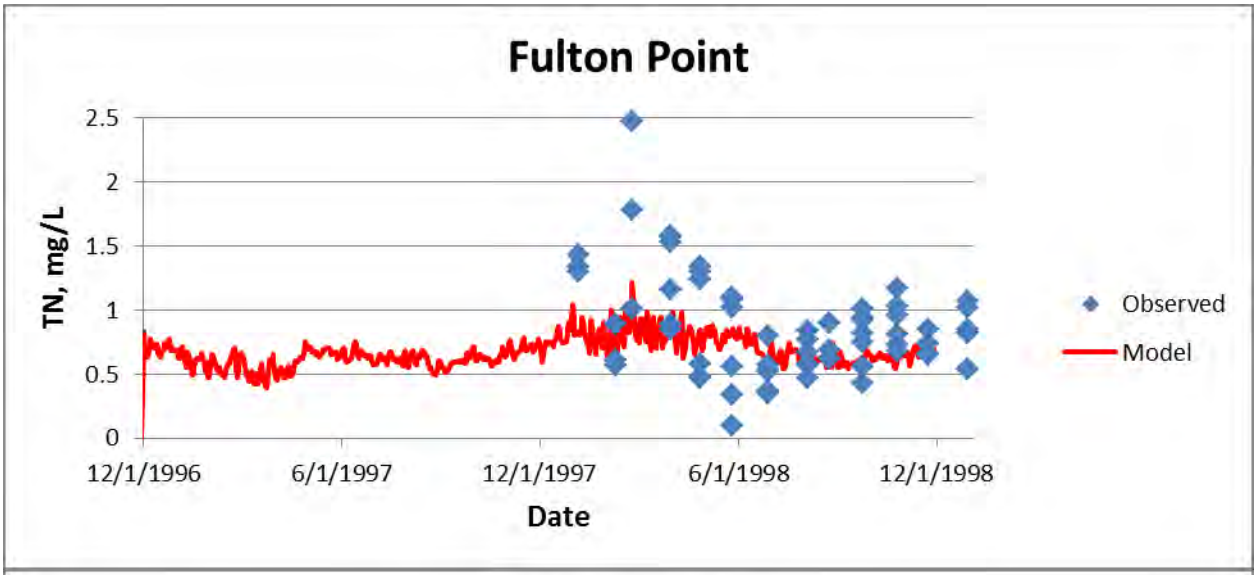
Fulton Point
TN, mg/L
2.5
2
1.5
1
0.5
0
12/1/1996
6/1/1997
12/1/1997
6/1/1998
12/1/1998
Date
Observed
Model

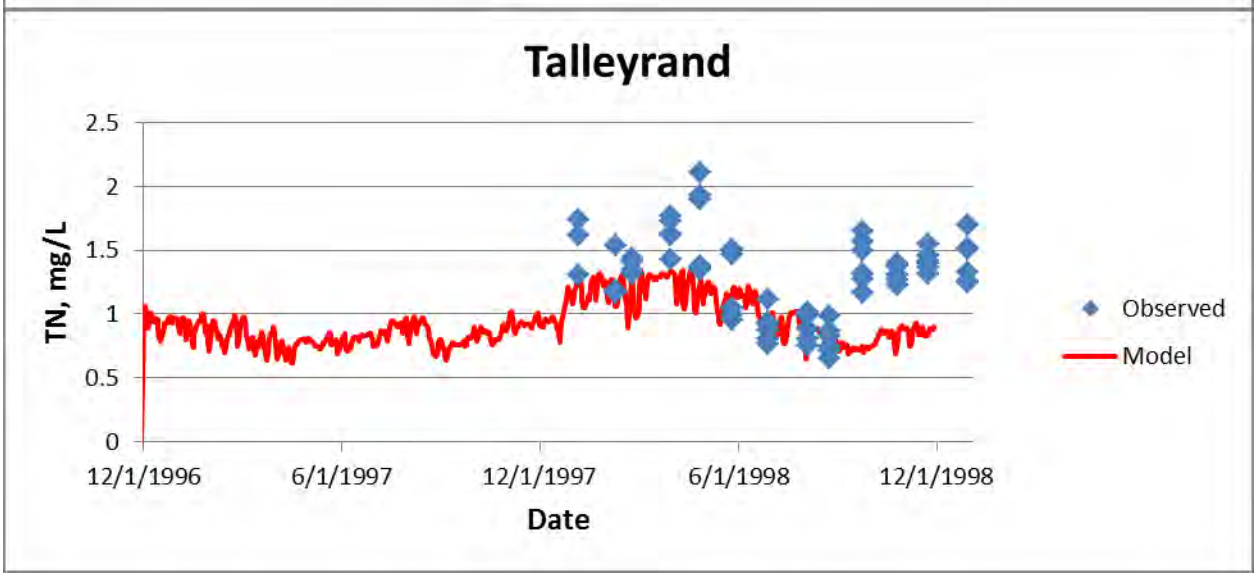
Talleyrand
TN, mg/L
2.5
2
1.5
1
0.5
0
12/1/1996
6/1/1997
12/1/1997
6/1/1998
12/1/1998
Date
Observed
Model

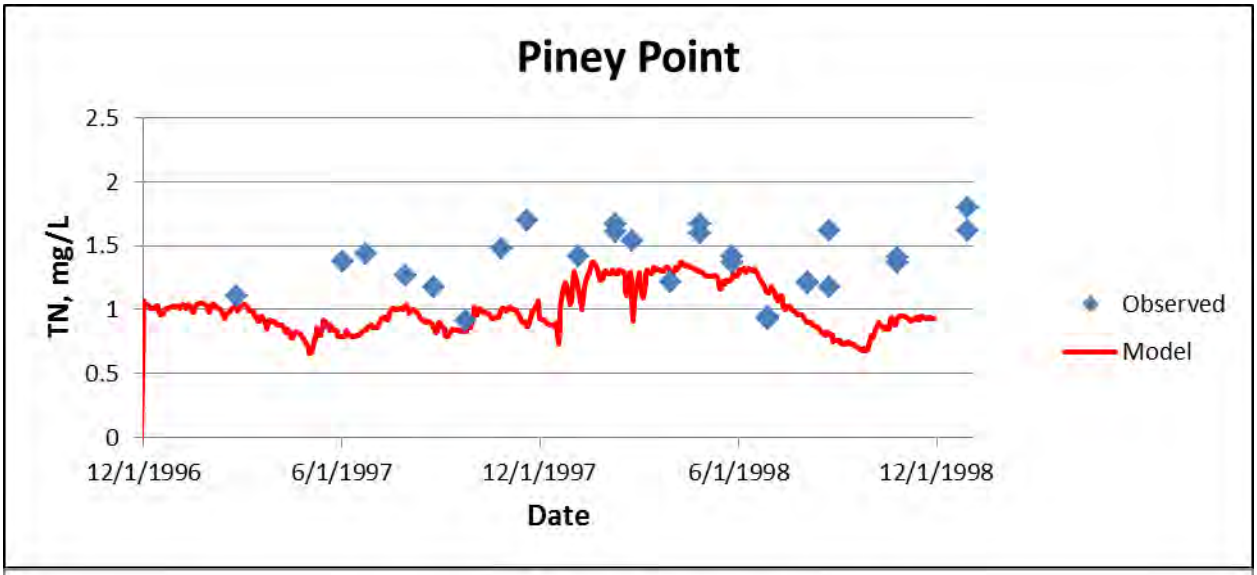
Piney Point
TN, mg/L
2.5
2
1.5
1
0.5
0
12/1/1996
6/1/1997
12/1/1997
6/1/1998
12/1/1998
Date
Observed
Model

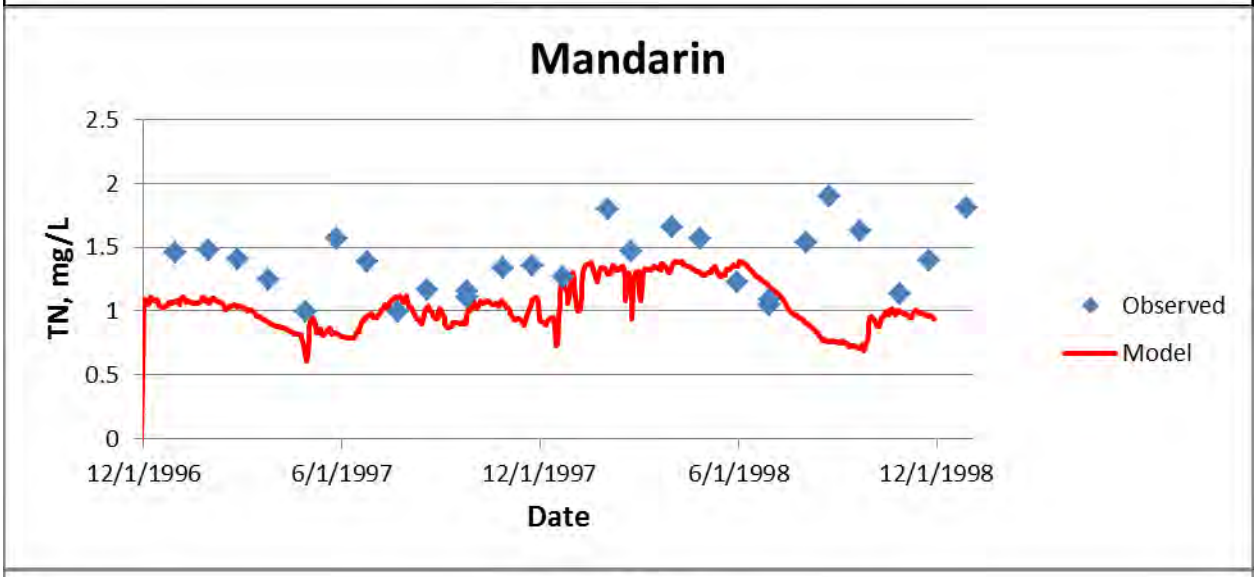
Mandarin
TN, mg/L
2.5
2
1.5
1
0.5
0
12/1/1996
6/1/1997
12/1/1997
6/1/1998
12/1/1998
Date
Observed
Model

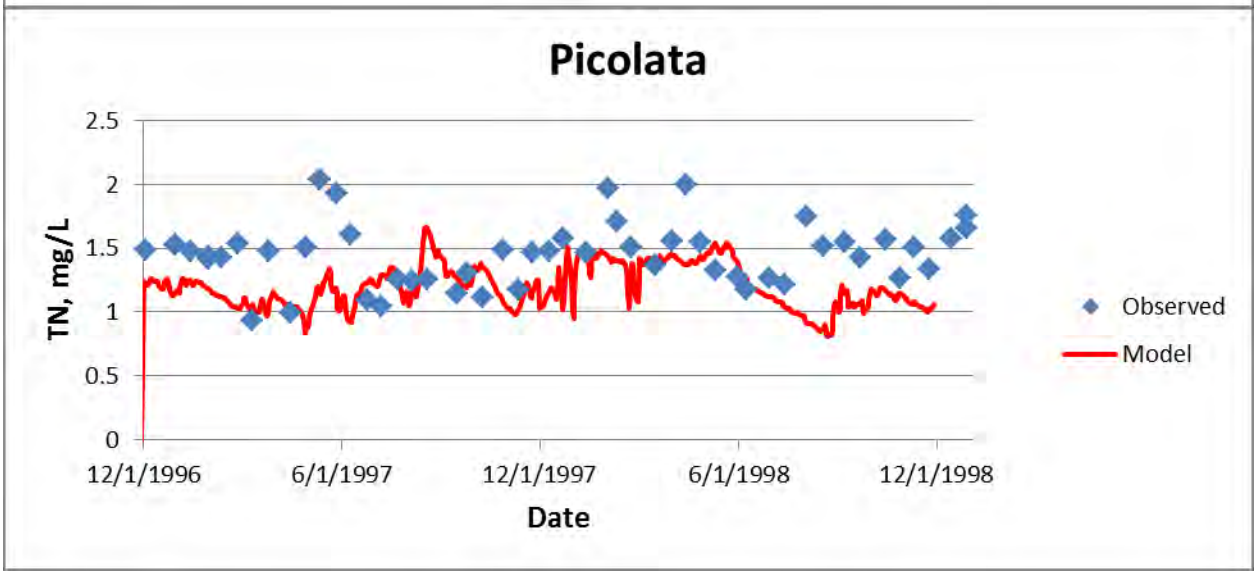
Picolata
TN, mg/L
2.5
2
1.5
1
0.5
0
12/1/1996
6/1/1997
12/1/1997
6/1/1998
12/1/1998
Date
Observed
Model

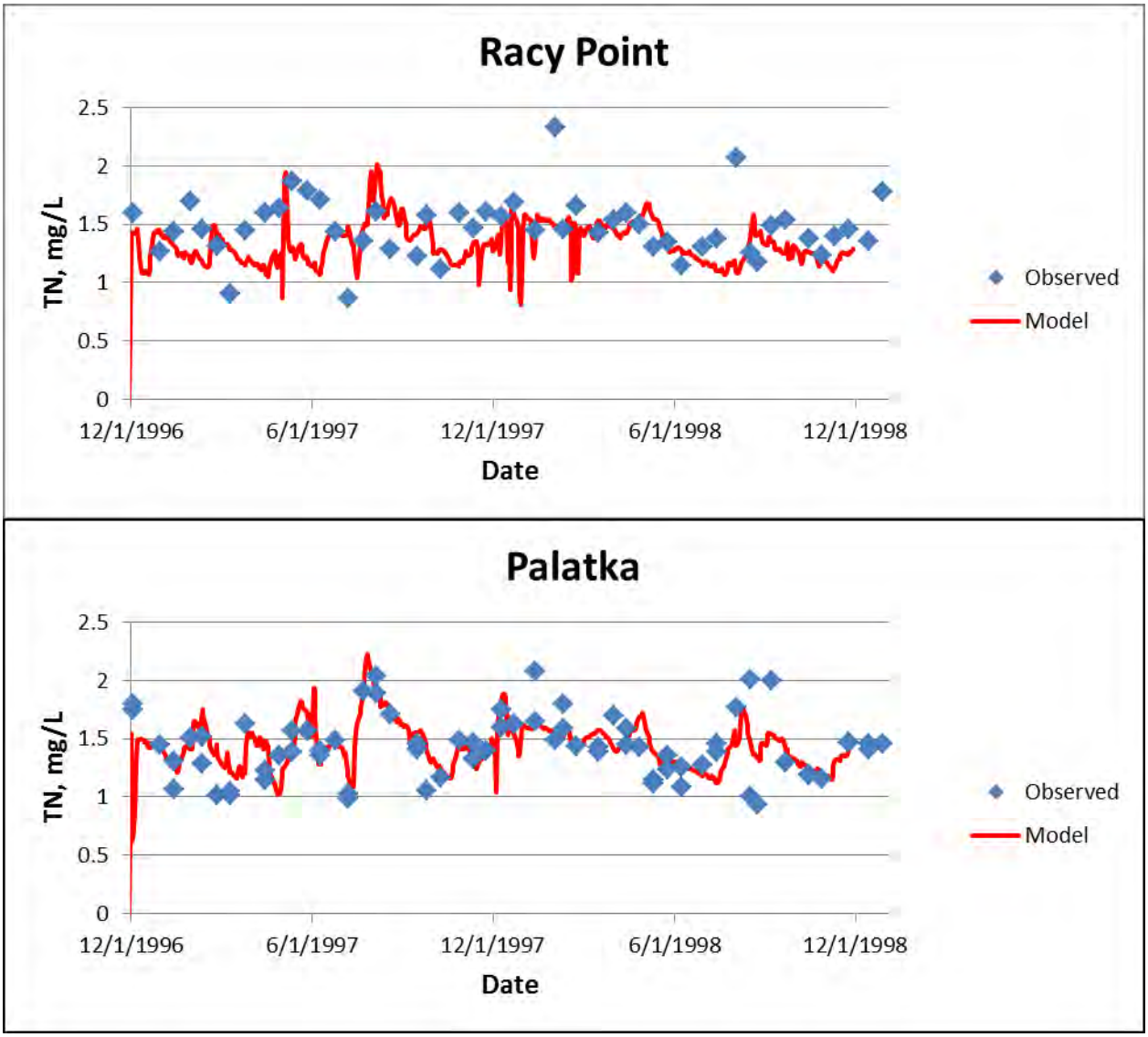


**Figure A3. Observed and depth-averaged, model-computed TN for seven stations**

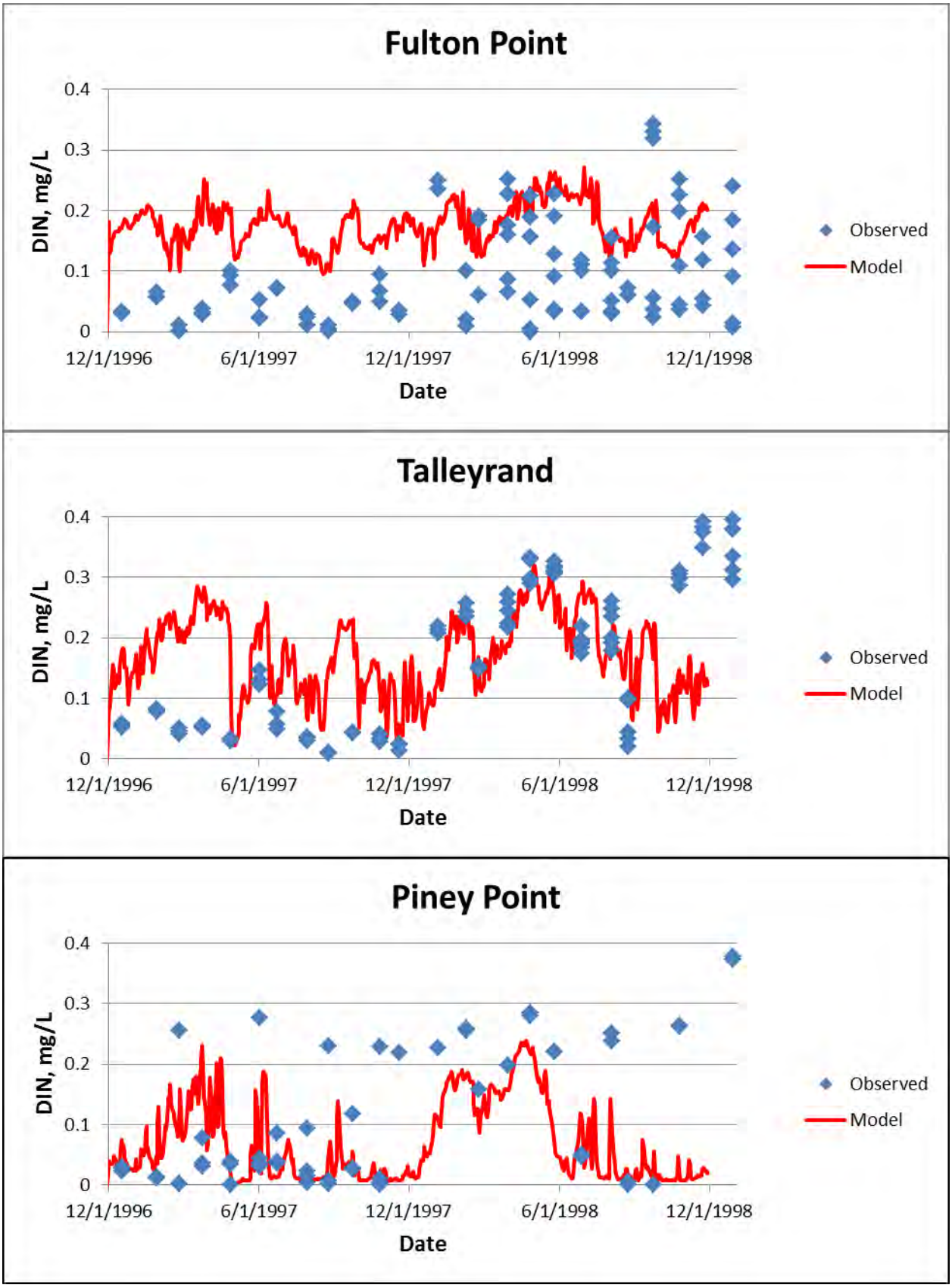
Fulton Point
DIN, mg/L
0.4
0.3
0.2
0.1
0
12/1/1996
6/1/1997
12/1/1997
6/1/1998
12/1/1998
Date
Observed
Model
Talleyrand
DIN, mg/L
0.4
0.3
0.2
0.1
0
12/1/1996
6/1/1997
12/1/1997
6/1/1998
12/1/1998
Date
Observed
Model
Piney Point
DIN, mg/L
0.4
0.3
0.2
0.1
0
12/1/1996
6/1/1997
12/1/1997
6/1/1998
12/1/1998
Date
Observed
Model

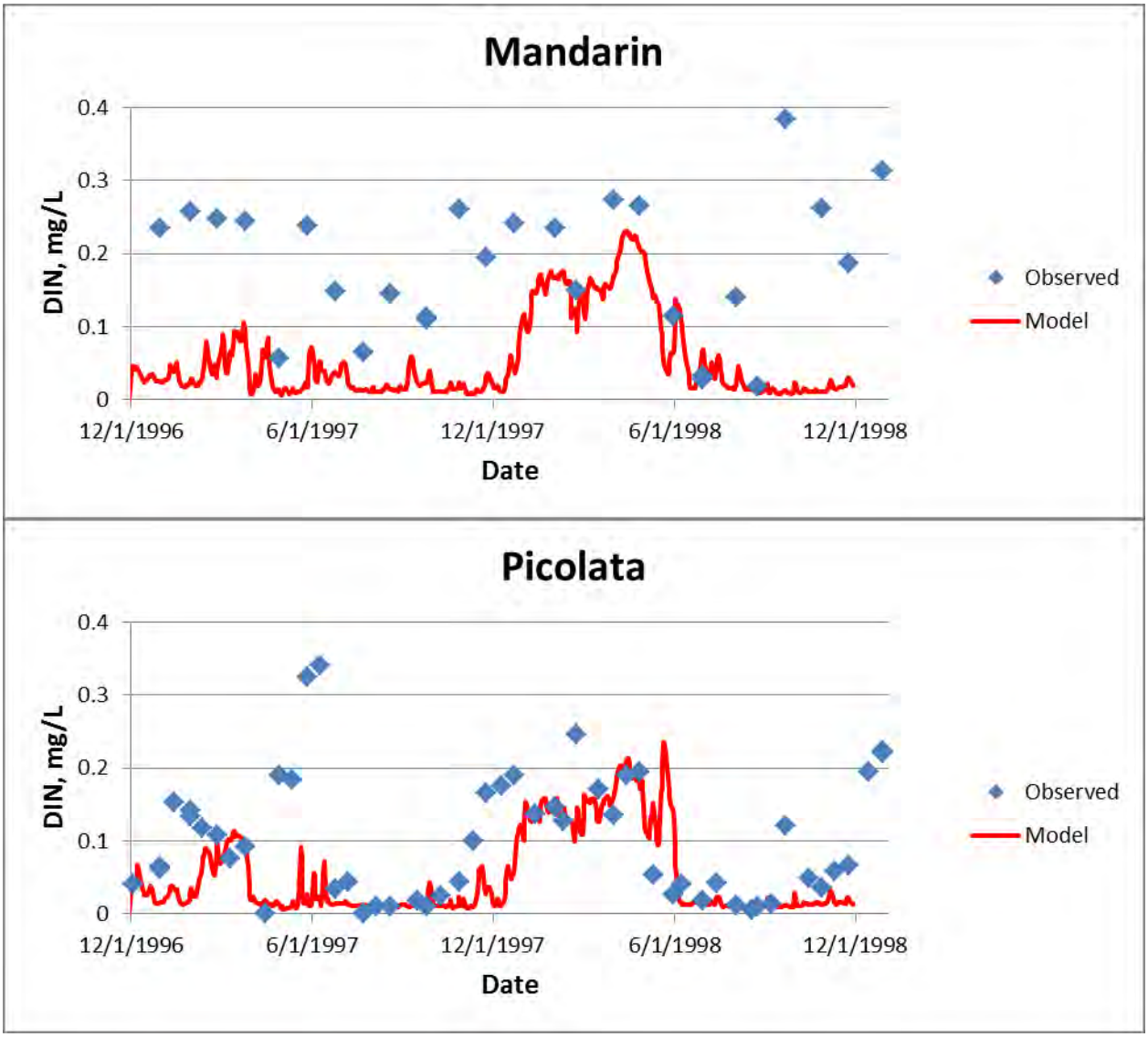
Mandarin
DIN, mg/L
0.4
0.3
0.2
0.1
0
12/1/1996
6/1/1997
12/1/1997
6/1/1998
12/1/1998
Date
Observed
Model
Picolata
DIN, mg/L
0.4
0.3
0.2
0.1
0
12/1/1996
6/1/1997
12/1/1997
6/1/1998
12/1/1998
Date
Observed
Model

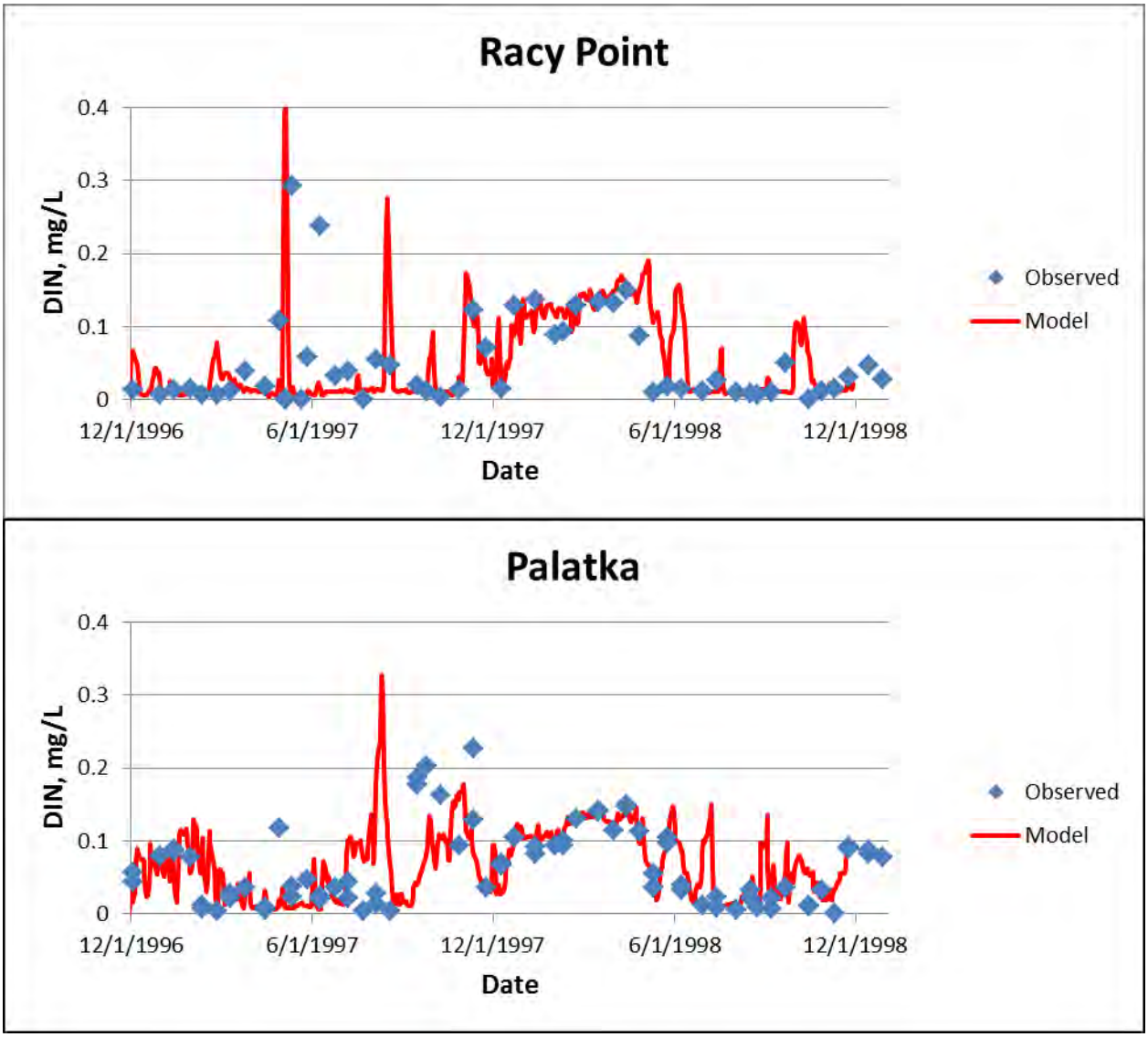


**Figure A4. Observed and depth-averaged, model-computed DIN for seven stations**

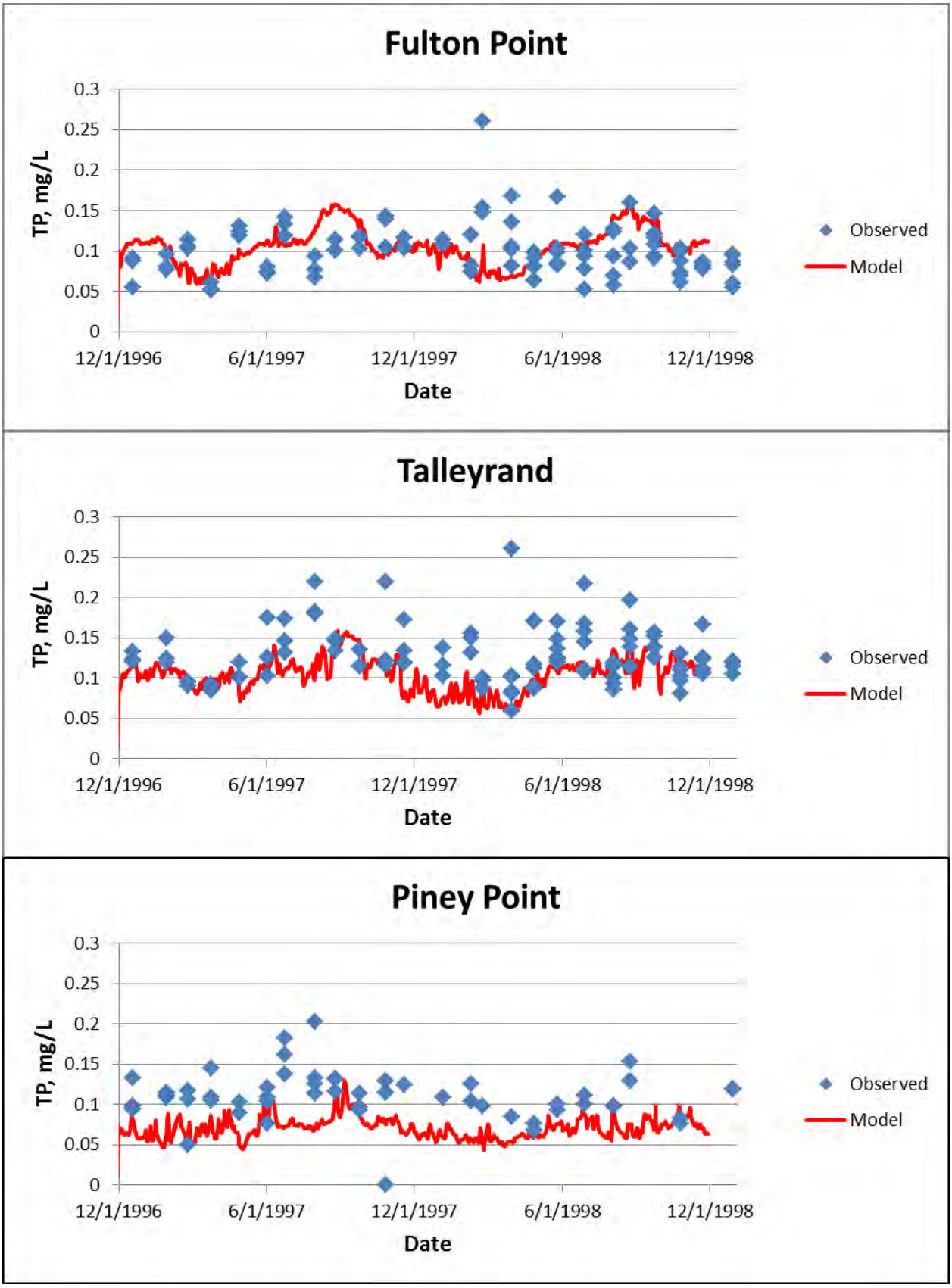
Fulton Point
TP, mg/L
0.3
0.25
0.2
0.15
0.1
0.05
0
12/1/1996
6/1/1997
12/1/1997
6/1/1998
12/1/1998
Date
Observed
Model
Talleyrand
TP, mg/L
0.3
0.25
0.2
0.15
0.1
0.05
0
12/1/1996
6/1/1997
12/1/1997
6/1/1998
12/1/1998
Date
Observed
Model
Piney Point
TP, mg/L
0.3
0.25
0.2
0.15
0.1
0.05
0
12/1/1996
6/1/1997
12/1/1997
6/1/1998
12/1/1998
Date
Observed
Model

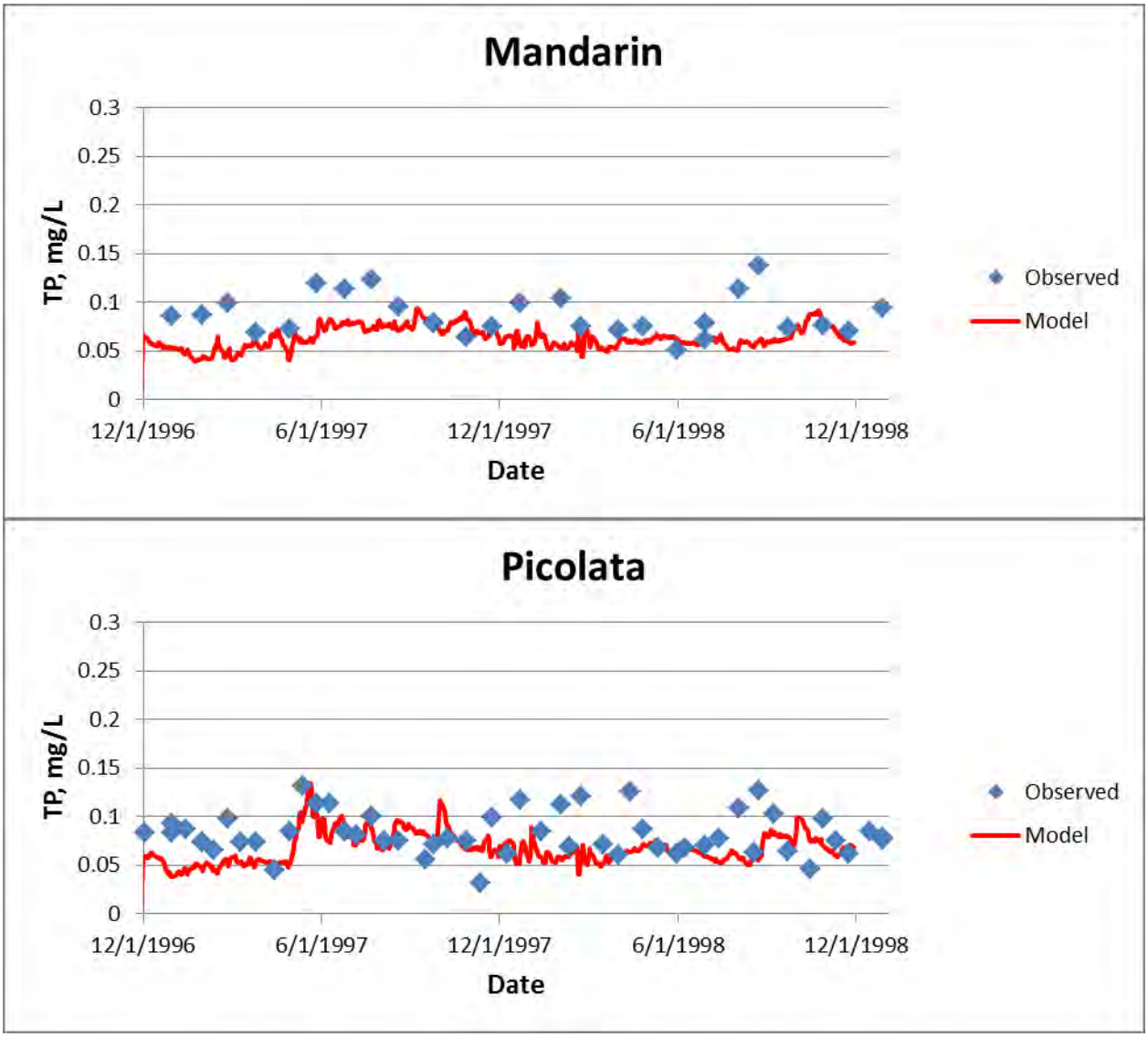
Mandarin
TP, mg/L
0.3
0.25
0.2
0.15
0.1
0.05
0
12/1/1996
6/1/1997
12/1/1997
6/1/1998
12/1/1998
Date
Observed
Model
Picolata
TP, mg/L
0.3
0.25
0.2
0.15
0.1
0.05
0
12/1/1996
6/1/1997
12/1/1997
6/1/1998
12/1/1998
Date
Observed
Model

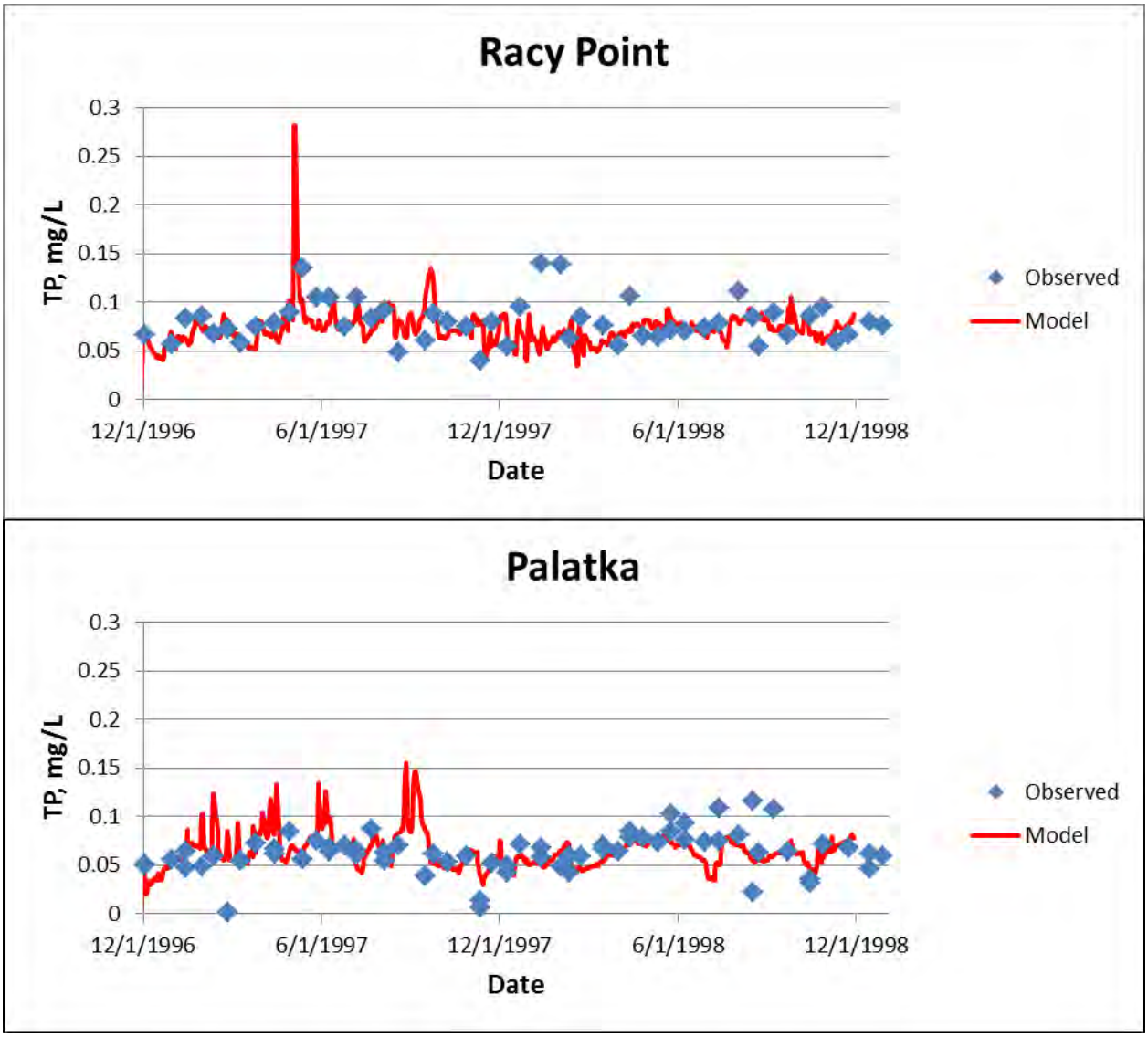


**Figure A5. Observed and depth-averaged, model-computed TP for seven stations**

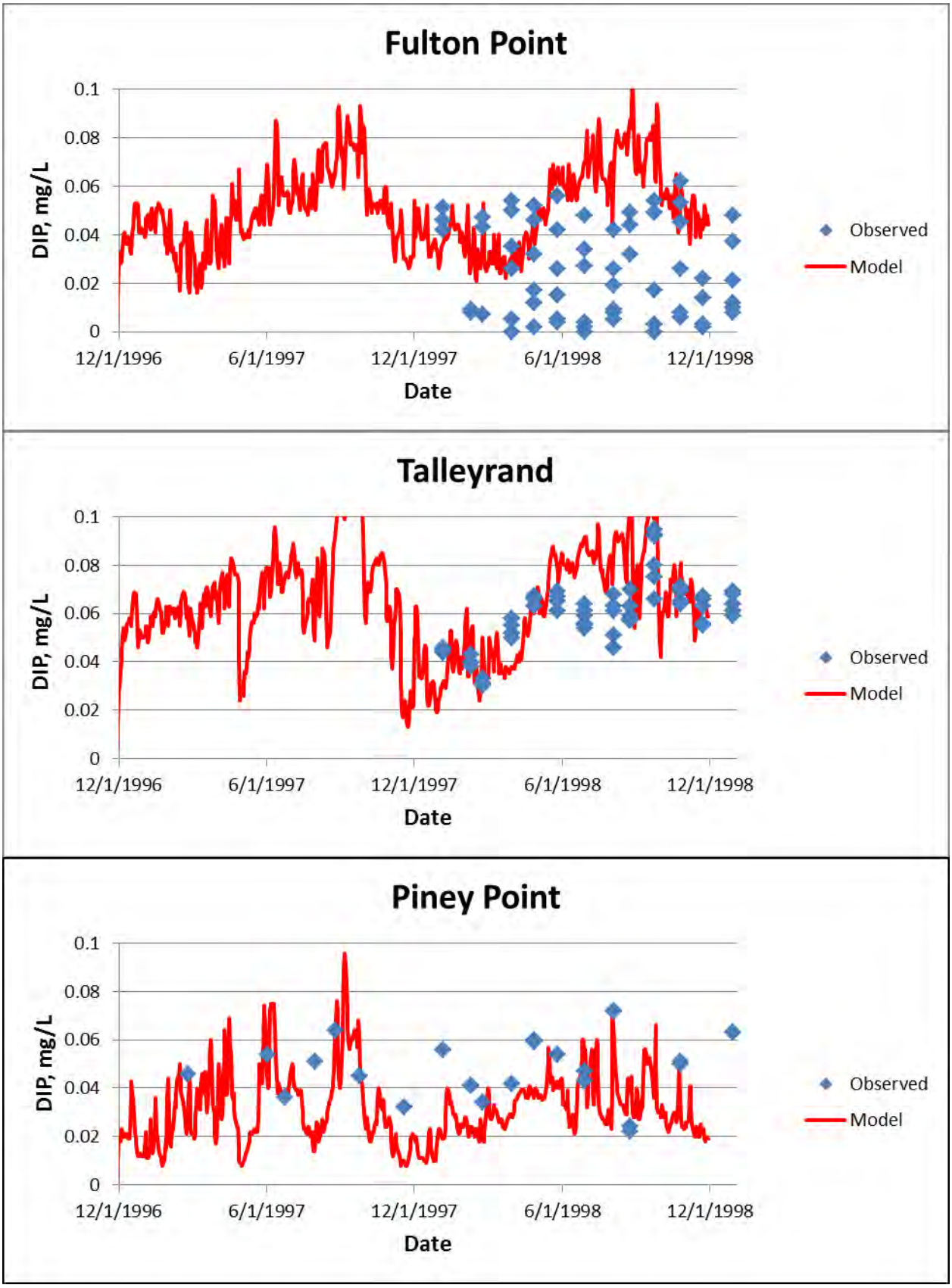
Fulton Point
DIP, mg/L
0.1
0.08
0.06
0.04
0.02
0
12/1/1996
6/1/1997
12/1/1997
6/1/1998
12/1/1998
Date
Observed
Model
Talleyrand
DIP, mg/L
0.1
0.08
0.06
0.04
0.02
0
12/1/1996
6/1/1997
12/1/1997
6/1/1998
12/1/1998
Date
Observed
Model
Piney Point
DIP, mg/L
0.1
0.08
0.06
0.04
0.02
0
12/1/1996
6/1/1997
12/1/1997
6/1/1998
12/1/1998
Date
Observed
Model

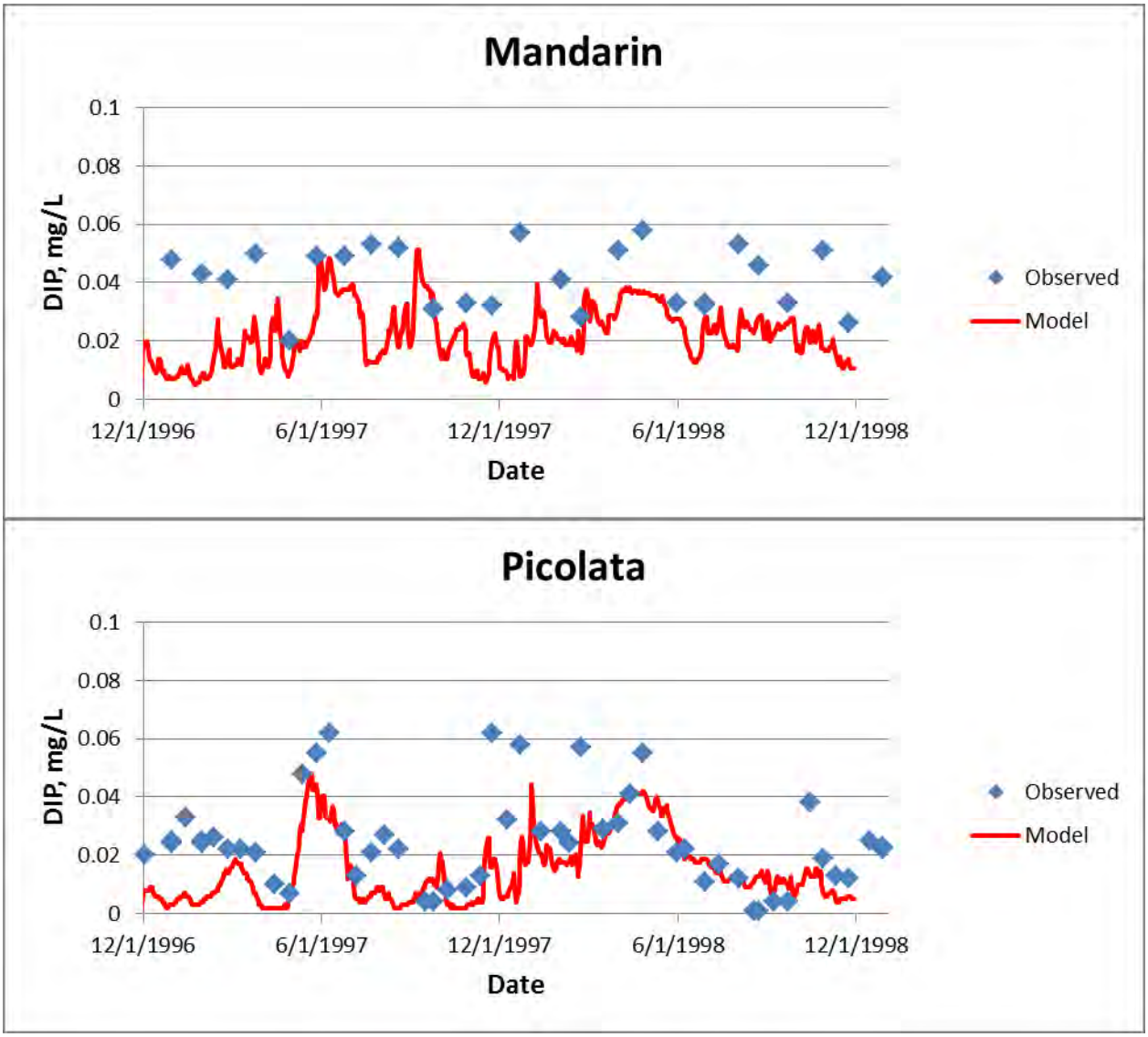
Mandarin
0.1
0.08
0.06
0.04
0.02
0
DIP, mg/L
12/1/1996
6/1/1997
12/1/1997
6/1/1998
12/1/1998
Date
Observed
Model
Picolata
0.1
0.08
0.06
0.04
0.02
0
DIP, mg/L
12/1/1996
6/1/1997
12/1/1997
6/1/1998
12/1/1998
Date
Observed
Model

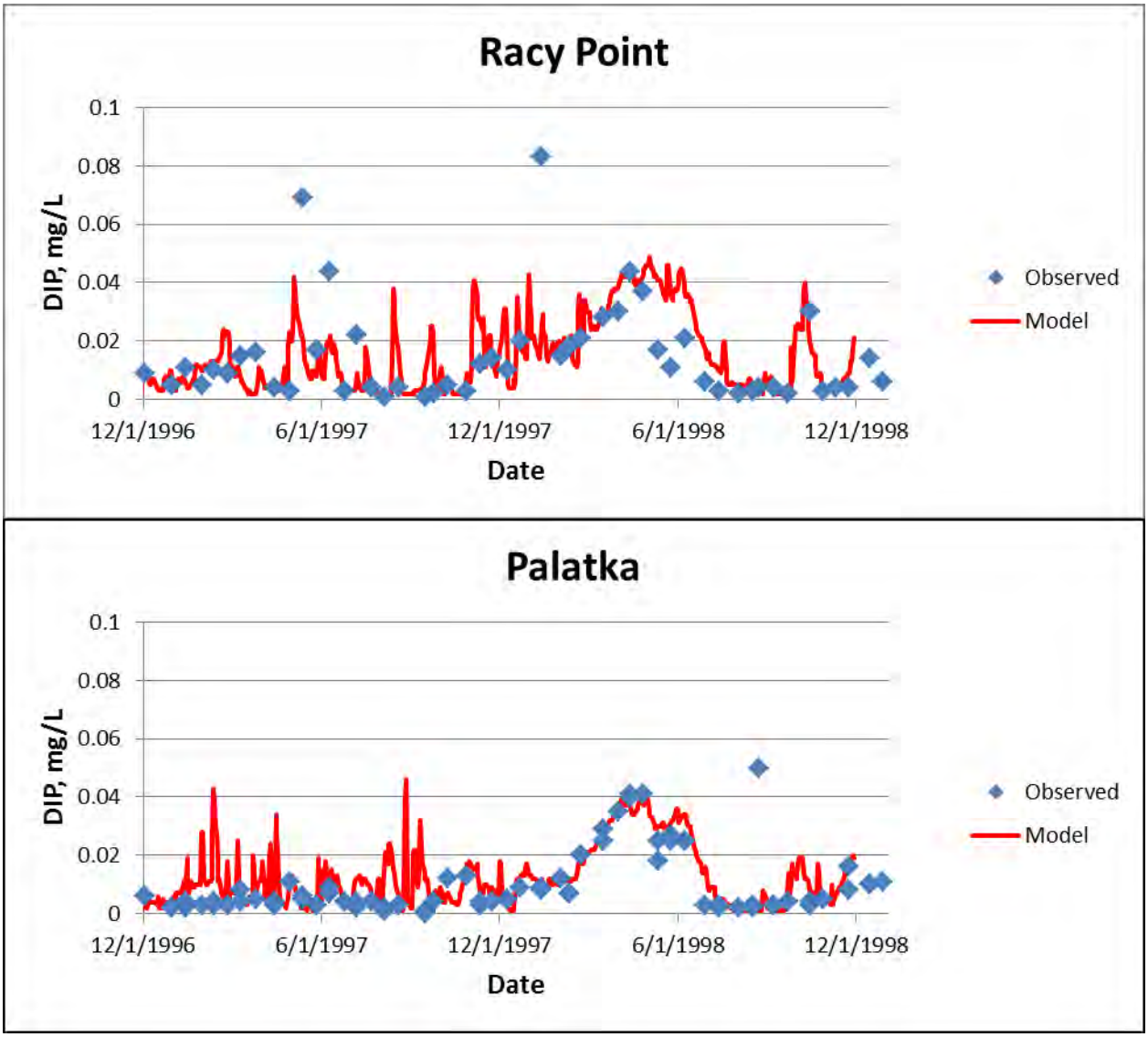


**Figure A6. Observed and depth-averaged, model-computed DIP for seven stations**

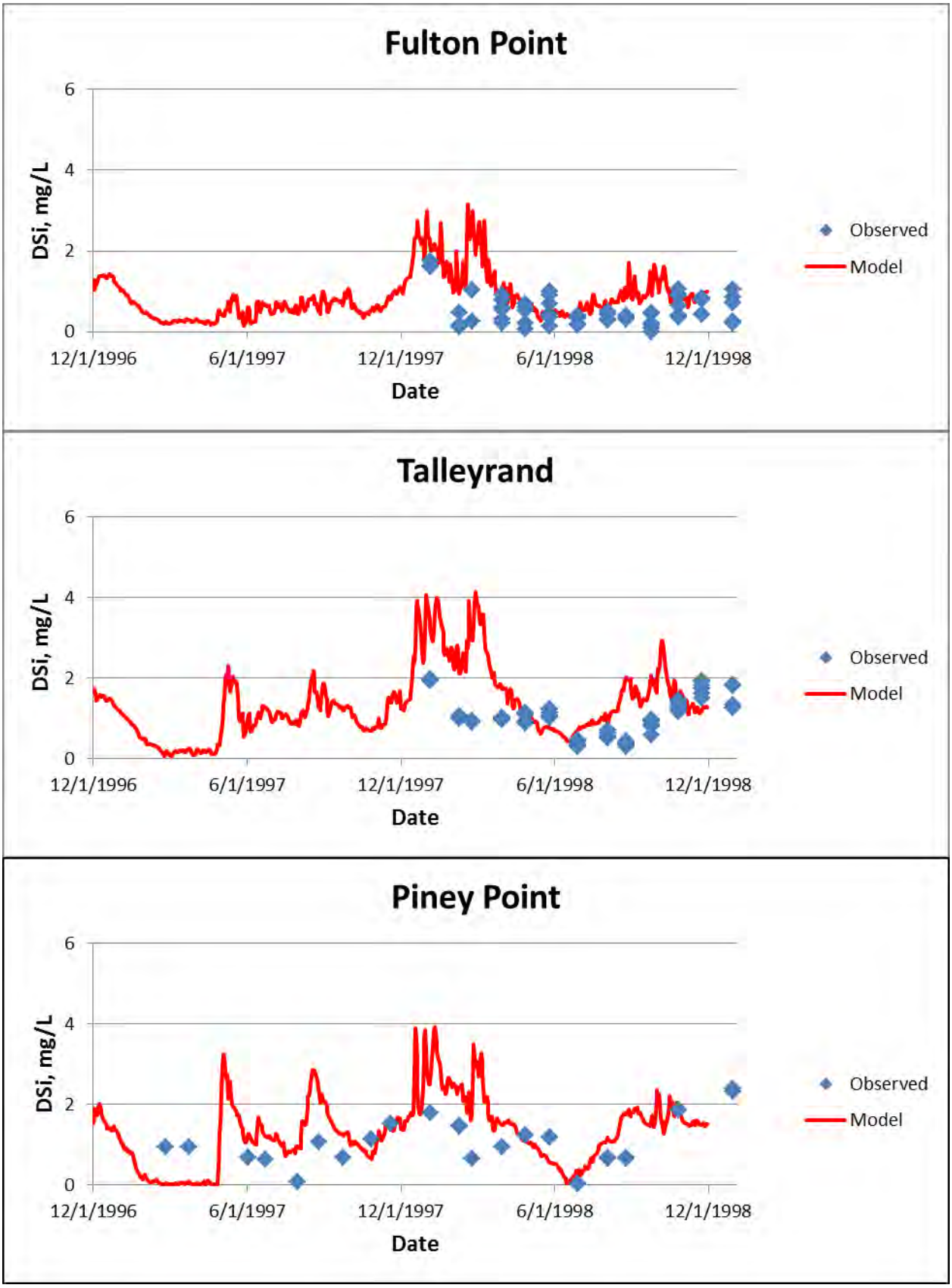
Fulton Point
DSi, mg/L
6
4
2
0
12/1/1996
6/1/1997
12/1/1997
6/1/1998
12/1/1998
Date
Observed
Model
Talleyrand
DSi, mg/L
6
4
2
0
12/1/1996
6/1/1997
12/1/1997
6/1/1998
12/1/1998
Date
Observed
Model
Piney Point
DSi, mg/L
6
4
2
0
12/1/1996
6/1/1997
12/1/1997
6/1/1998
12/1/1998
Date
Observed
Model

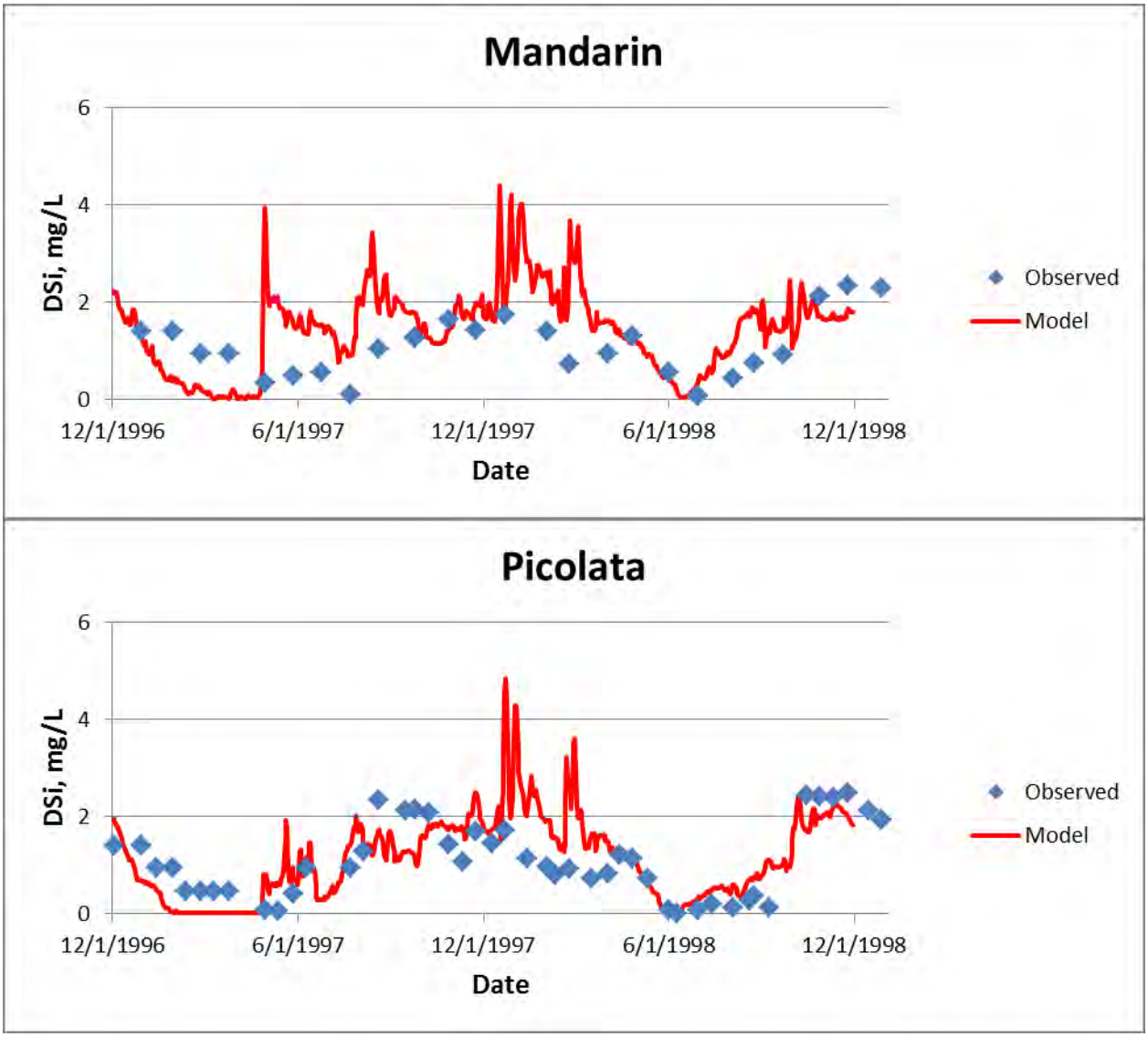
Mandarin
DSi, mg/L
6
4
2
0
12/1/1996
6/1/1997
12/1/1997
6/1/1998
12/1/1998
Date
Observed
Model
Picolata
DSi, mg/L
6
4
2
0
12/1/1996
6/1/1997
12/1/1997
6/1/1998
12/1/1998
Date
Observed
Model

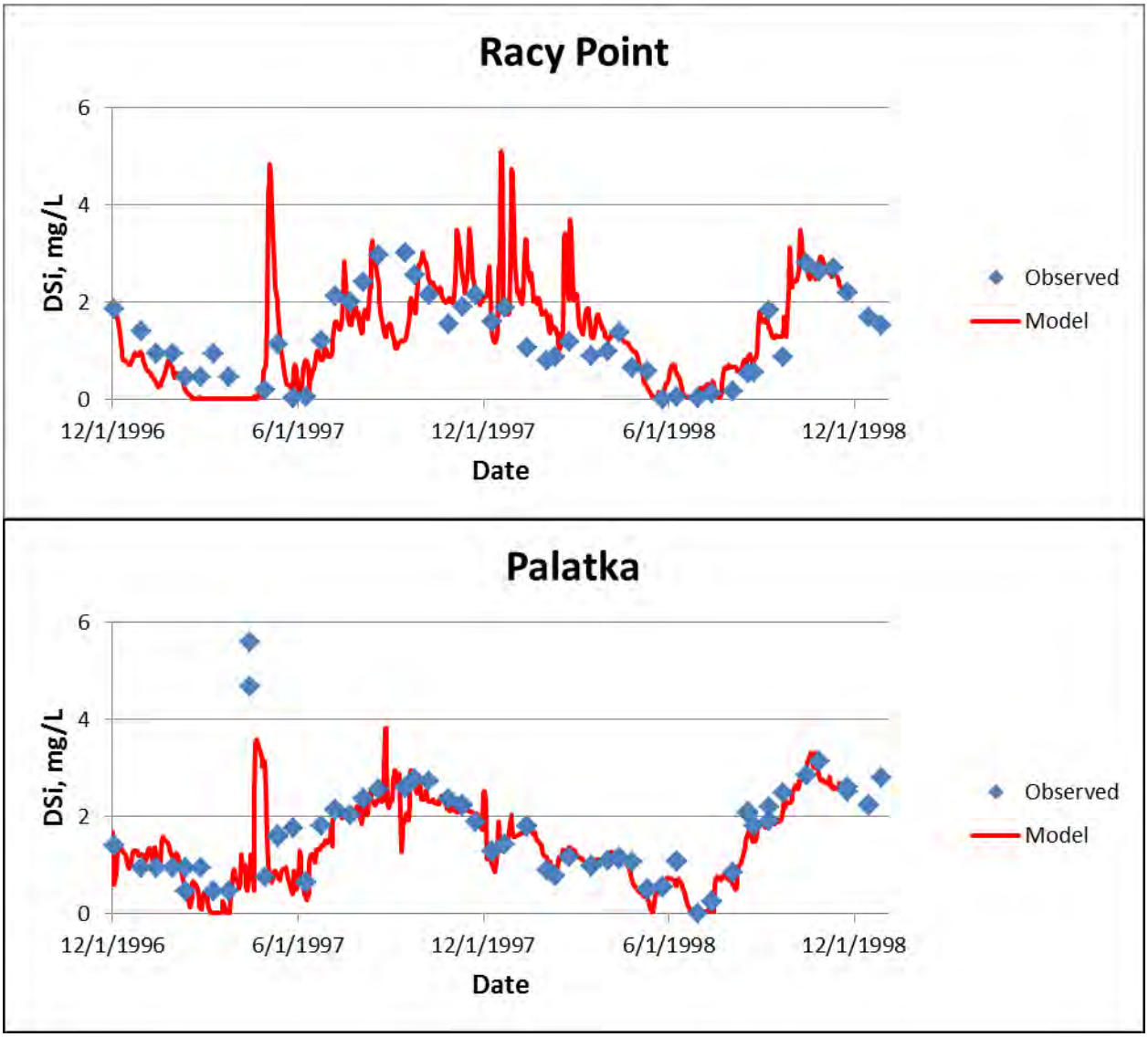


**Figure A7. Observed and depth-averaged, model-computed DSi for seven stations**

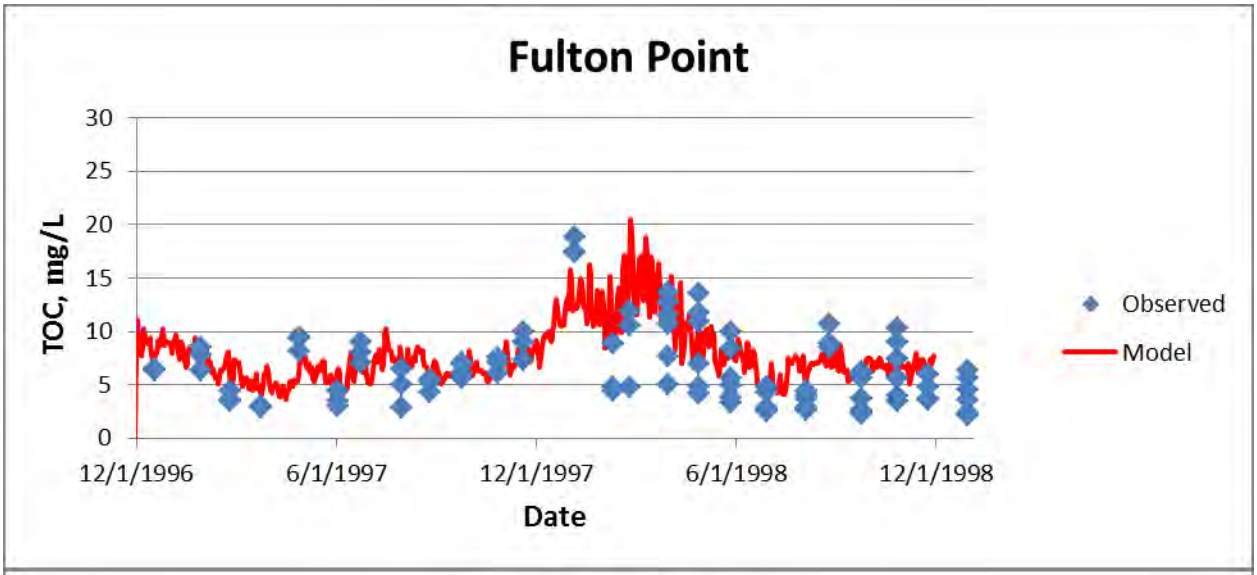
Fulton Point
TOC, mg/L
30
25
20
15
10
5
0
12/1/1996
6/1/1997
12/1/1997
6/1/1998
12/1/1998
Date
Observed
Model

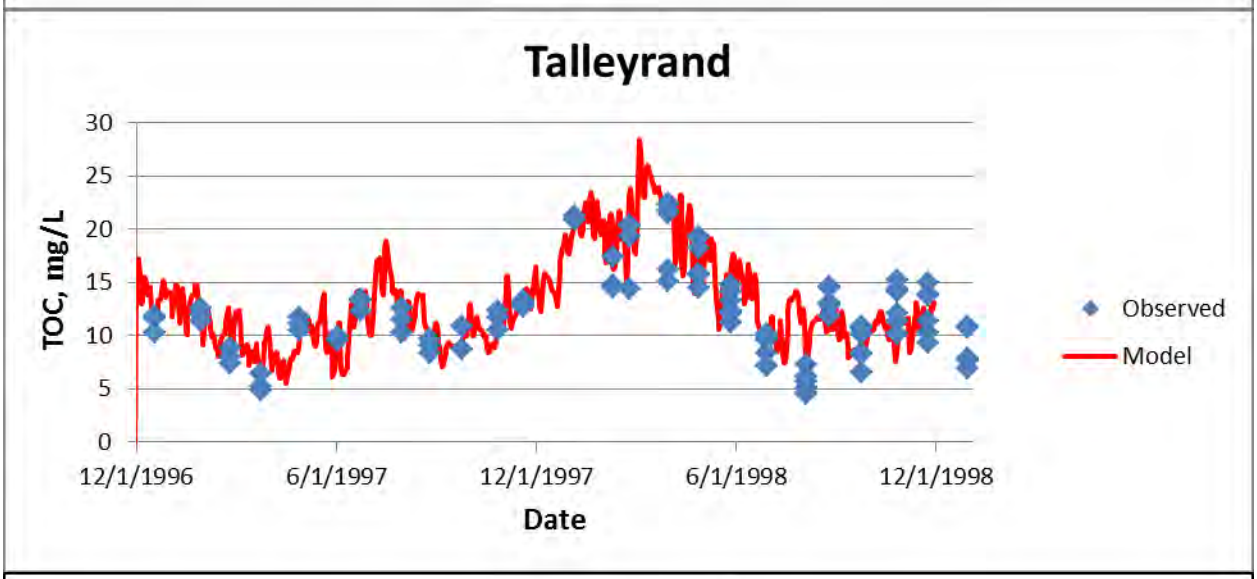
Talleyrand
TOC, mg/L
30
25
20
15
10
5
0
12/1/1996
6/1/1997
12/1/1997
6/1/1998
12/1/1998
Date
Observed
Model

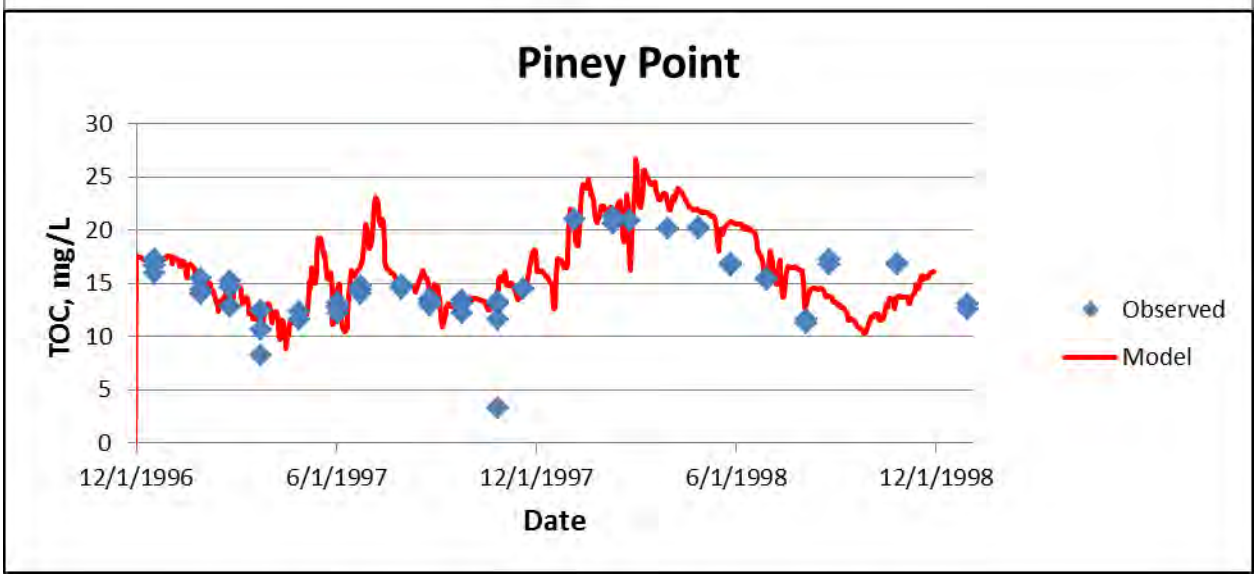
Piney Point
TOC, mg/L
30
25
20
15
10
5
0
12/1/1996
6/1/1997
12/1/1997
6/1/1998
12/1/1998
Date
Observed
Model

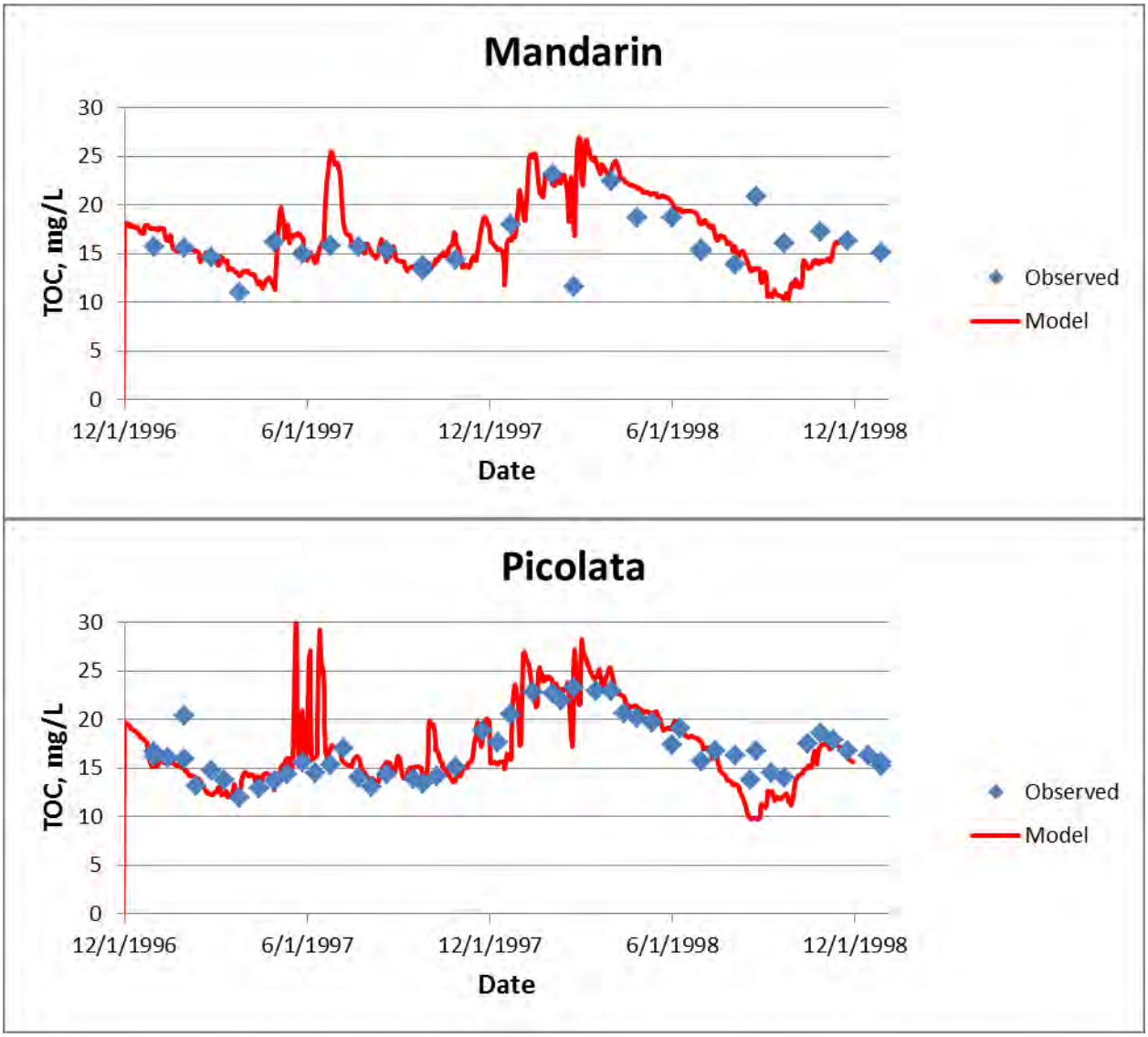
Mandarin
TOC, mg/L
30
25
20
15
10
5
0
12/1/1996
6/1/1997
12/1/1997
6/1/1998
12/1/1998
Date
Observed
Model
Picolata
TOC, mg/L
30
25
20
15
10
5
0
12/1/1996
6/1/1997
12/1/1997
6/1/1998
12/1/1998
Date
Observed
Model

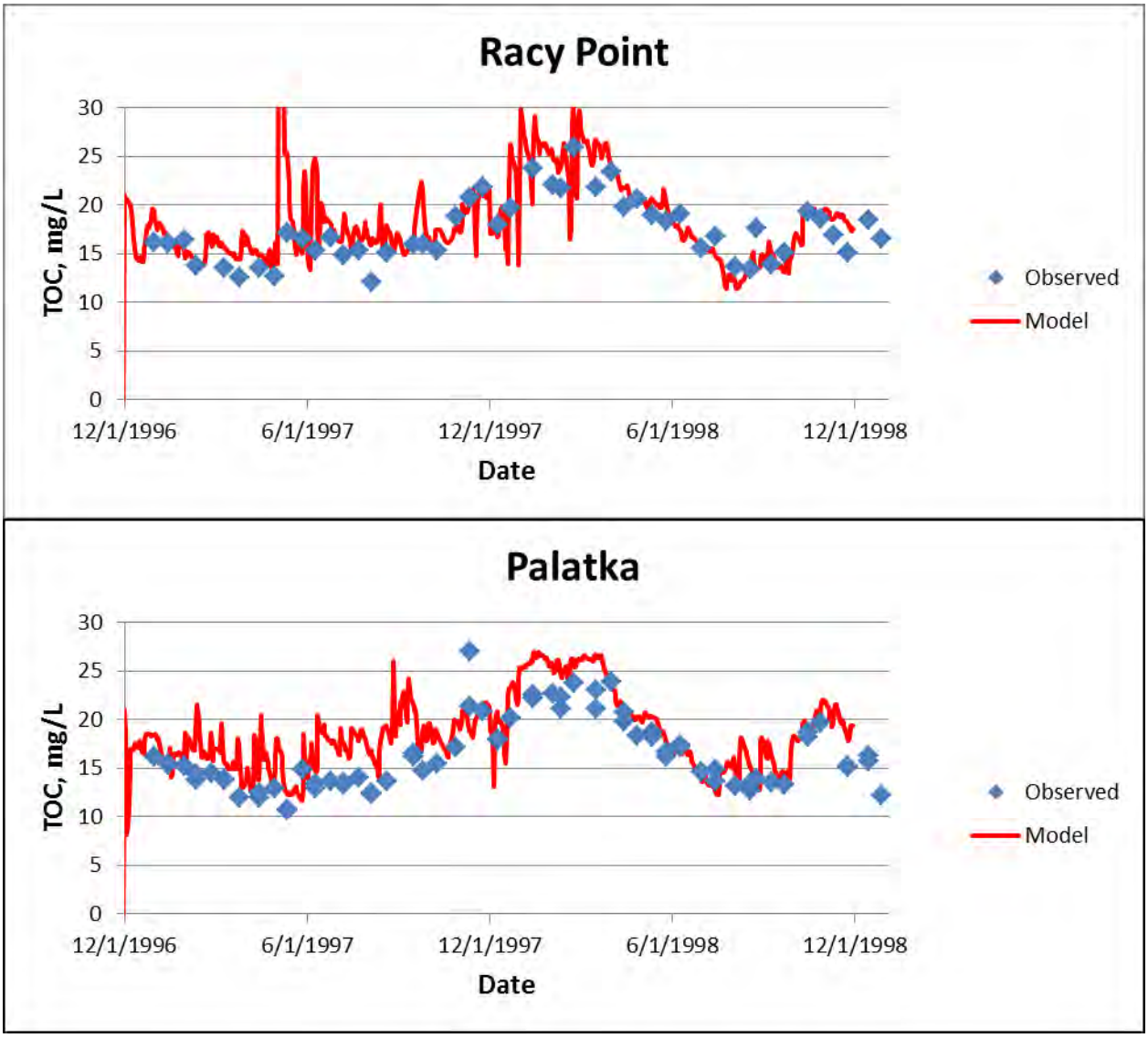


**Figure A8. Observed and depth-averaged, model-computed TOC for seven stations**